

# **Algal Bioproducts – Investigating the Effect of Light Quality on Metabolite Production by Photosynthetic Diatoms**

**Kenji Iwasaki**

B. Sci (Hons)

**Submitted in fulfilment of the requirements for the degree of Doctor of Philosophy  
in Science**

**Climate Change Cluster (C3), School of Life Sciences**

**University of Technology Sydney**

**October 2019**

**Supervised by: Prof. Peter Ralph & Dr. Milan Szabó**

## **Certificate of Original Authorship**

I, Kenji Iwasaki declare that this thesis, is submitted in fulfilment of the requirements for the award of Doctor of Philosophy, in the Climate Change Cluster, Faculty of Science at the University of Technology Sydney. This thesis is wholly my own work unless otherwise referenced or acknowledged. In addition, I certify that all information sources and literature used are indicated in the thesis. I certify that this document has not been submitted for qualifications at any other academic institution.

This research is supported by the Australian Government Research Training Program.

Production Note:

**Signature:** Signature removed prior to publication.

Kenji Iwasaki

Date: October 2019

## Acknowledgements

Thank you to my supervisors, Peter Ralph and Milán Szabó for their endless support, guidance and critique throughout my candidature. Thank you to all the past and present members of the Algae Biosystems and Biotechnology Group at UTS, Chris Evenhuis, Bojan Tamburic, Janice McCauley and Alonso Cordova, who have provided continuous support that has allowed for the completion of this thesis. Chris Evenhuis, in particular for developing the empirical model used in this thesis. Wayne O'Connor who had enabled facility visits to Port Stephens Fisheries Institute and provided invaluable insights to hatchery operations. Leo Hardtke and Phil Lawrence for their expertise in constructing the LED panel used in this thesis. Unnikrishnan Kuzhiumparambil and Taya Lapshina for their assistance and guidance in the chemical analysis required in this thesis. The technical staff who had maintained the laboratories and facilities that have allowed for experiments to run as smoothly as possible.

Lastly, to all my friends and colleagues at UTS who have made this PhD an enjoyable experience.

## **Preface**

This thesis has been prepared in publication format, whereby each chapter represents a manuscript ready for submission to a peer-reviewed journal. Therefore, there will be some duplication in Introduction and Materials and Methods. At present, no individual chapter has been submitted for publication in a peer-reviewed journal.

## Table of Content

Algal Bioproducts – Investigating the Effect of Light Quality on Metabolite Production by Photosynthetic Diatoms .....	i
Certificate of Original Authorship .....	ii
Acknowledgements .....	iii
Preface.....	iv
Table of Content.....	v
List of Figures .....	x
List of Tables.....	xix
Abstract of Thesis .....	xxi
Chapter 1 General Introduction.....	1
1.1. Introduction to Microalgae.....	1
1.2. Physiology and Importance of Diatoms.....	2
1.2.1. Importance of Diatoms in Aquaculture.....	5
1.2.2. Importance of <i>Chaetoceros muelleri</i> in Australian Aquaculture.....	8
1.2.3. Photosynthetic Mechanisms in Diatoms.....	10
1.3. Photosynthesis in Microalgae .....	11
1.4. Dynamics of CO <sub>2</sub> Availability in Microalgal Culture .....	15
1.5. Dynamics of Light Availability in Microalgal Culture .....	18
1.5.1. Light quality in aquatic environments.....	20
1.5.2. How Diatoms Respond to Light Intensity.....	21
1.5.3. Mechanisms to sense light quality in diatoms.....	22
1.6. Light Emitting Diodes as Light Source for Culturing Diatoms .....	24
1.6.1. Using light emitting diodes to manipulate biochemical content in diatoms ..	25
1.7. Summary .....	26
1.8. Aims of Thesis .....	26
1.9. Thesis structure .....	27
1.10. Ethics and Permits .....	28
1.11. References .....	28
Chapter 2 Light and CO <sub>2</sub> availability to enhance growth rate in the diatom <i>Chaetoceros muelleri</i> for aquaculture .....	49
2.1. Introduction.....	49
2.1.1. Diatoms as feed for aquaculture.....	49

2.1.2.	How diatoms respond to light .....	51
2.1.3.	How light effects diatom growth.....	52
2.1.4.	Light limitations in current aquaculture practices.....	54
2.1.5.	Light emitting diodes and their potential role in aquaculture .....	57
2.1.6.	Measuring steady-state light curves .....	58
2.1.7.	Carbon limitation in current aquaculture practices .....	59
2.2.	Aims and Objectives .....	61
2.3.	Material and Methods .....	62
2.3.1.	Culturing <i>Chaetoceros muelleri</i> .....	62
2.3.2.	Photobioreactor setup.....	63
2.3.3.	Experimental design.....	65
2.3.4.	Steady-state light curve measurements .....	67
2.3.5.	Dissolved oxygen measurements using optical sensors and measuring net photosynthesis .....	68
2.3.6.	Automated <i>Chaetoceros muelleri</i> growth measurements .....	69
2.3.7.	Light attenuation measurements .....	70
2.3.8.	Dissolved inorganic carbon.....	71
2.3.9.	Modelling net photosynthesis of <i>Chaetoceros muelleri</i> .....	71
2.4.	Results.....	72
2.4.1.	Steady-state light curve of <i>Chaetoceros muelleri</i> .....	72
2.4.2.	Growth rates of <i>Chaetoceros muelleri</i> under different light and CO <sub>2</sub> availability.....	73
2.4.3.	Modelling light availability of two LED configurations.....	77
2.4.4.	Net photosynthesis rates of <i>Chaetoceros muelleri</i> under varying light and carbon availability.....	82
2.4.5.	Observing carbon availability .....	86
2.5.	Discussion .....	87
2.5.1.	Growth .....	88
2.5.2.	Net photosynthesis .....	90
2.6.	Conclusion .....	91
2.7.	References .....	92
2.8.	Supplementary Materials .....	106

Chapter 3 Investigating the Effect of Light Quality on Primary Metabolite Production by <i>Chaetoceros muelleri</i> .....	109
3.1. Introduction .....	109
3.1.1. Diatoms .....	109
3.1.2. Importance of diatoms in aquaculture.....	110
3.1.3. Importance of <i>Chaetoceros muelleri</i> in aquaculture .....	112
3.1.4. Light emitting diodes and their potential role in aquaculture .....	113
3.1.5. Selecting light quality to grow microalgae .....	114
3.1.6. Defining cost efficiencies in using LEDs for microalgae culturing.....	117
3.1.7. Balancing light quality .....	119
3.1.8. Measuring photosynthetic performance from cultures grown using different light qualities .....	121
3.1.9. Light quality research in diatoms.....	122
3.2. Aims and Objectives .....	124
3.3. Material and Methods .....	125
3.3.1. Culturing <i>Chaetoceros muelleri</i> .....	125
3.3.2. Photobioreactor system .....	125
3.3.3. Growth light .....	126
3.3.4. Calculating growth rate .....	128
3.3.5. Light measurements and calibration .....	130
3.3.6. Dissolved oxygen measurements and measuring net photosynthesis using optical sensors .....	131
3.3.7. Rapid light curve measurement.....	132
3.3.8. Pigment analysis with high performance liquid chromatography.....	134
3.3.9. Sample preparation for protein, lipid and carbohydrate analysis.....	135
3.3.10. Total protein analysis from total nitrogen measurements.....	136
3.3.11. Total lipid and fatty acid methyl ester extraction and analysis .....	136
3.3.12. Total carbohydrate analysis .....	137
3.3.13. Cost efficiency of different light qualities.....	138
3.4. Results.....	139
3.4.1. Effects of light quality on <i>Chaetoceros muelleri</i> growth.....	139
3.4.2. Light attenuation in <i>Chaetoceros muelleri</i> cultures .....	141

3.4.3.	Primary metabolic composition of <i>Chaetoceros muelleri</i> grown with different light qualities .....	143
3.4.4.	Effects of light quality on the FAME composition of <i>Chaetoceros muelleri</i> .....	145
3.4.5.	Effects of different light quality on the pigment composition of <i>C. muelleri</i> .....	146
3.4.6.	Light quality and production efficiency .....	147
3.4.7.	Effects of different light quality on net photosynthesis rates of <i>Chaetoceros muelleri</i> .....	151
3.4.8.	Effects of light quality on rapid light curve .....	153
3.5.	Discussion .....	157
3.5.1.	Growth .....	157
3.5.2.	Metabolite production .....	159
3.5.3.	Pigments.....	159
3.5.4.	Photosynthesis.....	162
3.5.5.	Cost efficiency .....	164
3.6.	Conclusions .....	165
3.7.	References .....	166
3.8.	Supplementary Materials .....	186
Chapter 4 Change in photon diet – Light quality shifting to tailor metabolite content and their digestibility in <i>Chaetoceros muelleri</i> .....		187
4.1.	Introduction .....	187
4.1.1.	Diatoms in aquaculture .....	187
4.1.2.	Selecting light quality to grow diatoms in aquaculture.....	188
4.1.3.	Light shifting in microalgae .....	189
4.1.4.	Light shifts in diatoms.....	192
4.1.5.	Digestibility analysis.....	193
4.2.	Aims and Objectives .....	196
4.3.	Material and Methods .....	197
4.3.1.	Culturing <i>Chaetoceros muelleri</i> .....	197
4.3.2.	Photobioreactor system .....	198
4.3.3.	Growth light .....	199
4.3.4.	Growth rate.....	200



4.3.5. Light attenuation measurements .....	202
4.3.6. Rapid light curve measurements .....	202
4.3.7. Pigment analysis with HPLC .....	205
4.3.8. <i>In vitro</i> digestion assay.....	206
4.3.9. Sample preparation for protein and lipid analysis.....	208
4.3.10. Total protein analysis from total nitrogen measurements .....	209
4.3.11. Total lipid and fatty acid methyl ester extraction and analysis .....	209
4.4. Results.....	211
4.4.1. Effects of light shift on <i>Chaetoceros muelleri</i> growth.....	211
4.4.2. Light attenuations of <i>Chaetoceros muelleri</i> culture.....	213
4.4.3. Effects of light shift on rapid light curve parameters of <i>Chaetoceros muelleri</i> .....	214
4.4.4. Effect light shift on the pigment composition of <i>Chaetoceros muelleri</i> .....	216
4.4.5. Primary metabolic composition of <i>Chaetoceros muelleri</i> with light shift ..	217
4.4.6. Digestibility of desired metabolites .....	218
4.4.7. Effects of light shift on the fatty acid methyl ester composition of <i>Chaetoceros muelleri</i> .....	221
4.4.8. Digestibility of fatty acid methyl ester.....	222
4.5. Discussion .....	224
4.5.1. Growth rate.....	225
4.5.2. Metabolite production .....	226
4.5.3. Digestibility.....	228
4.5.4. Pigments.....	229
4.5.5. Photosynthesis.....	230
4.6. Conclusions.....	232
4.7. References .....	233
4.8. Supplementary Materials .....	248
Chapter 5 General Discussion.....	251
5.1. Key Findings .....	252
5.1.1. Chapter 2 .....	252
5.1.2. Chapter 3 .....	253
5.1.3. Chapter 4 .....	254
5.2. Future Research.....	254

5.2.1.	Chapter 2 .....	255
5.2.2.	Chapter 3 .....	255
5.2.3.	Chapter 4 .....	256
5.3.	Conclusion .....	257
5.4.	References .....	258

## List of Figures

Figure 1.1	Scanning electron image of different diatom species. A. <i>Thalassiosira pseudonana</i> , B. <i>Cocconeis</i> sp. C. <i>Lampricus</i> sp. D. <i>Gyosigma balticum</i> , E. <i>Cyclotella cryptica</i> , F. <i>Nitzschia</i> sp. G. <i>Thalassiosira weissflogii</i> , H. <i>Achnanthes</i> sp. Image from Hildebrand <i>et al.</i> (2012).....	2
Figure 1.2	Venn diagram representing shared/unique gene families in <i>Phaeodactylum tricornutum</i> , <i>Thalassiosira pseudonana</i> , <i>Viridiplantae</i> and red algae and other eukaryotes (including chromalveolates and opisthokonta (fungi and metazoan)). Gene families consisting of a single gene is denoted ‘orphans’. Image from Bowler <i>et al.</i> (2008). .....	4
Figure 1.3	Docosahexaenoic acid structure. Image from Ruxton <i>et al.</i> , (2007). .....	7
Figure 1.4	Average percentage of DHA, EPA, arachidonic acid (ARA) in 40 microalgae species held in the Australian National Algae Culture Collection. Image from Blackburn and Volkman, (2012). .....	8
Figure 1.5	Simplified scheme of photosynthesis water is consumed in the light reaction to produce oxygen, NADPH and ATP, which are then consumed alongside CO <sub>2</sub> to produce carbohydrates. Image from Masojídek, Torzillo and Koblížek (2013). .....	13
Figure 1.6	Carbon fixation and photorespiration pathways catalysed by RuBisCO, ribulose-1,5-biphosphate (RuBP) and both CO <sub>2</sub> or O <sub>2</sub> . In carbon fixation, the first stable product is 3-phosphoglycerate (PGA), and in photorespiration, the first stable product is a molecule of PGA and 2-phosphoglycolate (PG). Both reactions are facilitated by NADPH and ATP produced during the light stage of photosynthesis. Image from Bloom (2009).....	14
Figure 1.7	A schematic diagram of the carbon equilibrium in a PBR, where gaseous CO <sub>2</sub> and O <sub>2</sub> are introduced to the cultures and equilibrates with the CO <sub>2</sub> and O <sub>2</sub>	

- produced by the microalgae during photosynthesis (P) and photorespiration (R) at an overall mass transfer rate ( $k_{LA}$ ). Image from Tamburic *et al.* (2015). ..... 17
- Figure 1.8 The electromagnetic spectrum is shown, with the visible spectrum range (380 to 750 nm) enlarged. Within the visible range the photosynthetically active radiation (PAR) exists between 400 to 700 nm. Image from Masojídek, Torzillo and Koblížek (2013). ..... 19
- Figure 1.9 Rate of light transmission is dependent on the depth (metres) and wavelength (nm) of the light. In clear oceans the light becomes increasingly dominated by blue/green wavelengths at depths beyond 45 metres. Image adapted from Levine and MacNichol (1982). ..... 21
- Figure 2.1 Simplified relationship of increasing light intensity and cell growth of microalgae where regions are 1) light limited region where light is too low to grow, 2) region between light limited and light saturated ( $I_s$ ) where growth increases with light intensity 3) light saturated region where no increase in growth is seen with an increase in light intensity 4) photoinhibited ( $I_d$ ) region where a decrease in growth is seen with an increase in light intensity. Image from Carvalho *et al.*, 2011. .... 53
- Figure 2.2 Schematic of ePBR. Light is provided with a white LED array and culture temperature is controlled with a peltier jacket. pH, dissolved oxygen and temperature is measured with sensors. The culture was mixed with a magnetic stirrer. Image from Tamburic *et al.*, 2014. .... 64
- Figure 2.3 Side view schematic of experimental design. A) LL-CO<sub>2</sub>: LED illumination from the top (Top-LED) with no CO<sub>2</sub> addition. B) LL+CO<sub>2</sub>: LED illumination with Top-LED with CO<sub>2</sub> addition. C) HL-CO<sub>2</sub>: LED illumination from both sides (Side-LED) with no CO<sub>2</sub> addition. D) HL+CO<sub>2</sub>: LED illumination with Side-LED with CO<sub>2</sub> addition. All conditions were constantly aerated. .... 66
- Figure 2.4 Steady-state light curve (SSLC) of *C. muelleri* grown under standard growth conditions (section 2.4.1). Black dots indicate mean values of relative electron transfer rates (rETR) at each irradiance level, error bars indicate standard deviation ( $n = 3$ ) and red line indicates the fitted Platt function (Eqn. 2.4). Parameter values:  $\alpha = 0.278 \pm 0.007$ ,  $rETR_{max} = 59.867 \pm 1.877$ ,  $I_k = 215.5 \pm 9.614$ . .... 72

- Figure 2.5 The cell density for each condition as a function of time is shown in paired graphs (above and below), where: the black dots indicate mean cell density, error bars indicate standard deviation ( $n = 3$ ), the red line indicates the logistic function applied (Eqn. 2.5). Panels represent A) LL-CO<sub>2</sub> (low light without CO<sub>2</sub> addition), B) LL+CO<sub>2</sub> (low light with CO<sub>2</sub> addition), C) HL-CO<sub>2</sub> (high light without CO<sub>2</sub> addition) and D) HL+CO<sub>2</sub> (high light with CO<sub>2</sub> addition). ..... 73
- Figure 2.6 Measured photon flux density (PFD) values for each light condition as a function of cell density is shown where: the black circles indicate the measured PFD value (error bars indicate standard deviation ( $n = 3$ )) and the blue line indicates the fitted decay function and the red dotted line indicates 0 irradiance (Eqn. 2.7). LL samples had a path length of 20 cm (left panel) and HL cultures had a path length of 2.5 cm (right panel). ..... 77
- Figure 2.7 Modelled rate of light attenuation of two light conditions across the relevant path lengths: 20 cm for Top-LED (left panel) and 2.5 cm for Side-LED (right panel) with each line (blue, orange, green, red, purple, brown and pink) corresponding to incrementally increasing cell density ( $1 \times 10^6 \text{ mL}^{-1}$ ): 0, 0.5, 1, 2, 4, 8 and 12 respectively. Black dotted line indicates  $I_k$  ( $215.5 \pm 9.614$ ) (Calculated from Figure 2.4). ..... 79
- Figure 2.8 Modelled data of photosynthetic activity shown for each condition: A) Top-LED and B) Side-LED based on model explained in Eqn. 2.8 where black line indicates the rETR as a function of cell density of each culture, the dotted blue line indicates the initial cell density and red dotted line indicates the theoretical cell density limit where nitrogen is depleted. Modelled data assumes CO<sub>2</sub> replete conditions. .... 81
- Figure 2.9 An example dataset showing a typical spike in the dissolved oxygen (DO) in  $\mu\text{mol L}^{-1}$ , which was used to calculate net photosynthesis (photosynthesis – respiration). Dissolved oxygen equilibrium between microalgae photosynthesis during ‘Bubbling On’, aeration stopped during ‘Bubbling Off’ and photosynthetic DO is allowed to accumulate, DO equilibrium is allowed to be re-established once aeration restarts with ‘Bubbling On’. ..... 82
- Figure 2.10 Example dataset of dissolved oxygen (DO) represented with a black line during the light phase in early exponential phase with DO spikes occurring every 2 hr for 10 min (red zones indicate ‘Bubbling Off’ as in Figure 2.9). Small

- decreases in DO are due to CO<sub>2</sub> dosages, as shown by the pH data represented with a blue dashed line where a decrease in pH corresponds to CO<sub>2</sub> dosage. Grey zones indicate the dark phase. .... 84
- Figure 2.11 The calculated net photosynthetic oxygen production rates ..... 85
- Figure 2.12 Representative data of pH (red line) and calculated HCO<sub>3</sub><sup>-</sup> concentrations (blue broken line) of *C. muelleri* grown in conditions A) LL-CO<sub>2</sub>, B) HL-CO<sub>2</sub> and C) LL+CO<sub>2</sub> and HL+CO<sub>2</sub>. Grey areas indicate dark phase while white areas indicates light phase. .... 87
- Figure 2.13 The relative absorption spectra of *C. muelleri* represented with brown line and the spectra of the two LEDs used in this study: Top-LED represented as a broken black line and Side-LED represented as a black dotted line. .... 106
- Figure 2.14 View of the LED chips and their arrangements in the custom LED panel used in the study. The larger chips are the CREE® XLamp® XM-L Color and the smaller chips are the Cree® XLamp® XP-E photo-red. .... 107
- Figure 2.15 Comparison of conventional light sources with white LEDs of varying spectra. Power consumption (W), maximum intensity in lumens (lm), light output (lm/W), energy conversion efficiency (%) and theoretical maximum output (lm/W) are shown. Sourced from article published on DIAL website (<https://www.dial.de/en/blog/article/efficiency-of-ledsthe-highest-luminous-efficacy-of-a-white-led/>). .... 108
- Figure 3.1 Wavelength spectra of LEDs used in experiment and the relative absorption spectra of *C. muelleri*. Brown line represents the absorption spectra of *C. muelleri*, blue dotted line represents blue LED spectra, green ‘line & dot’ style line represents green LED spectra, red broken line represents red LED spectra, and black ‘long line & short line’ style line represents white LED spectra. .... 127
- Figure 3.2 Schematic of ePBR geometry (inverted conical frustum) and light measurement. A quantum 4π sensor were used to measure PFD *in situ*. There are three LED chips in each LED panel mounted at the front and back of ePBR vessel. LED illumination is showed for demonstrative purposes and are not illustrative of the actual LED emission angles. .... 130
- Figure 3.3 Cell density are shown as a function of time for four light qualities of equal photosynthetically utilized radiation (500 μmol photons m<sup>-2</sup> s<sup>-1</sup>). Blue circles indicate cultures grown using blue light (BL), green inverted triangles indicate

cultures grown using green light (GL), red squares indicate cultures grown using red light (RL) and black triangles indicate cultures grown using white light (WL). The data points prior to day zero indicate the cell density of the starting inoculum of cultures before the first experimental cell count (day one). The black dotted line indicates the target cell density of  $> 6 \times 10^6$  cells mL<sup>-1</sup> for metabolite analysis. Values represent the mean and standard deviation (n = 5).

..... 140

Figure 3.4 Irradiance measured *in situ* from cultures grown using different light qualities as a function of time. Blue circles represent BL, green inverted triangles represent GL, red squares represent RL and black triangles represent WL. Note that RL cultures were grown for five days and BL, GL and WL cultures were grown for three days, as growth rates were significantly lower and was hence grown for longer to harvest enough biomass for analysis. Irradiance at  $t_0$  represents the irradiance levels in media with no cells as detailed in section 3.3.5. Values represent the mean and standard deviation (n = 5)..... 142

Figure 3.5 Cellular content of total dry biomass (mg mL<sup>-1</sup>) on the left y-axis, total protein, lipid and carbohydrates (mg mg<sup>-1</sup>) on the right y-axis are shown for each light quality used to grow *C. muelleri*. Red bars with diagonal patterns represent dry weight, blue bars with horizontal patterns represent total protein, orange bars with vertical patterns represent total lipid and green bars with cross patterns represent total carbohydrates. Values represent mean and standard deviation of total metabolite samples (n = 3) and dry biomass samples (n = 9). One-way ANOVA performed with Tukey method at 95% confidence: the same letter indicates no significant difference, or if no letters are present, no significant differences between conditions were detected, and different letters indicate significant difference between light treatments. .... 144

Figure 3.6 Fatty acid methyl ester (FAME) content per mg dry weight ( $\mu\text{g mg}^{-1}$ ) of *C. muelleri* grown using different light qualities. Blue bars: BL cultures, green bars: GL cultures, red bars: RL cultures and black bars: WL cultures. One-way ANOVA performed with Tukey method at 95% confidence: same letter indicate no significant difference, different letters indicate significant difference, and where no letters are present no significant differences were detected between conditions. Values represents mean and standard deviation (n = 3). .... 145

- Figure 3.7 Pigment content per culture volume ( $\mu\text{g L}^{-1}$ ) of *C. muelleri* harvested after grown using different light qualities. Values are mean and error bars indicating standard deviation ( $n = 5$ ). Blue bars: BL grown cultures, green bars: GL grown cultures, red bars: RL grown cultures and black bars: WL grown cultures. One-way ANOVA performed with Tukey method at 95% confidence: the same letter indicates no significant difference and different letters indicate significant difference..... 147
- Figure 3.8 Dry biomass ( $\text{mg mL}^{-1} \text{kWh}^{-1}$ ; left y-axis) and total metabolite ( $\text{mg mg}^{-1} \text{kWh}^{-1}$ ; right y-axis) yield based on power consumption for each light quality is shown. Red bars with diagonal patterns represent dry weight, blue bars with horizontal patterns represent total protein, orange bars with vertical patterns represent total lipid and green bars with cross patterns represent total carbohydrates. One-way ANOVA performed with Tukey method at 95% confidence: the same letter indicates no significant difference and different letters indicate significant difference. Values represent mean and standard deviation of total metabolite samples ( $n = 3$ ) and dry biomass samples ( $n = 9$ ). ..... 148
- Figure 3.9 FAME content based on power consumption ( $\mu\text{g mg}^{-1} \text{kWh}^{-1}$ ) for each light quality is shown. Blue bars: BL grown cultures, green bars: GL grown cultures, red bars: RL grown cultures and black bars: WL grown cultures. One-way ANOVA performed with Tukey method at 95% confidence: same letter indicate no significant difference, different letters indicate significant difference, and where no letters are present no significant differences were detected between conditions. Values represents mean and standard deviation ( $n = 3$ ). ..... 149
- Figure 3.10 Pigment content as a function of power consumption ( $\mu\text{g L}^{-1} \text{kWh}^{-1}$ ) for each light quality is shown. Blue bars: BL grown cultures, green bars: GL grown cultures, red bars: RL grown cultures and black bars: WL grown cultures. One-way ANOVA performed with Tukey method at 95% confidence: same letter indicate no significant difference, different letters indicate significant difference, and where no letters are present no significant differences were detected between conditions. Values are mean and error bars indicating standard deviation ( $n = 5$ ). ..... 150

- Figure 3.11 Net photosynthesis of cultures grown using different light qualities as a function of time. Blue circle: BL grown cultures, green inverted triangle: GL grown cultures, red squares: RL grown cultures and black triangles: WL grown cultures. Dotted line indicates zero net photosynthesis. Values represent mean and standard deviation ( $n = 5$ )..... 152
- Figure 3.12 Rapid light curve plot parameters where  $\Phi_{PSII}$  (maximum quantum yield of photosystem II) are shown in boxes a, b, c and d,  $rETR_{max}$  (relative maximum electron transfer rate) in boxes e, f, g and h and NPQ (non-photochemical quenching) in boxes i, j, k and l. Condition blue light are shown in boxes a, e, and i, green light in boxes b, f and j, red light in boxes c, g, and k, and white light in boxes d, h and l. Measurements were taken at day one ( $t_0$ ) represented as blue circles and at day three ( $t_f$ ) represented as red squares. All samples at  $t_f$  were diluted with F/2 media to achieve similar  $F_0$  values prior to the measurement. Values represent mean and standard deviation ( $n = 5$ )..... 154
- Figure 3.13 View of the LED chips and their arrangements in the custom LED panel used in the study. The larger chips are the CREE® XLamp® XM-L Color and the smaller chips are the Cree® XLamp® XP-E photo-red. .... 186
- Figure 4.1 Conceptual diagram of a) traditional illumination of microalgae with white light b) illumination with constant red light c) a light shift from blue light to red light which induces an increase in division in *Chlamydomonas vulgaris* by increasing cell volume in blue light and subsequently shifting to red light to induce division (image adapted by Ooms *et al.* 2016; original image from Kim *et al.* 2014). .... 190
- Figure 4.2 Wavelength spectra of LEDs used in experiment and the relative absorption spectra of *C. muelleri*. Brown line represents the absorption spectra of *C. muelleri*, blue dotted line represents blue LED spectra, red broken line represents red LED spectra, and black ‘long line & short line’ style line represents white LED spectra.....200
- Figure 4.3 Cell concentration as a function of time and treatment. Black dots: cell count data, coloured shades indicating the light quality of growth light: blue for blue light, red for red light, white for white light and grey for dark phase. A) Constant blue light (BLctrl), B) BL shifted to red light for 10 h during day three (BLRL), C) constant white light (WLctrl) and D) WL shifted to red light for 10 h during



day three (WLRL). Values represents the mean and standard deviation (n = 7).

..... 211

Figure 4.4 Rate of light attenuation of different light qualities as a function of time. Blue circles: blue light grown (BL), blue squares: blue light grown subsequently red shifted on day three shown as blue/red square (BLRL), black circles: white light grown (WL) and black squares: white light grown subsequently red shifted on day three shown as black/red square (WLRL). Irradiance at  $t_0$  represents the initial irradiances as detailed in section 4.3.3. Grey area indicates dark phase and white area indicates light phase. Values represents the mean and standard deviation (n = 7). ..... 213

Figure 4.5 Rapid light curve plots where  $\Phi_{PSII}$  (a, b, c, d) is maximum electron transfer rate,  $rETR_{max}$  (e, f, g, h) is maximum quantum yield of photosystem II and NPQ (i, j, k, l) is non-photochemical quenching. Condition are grouped as: BLctrl (a, e, i), BLRL (b, f, j), WLctrl (c, g, k) and WLRL (d, h, l). Rapid light curve measurements were taken at day one ( $t_0$ ) represented as blue circle and at 3 time points at day three ( $t_f$ ): 0 h ( $t_{f0}$ ), 5 h ( $t_{f5}$ ) and 8 h after light shift ( $t_{f8}$ ); represented as red square, black inverted triangle and orange triangle respectively. All samples at  $T_f$  were diluted with F/2 media by  $\frac{1}{4}$  as to not oversaturate the measurement. Values represents the mean and standard deviation (n = 7). ..... 215

Figure 4.6 Pigment content of *C. muelleri* harvested after grown in different light qualities in  $\mu\text{g L}^{-1}$ . Blue bars: BLctrl, green bars: BLRL, black bars: WLctrl and orange: WLRL. One-way ANOVA performed with Tukey method at 95% confidence: same letter indicate no significant difference, different letters indicate significant difference, and where no letters are present no significant differences were detected between conditions. Values represents the mean and standard deviation (n = 7). ..... 217

Figure 4.7 Total and released protein and FAME from undigested and digested *C. muelleri* cultures grown under different light qualities. Blue bars with horizontal line pattern represent total protein in  $\text{mg mg}^{-1}$  dry weight (left y-axis), red bars with cross line pattern represent total FAME in  $\mu\text{g mg}^{-1}$  dry weight (right y-axis), green bars with diagonal line pattern represent released protein in  $\text{mg mg}^{-1}$  dry weight, and yellow bars with diagonal crossing line pattern represent

released FAME in  $\mu\text{g mg}^{-1}$  dry weight. One-way ANOVA performed with Tukey method at 95% confidence: same letter indicate no significant difference, different letters indicate significant difference, and where no letters are present no significant differences were detected between conditions. Values represents the mean and standard deviation ( $n = 3$ ). ..... 219

Figure 4.8 Percentage digested protein and total FAME shown where blue bars with horizontal line pattern represent total protein and red bars with crossing line pattern represent total FAME. One-way ANOVA performed with Tukey method at 95% confidence: same letter indicate no significant difference, different letters indicate significant difference, and where no letters are present no significant differences were detected between conditions. Values represents the mean and standard deviation ( $n = 3$ ). ..... 220

Figure 4.9 Total and released individual fatty acid species from undigested and digested *C. muelleri* cultures grown under different light qualities in  $\mu\text{g mg}^{-1}$  dry weight. Total FAME is represented by coloured bars with no line pattern, and released FAME is shown with diagonal line pattern. One-way ANOVA performed with Tukey method at 95% confidence: same letter indicate no significant difference, different letters indicate significant difference, and where no letters are present no significant differences were detected between conditions. Data represents the mean  $\pm$  standard deviation ( $n = 3$ ). ..... 222

Figure 4.10 Percentage FAME digestibility of *C. muelleri* grown under different light qualities are shown. One-way ANOVA performed with Tukey method at 95% confidence: same letter indicate no significant difference, different letters indicate significant difference, and where no letters are present no significant differences were detected between conditions. Data represents the mean  $\pm$  standard deviation ( $n = 3$ ). ..... 224

Figure 4.11 Total lipids from undigested and digested *C. muelleri* cultures grown under different light qualities. Purple bars with horizontal patterns represent total lipids in  $\mu\text{g mg}^{-1}$  dry weight from undigested samples and green bars with crossing patterns represent total lipids in  $\mu\text{g mg}^{-1}$  dry weight from digested samples. One-way ANOVA performed with Tukey method at 95% confidence: no letters indicate no significant difference and different letters indicate significant difference. Data represents the mean  $\pm$  standard deviation ( $n = 3$ ). ..... 250

## List of Tables

Table 1.1 Main chlorophyll, carotenoid and phycobilin of phototrophs. Image from Yen <i>et al.</i> (2013). .....	10
Table 2.1 Specific growth rate ( $\mu$ ), division rate ( $t_d$ ) and final cell density ( $t_f$ density) of <i>C. muelleri</i> in four different conditions LL-CO <sub>2</sub> , LL+CO <sub>2</sub> , HL-CO <sub>2</sub> and HL+CO <sub>2</sub> (mean $\pm$ stdev). One-way ANOVA performed with Tukey method at 95% confidence: same letter indicate no significant difference and different letters indicate significant difference. Values shown are the mean and standard deviation (n = 3). .....	75
Table 2.2 Comparison of growth rate of <i>C. muelleri</i> grown indoors in different light and carbon availabilities. Light intensity ( $\mu\text{mol photons m}^{-2} \text{s}^{-1}$ ), method of CO <sub>2</sub> addition and/or pH (representing carbon availability) control and specific growth rate ( $\mu$ ) are shown. p-test results (if available) are shown where same letters indicate no significant difference. ....	76
Table 3.1 Specific growth rates ( $\mu$ ), approximate doubling time ( $t_d$ ), mean final dry weight (mean dw) in $\text{mg mL}^{-1}$ and mean final cell density (mean $t_f$ cells) in $\text{cells mL}^{-1}$ . Treatments were BL for blue light grown cultures, GL for green light grown cultures, RL for red light grown cultures and WL for white light grown cultures. One-way ANOVA performed with Tukey method at 95% confidence: same or no letters indicate no significant difference and different letters indicate significant difference. Values represent mean and standard deviation (SD) (n = 5). ....	141
Table 3.2 Rapid light curve parameters are shown for cultures grown under blue (BL), green (GL), red (RL) and white (WL) light where $F_0$ and $F_m$ is minimum and maximum fluorescence yield of PSII in dark-adapted $a$ is slope of light-limited region, $rETR_{\text{max}}$ is maximum electron transfer rate, $I_k$ is minimum saturating irradiance and $\Phi_{\text{PSII}}$ is maximum quantum yield of photosystem II. Two RLC measurements were taken during each growth cycle at $t_0$ and $t_f$ . One-way ANOVA performed with Tukey method at 95% confidence: same or no letters indicates no significant difference and different letters indicate significant difference. Values indicate mean and standard deviation (n = 5). ....	156

Table 4.1 Conditions for the <i>in vitro</i> static digestion model using typical monogastric proteolytic enzymes pepsin and pancreatin. Based on modifications of Moyano & Savoie (2001). .....	208
Table 4.2 Specific growth rates ( $\mu$ ), division rate (td), average dry weight (mean dw) in $\text{mg mL}^{-1}$ , average final cell density (mean $t_f$ cells) in $\text{cells mL}^{-1}$ . One-way ANOVA performed with Tukey method at 95% confidence: same or no letters indicate no significant difference and different letters indicate significant difference. Data represents the mean and standard deviation ( $n = 7$ ). .....	212
Table 4.3 Rapid light curve data at $t_0$ where, $a$ is photosynthetic rate in light-limited region of RLC, $rETR_{\text{max}}$ is maximum electron transfer rate, $I_k$ is minimum saturating irradiance, $F_0$ is minimum fluorescence of dark-adapted microalgal culture, $F_m$ is maximum fluorescence yield of dark-adapted microalgal culture and $\Phi_{\text{PSII}}$ is maximum quantum yield of photosystem II. One-way ANOVA performed with Tukey method at 95% confidence: same letter indicate no significant difference and different letters indicate significant difference. Values shown are mean $\pm$ standard deviation ( $n = 7$ ). .....	248
Table 4.4 Rapid light curve data at $t_f$ where, $a$ is photosynthetic rate in light-limited region of RLC, $rETR_{\text{max}}$ is maximum electron transfer rate, $I_k$ is minimum saturating irradiance, $F_0$ is minimum fluorescence of dark-adapted microalgal culture, $F_m$ is maximum fluorescence yield of dark-adapted microalgal culture and $\Phi_{\text{PSII}}$ is maximum quantum yield of photosystem II. Measurements were taken at 3 time points during day three ( $T_f$ ): 0 h ( $T_f 0$ ), 5 h ( $T_f 5$ ) and 8 h after light shift ( $T_f 8$ ). One-way ANOVA performed with Tukey method at 95% confidence: same letter indicate no significant difference and different letters indicate significant difference. One-way ANOVA was used to analyse the same cultures at different time points. Values shown are mean $\pm$ standard deviation ( $n = 7$ ). .....	249

## Abstract of Thesis

In Australia, between 2016 and 2017, aquaculture products made up 44% of Australian seafood product in value, reaching over \$1.35 billion in production value. One of the top five profitable Australian aquaculture products during this period were edible oysters which is worth more than \$112 million in production value.

Oysters are fed with live microalgae (including diatoms) during the larval, juvenile and adult stages of growth, as are other shellfish, some crustaceans, shrimps/prawns and fish. The rearing of oysters and other aquaculture products rely on the constant production of live diatoms as feed. Diatom production in Australian hatcheries are commonly recognised as the major bottleneck in oyster production, estimated to be on average, 30-40% of hatchery operational cost. In order to meet the increasing production demand diatom production must be improved, while making it economically feasible and environmentally sustainable.

In this thesis, *Chaetoceros muelleri*, a common feed for oysters, was studied for their responses to a variety of environmental growth conditions including light. To achieve this, laboratory scale photobioreactors were used to continuously monitor environmental factors to record biological responses of *C. muelleri* to different environmental conditions including light wavelengths. A brief introduction to diatom physiology and its application to aquaculture will be provided in Chapter one. The

second chapter assessed the two key environmental limitations in diatom cultivation in aquaculture facilities, light and CO<sub>2</sub>. An empirical process model was developed to analyse the importance of light configuration to maximise light availability. High CO<sub>2</sub> availability coupled with high light availability significantly increased growth rates and maximum cell density. The third chapter then assessed the growth, metabolic content and cost efficiency of different colour LEDs (blue, green, red and white) based on the findings in Chapter 2. Blue light was found to be the most cost efficient in biomass and metabolite production, requiring less than half the Watt hours of other LEDs. In the fourth chapter, the wavelength of the growth light was shifted to assess its feasibility to modify metabolic content, as well as its effects on growth, photosynthesis and digestibility. The final chapter discussed the key findings of the thesis and the future research prospects. Several important avenues were identified to improve diatom production in aquaculture, such as improving light availability to increase the efficiency of CO<sub>2</sub> usage, blue LEDs to improve cost efficiency of biomass production and the utilization of wavelength shifting to manipulate diatom metabolite content.

## Chapter 1 General Introduction

### 1.1. Introduction to Microalgae

Microalgae are a diverse group of photosynthetic microorganisms that are able to grow rapidly and are present in virtually every habitat on Earth (Mata, Martins and Caetano, 2010). They are found in all aquatic environments, from the ocean to small freshwater ponds, as well as in some extreme environments, such as deserts and arctic waters (Aletsee and Jahnke, 1992; Blackburn and Volkman, 2012). They play a determinant role in the biogeochemical cycles of macroelements and CO<sub>2</sub> sequestration in aquatic ecosystems (Williams and Laurens, 2010; Farrelly *et al.*, 2013). It is estimated that microalgae can convert solar energy in to chemical energy 10-50 times more efficiently than terrestrial plants using CO<sub>2</sub> and/or bicarbonate as their primary source of carbon (Li, Du and Liu, 2008). Microalgae can also be cultivated without competing for agricultural resources such as water and land, as microalgae can be grown from water unsuitable for irrigation (e.g. salt water) and grown on non-arable land (Leu and Boussiba, 2014). This makes microalgae an attractive alternate source of fuel, nutraceuticals and pharmaceuticals (Chisti, 2008; Mimouni *et al.*, 2012; Guarnieri and Pienkos, 2015). Diatoms (Bacillariophyceae) are a group of microalgae, which have been a staple species for traditional applications such as aquaculture feed for decades, but are also becoming a candidate for other new industrial applications such as high

value products (Brown *et al.*, 1997, 1999; Lebeau and Robert, 2003b; Bozarth, Maier and Zauner, 2009; Peng *et al.*, 2011; Hildebrand *et al.*, 2012; Stonik and Stonik, 2015; Vinayak *et al.*, 2015).

## 1.2. Physiology and Importance of Diatoms

Diatoms are a group of microalgae with a distinctive siliceous cell wall known as frustules (Lebeau and Robert, 2003; Hildebrand *et al.*, 2012; Figure 1.1).

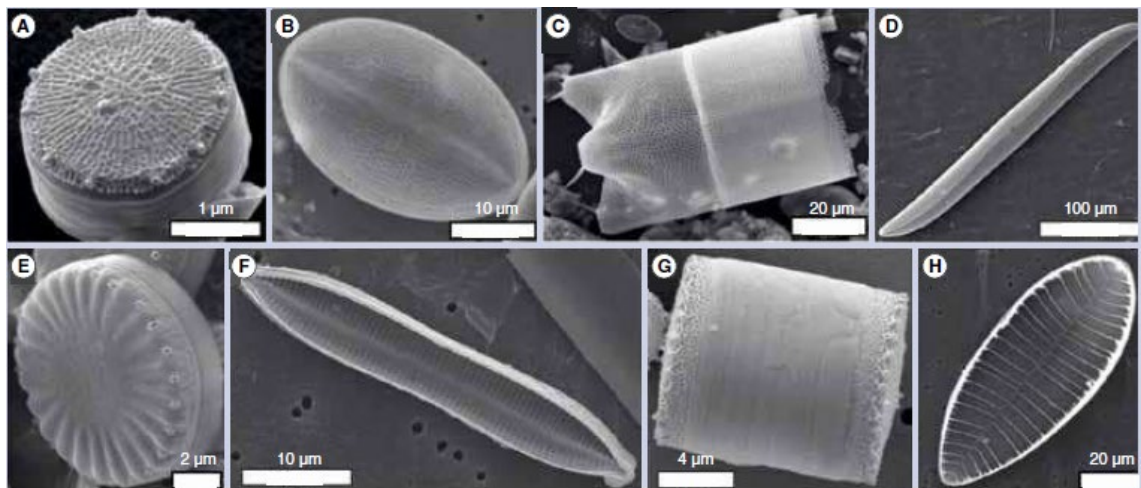


**Figure 1.1** Scanning electron image of different diatom species. A. *Thalassiosira pseudonana*, B. *Cocconeis* sp. C. *Lampricus* sp. D. *Gyosigma balticum*, E. *Cyclotella cryptica*, F. *Nitzschia* sp. G. *Thalassiosira weissflogii*, H. *Achnanthes* sp. Image from Hildebrand *et al.* (2012).



Diatoms are said to be one of the most species-rich groups of microalgae, recent estimates vary from 20,000 to up to 200,000 species (Guiry, 2012; Mann and Vanormelingen, 2013). They are also responsible for a significant portion (20-35%) of the marine primary productivity, up to 20% of the global carbon fixation and dominate the biogeochemical cycling of marine silicon (Nelson *et al.*, 1995; Tréguer, Nelson and Bennekom, 1995; Falkowski, Barber and Smetacek, 1998; Field *et al.*, 1998; Martin-Jezequel, Hildebrand and Brzezinski, 2000; Scala and Bowler, 2001).

Diatoms are thought to have evolved from a secondary endosymbiotic event between a red eukaryotic alga and a heterotrophic flagellate approximately 200 million years ago (Medlin, Kooistra & Schmid 2000). The recent full genome sequencing of two diatoms: the centric diatom *Thalassiosira pseudonana* and a pennate diatom *Phaeodactylum tricornutum* provided evidence of the complex genome of diatoms (Armbrust *et al.*, 2004; Bowler *et al.*, 2008). As seen in Figure 1.2, the genome of the two diatoms *P. tricornutum* and *T. pseudonana* has been shown to contain genes of red alga and other eukaryotes with a large portion of their genome being unique (not shared between the two species).

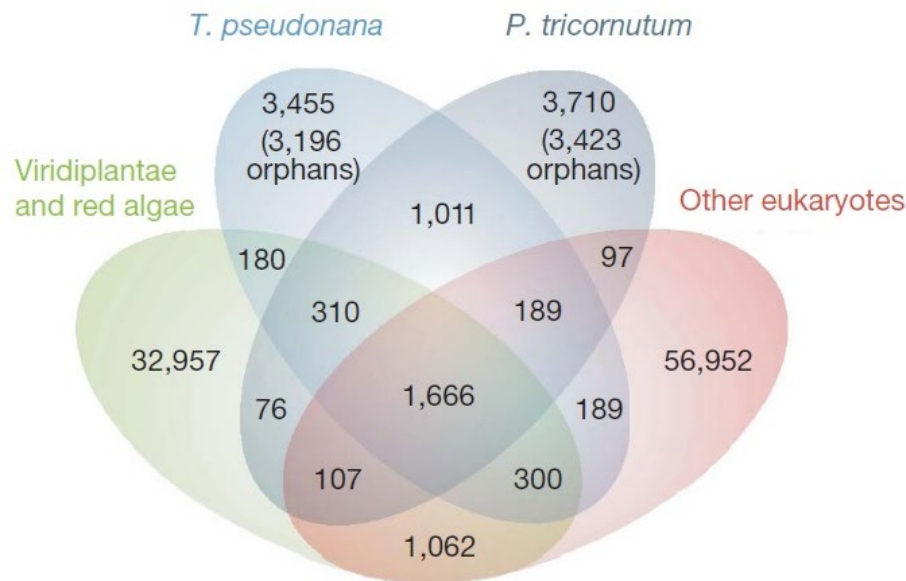


**Figure 1.2** Venn diagram representing shared/unique gene families in *Phaeodactylum tricornutum*, *Thalassiosira pseudonana*, *Viridiplantae* and red algae and other eukaryotes (including chromalveolates and opisthokonta (fungi and metazoan)). Gene families consisting of a single gene is denoted ‘orphans’. Image from Bowler *et al.* (2008).

Bowler *et al* (2008) concludes that at least 5% of diatom genes are of bacterial origin with only half of their genes shared between two diatom species. Thus the metabolism of diatoms is thought to be a complex mix of genes derived from highly divergent origins (Bowler *et al.*, 2008; Finazzi, Moreau and Bowler, 2010). Their ecological success and abundance has been attributed to their flexible metabolism which differs fundamentally from other algal classes (Wilhelm *et al.*, 2006). This abundance has resulted in diatoms being a major primary producer in many aquatic biospheres, making diatoms a natural choice for rearing several aquaculture species.

### 1.2.1. Importance of Diatoms in Aquaculture

With the world population predicted to surpass 9.5 billion people by the year 2050 (United Nation, 2015), food security and climate change will unquestionably be the major challenges facing humanity in the immediate future (Godfray *et al.*, 2010). Food sourced from aquatic environments such as fish, molluscs and crustaceans make an important contribution to the human diet. However, global wild fishery production has become stagnated since the 1990's at an estimate 90 million tonnes per annum (*The state of world fisheries and aquaculture 2018: Meeting the sustainable development goals*, 2018). Coupled with the increase in overfishing of the world's marine fish stocks, a steady increase in aquaculture production has been observed in recent decades with an estimate 80 million tonnes produced in 2016 (*The state of world fisheries and aquaculture 2018: Meeting the sustainable development goals*, 2018). In order to meet the increasing production demand, the efficiency of microalgal production must be improved; however, major challenges must be addressed to make production economically feasible and environmentally sustainable whilst still maintaining high feed quality.

Diatoms have been cultured in large-scale production systems for aquaculture feed for decades (Lebeau and Robert, 2003a). Diatoms are particularly important in feeding bivalves and shrimp larvae (Brown *et al.*, 1997; Lebeau and Robert, 2003b). Of the

hundreds of microalgal species tested as feed for aquaculture species in the past forty years, fewer than twenty species are used in commercial hatcheries today, of which notable diatom species include: *Chaetoceros* sp., *Thalassiosira* sp., *Skeletonema* sp. and *Nitzschia* sp. (Brown 2002). The reason for their small number is because microalgal species require particular cellular characteristics to be considered suitable as aquaculture feeds. Firstly, they must be of a suitable size for ingestion (e.g. 1-15  $\mu\text{m}$  for filter feeders and 10-100  $\mu\text{m}$  for grazers) and readily digestible (Webb and Chu, 1983; Jeffrey, Leroi and Brown, 1992; Kawamura, Roberts and Nicholson, 1998). Secondly, they must have a fast growth rate, must be amenable to mass culture, and tolerate fluctuations in temperature, light and nutrients which may occur in outdoor production sites (Brown, 2002). Lastly, they must not contain any toxins which will accumulate up the food chain and should have optimal nutritional content for the larvae (Brown, 2002; Spolaore *et al.*, 2006). Nutritional value of microalgae feeds have been a particular focus of research in aquaculture (Brown, 2002; Blackburn and Volkman, 2012; Guedes and Maccata, 2012). Polyunsaturated fatty acids (PUFAs) have been identified as an essential dietary requirement for marine animals (Nichols, 2003), as well as for the growth of many larvae (Becker 2004). The nomenclature of PUFAs are defined by the number of carbon atoms and the position of the C=C double bond (fatty acids with no double bonds are referred as saturated fatty acids) (Ruxton *et al.*, 2007). For example,

DHA (C22:6  $\omega$ -3) is a fatty acid with 22 carbons, 6 C=C double bonds, and the first double bond occurs between the 3<sup>rd</sup> and 4<sup>th</sup> carbon from the methyl group (CH<sub>3</sub>) of the molecule Figure 1.3).

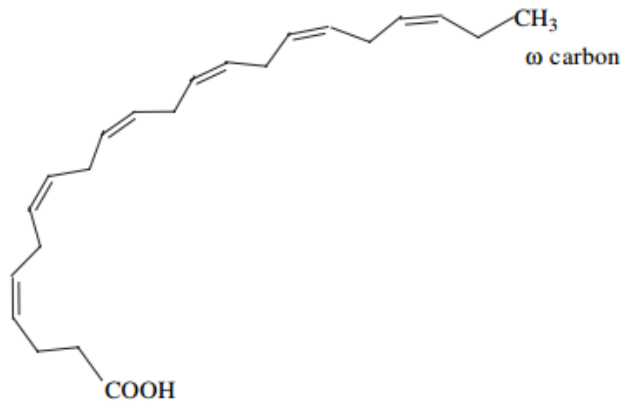


**Figure 1.3** Docosahexaenoic acid structure. Image from Ruxton *et al.*, (2007).

Among the various groups of microalgae, diatoms contain high levels of eicosapentaenoic acid (EPA C20:5  $\omega$ -3) and balanced levels of docosahexaenoic acid (DHA C22:6  $\omega$ -3) and arachidonic acid (ARA C20:5  $\omega$ -6) which have been shown to benefit larval growth (Nichols, 2003; Becker, 2004; Guedes and Malcata, 2012; Figure 1.4).

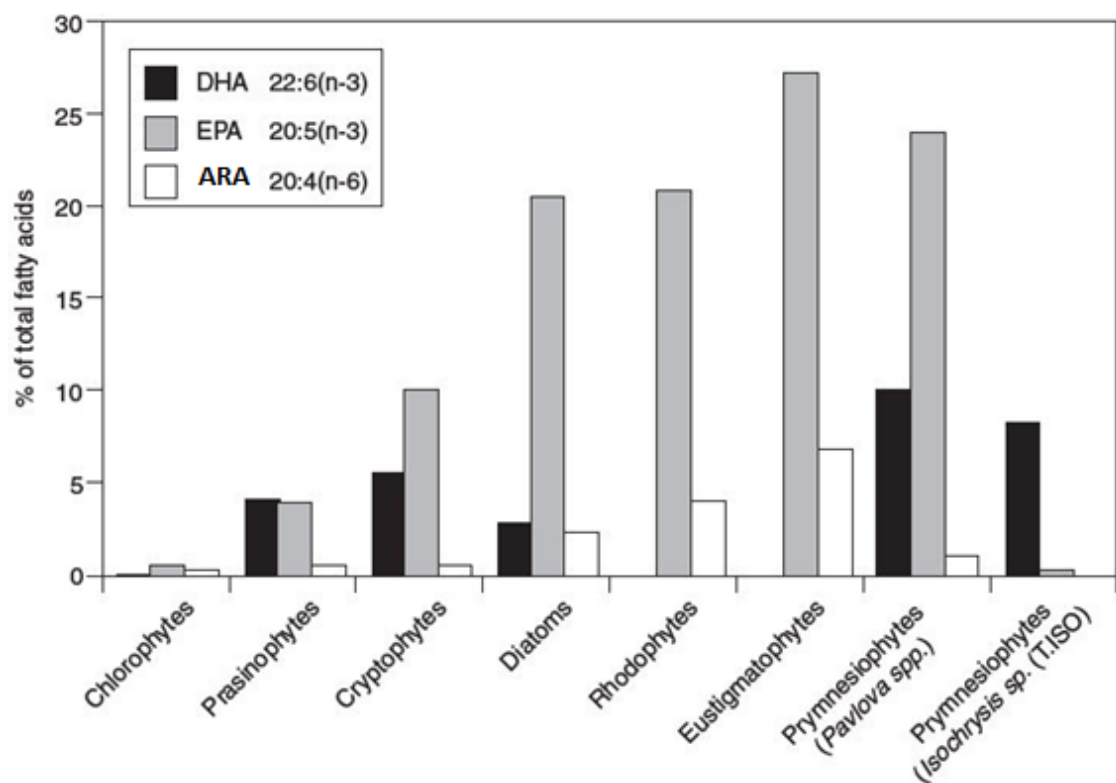


**Figure 1.4** Average percentage of DHA, EPA, arachidonic acid (ARA) in 40 microalgae species held in the Australian National Algae Culture Collection. Image from Blackburn and Volkman, (2012).

### 1.2.2. Importance of *Chaetoceros muelleri* in Australian Aquaculture

*Chaetoceros muelleri* is a marine diatom that is a particularly valuable species in Australian and Mexican hatcheries (Brown *et al.*, 1997; López Elías *et al.*, 2003). It is widely used in feeding, scallops, prawns and oysters at varying stages of growth (Brown *et al.*, 1997). The widespread usage of *C. muelleri* as feed is linked to increases in larval development and survivability which is attributed to a high proportion of unsaturated fatty acids such as: DHA, EPA and ARA (Parrish *et al.*,

1998; D'Souza and Loneragan, 1999). In Australia, *C. muelleri* is produced to feed edible oysters such as the Sydney rock oyster (*Saccostrea glomerata*) and the Pacific oyster (*Crassostrea gigas*) (Brown *et al.*, 1997; O'Connor *et al.*, 2008).

Between 2016 – 2017, edible oysters recorded a production value of approximately \$112 million (Department of Primary Industries, 2016). As these oysters (alongside other aquaculture species) require a constant supply of diatom feed, *C. muelleri* has been widely produced as feedstock in the aquaculture industry in Australia for decades (Brown *et al.*, 1997; Brown, 2002).

However, the productivity and operational costs of live diatom feed has been identified as a major bottleneck to further improve the oyster industry (Borowitzka, 1997; Knauer and Southgate, 1999; Camacho-Rodríguez *et al.*, 2016; Nielsen *et al.*, 2017). In order to improve feed production, one must first be aware of the environmental factors that limit photosynthesis, and hence growth. Environmental factors that limit diatom growth includes: temperature (Berges, Varela and Harrison, 2002), nutrient concentration (Fabregas *et al.*, 1986), salinity (Fabregas *et al.*, 1984; Renaud and Parry, 1994), carbon availability (Wang *et al.*, 2014) and light (Falkowski, Dubinsky and Wyman, 1985). The impact of these abiotic factors on biomass production and metabolite content of *C. muelleri* has been extensively characterized, however, this knowledge has seldom been applied in production

facilities in aquaculture (Harrison, Thompson and Calderwood, 1990; Borowitzka, 1997; Llorente and Luna, 2016). This may be due to a lack of knowledge in the aquaculture industry about the photophysiology of microalgae and diatoms.

### 1.2.3. Photosynthetic Mechanisms in Diatoms

Diatoms have a unique photosynthetic pigment composition of chlorophylls and carotenoids (Table 1.1). They contain chlorophyll *a* and *c*, as well as fucoxanthin as their main accessory pigment. Carotenoids are a structurally diverse class of isoprenoids present in all photosynthetic organisms from microalgae to higher plants (Table 1.1) (Jeffrey & Vesk 1997).

**Table 1.1** Main chlorophyll, carotenoid and phycobilin of phototrophs. Image from Yen *et al.* (2013).

Pigments	Characteristic absorption maxima (nm)	Occurrence
Chlorophylls	(in organic solvents)	
Chlorophyll <i>a</i>	420, 660	All higher plants and algae
Chlorophyll <i>b</i>	435, 643	All higher plants and green algae
Chlorophyll <i>c</i>	445, 625	Diatoms and brown algae
Chlorophyll <i>d</i>	450, 690	Red algae
Carotenoids	(in organic solvents)	
$\alpha$ -Carotene	420, 440, 470	Most plants and some algae
$\beta$ -Carotene	425, 450, 480	Higher plants and most algae
Luteol	425, 445, 475	Green algae, red algae, and higher plants
Fucoxanthol	425, 450, 475	Diatoms and brown algae
Peridinin	375, 495	Dinophytes
Phycobilins	(in water)	
Phycoerythrins	490, 546, 576	Red algae and some cyanobacteria
Phycocyanins	618	Cyanobacteria and some red algae
Allophycocyanins	650	Cyanobacteria and red algae

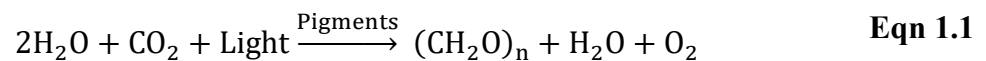
Carotenoids are essential components of the photosystems, where their primary role is to act as structural and functional components of the photosynthetic apparatus (Jin *et al.*, 2003; Cardozo *et al.*, 2007; Blackburn and Volkman, 2012) and have a secondary role as



a reactive oxygen scavenger to prevent photo-damage (photoinhibition) and as an antioxidant under stress conditions (Jin *et al.*, 2003; Cardozo *et al.*, 2007). These pigments are mostly bound to structural proteins and form the photosynthetic pigment-protein complexes, the functional units of photosynthetic reaction center (Falkowski and Raven, 2007).

### 1.3. Photosynthesis in Microalgae

While many factors affect photosynthesis, the most common limitation constraining photosynthesis in commercial-scale microalgae culture facilities is light and carbon availability (Beardall and Raven, 2013). Photosynthesis is the biological conversion of light energy to chemical energy and is one of the most ancient biological processes in nature (Falkowski and Raven, 2007). Oxygenic photosynthesis (Eqn 1.1) in all eukaryotic microalgae can be expressed as:

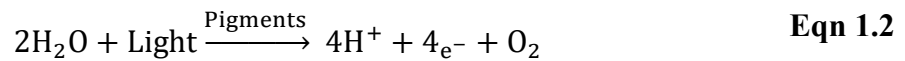


where light is a substrate and its energy is transferred to products and facilitated by photosynthetic pigments (further details in 1.2.4.).

Eqn 1.1 can be divided into two stages, the light-dependent stage (or light reactions) (Eqn 1.2), and the light-independent stage (or dark reactions) (Eqn 1.3; Figure 1.5).

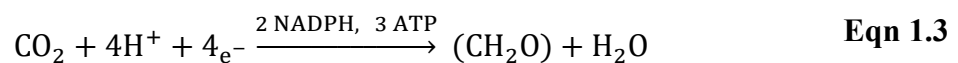
The light-dependent stage is where photosynthetic pigments catalyses a reaction or series of reactions to oxidize water in the presence of light as shown below

(Falkowski and Raven, 2007; Eqn 1.2).



In this reaction, light energy excites electrons into a higher energy state which is then used to produce the high energy product adenosine triphosphate (ATP) and the reductant nicotinamide adenine dinucleotide phosphate (NADPH) as shown below (Falkowski and Raven, 2007; Masojídek, Torzillo and Koblížek, 2013). Naturally, the main limiting factor during the light-dependent stage is light. As low light availability (light limitation) will limit the synthesis of NADPH and ATP which are required for the next stage, the light-independent stage.

During the light-independent stage, NADPH and ATP is used to fix carbon dioxide to carbohydrates as shown below (Falkowski and Raven, 2007; Masojídek, Torzillo and Koblížek, 2013; Eqn 1.3).



This second stage is also known as the Calvin-Benson cycle (alternatively the Calvin-Benson-Bassham cycle) where carbon fixation occurs (Falkowski and Raven, 2007).  $\text{CO}_2$  is fixed during the multi-step pathway of the Calvin-Benson cycle.

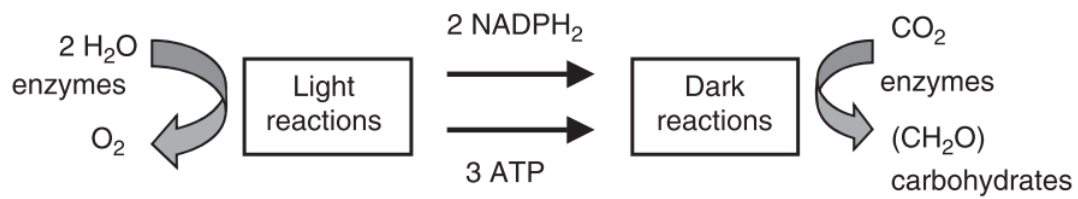


**Figure 1.5** Simplified scheme of photosynthesis water is consumed in the light reaction to produce oxygen, NADPH and ATP, which are then consumed alongside  $\text{CO}_2$  to produce carbohydrates. Image from Masojídek, Torzillo and Koblížek (2013).

In the Calvin-Benson cycle,  $\text{CO}_2$  fixation is catalysed by the carboxylation reaction of the enzyme RuBisCO (Ribulose-1,5-Bisphosphate Carboxylase/Oxygenase).

While the first light-dependent stage is strongly determined by light availability, the carboxylation reaction (or  $\text{C}_3$  carbon fixation reaction) is strongly dependent on the  $\text{O}_2/\text{CO}_2$  ratio. A high  $\text{O}_2/\text{CO}_2$  ratio stimulates the oxygenase reaction of RuBisCO commonly known as photorespiration, an energetically unfavourable reaction which consumes organic carbon to release  $\text{CO}_2$  with no metabolic gain (Masojídek, Torzillo and Koblížek, 2013; Figure 1.6).

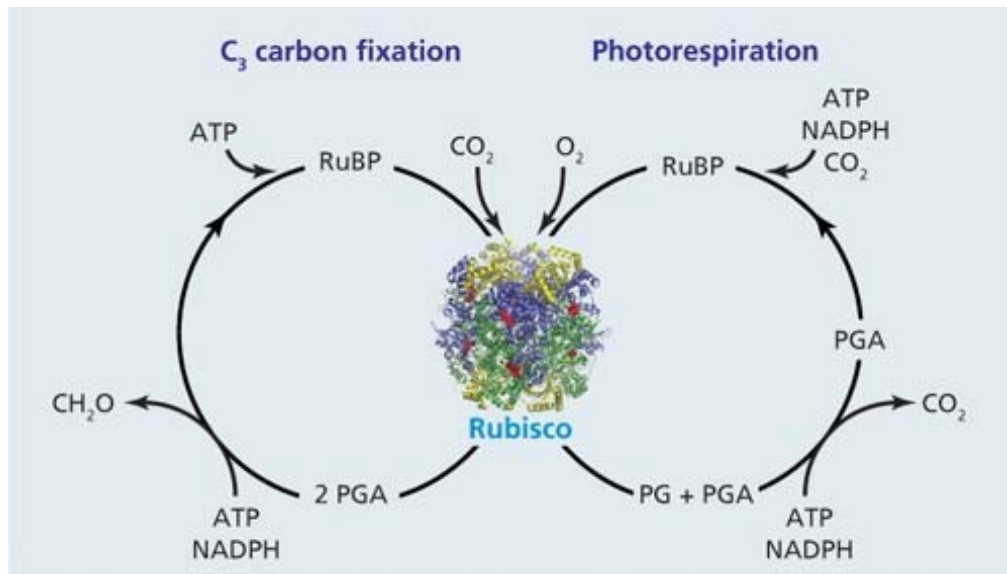


**Figure 1.6** Carbon fixation and photorespiration pathways catalysed by RuBisCO, ribulose-1,5-biphosphate (RuBP) and both CO<sub>2</sub> or O<sub>2</sub>. In carbon fixation, the first stable product is 3-phosphoglycerate (PGA), and in photorespiration, the first stable product is a molecule of PGA and 2-phosphoglycolate (PG). Both reactions are facilitated by NADPH and ATP produced during the light stage of photosynthesis. Image from Bloom (2009).

RuBisCO typically has low affinity to CO<sub>2</sub> and microalgae have developed carbon-concentrating mechanisms (CCMs) that assists in providing RuBisCO with high levels of CO<sub>2</sub> (Masojídek, Torzillo and Koblížek, 2013). Diatoms have been known to have highly efficient CCMs to achieve a high ratio of carboxylation to oxygenation (photorespiration) (Raven *et al.*, 2011; Gao and Campbell, 2014).

While not all microalgae possess CCMs, relying instead on diffusive CO<sub>2</sub> entry, they are advantageous to microalgae found in environments of variable and growth-

limiting low light (Raven, Beardall and Giordano, 2014). Diatoms have been shown to utilize both  $\text{CO}_2$  and  $\text{HCO}_3^-$  and concentrate them within their cells (Rost *et al.*, 2003; Giordano, Beardall and Raven, 2005; Trimborn *et al.*, 2008), while there are no known  $\text{CO}_3^{2-}$  transporters (Milligan, Mioni and Morel, 2009).

While several aspects of the diatom CCM is still unknown, the main steps can be summarised as: DIC taken up from the surrounding environment across the plasma membrane through  $\text{HCO}_3^-$  transporters (and possibly  $\text{CO}_2$  channels), transported across the chloroplast membrane, dehydrated to  $\text{CO}_2$  within the pyrenoid for RuBisCO to fix (Nakajima, Tanaka and Matsuda, 2013; Hopkinson, 2014; Kikutani *et al.*, 2016). It is estimated that the majority of the DIC utilized by diatoms are in the form of  $\text{HCO}_3^-$ , up to 95% in the centric diatom *Thalassiosira weissflogii* (Martin and Tortell, 2008). Therefore, the availability of both light and  $\text{CO}_2$  determines the rate of photosynthesis (Mata, Martins and Caetano, 2010; Masojídek, Torzillo and Koblížek, 2013; Gao and Campbell, 2014).

#### **1.4. Dynamics of $\text{CO}_2$ Availability in Microalgal Culture**

In order to understand the causes of carbon limitation in microalgae cultures, one must understand the equilibrium between the carbon species in aquatic environments. In an aquatic environment there is an equilibrium between the

different forms of dissolved inorganic carbon (DIC): carbon dioxide ( $\text{CO}_2$ ), carbonic acid ( $\text{H}_2\text{CO}_3$ ), bicarbonate ( $\text{HCO}_3^-$ ) and carbonate ( $\text{CO}_3^{2-}$ ), represented below in Eqn 1.4:



In aquaculture production facilities,  $\text{CO}_2$  is typically introduced to microalgal cultures via bubbling carbon-enriched air (Lavens and Sorgeloos, 1996). The introduced  $\text{CO}_2$  and  $\text{O}_2$  establishes an equilibrium within the culture medium. The  $\text{CO}_2$  and  $\text{O}_2$  equilibrium in the culture is expressed as the overall mass transfer rate ( $k_La$ ) which is derived from the introduced  $\text{CO}_2$  and  $\text{O}_2$  and the  $\text{CO}_2$  produced during respiration and  $\text{O}_2$  produced during photosynthesis (Zeebe and Wolf-Gladrow, 2001; Figure 1.7).

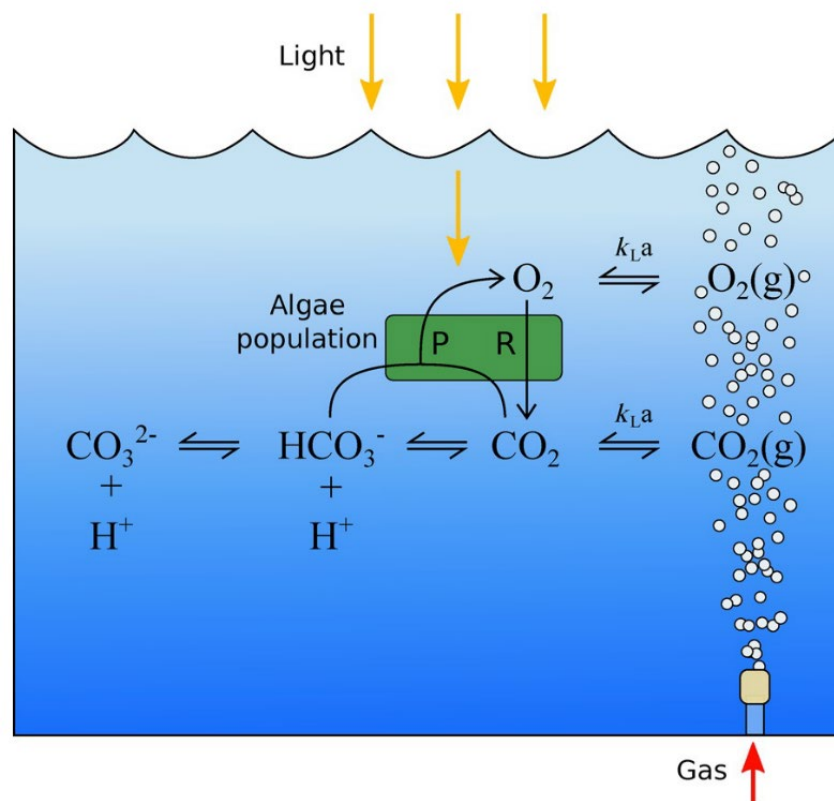


**Figure 1.7** A schematic diagram of the carbon equilibrium in a PBR, where gaseous  $\text{CO}_2$  and  $\text{O}_2$  are introduced to the cultures and equilibrates with the  $\text{CO}_2$  and  $\text{O}_2$  produced by the microalgae during photosynthesis (P) and photorespiration (R) at an overall mass transfer rate ( $k_L a$ ). Image from Tamburic *et al.* (2015).

As shown in Figure 1.7, cultures aerated with  $\text{CO}_2$  enriched air will decrease in pH as  $\text{H}^+$  is produced. This change in pH can be used to infer the dissolved inorganic carbon (DIC) concentration in the culture to estimate carbon availability (Al-Mashhadani, Bandulasena and Zimmerman, 2012; Tamburic *et al.*, 2015). However, if the culture struggles to maintain sufficient  $\text{CO}_2$  levels, due to limitations which

reduces the mass transfer rate of CO<sub>2</sub> (e.g. bubble size to surface ratio, high bubble rise velocity, insufficient bubble residence time, low CO<sub>2</sub> concentration, etc.), the culture will likely experience carbon limitation. While carbon availability is crucial for carbon fixation, light availability is also a major limiting factor of commercial microalgal cultures (Beardall and Raven, 2013).

### **1.5. Dynamics of Light Availability in Microalgal Culture**

The energy which drives photosynthesis is supplied in the form of light (photons). In nature, the sun emits electromagnetic radiation of which a small segment between 400 to 700 nm is usable to drive photosynthesis. This range is commonly referred to as the photosynthetically active radiation (PAR) range (Falkowski and Raven, 2007; Masojídek, Torzillo and Koblížek, 2013; Figure 1.8).



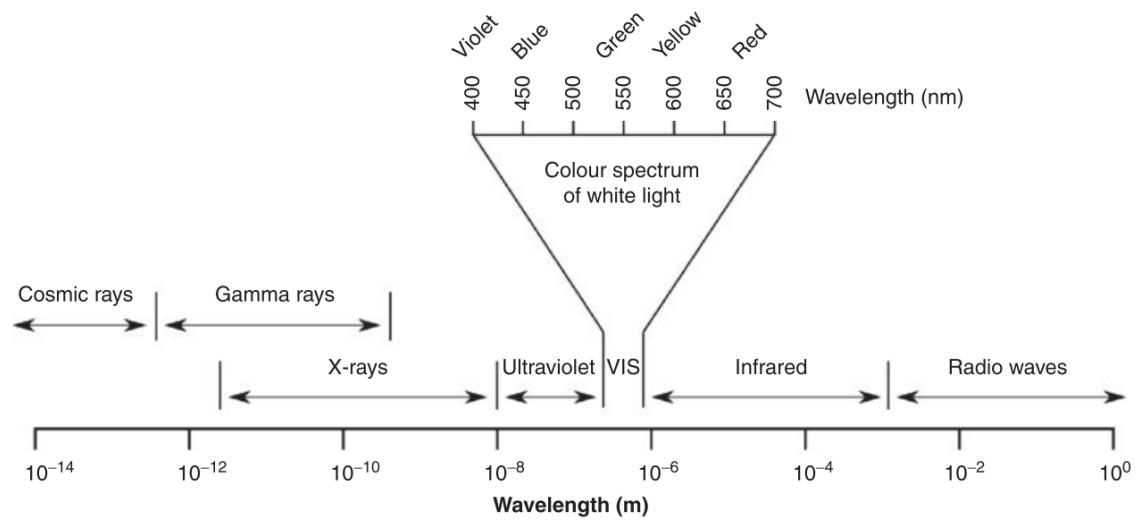


**Figure 1.8** The electromagnetic spectrum is shown, with the visible spectrum range (380 to 750 nm) enlarged. Within the visible range the photosynthetically active radiation (PAR) exists between 400 to 700 nm. Image from Masojídek, Torzillo and Koblížek (2013).

As photosynthesis is dependent on the number of photons reaching a unit of surface area in a unit time, in photobiological studies, it is common to measure light as photon flux density ( $\mu\text{mol quanta m}^{-2} \text{s}^{-1}$ ) (Masojídek, Torzillo and Koblížek, 2013). As light is crucial to drive photosynthesis, its uniform availability throughout a microalgal culture is essential in order to maximise biomass productivity (Salleh *et al.*, 2017). However, light levels in algal cultures exponentially decays as a function of path length and cell density due to a phenomenon known as light attenuation, commonly described by the Beer-Lambert's law (Yun and Park, 2001; Falkowski and Raven, 2007; Eqn 1.5).

$$I = I_0 e^{-\alpha x l} \quad \text{Eqn 1.5}$$

where  $I_0$  is light intensity,  $\alpha$  is the extinction coefficient,  $x$  is cell concentration and  $l$  is path length in cm

Thus, providing homogenous light availability is very difficult in dense cultures. An additional challenge to maintain light availability in microalgal cultures is to understand how dynamic light availability is in nature and how microalgae responds to it.

#### 1.5.1. Light quality in aquatic environments

A condition unique to aquatic phototrophs is that both light intensity and the wavelength composition of light (light quality or spectral quality) depends on the depth of the water column (Depauw *et al.*, 2012). The PAR region of the spectrum encompasses shorter wavelengths of blue/violet radiation to longer wavelengths of red/far red radiation.

Red/far red light are rapidly absorbed by water, which means a cell closer to the surface will experience more red-enriched light than a cell in deeper waters where blue/green wavebands dominate (Levine and MacNichol, 1982; Austin and Petzold, 1986; Kirk, 1994; Figure 1.9).

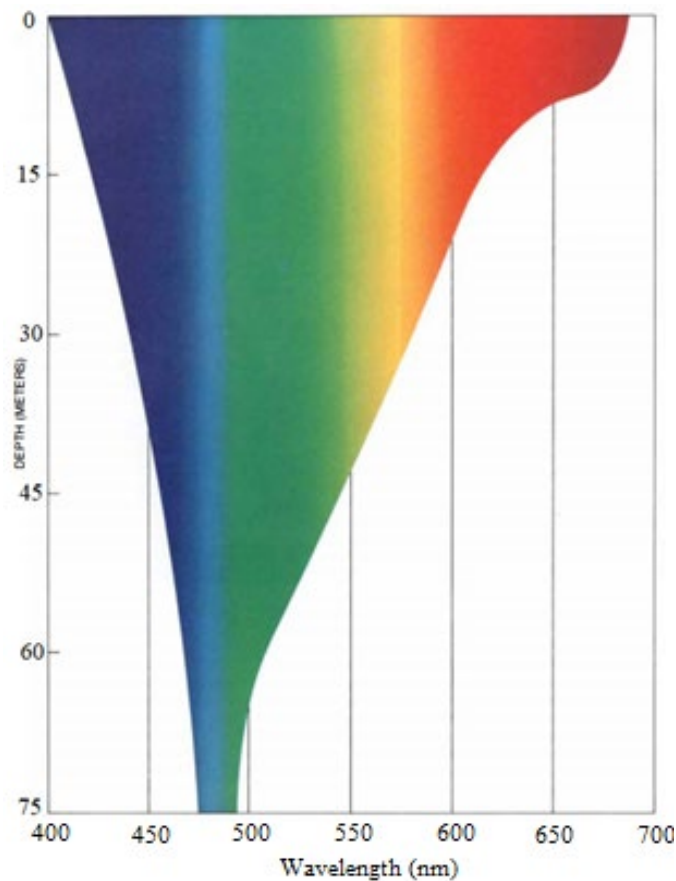


**Figure 1.9** Rate of light transmission is dependent on the depth (metres) and wavelength (nm) of the light. In clear oceans the light becomes increasingly dominated by blue/green wavelengths at depths beyond 45 metres. Image adapted from Levine and MacNichol (1982).

### 1.5.2. How Diatoms Respond to Light Intensity

Light intensity is dynamic in aquatic environments and affects all microalgae. They must adapt to their light condition rapidly in order to capture sufficient photons for photosynthesis (light harvesting), whilst also avoiding the damaging effects of excess energy of photons (photoprotection). Regardless of the light intensity or quality,

microalgae will attempt to acclimate to the available light within the limits of its genetic potential and environmental limits (Falkowski and Raven, 2007). Generally, under low light conditions, the primary response of microalgae is to maximize photon capture, which involves the optimisation of the light-harvesting pigment composition to the spectral distribution of incident light (Eberhard, Finazzi and Wollman, 2008; Depauw *et al.*, 2012). Conversely, under high irradiance, the primary response is protection against the damaging effects of light energy (photoprotection) and not photon capture. The photoprotection response is rapid and occurs at timescales of seconds or less (Eberhard, Finazzi and Wollman, 2008; Depauw *et al.*, 2012). Photoprotection occurs in a process known as non-photochemical quenching (NPQ), which involves dissipation of excess photon as heat, redistribution of energy between photosystems, the activation of photosystem II (PSII) repairing mechanisms and the activation of photoprotective pigments (such as xanthophylls) that quench excited states of chlorophylls and scavenge reactive oxygen species (Lohr and Wilhelm, 2001; Depauw *et al.*, 2012).

### 1.5.3. Mechanisms to sense light quality in diatoms

Diatoms are exposed to dynamic light availabilities and studies suggest their major ecological success is largely due to their capacity to acclimate to dynamic light conditions (Depauw *et al.*, 2012; Wilhelm *et al.*, 2014). They are able to adapt under

these conditions because they are able to sense and evaluate light quality via three main photoreceptors (Depauw *et al.*, 2012; Wilhelm *et al.*, 2014). Photoreceptors were first described in diatoms by Armbrust *et al.*, (2004) in *T. pseudonana* and subsequently by Bowler *et al.*, (2008) in *P. tricornutum*. They were phytochromes which sense red/far-red light (Rockwell and Lagarias, 2010, 2017) and cryptochromes and aureochromes which sense blue light (Takahashi *et al.*, 2007; Chaves *et al.*, 2011). First discovered in plants, phytochromes play a central role in developmental and morphological changes (i.e. photomorphogenesis) such as germination, growth, and flowering (Depauw *et al.*, 2012; Rockwell and Lagarias, 2017). Phytochromes have been identified in most phototrophs, ranging from higher plants, microalgae, even fungi; while it has been lost in some cyanobacteria (e.g. *Synechococcus* strains) (Ikeuchi and Ishizuka, 2008; Rockwell and Lagarias, 2017). In the model diatom *Phaeodactylum tricornutum*, phytochromes were found to regulate gene expression in response to red/far-red light (Fortunato *et al.*, 2016). Cryptochromes are an ancient group of proteins that contain photoreceptors which sense blue light and are present in almost all organisms ranging from archaea to eukaryotes (König, Juhas, *et al.*, 2017). In *Phaeodactylum tricornutum*, cryptochromes have been shown to regulate photosynthesis by regulating light-harvesting protein levels and other photoreceptors in response to blue light and darkness (König, Eisenhut, *et al.*, 2017; König, Juhas, *et al.*, 2017). Aureochromes are unique to

stramenopiles (which include diatoms) and represents a family of blue light photoreceptor (Takahashi *et al.*, 2007; Costa, Sachse, *et al.*, 2013). In *Phaeodactylum tricornutum*, aureochromes have been shown to control the initiation of cell division in response to blue light exposure and play a role in light acclimation (Costa, Sachse, *et al.*, 2013; Huysman *et al.*, 2013).

From the dynamic nature of light as experienced by diatoms in nature and the mechanisms in which these conditions are sensed, diatoms have been documented to respond to varying light conditions (Sánchez-Saavedra and Voltolina, 1996; Costa, Jungandreas, *et al.*, 2013; Jungandreas *et al.*, 2014; Wilhelm *et al.*, 2014; Schulze *et al.*, 2016).

### **1.6. Light Emitting Diodes as Light Source for Culturing Diatoms**

A particularly important question in applied phycology is the impact of light availability and quality on biomass production and metabolite content of diatoms. In commercial microalgal production using indoor aquaculture facilities, light is sourced through conventional light sources such as incandescent lamps, fluorescent tubes and metal halide lamps (Heasman *et al.*, 2001; Lebeau and Robert, 2003a; Blanken *et al.*, 2013; Borowitzka and Moheimani, 2013; Schulze *et al.*, 2016; Ramanna, Rawat and Bux, 2017). Alternatively, light emitting diodes (LEDs) offer several economic advantages

over traditional light sources, primarily, they can achieve higher light intensity while having a longer life-expectancy (up to 50,000 h) (Bourget, 2008; Carvalho *et al.*, 2011). These advantages, alongside the ability to accommodate different light qualities make LEDs an attractive alternate light source to be used in commercial microalgal production in hatcheries.

#### 1.6.1. Using light emitting diodes to manipulate biochemical content in diatoms

A further use of LEDs in aquaculture research is its use as a strategy to manipulating the biochemical content of cells without significantly changing the culture conditions such as pH and nutrient concentrations. Different colour LEDs have shown to have a profound effect on the biomass production and biochemical content of *Nannochloropsis* sp., *Chlamydomonas* sp., *Chlorella* sp., and *Dunaliella* sp. (de Mooij *et al.*, 2016; Glemser *et al.*, 2016; Ra *et al.*, 2016; Schulze *et al.*, 2016). While additional strategy may be light shifting (also known as spectral shift and wavelength shift), which refers to a shift in the spectrum of light during culture growth (e.g. blue light to red light). It has been shown that shifting the wavelength of light can stimulate a growth or metabolic response (Oldenhof, Zachleder and Van Den Ende, 2006; Kim *et al.*, 2014). However, studies investigating diatoms grown using these strategies are currently sparse and presents an attractive avenue of aquaculture research.

## 1.7. Summary

In this thesis, *Chaetoceros muelleri*, was studied for its physiological response to different CO<sub>2</sub> availability scenarios, light availability and light qualities. To achieve this, laboratory-scale photobioreactors were used to continuously measure environmental factors to record biological and photosynthetic responses of *C. muelleri* using sensors and fluorescence measurements.

## 1.8. Aims of Thesis

To improve the biomass productivity, cost-effectiveness and feed quality of *C. muelleri* cultures in aquaculture facilities, we must understand the physiological impact of growth limiting factors, light quality and digestibility. The main goal of this study was to improve biomass production and nutrient content of *C. muelleri* by assessing the advantages of LEDs to improve light availability and assess light quality, light shifts and digestibility. With these goals in mind, the three aims of this study were:

1. To improve biomass productivity by improving the areal availability of light, compare the carbon demand between two different light availability setups and to apply an empirical model to make an inference about photosynthesis rates based on light availability.



2. To assess the feasibility of using different colour LEDs as a means of improving biomass productivity, metabolic content and how it impacts the cost efficiency of culturing.
3. To evaluate the applicability of light shifts to manipulate growth and/or the metabolic content of *C. muelleri*, while assessing the feed quality by measuring digestibility.

### **1.9. Thesis structure**

This thesis is presented as a collection of data chapters planned for submission to scientific journals. The chapters are linked to answer the aims of the thesis while reviewing the existing literature in Chapter 1 and summarising the integrated results in Chapter 5.

**Chapter 1:** A brief introduction of diatom physiology, its application to aquaculture and current aquaculture culturing conditions are reviewed in this chapter.

**Chapter 2:** In this chapter, the two key environmental limitations in diatom cultivation in aquaculture, light and CO<sub>2</sub> availability was assessed. An empirical process model is be employed to make inferences of the importance of light availability to maximise photosynthesis.

**Chapter 3:** In this chapter, the growth, metabolic content and cost efficiency of different light quality LEDs was tested based on the findings in second chapter. Blue, green, red and white LEDs were employed to assess their viability as growth light in the aquaculture industry.

**Chapter 4:** In this chapter, the wavelength of the growth light was shifted to assess its feasibility as a possible non-invasive method to manipulate diatom metabolic content, as well as its effects on growth, photosynthesis and feed quality.

**Chapter 5:** In this chapter, the key findings of the study and its implications to future research avenues are discussed.

## **1.10. Ethics and Permits**

No ethical considerations nor permits were required for this study.

## **1.11. References**

Al-Mashhadani, M. K. H., Bandulasena, H. C. H. and Zimmerman, W. B. (2012) 'CO<sub>2</sub> mass transfer induced through an airlift loop by a microbubble cloud generated by fluidic oscillation', *Industrial & Engineering Chemistry Research*, 51(4), pp. 1864–

1877. doi: 10.1021/ie200960v.

Aletsee, L. and Jahnke, J. (1992) 'Growth and productivity of the psychrophilic marine diatoms *Thalassiosira antarctica* Comber and *Nitzschia frigida* Grunow in batch cultures at temperatures below the freezing point of sea water', *Polar Biology*, 11(8), pp. 643–647. doi: 10.1007/BF00237960.

Armbrust, E. V., Berges, J. A., Bowler, C., Green, B. R., Martinez, D., Putnam, N. H., Zhou, S., Allen, A. E., Apt, K. E., Bechner, M., Brzezinski, M. A., Chaal, B. K., Chiovitti, A., Davis, A. K., Demarest, M. S., Detter, J. C., Glavina, T., Goodstein, D., Hadi, M. Z., *et al.* (2004) 'The genome of the diatom *Thalassiosira Pseudonana*: Ecology, evolution, and metabolism', *Science*, 306(5693), pp. 79-86. doi: 10.1126/science.1101156.

Austin, R. W. and Petzold, T. J. (1986) 'Spectral dependence of the diffuse attenuation coefficient of light in ocean waters', *Optical Engineering*. International Society for Optics and Photonics, 25(3), pp. 253471. doi: 10.1117/12.7973845.

Beardall, J. and Raven, J. A. (2013) 'Limits to phototrophic growth in dense culture: CO<sub>2</sub> supply and light', in *Algae for Biofuels and Energy*. Dordrecht: Springer Netherlands, pp. 91–97. doi: 10.1007/978-94-007-5479-9\_5.

Becker, W. (2004) 'Microalgae for aquaculture: The nutritional value of microalgae for aquaculture', in Richmond, A. (ed.) *Handbook of Microalgal Culture: Biotechnology*

*and Applied Phycology*. Oxford, UK, pp. 380–391.

Berges, J. A., Varela, D. E. and Harrison, P. J. (2002) ‘Effects of temperature on growth rate, cell composition and nitrogen metabolism in the marine diatom *Thalassiosira pseudonana* (Bacillariophyceae)’, *Marine Ecology Progress Series*, 225, pp. 139–146.

doi: 10.3354/meps225139.

Blackburn, S. I. and Volkman, J. K. (2012) ‘Microalgae: A renewable source of bioproducts’, in Dunford, N. T. (ed.) *Food and Industrial Bioproducts and Bioprocessing*. 1st edn. Iowa: Iowa State University Press, pp. 221–241. doi:

10.1002/9781119946083.ch9.

Blanken, W., Cuaresma, M., Wijffels, R. H. and Janssen, M. (2013) ‘Cultivation of microalgae on artificial light comes at a cost’, *Algal Research*, 2(4), pp. 333–340. doi:

10.1016/j.algal.2013.09.004.

Bloom, A. J. (2009) ‘As carbon dioxide rises, food quality will decline without careful nitrogen management’, *California Agriculture*, 63(2), pp. 67–72. doi:

10.3733/ca.v063n02p67.

Borowitzka, M. A. (1997) ‘Microalgae for aquaculture: Opportunities and constraints’, *Journal of Applied Phycology*, 9(5), pp. 393–401. doi: 10.1023/A:1007921728300.

Borowitzka, M. A. and Moheimani, N. R. (eds) (2013) *Algae for Biofuels and Energy*.

Dordrecht: Springer Netherlands. doi: 10.1007/978-94-007-5479-9.

Bourget, C. M. (2008) 'An Introduction to Light-emitting Diodes', *American Society for Horticultural Science*, 43(7), pp. 1944–1946.

Bowler, C., Allen, A. E., Badger, J. H., Grimwood, J., Jabbari, K., Kuo, A., Maheswari, U., Martens, C., Maumus, F., Otiillar, R. P., Rayko, E., Salamov, A., Vandepoele, K., Beszteri, B., Gruber, A., Heijde, M., Katinka, M., Mock, T., Valentin, K., *et al.* (2008) 'The *Phaeodactylum* genome reveals the evolutionary history of diatom genomes', *Nature*, 456(7219), pp. 239–44. doi: 10.1038/nature07410.

Bozarth, A., Maier, U. G. and Zauner, S. (2009) 'Diatoms in biotechnology: Modern tools and applications', *Applied Microbiology and Biotechnology*, 82(2), pp. 195–201. doi: 10.1007/s00253-008-1804-8.

Brown, M. R. (2002) 'Nutritional value and use of microalgae in aquaculture', in Cruz-Suárez, L. E., Ricque-Marie, D., Tapia-Salazar, M., Gaxiola-Cortés, M. G., and Simoes, N. (eds) *Avances en nutrición acuícola VI. Memorias del VI Simposio Internacional de Nutrición Acuícola*. Quintana Roo, México, pp. 281–292. doi: 10.5772/1516.

Brown, M. R., Jeffrey, S. W., Volkman, J. K. and Dunstan, G. A. (1997) 'Nutritional properties of microalgae for mariculture', *Aquaculture*, 151(1–4), pp. 315–331. doi: 10.1016/S0044-8486(96)01501-3.

Brown, M. R., Mular, M., Miller, I., Farmer, C. and Trenerry, C. (1999) 'The vitamin content of microalgae used in aquaculture', *Journal of Applied Phycology*, 11(3), pp.

247–255. doi: 10.1023/A:1008075903578.

Camacho-Rodríguez, J., Cerón-García, M. C., Macías-Sánchez, M. D., Fernández-

Sevilla, J. M., López-Rosales, L. and Molina-Grima, E. (2016) ‘Long-term preservation of concentrated *Nannochloropsis gaditana* cultures for use in aquaculture’, *Journal of Applied Phycology*, 28(1), pp. 299–312. doi: 10.1007/s10811-015-0572-y.

Cardozo, K. H. M., Guaratini, T., Barros, M. P., Falcão, V. R., Tonon, A. P., Lopes, N. P.,

Campos, S., Torres, M. A., Souza, A. O., Colepicolo, P. and Pinto, E. (2007)

‘Metabolites from algae with economical impact’, *Comparative Biochemistry and Physiology - Part C*, 146(1–2), pp. 60–78. doi: 10.1016/j.cbpc.2006.05.007.

Carvalho, A. P., Silva, S. O., Baptista, J. M. and Malcata, F. X. (2011) ‘Light

requirements in microalgal photobioreactors: An overview of biophotonic aspects’,

*Applied Microbiology and Biotechnology*, 89(5), pp. 1275–1288. doi: 10.1007/s00253-010-3047-8.

Chaves, I., Pokorny, R., Byrdin, M., Hoang, N., Ritz, T., Brettel, K., Essen, L.-O., van

der Horst, G. T. J., Batschauer, A. and Ahmad, M. (2011) ‘The cryptochromes: Blue light photoreceptors in plants and animals’, *Annual Review of Plant Biology*, 62, pp.

335–364. doi: 10.1146/annurev-arplant-042110-103759.

Chisti, Y. (2008) ‘Biodiesel from microalgae beats bioethanol’, *Trends in*

*Biotechnology*, 26(3), pp. 126–131.

Costa, B. S., Jungandreas, A., Jakob, T., Weisheit, W., Mittag, M. and Wilhelm, C.

(2013) 'Blue light is essential for high light acclimation and photoprotection in the diatom *Phaeodactylum tricornutum*', *Journal of Experimental Botany*, 64(2), pp. 483–93. doi: 10.1093/jxb/ers340.

Costa, B. S., Sachse, M., Jungandreas, A., Bartulos, C. R., Gruber, A., Jakob, T., Kroth, P. G. and Wilhelm, C. (2013) 'Aureochrome 1a is involved in the photoacclimation of the diatom *Phaeodactylum tricornutum*', *PLoS ONE*, 8(9), pp. 1–14. doi: 10.1371/journal.pone.0074451.

D'Souza, F. M. L. and Loneragan, N. R. (1999) 'Effects of monospecific and mixed-algae diets on survival, development and fatty acid composition of penaeid prawn (*Penaeus* spp.) larvae', *Marine Biology*, 133(4), pp. 621–633.

Department of Primary Industries (2016) *NSW Oyster Industry Sustainable Aquaculture Strategy*. Nelson Bay.

Depauw, F. A., Rogato, A., D'Alcalá, M. R. and Falciatore, A. (2012) 'Exploring the molecular basis of responses to light in marine diatoms', *Journal of Experimental Botany*, 63(4), pp. 1575–1591. doi: 10.1093/jxb/ers005.

Eberhard, S., Finazzi, G. and Wollman, F.-A. (2008) 'The dynamics of photosynthesis', *Annual Review of Genetics*, 42(1), pp. 463–515. doi: 10.1146/annurev.genet.42.110807.091452.

Fabregas, J., Abalde, J., Herrero, C., Cabezas, B. and Veiga, M. (1984) 'Growth of the marine microalga *Tetraselmis suecica* in batch cultures with different salinities and nutrient concentrations', *Aquaculture*, 42, pp. 207–215.

Fabregas, J., Herrero, C., Cabezas, B. and Abalde, J. (1986) 'Biomass production and biochemical composition in mass cultures of the marine microalga *Isochrysis galbana* Parke at varying nutrient concentrations', *Aquaculture*, 53(2), pp. 101–113. doi: 10.1016/0044-8486(86)90280-2.

Falkowski, P. G., Barber, R. T. and Smetacek, V. (1998) 'Biogeochemical controls and feedbacks on ocean primary production', *Science*, 281(5374), pp. 200–207.

Falkowski, P. G., Dubinsky, Z. and Wyman, K. (1985) 'Growth-irradiance relationships in phytoplankton', *Limnology and Oceanography*, 30(2), pp. 311–321. doi: 10.4319/lo.1985.30.2.0311.

Falkowski, P. G. and Raven, J. A. (2007) *Aquatic photosynthesis*. 2nd Ed. New Jersey, USA: Princeton University Press.

FAO (2018) *The state of world fisheries and aquaculture 2018: Meeting the sustainable development goals*. Rome.

Farrelly, D. J., Everard, C. D., Fagan, C. C. and McDonnell, K. P. (2013) 'Carbon sequestration and the role of biological carbon mitigation: A review', *Renewable and Sustainable Energy Reviews*, 21, pp. 712–727. doi: 10.1016/j.rser.2012.12.038.



Field, C. B., Behrenfeld, M. J., Randerson, J. T. and Falkowski, P. (1998) 'Primary production of the biosphere: Integrating terrestrial and oceanic components', *Science*, 281(5374), pp. 237–240. doi: 10.1126/science.281.5374.237.

Finazzi, G., Moreau, H. and Bowler, C. (2010) 'Genomic insights into photosynthesis in eukaryotic phytoplankton', *Trends in Plant Science*, 15(10), pp. 565–572. doi: 10.1016/j.tplants.2010.07.004.

Fortunato, A. E., Jaubert, M., Enomoto, G., Bouly, J.-P., Raniello, R., Thaler, M., Malviya, S., Bernardes, J. S., Rappaport, F., Gentili, B., Huysman, M. J. J., Carbone, A., Bowler, C., D'Alcalà, M. R., Ikeuchi, M. and Falciatore, A. (2016) 'Diatom phytochromes reveal the existence of far-red-light-based sensing in the ocean', *The Plant Cell*, 28(3), pp. 616–628. doi: 10.1105/tpc.15.00928.

Gao, K. and Campbell, D. A. (2014) 'Photophysiological responses of marine diatoms to elevated CO<sub>2</sub> and decreased pH: A review', *Functional Plant Biology*, 41(5), pp. 449–459. doi: 10.1071/FP13247.

Giordano, M., Beardall, J. and Raven, J. A. (2005) 'CO<sub>2</sub> concentrating mechanisms in algae: Mechanisms, environmental modulation, and evolution', *Annual review of plant biology*, 56, pp. 99–131. doi: 10.1146/annurev.arplant.56.032604.144052.

Glemser, M., Heining, M., Schmidt, J., Becker, A., Garbe, D., Buchholz, R. and Brück, T. (2016) 'Application of light-emitting diodes (LEDs) in cultivation of phototrophic

microalgae: Current state and perspectives’, *Applied Microbiology and Biotechnology*, 100(3), pp. 1077–1088. doi: 10.1007/s00253-015-7144-6.

Godfray, H. C. J., Beddington, J. R., Crute, I. R., Haddad, L., Lawrence, D., Muir, J. F.,

Pretty, J., Robinson, S., Thomas, S. M. and Toulmin, C. (2010) ‘Food security: The challenge of feeding 9 billion people’, *Science*, 327, pp. 812–818.

Guarnieri, M. T. and Pienkos, P. T. (2015) ‘Algal omics: unlocking bioproduct diversity in algae cell factories’, *Photosynthesis research*, 123(3), pp. 255–263. doi: 10.1007/s11120-014-9989-4.

Guedes, A. C. and Malcata, F. X. (2012) ‘Nutritional value and uses of microalgae in aquaculture’, *Aquaculture*, p. 390. doi: 10.5772/1516.

Guiry, M. D. (2012) ‘How many species of algae are there?’, *Journal of Phycology*, 48(5), pp. 1057–1063. doi: 10.1111/j.1529-8817.2012.01222.x.

Harrison, P. J., Thompson, P. A. and Calderwood, G. S. (1990) ‘Effects of nutrient and light limitation on the biochemical composition of phytoplankton’, *Journal of Applied Phycology*, 2(1), pp. 45–56. doi: 10.1007/BF02179768.

Heasman, M. P., Sushames, T. M., Diemar, J. A., Connor, W. A. O. and Foulkes, L. A. (2001) *Production of micro-algal concentrates for aquaculture part 2: Development and evaluation of harvesting, preservation, storage and feeding technology*.

Hildebrand, M., Davis, A. K., Smith, S. R., Traller, J. C. and Abbriano, R. (2012) ‘The

place of diatoms in the biofuels industry', *Biofuels*, 3(2), pp. 221–240. doi:

10.4155/bfs.11.157.

Hopkinson, B. M. (2014) 'A chloroplast pump model for the CO<sub>2</sub> concentrating mechanism in the diatom *Phaeodactylum tricornutum*', *Photosynthesis Research*,

121(2–3), pp. 223–233. doi: 10.1007/s11120-013-9954-7.

Huysman, M. J. J., Fortunato, A. E., Matthijs, M., Costa, B. S., Vanderhaeghen, R., Van

den Daele, H., Sachse, M., Inzé, D., Bowler, C., Kroth, P. G., Wilhelm, C., Falciatore,

A., Vyverman, W. and De Veylder, L. (2013) 'Aureochrome1a-mediated induction of the diatom-specific cyclin dsCYC2 controls the onset of cell division in diatoms

(*Phaeodactylum tricornutum*)', *The Plant cell*, 25(1), pp. 215–28. doi:

10.1105/tpc.112.106377.

Ikeuchi, M. and Ishizuka, T. (2008) 'Cyanobacteriochromes: A new superfamily of tetrapyrrole-binding photoreceptors in cyanobacteria', *Photochemical &*

*Photobiological Sciences*, 7(10), p. 1159. doi: 10.1039/b802660m.

Jeffrey, S. W., Leroi, J.-M. and Brown, M. R. (1992) 'Characteristics of microalgal

species needed for Australian mariculture', in *Proceedings of the Aquaculture Nutrition Workshop*. Salamander Bay, NSW: Orange: NSW Fisheries, pp. 164–173.

Jin, E., Polle, J. E. W., Lee, H. K., Hyun, S. M. and Chang, M. (2003) 'Xanthophylls in microalgae: From biosynthesis to biotechnological mass production and application',

*Journal of Microbiology and Biotechnology*, 13(2), pp. 165–174. doi: <http://dx.doi.org/>.

Jungandreas, A., Costa, B. S., Jakob, T., Von Bergen, M., Baumann, S. and Wilhelm, C.

(2014) ‘The acclimation of *Phaeodactylum tricornutum* to blue and red light does not influence the photosynthetic light reaction but strongly disturbs the carbon allocation pattern’, *PLoS ONE*, 9(8), pp. 5–15. doi: 10.1371/journal.pone.0099727.

Kawamura, T., Roberts, R. D. and Nicholson, C. M. (1998) ‘Factors affecting the food value of diatom strains for post-larval abalone *Haliotis iris*’, *Aquaculture*, 160(1), pp. 81–88. doi: 10.1016/S0044-8486(97)00223-8.

Kikutani, S., Nakajima, K., Nagasato, C., Tsuji, Y., Miyatake, A. and Matsuda, Y. (2016) ‘Thylakoid luminal  $\theta$ -carbonic anhydrase critical for growth and photosynthesis in the marine diatom *Phaeodactylum tricornutum*’, *Proceedings of the National Academy of Sciences of the United States of America*, 113(35), pp. 9828–33. doi: 10.1073/pnas.1603112113.

Kim, D. G., Lee, C., Park, S.-M. and Choi, Y.-E. (2014) ‘Manipulation of light wavelength at appropriate growth stage to enhance biomass productivity and fatty acid methyl ester yield using *Chlorella vulgaris*’, *Bioresource Technology*, 159, pp. 240–248. doi: 10.1016/j.biortech.2014.02.078.

Kirk, J. T. O. (1994) *Light and photosynthesis in aquatic ecosystems*. 2nd edn.

Cambridge University Press.

- Knauer, J. and Southgate, P. C. (1999) 'A review of the nutritional requirements of bivalves and the development of alternative and artificial diets for bivalve aquaculture', *Reviews in Fisheries Science*, 7(3–4), pp. 241–280. doi: 10.1080/10641269908951362.
- König, S., Eisenhut, M., Bräutigam, A., Kurz, S., Weber, A. P. M. and Büchel, C. (2017) 'The influence of a cryptochrome on the gene expression profile in the diatom *Phaeodactylum tricornutum* under blue light and in darkness', *Plant and Cell Physiology*, 58(11), pp. 1914–1923. doi: 10.1093/pcp/pcx127.
- König, S., Juhas, M., Jäger, S., Kottke, T. and Büchel, C. (2017) 'The cryptochrome—photolyase protein family in diatoms', *Journal of Plant Physiology*, 217, pp. 15–19. doi: 10.1016/j.jplph.2017.06.015.
- Lavens, P. and Sorgeloos, P. (eds) (1996) *Manual on the production and use of live food for aquaculture*, *FAO Fisheries Technical Paper*. Rome: Food and Agriculture Organization of the United Nations.
- Lebeau, T. and Robert, J. M. (2003a) 'Diatom cultivation and biotechnologically relevant products. Part I: Cultivation at various scales', *Applied Microbiology and Biotechnology*, 60, pp. 612–623. doi: 10.1007/s00253-002-1176-4.
- Lebeau, T. and Robert, J. M. (2003b) 'Diatom cultivation and biotechnologically relevant products. Part II: Current and putative products', *Applied Microbiology and Biotechnology*, 60, pp. 624–632. doi: 10.1007/s00253-002-1177-3.

Leu, S. and Boussiba, S. (2014) 'Advances in the production of high-value products by microalgae', *Industrial Biotechnology*, 10(3), pp. 169–183. doi: 10.1089/ind.2013.0039.

Levine, J. S. and MacNichol, E. F. (1982) 'Color vision in fishes', *Scientific American*, 246(2), pp. 140–149. doi: 10.1038/scientificamerican0282-140.

Li, Q., Du, W. and Liu, D. (2008) 'Perspectives of microbial oils for biodiesel production', *Applied Microbiology and Biotechnology*, 80(5), pp. 749–756. doi: 10.1007/s00253-008-1625-9.

Llorente, I. and Luna, L. (2016) 'Bioeconomic modelling in aquaculture: an overview of the literature', *Aquaculture International*, 24(4), pp. 931–948. doi: 10.1007/s10499-015-9962-z.

Lohr, M. and Wilhelm, C. (2001) 'Xanthophyll synthesis in diatoms: Quantification of putative intermediates and comparison of pigment conversion kinetics with rate constants derived from a model', *Planta*, 212(3), pp. 382–391. doi: 10.1007/s004250000403.

López Elías, J. A., Voltolina, D., Chavira Ortega, C. O., Rodríguez Rodríguez, B. B., Sáenz Gaxiola, L. M., Cordero Esquivel, B. and Nieves, M. (2003) 'Mass production of microalgae in six commercial shrimp hatcheries of the Mexican northwest', *Aquacultural Engineering*, 29(3–4), pp. 155–164. doi: 10.1016/S0144-8609(03)00081-5.

Mann, D. G. and Vanormelingen, P. (2013) 'An inordinate fondness? The number, distributions, and origins of diatom species', *Journal of Eukaryotic Microbiology*, 60(4), pp. 414–420. doi: 10.1111/jeu.12047.

Martin-Jezequel, V., Hildebrand, M. and Brzezinski, M. A. (2000) 'Silicon metabolism in diatoms: Implications for growth', *Journal of Phycology*, 36(5), pp. 821–840. doi: 10.1046/j.1529-8817.2000.00019.x.

Martin, C. L. and Tortell, P. D. (2008) 'Bicarbonate transport and extracellular carbonic anhydrase in marine diatoms', *Physiologia Plantarum*, 133(1), pp. 106–116. doi: 10.1111/j.1399-3054.2008.01054.x.

Masojídek, J., Torzillo, G. and Koblížek, M. (2013) 'Photosynthesis in microalgae', in *Handbook of Microalgal Culture*. Oxford, UK: John Wiley & Sons, Ltd, pp. 21–36. doi: 10.1002/9781118567166.ch2.

Mata, T. M., Martins, A. A. and Caetano, N. S. (2010) 'Microalgae for biodiesel production and other applications: A review', *Renewable and Sustainable Energy Reviews*, 14(1), pp. 217–232. doi: 10.1016/j.rser.2009.07.020.

Milligan, A. J., Mioni, C. E. and Morel, F. M. M. (2009) 'Response of cell surface pH to pCO<sub>2</sub> and iron limitation in the marine diatom *Thalassiosira weissflogii*', *Marine Chemistry*, 114(1–2), pp. 31–36. doi: 10.1016/j.marchem.2009.03.003.

Mimouni, V., Ulmann, L., Pasquet, V., Mathieu, M., Picot, L., Bougaran, G., Cadoret,

- J.-P., Morant-Manceau, A. and Schoefs, B. (2012) 'The potential of microalgae for the production of bioactive molecules of pharmaceutical interest', *Current pharmaceutical biotechnology*, 13(15), pp. 2733–50. doi: 10.2174/138920112804724828.
- de Mooij, T., de Vries, G., Latsos, C., Wijffels, R. H. and Janssen, M. (2016) 'Impact of light color on photobioreactor productivity', *Algal Research*, 15, pp. 32–42. doi: 10.1016/j.algal.2016.01.015.
- Nakajima, K., Tanaka, A. and Matsuda, Y. (2013) 'SLC4 family transporters in a marine diatom directly pump bicarbonate from seawater', *Proceedings of the National Academy of Sciences of the United States of America*, 110(5), pp. 1767–72. doi: 10.1073/pnas.1216234110.
- Nelson, D. M., Tréguer, P., Brzezinski, M. A., Leynaert, A. and Quéguiner, B. (1995) 'Production and dissolution of biogenic silica in the ocean: Revised global estimates, comparison with regional data and relationship to biogenic sedimentation', *Global Biogeochemical Cycles*, 9(3), pp. 359–372. doi: 10.1029/95gb01070.
- Nichols, D. S. (2003) 'Prokaryotes and the input of polyunsaturated fatty acids to the marine food web', *FEMS Microbiology Letters*, 219(1), pp. 1–7. doi: 10.1016/S0378-1097(02)01200-4.
- Nielsen, R., Nielsen, M., Abate, T. G., Hansen, B. W., Jepsen, P. M., Nielsen, S. L., Støttrup, J. G. and Buchmann, K. (2017) 'The importance of live-feed traps - farming



marine fish species', *Aquaculture Research*, 48(6), pp. 2623–2641. doi:

10.1111/are.13281.

O'Connor, W., Dove, M., Finn, B. and O'Connor, S. (2008) *Manual for hatchery production of Sydney rock oysters (Saccostrea glomerata)*, NSW Department of Primary Industries – Fisheries Research Report Series.

Oldenhof, H., Zachleder, V. and Van Den Ende, H. (2006) 'Blue- and red-light regulation of the cell cycle in *Chlamydomonas reinhardtii* (Chlorophyta)', *European Journal of Phycology*, 41(3), pp. 313–320. doi: 10.1080/09670260600699920.

Parrish, C. C., Wells, J. S., Yang, Z. and Dabinett, P. (1998) 'Growth and lipid composition of scallop juveniles, *Placopecten magellanicus*, fed the flagellate *Isochrysis galbana* with varying lipid composition and the diatom *Chaetoceros muelleri*', *Marine Biology*, 133(3), pp. 461–471. doi: 10.1007/s002270050486.

Peng, J., Yuan, J. P., Wu, C. F. and Wang, J. H. (2011) 'Fucoxanthin, a marine carotenoid present in brown seaweeds and diatoms: Metabolism and bioactivities relevant to human health', *Marine Drugs*, 9(10), pp. 1806–1828. doi:

10.3390/md9101806.

Ra, C.-H., Kang, C.-H., Jung, J.-H., Jeong, G.-T. and Kim, S.-K. (2016) 'Effects of light-emitting diodes (LEDs) on the accumulation of lipid content using a two-phase culture process with three microalgae', *Bioresource Technology*, 212, pp. 254–261. doi:

10.1016/j.biortech.2016.04.059.

Ramanna, L., Rawat, I. and Bux, F. (2017) 'Light enhancement strategies improve microalgal biomass productivity', *Renewable and Sustainable Energy Reviews*, 80, pp. 765–773. doi: 10.1016/J.RSER.2017.05.202.

Raven, J. A., Beardall, J. and Giordano, M. (2014) 'Energy costs of carbon dioxide concentrating mechanisms in aquatic organisms', *Photosynthesis Research*, 121(2–3), pp. 111–124. doi: 10.1007/s11120-013-9962-7.

Raven, J. A., Giordano, M., Beardall, J. and Maberly, S. C. (2011) 'Algal and aquatic plant carbon concentrating mechanisms in relation to environmental change', *Photosynthesis Research*, 109, pp. 281–296. doi: 10.1007/s11120-011-9632-6.

Renaud, S. M. and Parry, D. L. (1994) 'Microalgae for use in tropical aquaculture II: Effect of salinity on growth, gross chemical composition and fatty acid composition of three species of marine microalgae', *Journal of Applied Phycology*, 6(3), pp. 347–356. doi: 10.1007/BF02181949.

Rockwell, N. C. and Lagarias, J. C. (2010) 'A brief history of phytochromes', *Chem Phys Chem*, 11(6), pp. 1172–1180. doi: 10.1002/cphc.200900894.

Rockwell, N. C. and Lagarias, J. C. (2017) 'Phytochrome diversification in cyanobacteria and eukaryotic algae', *Current Opinion in Plant Biology*, 37, pp. 87–93. doi: 10.1016/j.pbi.2017.04.003.

Rost, B., Riebesell, U., Burkhardt, S. and Sültemeyer, D. (2003) 'Carbon acquisition of bloom-forming marine phytoplankton', *Limnology and Oceanography*, 48(1), pp. 55–67. doi: 10.4319/lo.2003.48.1.0055.

Ruxton, C. H. S., Reed, S. C., Simpson, J. A. and Millington, K. J. (2007) 'The health benefits of omega-3 polyunsaturated fatty acids: A review of the evidence', *Journal of Human Nutrition and Dietetics*, 20(3), pp. 275–285. doi: 10.1111/j.1365-277X.2007.00770.x.

Salleh, S. F., Kamaruddin, A., Uzir, M. H., Mohamed, A. R. and Shamsuddin, A. H. (2017) 'Modeling the light attenuation phenomenon during photoautotrophic growth of *A. variabilis* ATCC 29413 in a batch photobioreactor', *Journal of Chemical Technology & Biotechnology*, 92(2), pp. 358–366. doi: 10.1002/jctb.5013.

Sánchez-Saavedra, M. P. and Voltolina, D. (1996) 'Effect of blue-green light on growth rate and chemical composition of three diatoms', *Journal of Applied Phycology*, 8, pp. 131–137.

Scala, S. and Bowler, C. (2001) 'Molecular insights into the novel aspects of diatom biology', *Cellular and Molecular Life Sciences CMLS*, 58(11), pp. 1666–1673. doi: 10.1007/pl00000804.

Schulze, P. S. C., Pereira, H. G. C., Santos, T. F. C., Schueler, L., Guerra, R., Barreira, L. A., Perales, J. A. and Varela, J. C. S. (2016) 'Effect of light quality supplied by light

emitting diodes (LEDs) on growth and biochemical profiles of *Nannochloropsis oculata* and *Tetraselmis chuii*', *Algal Research*, 16, pp. 387–398. doi:

10.1016/j.algal.2016.03.034.

Spolaore, P., Joannis-Cassan, C., Duran, E. and Isambert, A. (2006) 'Commercial applications of microalgae', *Journal of Bioscience and Bioengineering*, 101(2), pp. 87–96. doi: <http://dx.doi.org/10.1263/jbb.101.87>.

Stonik, V. and Stonik, I. (2015) 'Low-molecular-weight metabolites from diatoms: Structures, biological roles and biosynthesis', *Marine Drugs*, 13(6), pp. 3672–3709. doi: 10.3390/md13063672.

Takahashi, F., Yamagata, D., Ishikawa, M., Fukamatsu, Y., Ogura, Y., Kasahara, M., Kiyosue, T., Kikuyama, M., Wada, M. and Kataoka, H. (2007) 'Aureochrome, a photoreceptor required for photomorphogenesis in stramenopiles.', *Proceedings of the National Academy of Sciences of the United States of America*, 104(49), pp. 19625–19630. doi: 10.1073/pnas.0707692104.

Tamburic, B., Evenhuis, C. R., Suggett, D. J., Larkum, A. W. D., Raven, J. A. and Ralph, P. J. (2015) 'Gas transfer controls carbon limitation during biomass production by marine microalgae', *Chem Sus Chem*, 8(16), pp. 2727–2736. doi: 10.1002/cssc.201500332.

Tréguer, P., Nelson, D. and Bennekom, A. Van (1995) 'The silica balance in the world

ocean: A reestimate', *Science*, 268(5209), pp. 375–379.

Trimborn, S., Lundholm, N., Thoms, S., Richter, K.-U., Krock, B., Hansen, P. J. and

Rost, B. (2008) 'Inorganic carbon acquisition in potentially toxic and non-toxic

diatoms: The effect of pH-induced changes in seawater carbonate chemistry',

*Physiologia Plantarum*, 133(1), pp. 92–105. doi: 10.1111/j.1399-3054.2007.01038.x.

United Nation (2015) *World Population Prospects: The 2015 Revision, Key Findings and Advance Tables*.

Vinayak, V., Manoylov, K. M., Gateau, H., Blanckaert, V., Hérault, J., Pencréac'H, G.,

Marchand, J., Gordon, R. and Schoefs, B. (2015) 'Diatom milking? A review and new

approaches', *Marine Drugs*, 13(5), pp. 2629–2665. doi: 10.3390/md13052629.

Wang, X.-W., Liang, J.-R., Luo, C.-S., Chen, C.-P. and Gao, Y.-H. (2014) 'Biomass,

total lipid production, and fatty acid composition of the marine diatom *Chaetoceros*

*muelleri* in response to different CO<sub>2</sub> levels', *Bioresource Technology*, 161, pp. 124–

130. doi: 10.1016/j.biortech.2014.03.012.

Webb, K. L. and Chu, F. E. (1983) 'Phytoplankton as a food source for bivalve larvae',

in Pruder, G. D., Langdon, C., and Conklin, D. (eds) *Proceedings of the Second*

*International conference on Aquaculture Nutrition: Biochemical and physiological*

*approaches to shellfish nutrition, Lewes/Rehoboth Beach, Delaware, October 27-29*

*1981*. LA: Louisiana State University, pp. 272–291.

Wilhelm, C., Büchel, C., Fisahn, J., Goss, R., Jakob, T., LaRoche, J., Lavaud, J., Lohr, M., Riebesell, U., Stehfest, K., Valentin, K. and Kroth, P. G. (2006) 'The regulation of carbon and nutrient assimilation in diatoms is significantly different from green algae', *Protist*, 157(2), pp. 91–124. doi: 10.1016/j.protis.2006.02.003.

Wilhelm, C., Jungandreas, A., Jakob, T. and Goss, R. (2014) 'Light acclimation in diatoms: From phenomenology to mechanisms', *Marine Genomics*, 16, pp. 5–15. doi: 10.1016/j.margen.2013.12.003.

Williams, P. and Laurens, L. (2010) 'Microalgae as biodiesel biomass & feedstocks: Review & analysis of the biochemistry, energetics & economics', *Energy & Environmental Science*, 3(5), p. 554. doi: 10.1039/b924978h.

Yen, H. W., Hu, I. C., Chen, C. Y., Ho, S. H., Lee, D. J. and Chang, J. S. (2013) 'Microalgae-based biorefinery - From biofuels to natural products', *Bioresource Technology*, 135, pp. 166–174. doi: 10.1016/j.biortech.2012.10.099.

Yun, Y. S. and Park, J. M. (2001) 'Attenuation of monochromatic and polychromatic lights in *Chlorella vulgaris* suspensions', *Applied Microbiology and Biotechnology*, 55(6), pp. 765–770. doi: 10.1007/s002530100639.

Zeebe, R. E. and Wolf-Gladrow, D. A. (2001) *CO<sub>2</sub> in seawater : Equilibrium, kinetics, isotopes*. 1st Ed. Amsterdam: Elsevier.

## **Chapter 2 Light and CO<sub>2</sub> availability to enhance growth rate in the diatom *Chaetoceros muelleri* for aquaculture**

Kenji Iwasaki, Christian Evenhuis, Milán Szabó, Bojan Tamburic,

Unnikrishnan Kuzhiumparambil & Peter Ralph

Climate Change Cluster (C3), Faculty of Science, University of Technology Sydney,

Australia

### **2.1.Introduction**

#### **2.1.1. Diatoms as feed for aquaculture**

Diatoms are a major group of microalgae that have been cultured in large-scale production systems as aquaculture feed for decades (Lebeau and Robert, 2003a).

Diatoms are particularly important in feeding bivalve, mollusc and shrimp larvae (Brown *et al.*, 1997; Lebeau and Robert, 2003b). The nutritional value of diatom feed has been a long-term focus of research in aquaculture (Brown, 2002; Blackburn and Volkman, 2012; Guedes and Malcata, 2012). In particular, a high dietary protein diet has been proven to improve growth for a number of juvenile shellfish species (Kreeger and Langdon, 1993; Knuckey *et al.*, 2002). While the role of live microalgae (including diatoms) in the commercial rearing of larvae and juveniles have been recognised

worldwide, it is also considered a major bottleneck for aquaculture operations (Heasman *et al.*, 2000; Chen *et al.*, 2016). The on-site production of live microalgae for hatcheries is costly, estimated to be 30-40% of total hatchery operation costs (Fabregas *et al.*, 1986; Fulks and Main, 1991; Lavens and Sorgeloos, 1996; Hemaiswarya *et al.*, 2011).

Culture systems used most commonly in commercial aquaculture facilities includes closed bags, open ponds, raceway ponds and tanks (de la Noue and de Pauw, 1988; Borowitzka, 1997; Pulz, 2001; Raja *et al.*, 2008). Regardless of the approach used for culturing, there will be one or more systemic limitations that will limit productivity.

Possible limitations include light, CO<sub>2</sub>, mixing/oxygen removal and temperature control (Harrison, Thompson and Calderwood, 1990; Lee, 1999; Kumar *et al.*, 2010; Borowitzka and Moheimani, 2013b; Tamburic *et al.*, 2015). The potential for increased productivity has motivated research into alternate feeds for rearing bivalves (Knauer and Southgate, 1999). Some candidate feeds that have been considered include; freeze-dried microalgal biomass (Hidu and Ukeles, 1964), frozen microalgal biomass (Mock and Murphy, 1970) and microalgae paste/concentrates (Heasman *et al.*, 2000; Knuckey *et al.*, 2006).

While alternative feeds continue to be researched, it is thought to be unlikely that live microalgal feed will be totally replaced (Borowitzka, 1997; Hemaiswarya *et al.*, 2011).

Hence, it is of key importance to understand which limitations are responsible for the



growth rates observed in current microalgal culture systems. To understand what is limiting growth, one needs to understand the physiological responses of the diatom, under simulated conditions that represent large scale systems.

### 2.1.2. How diatoms respond to light

Photosynthetic diatoms, like all other photoautotrophs use energy from light to convert CO<sub>2</sub> into chemical energy in the form of organic compounds via photosynthesis (Borowitzka and Moheimani, 2013b). Photoautotrophs must reconcile two inevitable consequences of utilising light energy; 1) to capture enough photons to drive photosynthesis 2) to avoid the damaging effects of excess photons (photodamage) (Depauw *et al.*, 2012). Upon exposure to low irradiance, generally, the primary focus is to increase photocapture (photons captured for photosynthesis) (Eberhard, Finazzi and Wollman, 2008). Conversely, exposure to high irradiance, the primary focus becomes photoprotection (protection mechanisms against photodamage) (Eberhard, Finazzi and Wollman, 2008). This excess energy is rapidly dissipated as either heat and redistributed between photosystems in a mechanism known as non-photochemical quenching (NPQ) (Lavaud, Strzepek and Kroth, 2007; Depauw *et al.*, 2012). However, under prolonged exposure to high irradiance, the excess energy will exceed the capacity of photosystem

If repair mechanisms and gene expression is activated to modify the photosynthetic apparatus (Depauw *et al.*, 2012).

### 2.1.3. How light effects diatom growth

The physiological relationship between light and diatom growth rate is illustrated in Figure 2.1. At zero irradiance (phase 1 in Figure 2.1) diatom growth is limited by a lack of light. As irradiance steadily increases (phase 2 in Figure 2.1), light availability is sufficient to reach a hypothetical maximum growth rate (phase 3 in Figure 2.1). However, if irradiance increases further, cells will become photoinhibited (phase 4 in Figure 2.1). Hence, a decrease or an increase of irradiance from the hypothetical optimal irradiance where maximum growth rate is achieved there will be a decrease in growth rate as either light is not sufficient to sustain growth or it has caused photoinhibition (Chisti, 2007).

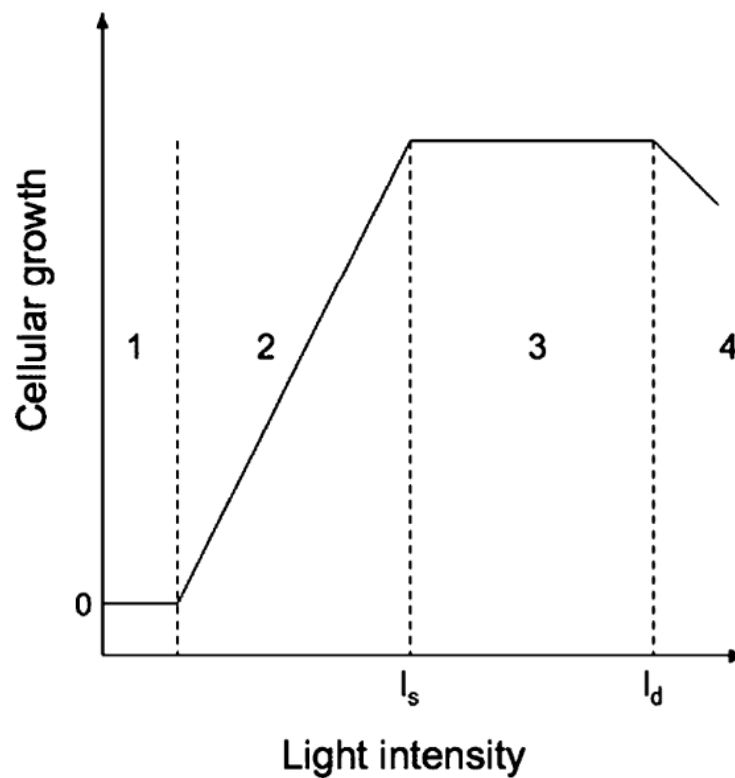
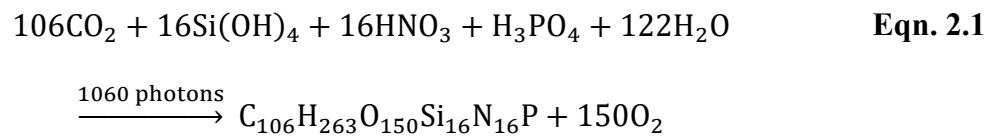


**Figure 2.1** Simplified relationship of increasing light intensity and cell growth of microalgae where regions are 1) light limited region where light is too low to grow, 2) region between light limited and light saturated ( $I_s$ ) where growth increases with light intensity 3) light saturated region where no increase in growth is seen with an increase in light intensity 4) photoinhibited ( $I_d$ ) region where a decrease in growth is seen with an increase in light intensity. Image from Carvalho *et al.*, 2011.

The light intensity of light saturation varies greatly between microalgal species; for example, the light saturation intensity is  $185 \mu\text{mol photons m}^{-2} \text{s}^{-1}$  in *Phaeodactylum tricornutum* (Mann and Myers, 1968), approximately  $200 \mu\text{mol photons m}^{-2} \text{s}^{-1}$  in *Porphyridium cruentum* (Molina *et al.*, 2000) and  $400 \mu\text{mol photons m}^{-2} \text{s}^{-1}$  in

*Cosmarium subprotumidum* (Bouterfas, Belkoura and Dauta, 2002). Hence, in order to efficiently grow diatoms, one must understand what the optimal irradiance for growth is and how that will be provided to the culture. Additionally, the acclimation state of the microalgae plays a role in dictating the growth rate, as a high-light acclimated culture will have higher photosynthesis rates as a function of intensity and conversely, low-light or photoinhibited culture will have lower rates (Tredici, 2010).

It is estimated that the minimum number of photons to fix one unit of carbon is around 7.8 –9.6 for diatoms (Raven, Beardall and Giordano, 2014). This indicates that each diatom cell requires up to 10 photons to initiate photosynthesis to fix a unit of carbon (as defined in Eqn. 2.1), which highlights how crucial it is to supply ample light to sustain optimal photosynthesis. Below is a modified Redfield equation to include silicate (which is estimated to be 1:1 Si:N) and simplified to 10 photons to fix one unit of carbon (Redfield, Ketchum and Richards, 1963; Louanchi and Nasjjar, 2000).



#### 2.1.4. Light limitations in current aquaculture practices

Light is the energy input which initiates photosynthesis, thus the irradiance and its availability needs to be optimized to ensure an efficient culture system. Light availability decreases exponentially with path length and cell density; this phenomenon

is called light attenuation and is the most challenging bottleneck limiting feed productivity (Yun and Park, 2001; Schulze *et al.*, 2017). While path length and cell density are the main factors influencing the light attenuation rate, other factors include: wavelength, cell morphology (e.g. cell size) and pigmentation (Kumar *et al.*, 2011; Kandilian, Lee and Pilon, 2013). Also, due to their high efficiency of photosynthetic antennas, microalgae will absorb photons in excess of its photosynthetic requirements (Lee, 1999). This makes light availability one of the most significant bottlenecks for efficient culturing of diatoms at commercial scales in aquaculture facilities which rely on low intensity light sources typically  $\approx 100 \mu\text{mol photons m}^{-2} \text{ s}^{-1}$  (Brown *et al.*, 1996).

Light attenuation, typically expressed by the Beer-Lambert law (Eqn. 2.2) is a complex function of both biological and physical properties such as the absorption properties, biomass concentration, irradiance and the geometry of the culture vessel (which dictates the path length and mixing efficiency) (Yun and Park, 2001; Ooms *et al.*, 2017; Straka and Rittmann, 2017).

$$I = I_0 e^{-\alpha x l} \quad \text{Eqn. 2.2}$$

where  $I_0$  is light intensity,  $\alpha$  is the extinction coefficient,  $x$  is cell concentration and  $l$  is path length.

There are three ways to reduce light attenuation for a fixed concentration of cells: i) increase the incident light intensity, ii) reduce the path length or iii) decrease the light absorption per cell. However, increasing light intensity may significantly decrease photosynthetic efficiency as a major consequence of photoinhibition, especially to cells closer to the light source (Tredici, 2010; Borowitzka and Moheimani, 2013b).

Decreasing path length will increase the surface area to volume ratio of irradiance; however, it may increase the cost of the system, reduce mixing and increase the heat transfer rate. Also, a microalga may reduce its photosynthetic antenna size in order to decrease photocapture. This process has prompted research into engineering microalga that have smaller antenna; however, difficulties have been observed in reducing non-photochemical absorption without impacting light harvesting (Beckmann *et al.*, 2009).

Hence, simply increasing light intensity is economically and energetically inefficient to maintain sufficient light availability. Instead, optimizing light configuration to minimize factors that cause light attenuation (such as path length) is superior from the perspective of economics and energetics, while maintaining healthy growth and photosynthesis.

### 2.1.5. Light emitting diodes and their potential role in aquaculture

Many aquaculture facilities rely on conventional light sources such as fluorescent and metal halide lamps. Light emitting diodes (LEDs) offer several economic advantages over more traditional light sources, such as: lower heat generated when emitting light, can achieve higher light intensity, has a longer life-expectancy (up to 50,000 h) and have higher energy conversion efficiency (produce more light per Watt of power consumed) (Bourget, 2008; Carvalho *et al.*, 2011). Light emitting diodes may potentially be used in aquaculture facilities as the primary light source from the reasons mentioned above, as well as lowering costs in energy (due to higher conversion efficiency) (Figure 2.15 in Supplementary Material of this chapter) and require less maintenance (Schulze *et al.*, 2014). It is also noteworthy to mention that while LED-based lighting has significantly decreased in cost over the last few years, LEDs are still four times more expensive than conventional fluorescent lamps on average. However, this higher initial cost can be offset by the longer life-expectancy and higher conversion efficiency as previously mentioned (Schulze *et al.*, 2014). In addition, conventional light sources (such as fluorescent lamps) have a wide emission spectrum, which include wavelengths that are not strongly absorbed by some microalgae, reducing its energy conversion efficiency. However, LED arrays can be designed to have an optimized emission spectrum for a specific microalga to emit wavelengths that are highly relevant

for photosynthesis. Thus, LEDs could be a suitable replacement for conventional light sources to cultivate microalgae.

#### 2.1.6. Measuring steady-state light curves

The photosynthetic performances of microalgae with increasing irradiances can be observed with a standard photosynthesis vs. irradiance (PI) curve in the form of a steady-state light curve (SSLC). A steady-state light curve measures the photosynthetic rate in steady-state conditions via chlorophyll *a* fluorescence, which gives the microalga sufficient time for the photosynthetic apparatus to acclimatize to incremental increases in irradiance (Ralph and Gademann, 2005). Steady-state light curves are therefore used to observe long-term acclimation states and potential photosynthetic performances as a function of irradiance (Ralph and Gademann, 2005). The SSLC has three distinct regions: light-limited and light-saturated regions and a photoinhibited region (MacIntyre *et al.*, 2002; Ralph and Gademann, 2005). Both light-limited region and the photoinhibited region are not ideal for microalgal photosynthesis or growth. In the light-limited region, there is a limitation in light availability to drive photosynthesis and in the photoinhibited region, there is an excess of light availability, whereby the excess energy is dissipated as heat (in a form of NPQ) instead of being utilised for

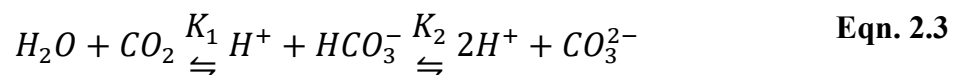


photochemistry. Alternatively, the light-saturated region, between the light-limited and photoinhibited region is the ideal region for microalgal photosynthesis and growth.

While a SSLC can give a good indication of the irradiance with the highest potential photosynthetic activity, it is difficult to maintain that irradiance in mass culture (Borowitzka and Moheimani, 2013a). As light availability rises, the rate of photosynthesis increases as discussed above, this will also increase the rate of carbon fixation, which in turn, increases the demand for carbon until the light intensity becomes photoinhibiting.

#### 2.1.7. Carbon limitation in current aquaculture practices

Carbon is considered as one of the most important limiting nutrients for culturing microalgae (Doucha, Straka and Lívanský, 2005). Carbon is typically added as CO<sub>2</sub> gas and bubbled into microalgal cultures. In water, dissolved inorganic carbon (DIC) consists of CO<sub>2</sub>, HCO<sub>3</sub><sup>-</sup>, and CO<sub>3</sub><sup>2-</sup> in a state of equilibrium (Eqn. 2.3) (Falkowski and Raven, 2007; Reinfelder, 2011). The relative proportions of the DIC components depend on the alkalinity, salinity and temperature (Borowitzka & Moheimani 2013).



where  $K_1$  and  $K_2$  are the respective dissociation constants (Zeebe and Wolf-Gladrow, 2001).

All microalgae can utilize  $\text{CO}_2$  and many (including diatoms) have carbon concentrating mechanisms (CCMs) that allow them to convert  $\text{HCO}_3^-$  to  $\text{CO}_2$  for photosynthesis; however, no microalgae are known to utilize  $\text{CO}_3^{2-}$  (Tortell, Reinfelder and Morel, 1997; Reinfelder, 2011). When the  $\text{HCO}_3^-$  and  $\text{CO}_2$  concentration is low, the pH of microalgae cultures will be high, typically greater than 9.5, and the equilibrium shown in Eqn. 2.3 shifts to the right where the majority of DIC is  $\text{CO}_3^{2-}$  which is unusable for photosynthesis (Borowitzka & Moheimani 2013; Richmond & Grobbelaar 1986; Valle *et al.* 2014). A high pH should be avoided as it starves the diatoms of the carbon required for photosynthesis. However, with efficient  $\text{CO}_2$  addition, the equilibrium in Eqn. 2.3 shifts to the left where the dominant DIC component becomes  $\text{HCO}_3^-$  (and very low  $\text{CO}_{2(\text{aq})}$ ), therefore fulfilling the carbon requirements of photosynthesis. As carbon limitation negatively impacts growth (Jaworski, Talling and Heaney, 1981),  $\text{CO}_2$  addition is a necessity for efficient diatom cultures. Although bicarbonate salts such as sodium bicarbonate ( $\text{NaHCO}_3$ ) can be used to replace  $\text{CO}_2$  gas as the source of inorganic carbon, this is usually not done on an industrial scale for two main reasons. Firstly,  $\text{NaHCO}_3$  is more expensive than  $\text{CO}_2$  gas and second, the addition of  $\text{NaHCO}_3$  increases the alkalinity of the medium which may lead to issues in some algal cultures (Borowitzka & Moheimani 2013). Conversely, the addition of  $\text{CO}_2$  gas does not affect the alkalinity and will decrease the pH, which shifts the DIC equilibrium to increase the

concentrations of  $\text{CO}_2$  and  $\text{HCO}_3^-$  which can both be utilized for photosynthesis (Borowitzka & Moheimani 2013). Hence, pH control via direct gaseous  $\text{CO}_2$  addition is the most economical and most convenient method to maintain  $\text{CO}_2$  levels and pH for mass microalgae cultures (Borowitzka & Moheimani 2013; Grobbelaar 2004). Both light and  $\text{CO}_2$  are fundamental requirements for photosynthesis and microalgal growth and hence the steady availability of these components dictates the productivity and efficiency of microalgal cultures. In this study, an empirical model was developed to infer the timing and severity of light limitation which limits net photosynthesis and growth.

## **2.2. Aims and Objectives**

Although light and  $\text{CO}_2$  are generally considered major limiting factors in algal growth, most of the studies conducted do not conduct *in situ* continuous measurements of these limiting factors in a standardised platform. Therefore, it is difficult to compare various studies/results investigating ‘optimal’ conditions. Moreover, most aquaculture facilities do not monitor physiological parameters continuously over the entire growth phase, which lead to an incomplete understanding of culture health. Higher temporal resolution of physiological and environmental measurements will allow for rigorous assessment of growth limitations, which is often missing in culturing facilities.

Therefore, the overall aim of this study was to assess the growth rate of the aquaculture feed *C. muelleri* in a photobioreactor system as a standardized platform by comparing light configurations and CO<sub>2</sub> addition which was then simulated against aquaculture relevant conditions; where light and carbon are both limited. The specific aims of the experiment were to compare the specific growth rates and photosynthesis rates of *C. muelleri* cultures grown under four conditions of light and CO<sub>2</sub> availability.

Physiochemical parameters such as pH, dissolved oxygen, light availability and temperature were monitored. Light availability, growth rates, and photosynthesis rates were fitted to an empirical process model to infer limitations in growth (section 2.4.9).

## **2.3. Material and Methods**

### **2.3.1. Culturing *Chaetoceros muelleri***

*Chaetoceros muelleri* (CS-176) obtained from the Australian National Algae Culture Collection (ANACC; CSIRO, Hobart, Australia) was grown in artificial seawater enriched with F/2 nutrients with silica following the methods of Guillard (1975).

Artificial seawater was prepared by filter sterilising artificial sea salt (Aquasonic) dissolved in milli-Q water through a 0.2 µm filter made to 35 practical salinity units (PSU). Growth medium was made fresh and stored in the dark at 4°C until needed.

Stock cultures were maintained in 250 mL conical flasks in an incubator (Labec Pty.

Ltd.) at 22°C under a 12 h:12 h light:dark cycle at incident irradiance of approximately 40  $\mu\text{mol photons m}^{-2} \text{s}^{-1}$ .

### 2.3.2. Photobioreactor setup

*Chaetoceros muelleri* was cultured in vertical photobioreactors (ePBR, Phenometrics, Lansing, MI, USA) with inverted conical frustum geometry and a working volume of 450 mL (Figure 2.2). A peltier jacket encasing the ePBR controlled the temperature of the cultures. Temperature sensors (Phenometrics, Lansing, MI, USA) and pH electrodes (Van London pH electrode, Houston, TX, USA) were used to continuously monitor (every 5 min) algal growth. All PBRs were aerated constantly with 0.2  $\mu\text{m}$  filtered (oil-free) ambient air ( $\text{CO}_2 \approx 0.04\% \text{ v/v}$ ) which was humidified by passing it through Milli-Q water and delivered from the bottom of the vessel with a 0.4 mm hypodermic needle. The humidifying step was added to prevent blockages forming inside the needle as a result of dried salt, which disrupts the aeration of cultures. The pH was maintained via 5%  $\text{CO}_2$  addition (food grade, BOC) using an inbuilt solenoid valve programmed to maintain the pH at approximately  $8.0 \pm 0.2$ . Carbon dioxide was bubbled from the bottom of the PBR with an SGE needle (SGE, 5/10 ADT (N) 6cm). The cultures were magnetically stirred with a Teflon-coated magnetic stirrer bars at 120 rpm to prevent cells from sinking to the bottom of the ePBR flask, combined with the constant aeration

kept the cultures homogeneous. This ensures that the samples taken were a close representation of the cell population of the culture.

Experimental cultures were operated in batch mode, where cultures were grown for 7 days and harvested at the end of the period. As the aim was to observe the growth, the cultures were grown for 7 days to allow observations until the stationary phase was reached.

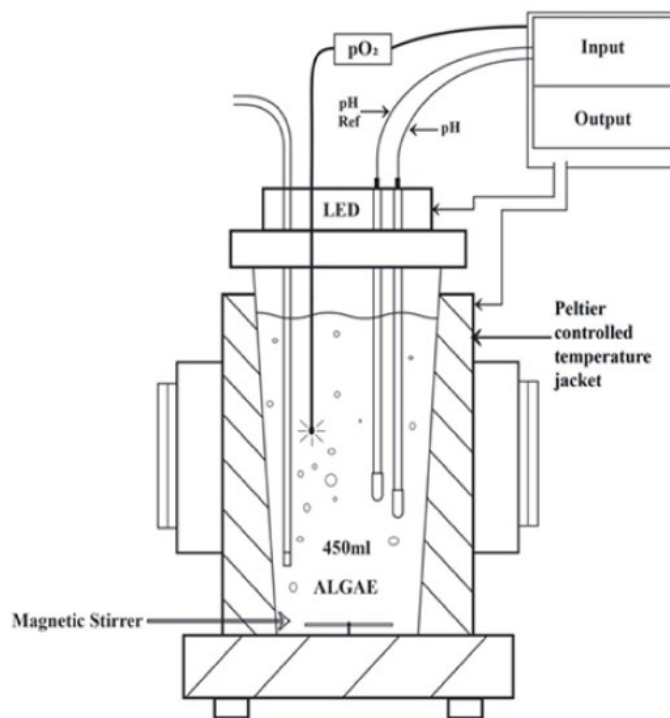


**Figure 2.2** Schematic of ePBR. Light is provided with a white LED array and culture temperature is controlled with a peltier jacket. pH, dissolved oxygen and temperature is measured with sensors. The culture was mixed with a magnetic stirrer. Image from Tamburic *et al.*, 2014.

### 2.3.3. Experimental design

The experiment utilised two LED configurations set to  $500 \mu\text{mol photons m}^{-2} \text{ s}^{-1}$ . One configuration had LEDs mounted on the top of the culture vessel (Top-LED) to simulate the light of typical bag/pond systems illuminated from a single side with a long path length. A custom LED (Side-LED) panel was built to fit between the two peltier heater-cooler units both front and back of the ePBR (Figure 2.3). This increased the areal exposure of light to increase light availability into the culture and was hypothesised to largely eliminate premature light limitation due to the shorter path length. Six LED chips (3 CREE® XLamp® XM-L Color and 3 Cree® XLamp® XP-E photo-red) were used for the custom LED panel. The chips were arranged equidistant apart and arranged in an alternating pattern to avoid bright and dark spots in the water column, such that the light was as homogenous as possible (Figure 2.14 in Supplementary Materials). The emission spectra of the Top-LED and Side-LED were measured with a Jaz spectrometer (Ocean Optics, USA) and is shown in Figure 2.13 alongside the absorption spectra of *C. muelleri* which was measured with a microplate reader (Infinite 200 PRO, Tecan, Switzerland) (Figure 2.13 in Supplementary Materials). The ePBRs were arranged to test four conditions (Figure 2.3). Light configuration Top-LED was used to simulate a typical pond/bag experiencing low light availability (LL) with and without CO<sub>2</sub> limitation (LL+CO<sub>2</sub> and LL-CO<sub>2</sub> respectively). While Side-LED was used to simulate a

culture with higher light availability (HL) with and without CO<sub>2</sub> addition (HL+CO<sub>2</sub> and HL-CO<sub>2</sub> respectively). In summary, the conditions simulated low light and carbon limited culture (LL-CO<sub>2</sub>), low light and carbon replete culture (LL+CO<sub>2</sub>), high light and carbon limited culture (HL-CO<sub>2</sub>) and light and carbon replete culture (HL+CO<sub>2</sub>).

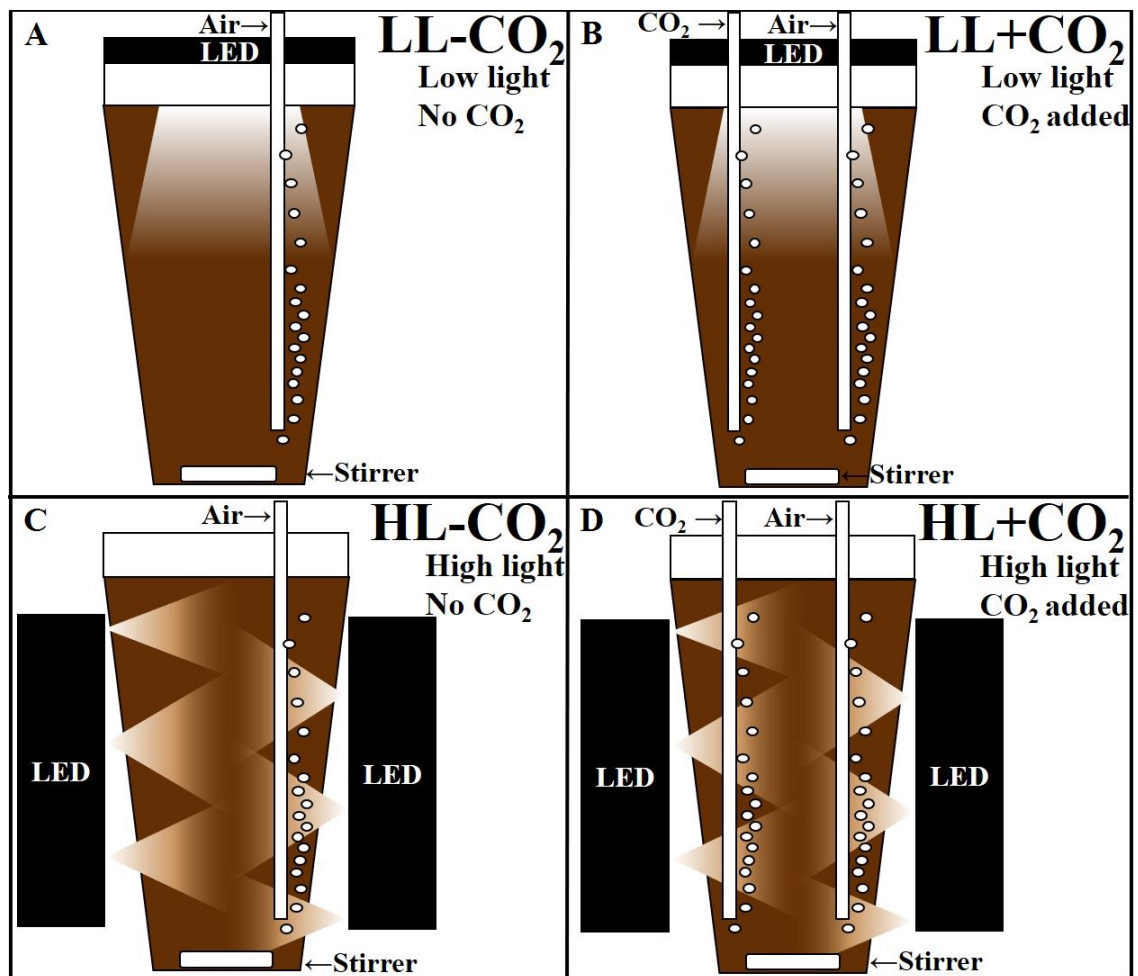


**Figure 2.3** Side view schematic of experimental design. A) LL-CO<sub>2</sub>: LED illumination from the top (Top-LED) with no CO<sub>2</sub> addition. B) LL+CO<sub>2</sub>: LED illumination with Top-LED with CO<sub>2</sub> addition. C) HL-CO<sub>2</sub>: LED illumination from both sides (Side-LED) with no CO<sub>2</sub> addition. D) HL+CO<sub>2</sub>: LED illumination with Side-LED with CO<sub>2</sub> addition. All conditions were constantly aerated.



#### 2.3.4. Steady-state light curve measurements

The Multi-Colour-PAM (Pulse Amplitude Modulation) fluorometer (MC-PAM, Heinz Walz GmbH, Germany) was used to measure a SSLC with three biological replicates. Cultures of *C. muelleri* used for the SSLC were incubated under standard incubation conditions of 22°C under a 12 h:12 h light:dark cycle at a light intensity of 40  $\mu\text{mol photons m}^{-2} \text{s}^{-1}$ . The PAR list used in the SSLC in  $\mu\text{mol photons m}^{-2} \text{s}^{-1}$  was 0, 1, 3, 8, 51, 96, 141, 209, 297, 406, 576, 759, 957, 1186, 1407, 1681, 1990, 2299, 2646, 3112 and 3586. Measuring light and saturation pulse intensity were approximately 0.4  $\mu\text{mol photons m}^{-2} \text{s}^{-1}$  at 440 nm and approximately 2500  $\mu\text{mol photons m}^{-2} \text{s}^{-1}$  at 440 nm respectively and saturation pulse length was 0.8s. White light was used as actinic light and 440 nm was used as measuring light. Each irradiance interval was set to 180s. Relative electron transfer rate (rETR) values were fitted against PAR with the formula detailed in (Platt, Gallegos and Harrison, 1980) which is shown below (Eqn. 2.4).

$$P = P_{max} \left( 1 - e^{-\alpha I / P_{max}} \right) e^{-\beta I / P_{max}} \quad \text{Eqn. 2.4}$$

where  $P$  is rate of photosynthesis at a given irradiance,  $P_{max}$  is maximum rate of photosynthesis,  $\alpha$  is the initial slope of the curve before the onset of light saturation,  $I$  is irradiance and  $\beta$  is the slope of the curve after the onset a condition known as photoinhibition (Falkowski and Raven, 2007).

The rise of the curve in the light-limited region ( $\alpha$ ) is virtually linear to irradiance as irradiance increases into the light-saturated region, where the minimum saturating irradiance occurs ( $I_k$ ) which is determined by finding the intercept of  $\alpha$  with the maximum relative electron transfer rate between photosystem II (PSII) and photosystem I (PSI) ( $rETR_{max}$ ) (MacIntyre *et al.* 2002; Sakshaug *et al.* 1997; Schreiber 2004). The  $I_k$  value therefore is an intercept between the light-limited and light-saturated region, and was hence used as an indicator to avoid light limitation in this study.

#### 2.3.5. Dissolved oxygen measurements using optical sensors and measuring net photosynthesis

Dissolved oxygen (DO) was logged every 30s (FireSting logger; PyroScience GmbH) with 3 mm oxygen optical minisensors with optical isolation (OXROB10-OI; PyroScience GmbH). A two-point calibration against air-saturated water and sodium dithionate solution (zero DO) was performed for all oxygen probes prior to all experiments. A solenoid valve (SMC Pneumatics Pty. Ltd.) controlled via an Arduino was used to intermittently stop the aeration in the ePBRs for 10 min every 2 h to produce a ‘spike’ (Figure 2.9). These spikes were used to monitor the linear change of DO concentration linked to photosynthesis during the light cycle and respiration during the dark cycle (Figure 2.10). This technique has been outlined in previous studies

(Tamburic *et al.*, 2015, 2018). Net photosynthesis (photosynthesis - respiration [p-r])

were calculated by applying a linear regression to each spike, which is then normalized to cell density (section 2.4.4).

### 2.3.6. Automated *Chaetoceros muelleri* growth measurements

Microscopic cell counting was conducted with a haemocytometer (Neubauer, Germany) and a digital imaging microscope (BX50 with analySIS software Olympus, Victoria, Australia) twice a day at 10x magnification (2 h before/after lights off/on respectively).

Cells were allowed to settle (5 min) before 32 images of each sample was taken at different coordinates across the haemocytometer. A custom ImageJ script was used to calculate cell density from the resulting images (Tamburic *et al.*, 2015). The script is also able to distinguish between cells, detritus, dust and air bubbles.

Specific growth rate ( $\mu$ ) was calculated using the Verhulst equation (Eqn. 2.5) which is a logistic equation to describe self-limiting population growth (Bacaër, 2011). Division rate was calculated by applying equation Eqn. 2.5.

$$\mu = \frac{P_M P_0 e^{kt}}{(P_M + P_0 (e^{kt} - 1))} \quad \text{Eqn. 2.6}$$

where  $P_M$  = maximum cell density,  $t$  = time,  $P_0$  = minimum cell density,  $k$  is growth rate

$$t_d = \frac{\ln(2)}{\mu} \quad \text{Eqn. 2.7}$$

where  $\mu$  = specific growth rate

### 2.3.7. Light attenuation measurements

Two different quantum sensors ( $2\pi$  and  $4\pi$  LI-COR Inc., Lincoln, Nebraska, U.S.) and light meter (LI-250A, LI-COR Inc., Lincoln, Nebraska, U.S.) were used to measure the photon flux density (PFD) at the longest path length of the ePBR vessel to determine the attenuated light of the two light configurations. For LL cultures using Top-LEDs, the  $2\pi$  sensor was used to measure PFD from the bottom of the ePBR ( $\approx 20$  cm path length) and for HL cultures using Side-LEDs, the  $4\pi$  sensor (after sterilizing with 75% ethanol) was suspended inside the culture by 2.5 cm from the culture surface to measure PFD from the centre of the culture ( $\approx 2.5$  cm path length). Light calibration was done with this method before the experiment to produce PFD of  $500 \mu\text{mol photons m}^{-2} \text{s}^{-1}$  in water without cells. The attenuation was measured twice a day prior to sampling for cell counts. The measured values were then fitted against a modified Beer-Lambert equation by adding a parameter  $I_b$  to take into consideration the attenuation that takes place in the absence of cells (Eqn. 2.7).

$$A = I_0 e^{-(axl+Ib)} \quad \text{Eqn. 2.8}$$

where  $I_0$  = incident irradiance,  $a$  = attenuation due to cells (cells/cm),  $x$  = cell density,  $l$  = path length (cm),  $Ib$  = attenuation without cells

### 2.3.8. Dissolved inorganic carbon

In order to calculate  $\text{HCO}_3^-$ , the salinity and total alkalinity were first measured at the beginning of the experiment, as well as pH and temperature which were measured continuously. Total alkalinity titration was performed with 0.1 M hydrochloric acid with 50 mL of medium using an auto-titrator (800 Dosino; Metrohm AG). With these parameters,  $\text{HCO}_3^-$  was calculated using the CO2SYS model (Lewis and Wallace, 1998).

### 2.3.9. Modelling net photosynthesis of *Chaetoceros muelleri*

An empirical model combining simple equations and physiological measurements was applied to examine the implications of systemic light limitations in *C. muelleri* cultures and their respective effects on growth rate and potential photosynthetic activity. All modelling, data visualisation and statistics were done with Python programming language (Python 3.6.1. from Spyder 3.1.4.) and Minitab® Statistical Software (Minitab 17).

## 2.4. Results

### 2.4.1. Steady-state light curve of *Chaetoceros muelleri*

To understand the optimal irradiance required for photosynthetic activity, a SSLC was measured (Figure 2.4).

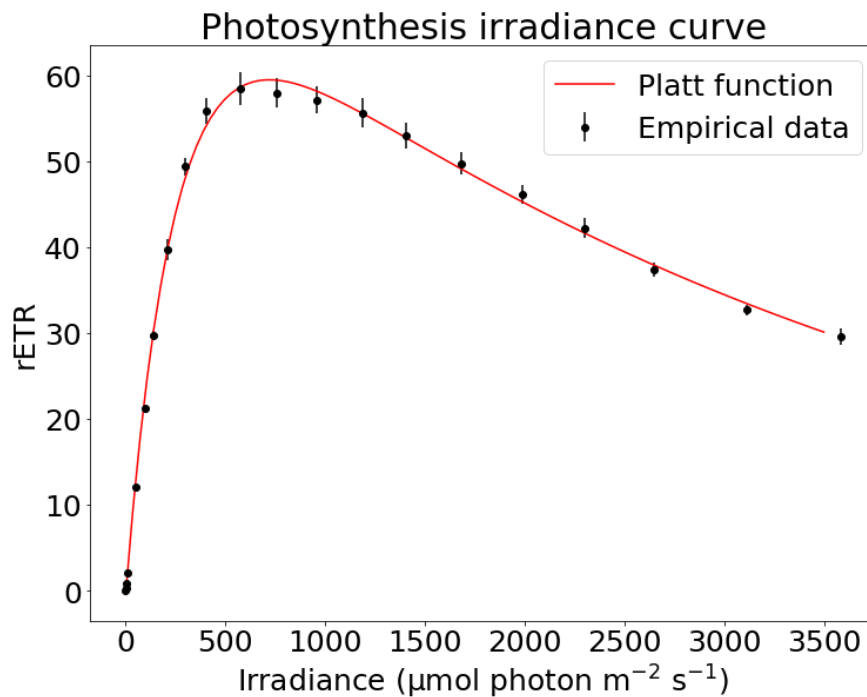


**Figure 2.4** Steady-state light curve (SSLC) of *C. muelleri* grown under standard growth conditions (section 2.4.1). Black dots indicate mean values of relative electron transfer rates (rETR) at each irradiance level, error bars indicate standard deviation ( $n = 3$ ) and red line indicates the fitted Platt function (Eqn. 2.4). Parameter values:  $\alpha = 0.278 \pm 0.007$ ,  $\text{rETR}_{\text{max}} = 59.867 \pm 1.877$ ,  $I_k = 215.5 \pm 9.614$

The SSLC gives an indication of photosynthetic activity as a function of irradiance.

From Figure 2.4 the maximum irradiance to be used in the experiment was determined

to be  $500 \mu\text{mol photons m}^{-2} \text{ s}^{-1}$ , and as  $I_k$  was determined, the minimum irradiance to avoid light limitation was found to be  $\approx 215 \mu\text{mol photons m}^{-2} \text{ s}^{-1}$ .

#### 2.4.2. Growth rates of *Chaetoceros muelleri* under different light and CO<sub>2</sub>

availability

A logistic function (Eqn. 2.5) was fitted against cell density of *C. muelleri* grown under four conditions of light and carbon availability which are shown for each condition

(Figure 2.5).

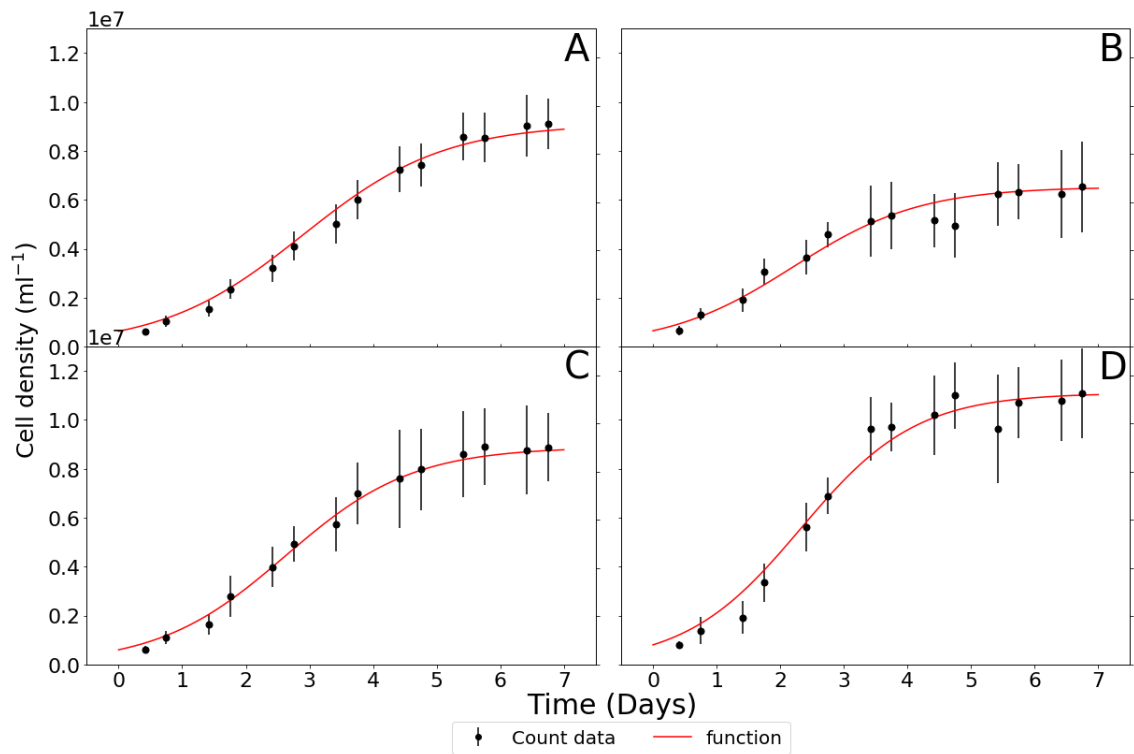


**Figure 2.5** The cell density for each condition as a function of time is shown in paired graphs (above and below), where: the black dots indicate mean cell density, error bars indicate standard deviation ( $n = 3$ ), the red line indicates the logistic function applied (Eqn. 2.5). Panels represent A) LL-CO<sub>2</sub> (low light without CO<sub>2</sub> addition), B) LL+CO<sub>2</sub>

(low light with CO<sub>2</sub> addition), C) HL-CO<sub>2</sub> (high light without CO<sub>2</sub> addition) and D) HL+CO<sub>2</sub> (high light with CO<sub>2</sub> addition).

Specific growth rate, maximum cell density and division rates were highest in HL+CO<sub>2</sub> (Table 2.1 & Figure 2.5D), which provided light availability from both sides of the reactor vessel with CO<sub>2</sub> addition triggered by photosynthetic demand. All culture conditions displayed a lag phase within the day one. By day two, all cultures had entered exponential or linear growth phase and subsequently stationary phase by day four or five. Specific growth rates shown in Table 2.1, calculated from cell count data, showed no significant difference with increasing light availability when carbon was not added (LL-CO<sub>2</sub> & HL-CO<sub>2</sub>); however between the cultures with different carbon availabilities (LL-CO<sub>2</sub> & LL+CO<sub>2</sub> and HL-CO<sub>2</sub> & HL+CO<sub>2</sub>), a significant difference was observed. Final cell density showed no significant differences by increasing light availability (LL-CO<sub>2</sub> & HL-CO<sub>2</sub>); however, in LL+CO<sub>2</sub> the final cell density significantly decreased, while in HL+CO<sub>2</sub> final cell density significantly increased.



**Table 2.1** Specific growth rate ( $\mu$ ), division rate ( $t_d$ ) and final cell density ( $t_f$  density) of *C. muelleri* in four different conditions LL-CO<sub>2</sub>, LL+CO<sub>2</sub>, HL-CO<sub>2</sub> and HL+CO<sub>2</sub> (mean  $\pm$  stdev). One-way ANOVA performed with Tukey method at 95% confidence: same letter indicate no significant difference and different letters indicate significant difference. Values shown are the mean and standard deviation (n = 3).

Treatments	$\mu$	$t_d$	$t_f$ density
LL-CO <sub>2</sub>	$0.84 \pm 0.08^c$	$0.83 \pm 0.08^a$	$9.04 \times 10^6 \pm 1.11 \times 10^6^b$
LL+CO <sub>2</sub>	$1.14 \pm 0.05^b$	$0.61 \pm 0.02^{bc}$	$6.63 \times 10^6 \pm 1.84 \times 10^6^c$
HL-CO <sub>2</sub>	$0.98 \pm 0.16^{bc}$	$0.72 \pm 0.13^{ab}$	$9.10 \times 10^6 \pm 1.89 \times 10^6^b$
HL+CO <sub>2</sub>	$1.59 \pm 0.12^a$	$0.44 \pm 0.03^c$	$1.11 \times 10^7 \pm 1.84 \times 10^6^a$

The growth rates in Table 2.1 were compared with those that have reported *C. muelleri* specific growth rates under varying availabilities of light and CO<sub>2</sub> in Table 2.2, which show that the highest specific growth rates have been obtained in this study.

**Table 2.2** Comparison of growth rate of *C. muelleri* grown indoors in different light and carbon availabilities. Light intensity ( $\mu\text{mol photons m}^{-2} \text{s}^{-1}$ ), method of CO<sub>2</sub> addition and/or pH (representing carbon availability) control and specific growth rate ( $\mu$ ) are shown. p-test results (if available) are shown where same letters indicate no significant difference.

Light intensity	CO <sub>2</sub> availability	pH	$\mu$ (day <sup>-1</sup> )	Reference
45 <sup>1</sup>	Air (0.03%)		0.38	Velasco <i>et al.</i> 2016
50 <sup>2</sup>	Acid titration	8.23 $\pm$ 0.05	0.25 $\pm$ 0.01 <sup>a</sup>	Thornton 2009
50 <sup>2</sup>	Acid addition	7.93 $\pm$ 0.04	0.25 $\pm$ 0.01 <sup>a</sup>	Thornton 2009
50 <sup>2</sup>	Acid addition	7.42 $\pm$ 0.04	0.24 $\pm$ 0.02 <sup>a</sup>	Thornton 2009
50 <sup>2</sup>	Acid addition	6.82 $\pm$ 0.04	0.19 $\pm$ 0.01 <sup>b</sup>	Thornton 2009
140 <sup>1</sup>	Air (0.03%)		0.45	Størseth <i>et al.</i> 2005
140 <sup>1</sup>	Air (0.03%)		0.69	Smith-Harding, Beardall and Mitchell, 2017
150 <sup>1</sup>	Air (0.03%)	9.50 $\pm$ 0.17	0.44 $\pm$ 0.03 <sup>b</sup>	Wang <i>et al.</i> 2014
150 <sup>1</sup>	10%	6.32 $\pm$ 0.10	0.87 $\pm$ 0.05 <sup>a</sup>	Wang <i>et al.</i> 2014
150 <sup>1</sup>	20%	5.90 $\pm$ 0.08	0.42 $\pm$ 0.03 <sup>b</sup>	Wang <i>et al.</i> 2014
150 <sup>1</sup>	30%	5.66 $\pm$ 0.08	0.30 $\pm$ 0.02 <sup>c</sup>	Wang <i>et al.</i> 2014
500 <sup>3</sup>	Air (0.03%)	8.42 $\pm$ 0.35	0.84 $\pm$ 0.08 <sup>c</sup>	This study
500 <sup>3</sup>	pH-stat	7.61 $\pm$ 0.47	1.14 $\pm$ 0.05 <sup>b</sup>	This study
500 <sup>4</sup>	Air (0.03%)	8.93 $\pm$ 0.81	0.98 $\pm$ 0.16 <sup>bc</sup>	This study
500 <sup>4</sup>	pH-stat	7.52 $\pm$ 0.38	1.59 $\pm$ 0.12 <sup>a</sup>	This study

<sup>1</sup> continuous illumination

<sup>2</sup> 14 hour light cycle

<sup>3</sup> Irradiance, 12 hour light cycle, Top-LEDs (Figure 2.3)

<sup>4</sup> Irradiance, 12 hour light cycle, Side-LEDs (Figure 2.3)

### 2.4.3. Modelling light availability of two LED configurations

A modified Beer-lambert function (Eqn. 2.7) was fitted to empirical measurements of PFD in cultures of *C. muelleri* (Figure 2.6). As both Top-LED and Side-LED cultures were calibrated to  $500 \mu\text{mol photons m}^{-2} \text{s}^{-1}$  at their respective maximum path lengths (20 cm and 2.5 cm), all changes in PFD were indicative of the self-shading effects of the culture.

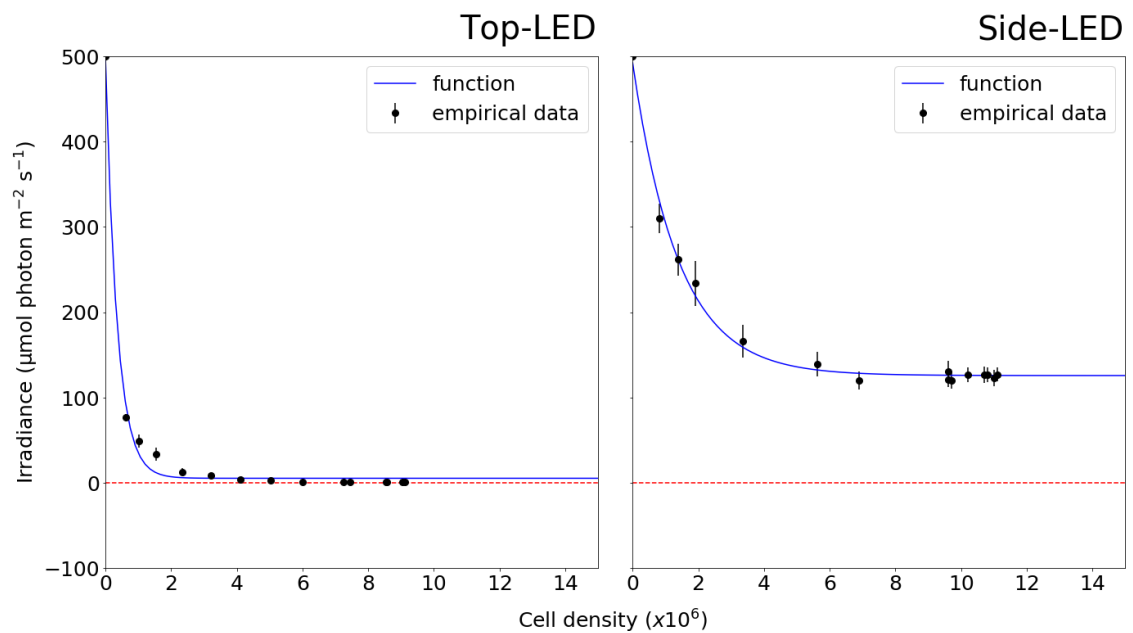


**Figure 2.6** Measured photon flux density (PFD) values for each light condition as a function of cell density is shown where: the black circles indicate the measured PFD value (error bars indicate standard deviation ( $n = 3$ )) and the blue line indicates the fitted decay function and the red dotted line indicates 0 irradiance (Eqn. 2.7). LL samples had a path length of 20 cm (left panel) and HL cultures had a path length of 2.5 cm (right panel).

At the initial cell density approximately  $5 \times 10^5$  cell mL<sup>-1</sup>, the PFD was significantly higher in the Side-LED with  $\approx 320$   $\mu\text{mol photons m}^{-2} \text{s}^{-1}$ , compared to  $\approx 75$   $\mu\text{mol photons m}^{-2} \text{s}^{-1}$  of the Top-LED on day one; a value that is notably lower than the determined  $I_k$  (Figure 2.4). The PFD in both cultures stabilize by the fourth day, at  $\approx 150$   $\mu\text{mol photons m}^{-2} \text{s}^{-1}$  for the Side-LED panel and  $< 1$   $\mu\text{mol photons m}^{-2} \text{s}^{-1}$  for the Top-LED.

From the empirical light measurements and decay fit in Figure 2.6, attenuation rates were modelled based on Eqn. 2.7 to demonstrate the dramatic difference light configuration can have in defining light availability (Figure 2.7).

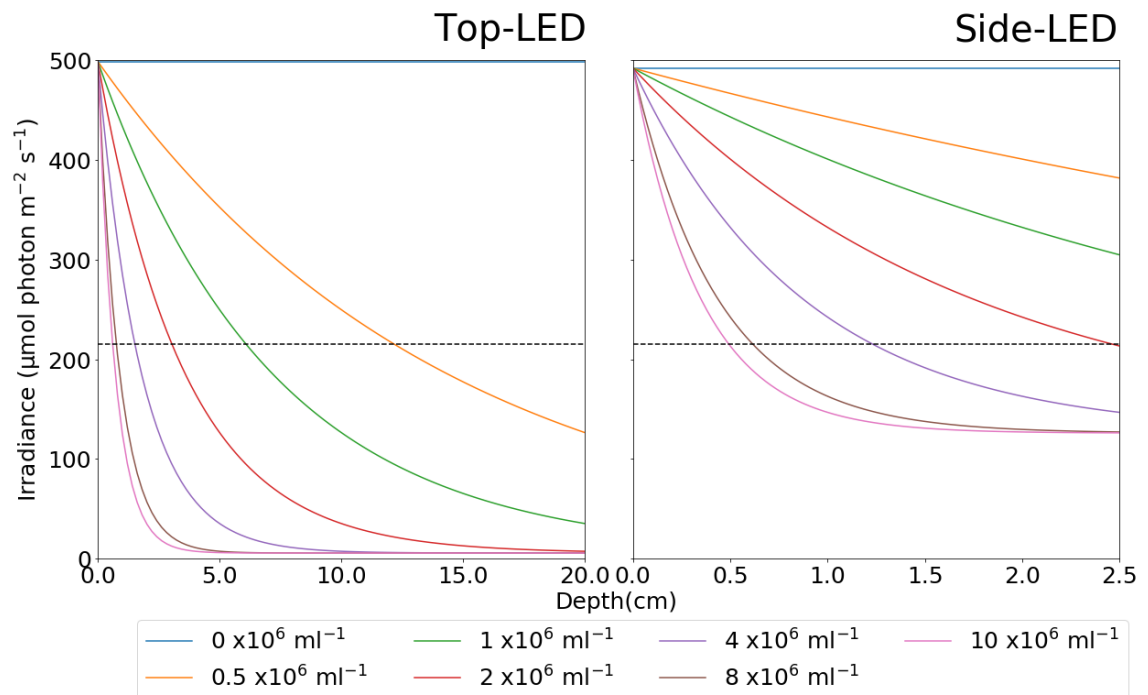


**Figure 2.7** Modelled rate of light attenuation of two light conditions across the relevant

path lengths: 20 cm for Top-LED (left panel) and 2.5 cm for Side-LED (right panel)

with each line (blue, orange, green, red, purple, brown and pink) corresponding to

incrementally increasing cell density ( $1 \times 10^6 \text{ mL}^{-1}$ ): 0, 0.5, 1, 2, 4, 8 and 12 respectively.

Black dotted line indicates  $I_k$  ( $215.5 \pm 9.614$ ) (Calculated from Figure 2.4).

As shown in Figure 2.7, between the two light configurations the initial irradiance level

with approximately  $5 \times 10^5 \text{ cell mL}^{-1}$  in LL is less than a third compared to the HL

cultures. In addition to the lower initial irradiance (orange line in Figure 2.7 left panel),

the rate of attenuation is significantly higher in LL cultures illuminated with the Top-

LED, especially in the first 5 cm where the majority of light is attenuated (Figure 2.7

left panel). In contrast, the HL cultures that were illuminated with the Side-LED, were

more efficient at maintaining higher light availability as a result of the lower attenuation rate, which is due to its significantly shorter path length. Moreover, the Side-LEDs were able to produce the minimum irradiance requirements as suggested by  $I_k$  for the first  $\approx 2 \times 10^6 \text{ mL}^{-1}$  cells during exponential growth phase, while the Top-LED struggled to provide sufficient irradiance over the maximum path length from the beginning of the experiment.

The equation shown below was developed to integrate the light and growth function results (Figure 2.4, Figure 2.5 and Figure 2.7) to estimate net photosynthetic activity ( $P_{\text{net}}$ ) as a function of cell density ( $P$ ).

$$P_{\text{net}}(P) = \int_{z_0}^{z_f} PI(I_{\text{react}}(z, P, I_0, a, b)) P \text{ area } dz \quad \text{Eqn. 2.9}$$

where  $z_0$  is path length of 0 cm,  $z_f$  is the full path length (20 cm or 2.5 cm),  $PI$  is the function results shown in Figure 2.4,  $I_{\text{react}}$  is the function results shown in Figure 2.7 and  $P$  is the function results shown in Figure 2.5.

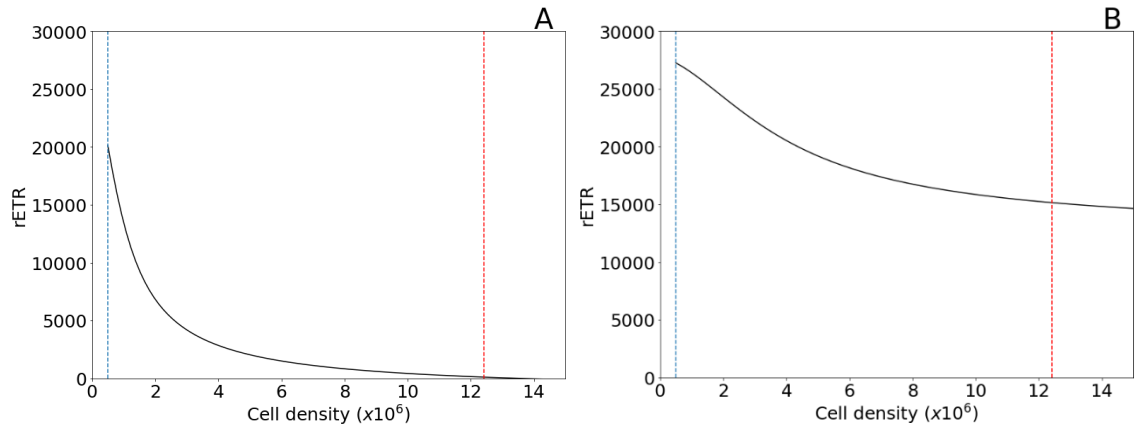


**Figure 2.8** Modelled data of photosynthetic activity shown for each condition: A) Top-LED and B) Side-LED based on model explained in Eqn. 2.8 where black line indicates the rETR as a function of cell density of each culture, the dotted blue line indicates the initial cell density and red dotted line indicates the theoretical cell density limit where nitrogen is depleted. Modelled data assumes CO<sub>2</sub> replete conditions.

As shown in Figure 2.8, Top-LEDs (Figure 2.8A) shows a rapid decline in photosynthetic activity (rETR) with increases in cell density. While in Side-LEDs (Figure 2.8B) the decline in photosynthetic activity is slower in comparison to Top-LEDs. The difference is highlighted in Figure 2.7, where a rapid decay of light is observed in Top-LEDs as opposed to Side-LEDs, due to the increase of areal light availability.

The effects of light availability have been measured and how it potentially effects net photosynthesis. Empirical measurements of DO have been used to calculate net photosynthesis per cell per minute.

#### 2.4.4. Net photosynthesis rates of *Chaetoceros muelleri* under varying light and carbon availability

To determine whether light and carbon availability influences the net photosynthesis rates of *C. muelleri*, DO concentration was monitored over the course of the experiment and artificially ‘spiked’ to monitor the accumulation of DO when aeration is temporarily stopped (Figure 2.9).

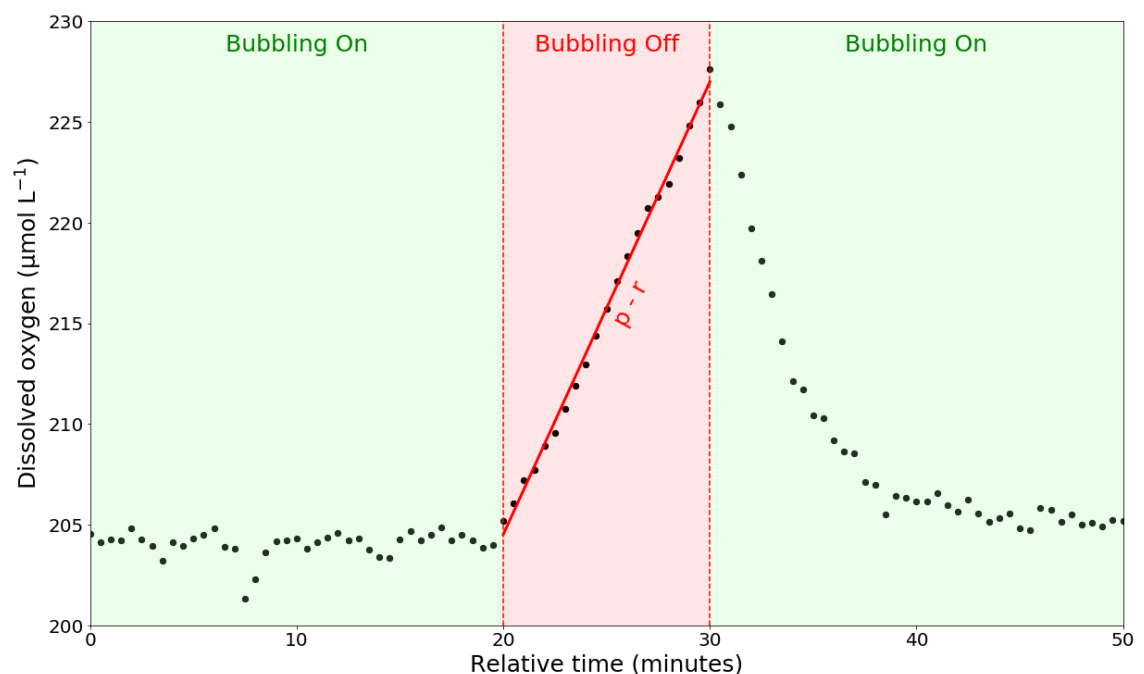


**Figure 2.9** An example dataset showing a typical spike in the dissolved oxygen (DO) in  $\mu\text{mol L}^{-1}$ , which was used to calculate net photosynthesis (photosynthesis – respiration).



Dissolved oxygen equilibrium between microalgae photosynthesis during ‘Bubbling On’, aeration stopped during ‘Bubbling Off’ and photosynthetic DO is allowed to accumulate, DO equilibrium is allowed to be re-established once aeration restarts with ‘Bubbling On’.

Net photosynthesis was calculated for each condition at 12 time points per day, 6 during the light phase and 6 during the dark phase. While cell density measurements were taken only twice a day, values were extrapolated from the logistic function (Eqn. 2.5) to estimate each corresponding time points to normalize each time point to cell density. A typical raw DO dataset during light phase is shown in Figure 2.10, as the light phase begins at  $\approx 0.5$  h and end at  $\approx 12.5$  h. The height of the DO spikes is primarily attributed to cell density, but also irradiance, carbon availability and nitrogen availability. In the example, the spikes in DO begin low in height and increase as the light phase progresses. This is because the culture was in lag/early exponential phase with minimal self-shading, giving the culture sufficient light, CO<sub>2</sub> and nutrients and is able to progressively increase photosynthetic oxygen production as cell density increases.

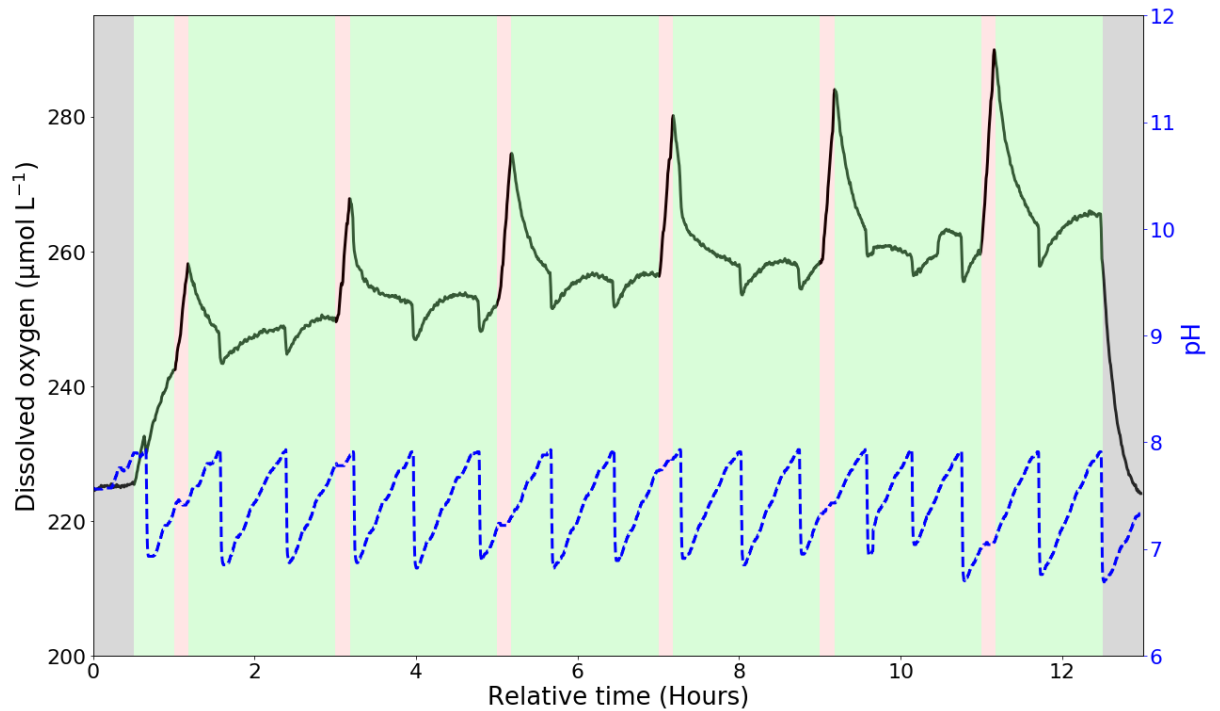


**Figure 2.10** Example dataset of dissolved oxygen (DO) represented with a black line during the light phase in early exponential phase with DO spikes occurring every 2 hr for 10 min (red zones indicate ‘Bubbling Off’ as in Figure 2.9). Small decreases in DO are due to CO<sub>2</sub> dosages, as shown by the pH data represented with a blue dashed line where a decrease in pH corresponds to CO<sub>2</sub> dosage. Grey zones indicate the dark phase.

The DO profile and oxygen production rates of *C. muelleri* were significantly affected by the availability of carbon. In Figure 2.11, there is little difference in net photosynthesis observed with increasing light availability between cultures with no CO<sub>2</sub> addition (LL-CO<sub>2</sub> and HL-CO<sub>2</sub>). While a greater difference can be observed between cultures with CO<sub>2</sub> addition (LL+CO<sub>2</sub> and HL+CO<sub>2</sub>). In Figure 2.11, HL+CO<sub>2</sub> had the highest net photosynthesis rates in the first 3 days compared to all conditions

(Figure 2.11). On day one, LL+CO<sub>2</sub> displayed higher net photosynthesis rates than its counterpart without CO<sub>2</sub> addition (LL-CO<sub>2</sub>). The difference in net photosynthesis rate became smaller as the experiment continued; however, the cultures with CO<sub>2</sub> addition continued to display a slightly higher rate until the end of the experiment (Figure 2.11).

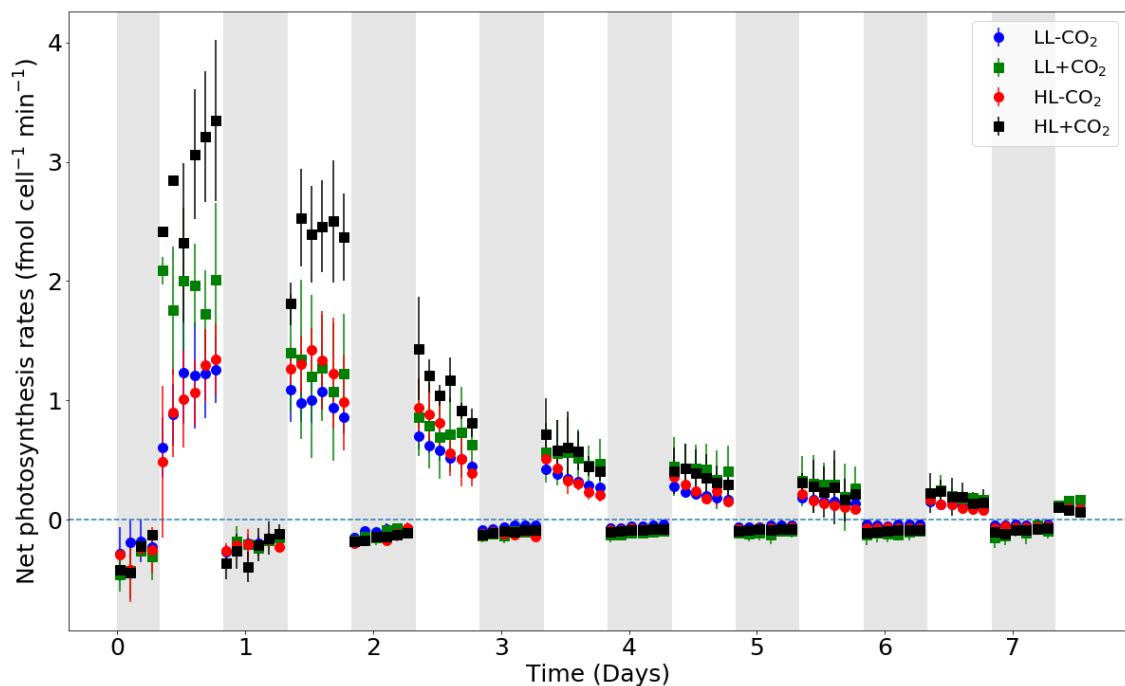


**Figure 2.11** The calculated net photosynthetic oxygen production rates

(fmol cell<sup>-1</sup> min<sup>-1</sup>) as a function of time. Blue dots represent LL-CO<sub>2</sub>, red dots represent HL-CO<sub>2</sub>, green squares represent LL+CO<sub>2</sub> and black squares represent HL+CO<sub>2</sub>. Values represent the mean and standard deviation (n = 3) and dotted blue line shows net photosynthesis rate of zero. Grey areas indicate dark phase while white areas indicates light phase.

#### 2.4.5. Observing carbon availability

Significantly higher growth rates were observed in condition HL+CO<sub>2</sub> (Table 2.1). This can be attributed to the higher light and HCO<sub>3</sub><sup>-</sup> availability during the exponential growth phase (Figure 2.12C). In condition LL-CO<sub>2</sub> the HCO<sub>3</sub><sup>-</sup> concentration fluctuated approximately between 1800 mmol kg<sup>-1</sup> and 600 mmol kg<sup>-1</sup>, as the culture was severely light limited the culture did not have a high enough photosynthetic demand of HCO<sub>3</sub><sup>-</sup> to deplete the total HCO<sub>3</sub><sup>-</sup> pool (Figure 2.12A). The lowest HCO<sub>3</sub><sup>-</sup> concentration ( $\approx$  600 mmol kg<sup>-1</sup>) of LL-CO<sub>2</sub> was observed during the exponential and linear growth phase (days 2 - 4) (Figure 2.12A). While in HL-CO<sub>2</sub>, HCO<sub>3</sub><sup>-</sup> concentration fluctuated approximately between 1800 mmol kg<sup>-1</sup> and 0 mmol kg<sup>-1</sup> as the availability of light was higher, the demand for HCO<sub>3</sub><sup>-</sup> was significant enough to completely deplete the HCO<sub>3</sub><sup>-</sup> pool (Figure 2.12B). In condition HL-CO<sub>2</sub> the HCO<sub>3</sub><sup>-</sup> concentration became largely depleted during the growth and stationary phase (days 2 - 5) (Figure 2.12B). This fluctuation was not seen in LL+CO<sub>2</sub> and HL+CO<sub>2</sub> as CO<sub>2</sub> was added to maintained HCO<sub>3</sub><sup>-</sup> concentrations between 1600 and 1800 mmol kg<sup>-1</sup> (Figure 2.12C).

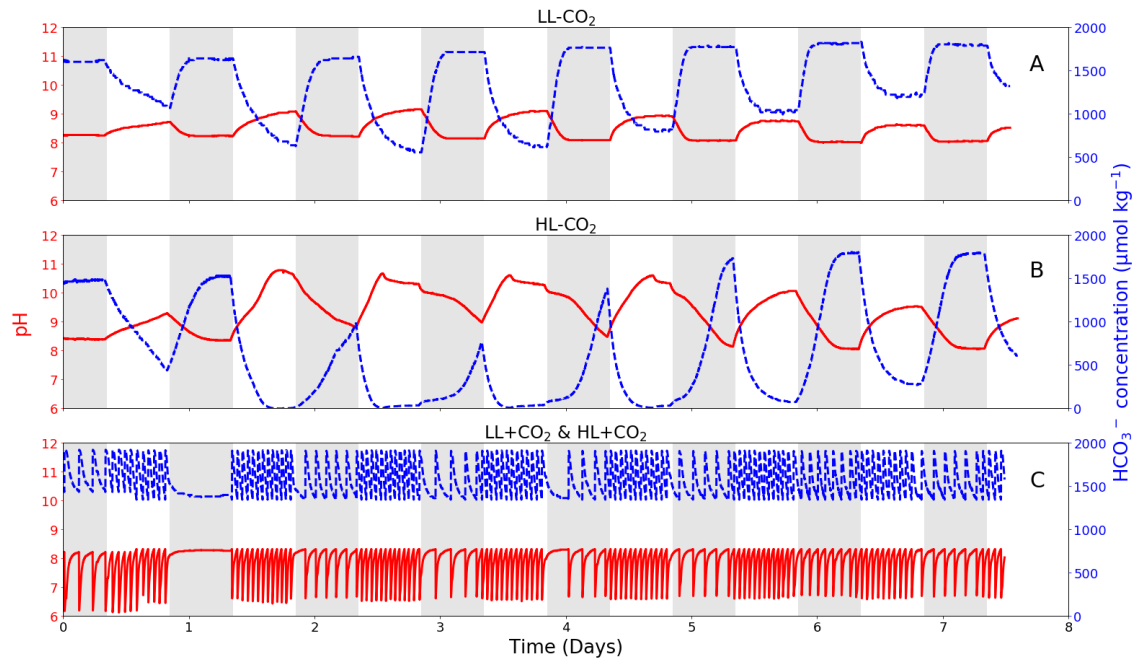


**Figure 2.12** Representative data of pH (red line) and calculated HCO<sub>3</sub><sup>-</sup> concentrations (blue broken line) of *C. muelleri* grown in conditions A) LL-CO<sub>2</sub>, B) HL-CO<sub>2</sub> and C) LL+CO<sub>2</sub> and HL+CO<sub>2</sub>. Grey areas indicate dark phase while white areas indicates light phase.

## 2.5. Discussion

This study investigated the response of *C. muelleri* to two different light availabilities (LL and HL with respective path lengths of 20 cm and 2.5 cm) and two CO<sub>2</sub> availabilities. By applying calibrated irradiances of 500 μmol photons m<sup>-2</sup> s<sup>-1</sup> at each respective path length, this study aimed to investigate the effects of light and CO<sub>2</sub> availability on growth rate and net photosynthesis.

### 2.5.1. Growth

From the cell count data shown in Figure 2.5 and other growth data shown in Table 2.1, a significant increase in growth rate, division rate and final cell density was observed in HL+CO<sub>2</sub> cultures as a result of the improved light and CO<sub>2</sub> availability. In HL+CO<sub>2</sub> cultures, the addition of CO<sub>2</sub> resulted in significantly improved specific growth rates compared to those without CO<sub>2</sub> addition (Table 2.1). A similar result was observed by Wang *et al.* (2014) when comparing the specific growth rate of *C. muelleri* cultures with and without CO<sub>2</sub> addition (air and 10% CO<sub>2</sub> concentration). The highest growth rate observed by Wang *et al.* (2014) was in cultures grown with 10% CO<sub>2</sub> (average pH  $6.32 \pm 0.10$ ), followed by cultures grown with just air (Table 2.2). Cultures grown with 20% and 30% CO<sub>2</sub> had lower growth rates than cultures bubbled with only air (Wang *et al.* 2014, Table 2.2). Their work however, overlooked a large gap in pH between 9.50 and 6.32 (Wang *et al.*, 2014). In the work by Thornton (2009), pHs 6.8, 7.4, 7.9 and 8.2 were maintained via manual acid (HCl) addition and tested for growth rate alongside other parameters with *C. muelleri*. Thornton (2009) concluded that there were no significant differences in growth rate between cultures grown in pHs 7.4 to 8.2, while growth rate decreased at pH 6.8 as shown in Table 2.2. The lower growth rate values observed by Thornton (2009) compared to Wang *et al.* (2014) can be attributed to two main factors: light availability (both intensity and light cycle length) and carbon

availability (no CO<sub>2</sub> bubbling), which Thornton (2009) noted would be a more suitable way to control pH and DIC concentration compared to acid addition. From Table 2.2, a positive correlation of light availability and growth rate can be seen. Ihnken *et al.*

(2011) also observed this positive trend when screening *C. muelleri* under different continuous irradiances from approximately 0 to 400  $\mu\text{mol photons m}^{-2} \text{s}^{-1}$ , as growth rates increased to follow a classic Michaelis-Menten curve. Another observation made by Ihnken *et al.* (2011) who compared growth rates of cultures in different pHs under high light which complemented the observations by Thornton (2009) in low light as neither groups observed a difference in growth rates at pHs 8.2, 7.8 and 7.4. These observations suggest a broad pH range between 8.2 and 7.4 is ideal to grow *C. muelleri* and pHs higher or lower will not grow optimally.

This study observed a specific growth rate of  $0.98 \pm 0.16$  and  $1.59 \pm 0.12$  with HL-CO<sub>2</sub> cultures (average pH  $9.29 \pm 0.76$ ) and HL+CO<sub>2</sub> cultures (average pH  $7.45 \pm 0.35$ ) respectively. This increase in growth rate was similar to the observations by Wang *et al.* (2014) in air and 10% CO<sub>2</sub> cultures, but under a lower light intensity than this study ( $150 \mu\text{mol photons m}^{-2} \text{s}^{-1}$  continuous illumination). It is difficult, however, to assess the cause of growth limitations in the study by Wang *et al.* (2014), as pH was only measured daily, as opposed to high frequency measurements and only incident irradiance is mentioned and not measured *in situ*.

### 2.5.2. Net photosynthesis

While many works have cited light intensity, this can be misleading, as light intensity is not indicative of the PFD received by the diatom culture, as light availability will vary based on the distance from the light source to the culture vessel, the geometry and the material of the vessel. As light intensity is strictly proportional to the power output of the light at the source, it will not reflect the light available to the culture, which can only be measured by recording irradiance (light received by a surface). This is because over time, algal cells undergo self-shading due to an increase in cell density, and this accelerates light attenuation, the impacts of which on photosynthetic light utilization and growth is poorly characterised.

In this study we have demonstrated that an increase in both light and CO<sub>2</sub> significantly improved net photosynthesis rates during the exponential growth phase (Figure 2.11).

Both cultures experiencing CO<sub>2</sub> limitation (LL-CO<sub>2</sub> and HL-CO<sub>2</sub>) exhibited net photosynthesis rates of approximately 1.2 (fmol cell<sup>-1</sup> min<sup>-1</sup>) at its highest. These cultures were limited by CO<sub>2</sub> availability in varying degree as observed in Figure 2.12.

In LL-CO<sub>2</sub>, photosynthesis was only supported by the ambient CO<sub>2</sub> in the air (0.03%) and the Top-LEDs limited light availability, which limited both specific growth rate and photosynthesis rates (Figure 2.5 & Figure 2.11). While LL+CO<sub>2</sub> exhibited higher net photosynthesis rates on day one (approximately 2 fmol cell<sup>-1</sup> min<sup>-1</sup>) the rate decreased as



irradiance decreased as a consequence of increased cell density by the second day.

Condition HL-CO<sub>2</sub> had higher photosynthetic rates during the early hours of the light cycle compared to LL-CO<sub>2</sub> on day two and three and rapidly declines to similar photosynthetic rates as LL-CO<sub>2</sub> during the late hours of the light cycle. The higher rate of photosynthesis is due to the high light availability coupled with HCO<sub>3</sub><sup>-</sup> availability as a result of respiration during the dark phase which decreases rapidly (Figure 2.12).

Condition HL+CO<sub>2</sub> exhibited the highest net photosynthesis rates of approximately 3.5 fmol cell<sup>-1</sup> min<sup>-1</sup> at its highest and consistently demonstrated the highest rates of all treatments during the first three days. In this study we have shown that in order to maximise biomass productivity and net photosynthesis improved availability of both light and CO<sub>2</sub> is crucial, as a limitation in either or both will result in decreased productivity and net photosynthesis. This understanding is vital for microalgae facilities in aquaculture looking to improve biomass productivity, as an improvement in both their light source and CO<sub>2</sub> delivery is needed.

## **2.6. Conclusion**

Four conditions of light and CO<sub>2</sub> availability have been monitored to assess the specific growth rate and net photosynthesis rates with an empirical model. A significant increase in growth rate, maximum cell density and net photosynthesis rates (in exponential

phase) was highest with HL+CO<sub>2</sub> treatment as it was able to maintain optimal light and CO<sub>2</sub> availability for the longest duration.

The empirical model was applied to understand the importance of light availability and how it in turn dictates growth and net photosynthesis. This work has demonstrated how light availability can be improved by minimizing the path length of light through the culture and the subsequent importance of CO<sub>2</sub> availability. Once these two primary limitations are minimized, this has a great impact on growth and photosynthesis.

## 2.7. References

- Bacaër, N. (2011) ‘Verhulst and the logistic equation (1838)’, in *A Short History of Mathematical Population Dynamics*. 1st edn. London: Springer-Verlag London, pp. 35–39. doi: 10.1007/978-0-85729-115-8\_6.
- Beckmann, J., Lehr, F., Finazzi, G., Hankamer, B., Posten, C., Wobbe, L. and Kruse, O. (2009) ‘Improvement of light to biomass conversion by de-regulation of light-harvesting protein translation in *Chlamydomonas reinhardtii*’, *Journal of Biotechnology*, 142(1), pp. 70–77. doi: 10.1016/j.jbiotec.2009.02.015.
- Blackburn, S. I. and Volkman, J. K. (2012) ‘Microalgae: A renewable source of bioproducts’, in Dunford, N. T. (ed.) *Food and Industrial Bioproducts and Bioprocessing*. 1st edn. Iowa: Iowa State University Press, pp. 221–241. doi:

10.1002/9781119946083.ch9.

Borowitzka, M. A. (1997) 'Microalgae for aquaculture: Opportunities and constraints', *Journal of Applied Phycology*, 9(5), pp. 393–401. doi: 10.1023/a:1007921728300.

Borowitzka, M. A. and Moheimani, N. R. (eds) (2013a) *Algae for biofuels and energy*. Dordrecht: Springer Netherlands. doi: 10.1007/978-94-007-5479-9.

Borowitzka, M. A. and Moheimani, N. R. (2013b) 'Open Pond Culture Systems', in Borowitzka, M. A. and Moheimani, N. R. (eds) *Algae for Biofuels and Energy*. Dordrecht: Springer Netherlands, pp. 133–152. doi: 10.1007/978-94-007-5479-9\_8.

Bourget, C. M. (2008) 'An Introduction to Light-emitting Diodes', *American Society for Horticultural Science*. American Society for Horticultural Science, 43(7), pp. 1944–1946.

Bouterfas, R., Belkoura, M. and Dauta, A. (2002) 'Light and temperature effects on the growth rate of three freshwater algae isolated from a eutrophic lake', *Hydrobiologia*, 489, pp. 207–217.

Brown, M. R. (2002) 'Nutritional value and use of microalgae in aquaculture', in Cruz-Suárez, L. E., Ricque-Marie, D., Tapia-Salazar, M., Gaxiola-Cortés, M. G., and Simoes, N. (eds) *Avances en nutrición acuícola VI. Memorias del VI Simposio Internacional de Nutrición Acuícola*. Quintana Roo, México, pp. 281–292. doi: 10.5772/1516.

Brown, M. R., Dunstan, G. A., Norwood, S. J. and Miller, K. A. (1996) 'Effects of harvest stage and light on the biochemical composition of the diatom *Thalassiosira pseudonana*', *Journal of Phycology*, 32, pp. 64–73.

Brown, M. R., Jeffrey, S. W., Volkman, J. K. and Dunstan, G. A. (1997) 'Nutritional properties of microalgae for mariculture', *Aquaculture*, 151(1–4), pp. 315–331. doi: 10.1016/S0044-8486(96)01501-3.

Carvalho, A. P., Silva, S. O., Baptista, J. M. and Malcata, F. X. (2011) 'Light requirements in microalgal photobioreactors: An overview of biophotonic aspects', *Applied Microbiology and Biotechnology*, 89(5), pp. 1275–1288. doi: 10.1007/s00253-010-3047-8.

Chen, J., Wang, Y., Benemann, J. R., Zhang, X., Hu, H. and Qin, S. (2016) 'Microalgal industry in China: Challenges and prospects', *Journal of Applied Phycology*, 28(2), pp. 715–725. doi: 10.1007/s10811-015-0720-4.

Chisti, Y. (2007) 'Biodiesel from microalgae', *Biotechnology Advances*, 25(3), pp. 294–306.

Depauw, F. A., Rogato, A., D'Alcalá, M. R. and Falciatore, A. (2012) 'Exploring the molecular basis of responses to light in marine diatoms', *Journal of Experimental Botany*, 63(4), pp. 1575–1591. doi: 10.1093/jxb/ers005.

Doucha, J., Straka, F. and Lívanský, K. (2005) 'Utilization of flue gas for cultivation of microalgae (*Chlorella* sp.) in an outdoor open thin-layer photobioreactor', *Journal of Applied Phycology*, 17(5), pp. 403–412. doi: 10.1007/s10811-005-8701-7.

Eberhard, S., Finazzi, G. and Wollman, F.-A. (2008) 'The dynamics of photosynthesis', *Annual Review of Genetics*, 42(1), pp. 463–515. doi: 10.1146/annurev.genet.42.110807.091452.

Fabregas, J., Herrero, C., Cabezas, B. and Abalde, J. (1986) 'Biomass production and biochemical composition in mass cultures of the marine microalga *Isochrysis galbana* Parke at varying nutrient concentrations', *Aquaculture*, 53(2), pp. 101–113. doi: 10.1016/0044-8486(86)90280-2.

Falkowski, P. G. and Raven, J. A. (2007) *Aquatic photosynthesis*. 2nd Ed. New Jersey, USA: Princeton University Press.

Fulks, W. and Main, K. L. (1991) 'Rotifer and microalgae culture systems', in Fulks, W. and Main, K. L. (eds) *Proceeding of a U.S. -Asia workshop; 1991 January 28-31*; Honolulu, Hawaii: The Oceanic Institute, pp. 1–364.

Grobbelaar, J. U. (2003) 'Algal nutrition mineral nutrition', in Richmond, A. (ed.) *Handbook of microalgal culture: Biotechnology and applied phycology*. Oxford, UK: Blackwell Publishing Ltd, pp. 97–115.

Guedes, A. C. and Malcata, F. X. (2012) 'Nutritional value and uses of microalgae in aquaculture', *Aquaculture*, p. 390. doi: 10.5772/1516.

Guillard, R. R. L. (1975) 'Culture of Phytoplankton for Feeding Marine Invertebrates', in Smith, W. L. and Chanley, M. H. (eds) *Culture of marine invertebrate animals*. Boston, MA: Springer US, pp. 29–60. doi: 10.1007/978-1-4615-8714-9\_3.

Harrison, P. J., Thompson, P. A. and Calderwood, G. S. (1990) 'Effects of nutrient and light limitation on the biochemical composition of phytoplankton', *Journal of Applied Phycology*, 2(1), pp. 45–56. doi: 10.1007/BF02179768.

Heasman, M., Diemar, J., O'connor, W., Sushames, T. and Foulkes, L. (2000) 'Development of extended shelf-life microalgae concentrate diets harvested by centrifugation for bivalve molluscs - A summary', *Aquaculture Research*, 31(8–9), pp. 637–659. doi: 10.1046/j.1365-2109.2000.318492.x.

Hemaiswarya, S., Raja, R., Kumar, R. R., Ganesan, V. and Anbazhagan, C. (2011) 'Microalgae: A sustainable feed source for aquaculture', *World Journal of Microbiology and Biotechnology*, 27(8), pp. 1737–1746. doi: 10.1007/s11274-010-0632-z.

Hidu, H. and Ukeles, R. (1964) 'Dried unicellular algae as food for larvae of the hard shell clam, *Mercenaria mercenaria*', in *Proceedings of the National Shellfisheries Association; August 1962*, pp. 85–101.

Ihnken, S., Roberts, S. and Beardall, J. (2011) 'Differential responses of growth and photosynthesis in the marine diatom *Chaetoceros muelleri* to CO<sub>2</sub> and light availability', *Phycologia*, 50(2), pp. 182–193. doi: 10.2216/10-11.1.

Jaworski, G. H. M., Talling, J. F. and Heaney, S. I. (1981) 'The influence of carbon dioxide-depletion on growth and sinking rate of two planktonic diatoms in culture', *British Phycological Journal*, 16(4), pp. 395–410.

Kandilian, R., Lee, E. and Pilon, L. (2013) 'Radiation and optical properties of *Nannochloropsis oculata* grown under different irradiances and spectra', *Bioresource Technology*, 137, pp. 63–73. doi: 10.1016/j.biortech.2013.03.058.

Knauer, J. and Southgate, P. C. (1999) 'A review of the nutritional requirements of bivalves and the development of alternative and artificial diets for bivalve aquaculture', *Reviews in Fisheries Science*, 7(3–4), pp. 241–280. doi: 10.1080/10641269908951362.

Knuckey, R. M., Brown, M. R., Barrett, S. M. and Hallegraeff, G. M. (2002) 'Isolation of new nanoplanktonic diatom strains and their evaluation as diets for juvenile Pacific oysters (*Crassostrea gigas*)', *Aquaculture*, 211(1–4), pp. 253–274. doi: 10.1016/S0044-8486(02)00010-8.

Knuckey, R. M., Brown, M. R., Robert, R. and Frampton, D. M. F. (2006) 'Production of microalgal concentrates by flocculation and their assessment as aquaculture feeds',

*Aquacultural Engineering*, 35(3), pp. 300–313. doi: 10.1016/j.aquaeng.2006.04.001.

Kreeger, D. A. and Langdon, C. J. (1993) ‘Effect of dietary protein content on growth of juvenile mussels, *Mytilus trossulus* (Gould 1850)’, *Biological Bulletin*, 185, pp. 123–139. doi: 10.2307/1542136.

Kumar, A., Ergas, S., Yuan, X., Sahu, A., Zhang, Q., Dewulf, J., Malcata, F. X. and van Langenhove, H. (2010) ‘Enhanced CO<sub>2</sub> fixation and biofuel production via microalgae: Recent developments and future directions’, *Trends in Biotechnology*, 28(7), pp. 371–380. doi: 10.1016/j.tibtech.2010.04.004.

Kumar, K., Dasgupta, C. N., Nayak, B., Lindblad, P. and Das, D. (2011) ‘Development of suitable photobioreactors for CO<sub>2</sub> sequestration addressing global warming using green algae and cyanobacteria’, *Bioresource Technology*, 102(8), pp. 4945–4953. doi: 10.1016/j.biortech.2011.01.054.

de la Noue, J. and de Pauw, N. (1988) ‘The potential of microalgal biotechnology: A review of production and uses of microalgae’, *Biotechnology Advances*, 6(4), pp. 725–770. doi: 10.1016/0734-9750(88)91921-0.

Lavaud, J., Strzepek, R. F. and Kroth, P. G. (2007) ‘Photoprotection capacity differs among diatoms: Possible consequences on the spatial distribution of diatoms related to fluctuations in the underwater light climate’, *Limnology and Oceanography*, 52(3), pp.



1188–1194. doi: 10.4319/lo.2007.52.3.1188.

Lavens, P. and Sorgeloos, P. (eds) (1996) *Manual on the production and use of live food for aquaculture, FAO Fisheries Technical Paper*. Rome: Food and Agriculture Organization of the United Nations.

Lebeau, T. and Robert, J. M. (2003a) 'Diatom cultivation and biotechnologically relevant products. Part I: Cultivation at various scales', *Applied Microbiology and Biotechnology*, 60, pp. 612–623. doi: 10.1007/s00253-002-1176-4.

Lebeau, T. and Robert, J. M. (2003b) 'Diatom cultivation and biotechnologically relevant products. Part II: Current and putative products', *Applied Microbiology and Biotechnology*, 60, pp. 624–632. doi: 10.1007/s00253-002-1177-3.

Lee, C.-G. (1999) 'Calculation of light penetration depth in photobioreactors', *Biotechnology and Bioprocess Engineering*, 4(1), pp. 78–81. doi: 10.1007/BF02931920.

Lewis, E. and Wallace, D. W. R. (1998) 'Program developed for CO<sub>2</sub> system calculations'. Tennessee: Carbon Dioxide Information Analysis Centre, pp. 1–38. doi: 10.2172/639712.

Louanchi, F. and Najjar, R. G. (2000) 'A global monthly climatology of phosphate, nitrate, and silicate in the upper ocean: Spring-summer export production and shallow remineralization', *Global Biogeochemical Cycles*, 14(3), pp. 957–977. doi:

10.1029/1999GB001215.

MacIntyre, H. L., Kana, T. M., Anning, T. and Geider, R. J. (2002) 'Photoacclimation of photosynthesis irradiance response curves and photosynthetic pigments in microalgae and cyanobacteria', *Journal of Phycology*, 38(1), pp. 17–38. doi: 10.1046/j.1529-8817.2002.00094.x.

Mann, J. E. and Myers, J. (1968) 'On pigments, growth, and photosynthesis of *Phaeodactylum tricornutum*', *Journal of Phycology*, 4(4), pp. 349–355. doi: 10.1111/j.1529-8817.1968.tb04707.x.

Mock, C. R. and Murphy, M. A. (1970) 'Techniques for raising penaeid shrimp from the egg to post-larvae', *Proceedings of the annual workshop - World Mariculture Society; February 9-10 1970*, 1(1–4), pp. 143–158. doi: 10.1111/j.1749-7345.1970.tb00022.x.

Molina, E., Acién Fernández, F. G., García Camacho, F., Camacho Rubio, F. and Chisti, Y. (2000) 'Scale-up of tubular photobioreactors', *Journal of Applied Phycology*, 12(3/5), pp. 355–368. doi: 10.1023/A:1008110819338.

Ooms, M. D., Graham, P. J., Nguyen, B., Sargent, E. H. and Sinton, D. (2017) 'Light dilution via wavelength management for efficient high-density photobioreactors', *Biotechnology and Bioengineering*, 114(6), pp. 1160–1169. doi: 10.1002/bit.26261.

Platt, T., Gallegos, C. and Harrison, W. (1980) 'Photoinhibition of photosynthesis in

natural assemblages of marine phytoplankton', *Journal of Marine Research*, 38(4), pp. 687–701.

Pulz, O. (2001) 'Photobioreactors: Production systems for phototrophic microorganisms', *Applied Microbiology and Biotechnology*, 57(3), pp. 287–293. doi: 10.1007/s002530100702.

Raja, R., Hemaiswarya, S., Kumar, N. A., Sridhar, S. and Rengasamy, R. (2008) 'A perspective on the biotechnological potential of microalgae.', *Critical reviews in microbiology*, 34(2), pp. 77–88. doi: 10.1016/0167-7799(92)90282-Z.

Ralph, P. J. and Gademann, R. (2005) 'Rapid light curves: A powerful tool to assess photosynthetic activity', *Aquatic Botany*, 82(3), pp. 222–237. doi: 10.1016/j.aquabot.2005.02.006.

Raven, J. A., Beardall, J. and Giordano, M. (2014) 'Energy costs of carbon dioxide concentrating mechanisms in aquatic organisms', *Photosynthesis Research*, 121(2–3), pp. 111–124. doi: 10.1007/s11120-013-9962-7.

Redfield, A. C., Ketchum, B. H. and Richards, F. A. (1963) 'The influence of organisms on the composition of the sea water', in Hill, M. N. (ed.) *The sea: Ideas and observations on progress in the study of the seas*. New York: Interscience Publishers, pp. 26–77.

Reinfelder, J. R. (2011) 'Carbon concentrating mechanisms in eukaryotic marine phytoplankton', *Annual Review of Marine Science*, 3(1), pp. 291–315. doi: 10.1146/annurev-marine-120709-142720.

Richmond, A. and Grobbelaar, J. U. (1986) 'Factors affecting the output rate of *Spirulina platensis* with reference to mass cultivation', *Biomass*, 10(4), pp. 253–264.

Sakshaug, E., Bricaud, A., Dandonneau, Y., Falkowski, P. G., Kiefer, D. A., Legendre, L., Morel, A., Parslow, J. and Takahashi, M. (1997) 'Parameters of photosynthesis: Definitions, theory and interpretation of results', *Journal of Plankton Research*, 19(11), pp. 1637–1670. doi: 10.1093/plankt/19.11.1637.

Schreiber, U. (2005) 'Pulse-amplitude-modulation (PAM) fluorometry and saturation pulse method: An overview', in Papageorgiou, G. C. and Govindjee (eds) *Advances in Photosynthesis and Respiration*. Dordrecht: Springer Netherlands, pp. 279–319. doi: 10.1007/978-1-4020-3218-9\_11.

Schulze, P. S. C., Barreira, L. A., Pereira, H. G. C., Perales, J. A. and Varela, J. C. S. (2014) 'Light emitting diodes (LEDs) applied to microalgal production', *Trends in Biotechnology*, 32(8), pp. 422–430. doi: 10.1016/j.tibtech.2014.06.001.

Schulze, P. S. C., Guerra, R., Pereira, H., Schüller, L. M. and Varela, J. C. S. (2017) 'Flashing LEDs for microalgal production', *Trends in Biotechnology*, 35(11), pp. 1088–

1101. doi: 10.1016/j.tibtech.2017.07.011.

Smith-Harding, T. J., Beardall, J. and Mitchell, J. G. (2017) ‘The role of external carbonic anhydrase in photosynthesis during growth of the marine diatom *Chaetoceros muelleri*’, *Journal of Phycology*, 53(6), pp. 1159–1170. doi: 10.1111/jpy.12572.

Størseth, T. R., Hansen, K., Reitan, K. I. and Skjermo, J. (2005) ‘Structural characterization of  $\beta$ -D-(1 $\rightarrow$ 3)-glucans from different growth phases of the marine diatoms *Chaetoceros m  lleri* and *Thalassiosira weissflogii*’, *Carbohydrate Research*, 340(6), pp. 1159–1164. doi: 10.1016/j.carres.2004.12.036.

Straka, L. and Rittmann, B. E. (2017) ‘Light attenuation changes with photo-acclimation in a culture of *Synechocystis* sp. PCC 6803’, *Algal Research*, 21, pp. 223–226. doi: 10.1016/j.algal.2016.11.024.

Tamburic, B., Evenhuis, C. R., Crosswell, J. R. and Ralph, P. J. (2018) ‘An empirical process model to predict microalgal carbon fixation rates in photobioreactors’, *Algal Research*, 31, pp. 334–346. doi: 10.1016/j.algal.2018.02.014.

Tamburic, B., Evenhuis, C. R., Suggett, D. J., Larkum, A. W. D., Raven, J. A. and Ralph, P. J. (2015) ‘Gas transfer controls carbon limitation during biomass production by marine microalgae’, *Chem Sus Chem*, 8(16), pp. 2727–2736. doi: 10.1002/cssc.201500332.

- Tamburic, B., Guruprasad, S., Radford, D. T., Szabó, M., Lilley, R. M., Larkum, A. W. D., Franklin, J. B., Kramer, D. M., Blackburn, S. I., Raven, J. A., Schliep, M. and Ralph, P. J. (2014) 'The effect of diel temperature and light cycles on the growth of *Nannochloropsis oculata* in a photobioreactor matrix', *PLoS ONE*, 9(1), pp. 1–13. doi: 10.1371/journal.pone.0086047.
- Thornton, D. C. O. (2009) 'Effect of low pH on carbohydrate production by a marine planktonic diatom (*Chaetoceros muelleri*)', *Research Letters in Ecology*, 2009, pp. 4–8. doi: 10.1155/2009/105901.
- Tortell, P. D., Reinfelder, J. R. and Morel, F. M. M. (1997) 'Active uptake of bicarbonate by diatoms', *Nature*, 390(6657), pp. 243–244. doi: 10.1038/36765.
- Tredici, M. R. (2010) 'Photobiology of microalgae mass cultures: understanding the tools for the next green revolution', *Biofuels*, 1(1), pp. 143–162. doi: 10.4155/bfs.09.10.
- Valle, K. C., Nymark, M., Aamot, I., Hancke, K., Winge, P., Andresen, K., Johnsen, G., Brembu, T. and Bones, A. M. (2014) 'System responses to equal doses of photosynthetically usable radiation of blue, green, and red light in the marine diatom *Phaeodactylum tricornutum*', *PLoS ONE*, 9(12), pp. 1–37. doi: 10.1371/journal.pone.0114211.
- Velasco, L. A., Carrera, S. and Barros, J. (2016) 'Isolation, culture and evaluation of

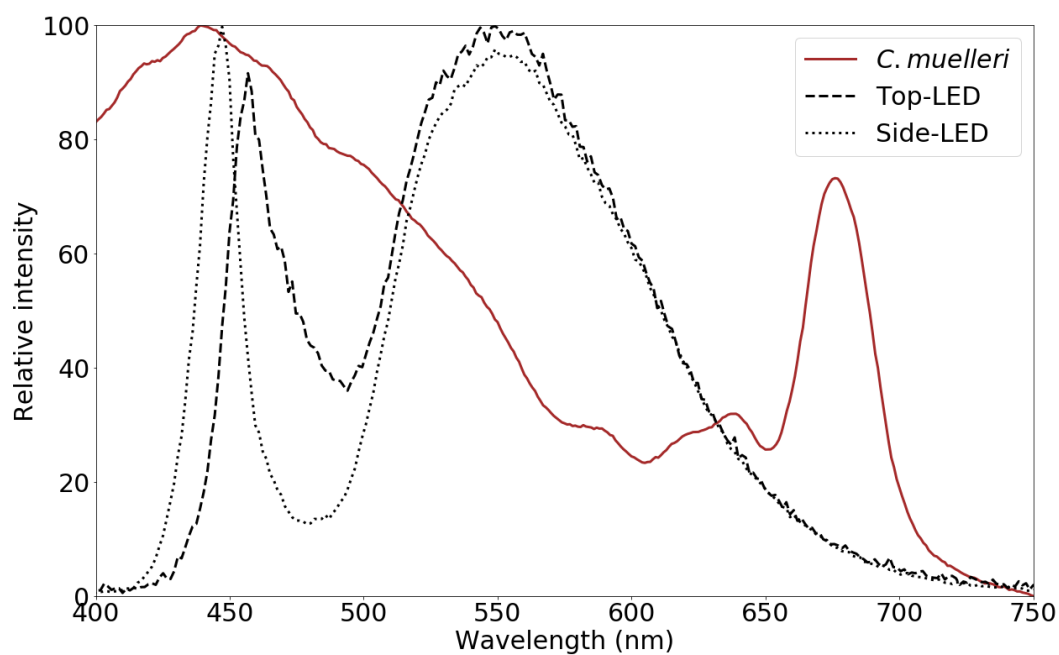
*Chaetoceros muelleri* from the Caribbean as food for the native scallops, *Argopecten nucleus* and *Nodipecten nodosus*', *Latin American Journal of Aquatic Research*, 44(3), pp. 557–568.

Wang, X.-W., Liang, J.-R., Luo, C.-S., Chen, C.-P. and Gao, Y.-H. (2014) 'Biomass, total lipid production, and fatty acid composition of the marine diatom *Chaetoceros muelleri* in response to different CO<sub>2</sub> levels', *Bioresource Technology*, 161, pp. 124–130. doi: 10.1016/j.biortech.2014.03.012.

Yun, Y. S. and Park, J. M. (2001) 'Attenuation of monochromatic and polychromatic lights in *Chlorella vulgaris* suspensions', *Applied Microbiology and Biotechnology*, 55(6), pp. 765–770. doi: 10.1007/s002530100639.

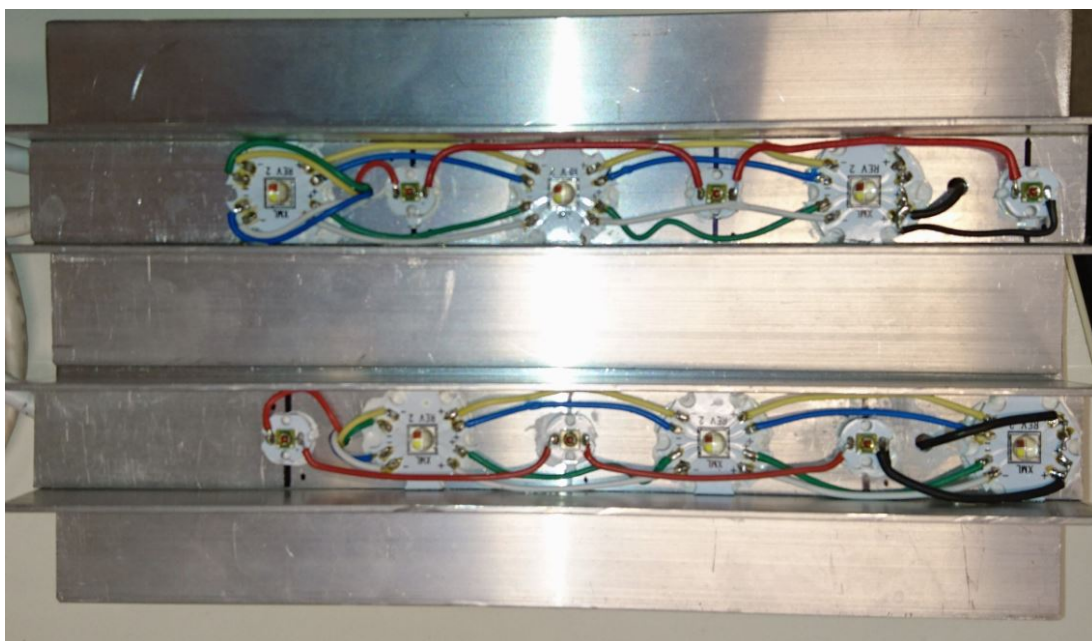
Zeebe, R. E. and Wolf-Gladrow, D. A. (2001) *CO<sub>2</sub> in seawater : Equilibrium, kinetics, isotopes*. 1st Ed. Amsterdam: Elsevier.

## 2.8. Supplementary Materials

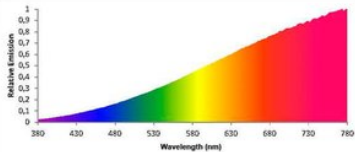
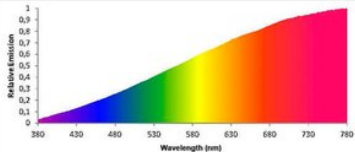
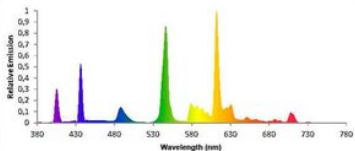
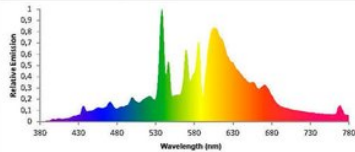
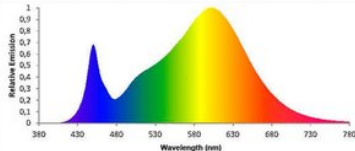
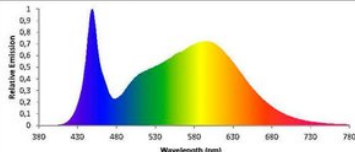
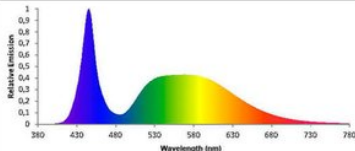


**Figure 2.13** The relative absorption spectra of *C. muelleri* represented with brown line and the spectra of the two LEDs used in this study: Top-LED represented as a broken black line and Side-LED represented as a black dotted line.





**Figure 2.14** View of the LED chips and their arrangements in the custom LED panel used in the study. The larger chips are the CREE® XLamp® XM-L Color and the smaller chips are the Cree® XLamp® XP-E photo-red.

Description	Spectrum	System power consumption, measured (W)	Lamp or module luminous flux, measured (lm)	System luminous efficacy (lm/W)	Energy conversion efficiency	Theoretical maximum luminous efficacy (lm/W)
High voltage halogen, 120 W		127,4	2.249	17,7	11,9	148,7
Low voltage halogen, 60 W		59,9	1.535	25,6	15,4	166,3
Fluorescent lamp T 5, 54 W, 830		51,3	4.184	81,6	23,7	344,4
Metal halide lamp, 70 W, 830		79,8	7.912	99,2	31,5	314,5
LED, 35 W, 830		34,2	4.739	138,6	42,3	327,6
LED, 35 W, 840		34,5	4.806	139,3	43,7	318,8
LED, 16 W, 750		16,2	2.436	150,5	48,7	309,0

**Figure 2.15** Comparison of conventional light sources with white LEDs of varying

spectra. Power consumption (W), maximum intensity in lumens (lm), light output

(lm/W), energy conversion efficiency (%) and theoretical maximum output (lm/W) are

shown. Sourced from article published on DIAL website

(<https://www.dial.de/en/blog/article/efficiency-of-leds-the-highest-luminous-efficacy-of-a-white-led/>).

## **Chapter 3 Investigating the Effect of Light Quality on Primary Metabolite Production by *Chaetoceros muelleri***

Kenji Iwasaki, Milán Szabó, Bojan Tamburic, Christian Evenhuis,

Unnikrishnan Kuzhiumparambil & Peter Ralph

Climate Change Cluster (C3), Faculty of Science, University of Technology Sydney,

Australia

### **3.1. Introduction**

#### **3.1.1. Diatoms**

Diatoms (Bacillariophyceae) are a distinct group of microalgae with their most unique feature being its siliceous cell wall (Lebeau and Robert, 2003b; Hildebrand *et al.*, 2012).

Diatoms are one of the most species-rich groups of microalgae, with recent estimates varying from 20,000 (Guiry, 2012) to up to 200,000 species (Mann and Vanormelingen, 2013). They are responsible for a significant portion (20-35%) of the marine primary productivity (Nelson *et al.*, 1995; Falkowski, Barber and Smetacek, 1998; Field *et al.*, 1998; Scala and Bowler, 2001) and approximately 20% of the global carbon fixation (Tréguer, Nelson and Bennekom, 1995). They also dominate the biogeochemical cycling of marine silicon (Tréguer, Nelson and Bennekom, 1995; Martin-Jezequel, Hildebrand and Brzezinski, 2000). Diatoms are exceptionally robust and have been

known to inhabit virtually all photic zones from tropic to arctic environments, with some diatoms possessing the capacity to produce ice-binding proteins to protect the cells from freezing (Janech *et al.*, 2006; Sims, Mann and Medlin, 2006). In part, due to this high degree of physiological flexibility to grow in a range of environments, diatoms can potentially be cultured to produce biotechnologically relevant metabolites.

Applications for such metabolites include utilisation in cosmetics, food supplements, nano-materials, pharmaceuticals, aquaculture feed, as well as a feedstock for biofuels (Bozarth, Maier and Zauner, 2009; Williams and Laurens, 2010).

### 3.1.2. Importance of diatoms in aquaculture

Diatoms have been cultured in large-scale production systems for aquaculture feed for decades (Lebeau and Robert, 2003a). Diatoms are particularly important in feeding bivalve, mollusc and shrimp larvae (Brown *et al.*, 1997; Lebeau and Robert, 2003b). Of the hundreds of microalgal species tested as feed for aquaculture species in the past forty years, fewer than twenty species are used in commercial aquaculture today, of which notable diatom species include: *Chaetoceros* sp., *Thalassiosira* sp., *Skeletonema* sp. and *Nitzschia* sp. (Brown, 2002). The reason for this small number is because microalgal species require particular characteristics to be considered suitable as aquaculture feeds. Firstly, they must be of a suitable size for ingestion (e.g. 1-15 µm for

filter feeders and 10-100  $\mu\text{m}$  for grazers) and readily digestible (Webb and Chu, 1983; Jeffrey, Leroi and Brown, 1992; Kawamura, Roberts and Nicholson, 1998). Secondly, they must have a fast growth rate, must be amenable to mass culture, and tolerate fluctuations in temperature, light and nutrients which may occur in outdoor hatchery sites (Brown, 2002). Lastly, they must not contain any toxins or other deleterious constituents which will accumulate in the food chain, and should have suitable nutritional content for larval growth (Brown, 2002; Spolaore *et al.*, 2006).

Nutritional value of microalgae feeds has been a focus of research in aquaculture (Brown, 2002; Blackburn and Volkman, 2012; Guedes and Malcata, 2012). Particular lipids such as polyunsaturated fatty acids (PUFAs) have been identified as an essential dietary requirement for marine animals (Nichols, 2003), as well as for the growth of many larvae (Becker, 2004). Among the various groups of microalgae, diatoms contain high levels of the PUFAs eicosapentaenoic acid (EPA C20:5 omega-3) with a balanced level of docosahexaenoic acid (DHA C22:6 omega-3) and arachidonic acid (ARA C20:5 omega-6) which have been shown to benefit larval growth (Blackburn and Volkman, 2012).

In addition to their high lipid content, some diatom species contain high amounts of vitamins which improve growth of aquaculture species. Thiamine (vitamin B<sub>1</sub>) is an example of a vitamin which has been shown to improve growth of juvenile abalone

(*Haliotis discus hannoi* Ino) (Zhu, Mai and Wu, 2002) and juvenile Jian carp (*Cyprinus carpio* var. Jian) (Huang *et al.*, 2011). Brown *et al.* (1999) showed both *Chaetoceros muelleri* and *Thalassiosira pseudonana*, two important diatom species in aquaculture, containing high levels of thiamine under stationary growth phase, with amounts of 125 µg and 90 µg of thiamine per gram of dry weight, respectively.

### 3.1.3. Importance of *Chaetoceros muelleri* in aquaculture

From the microalgae tested for the criteria mentioned above, *Chaetoceros muelleri* (*C. muelleri*) has become a particularly important species in aquaculture.

*Chaetoceros muelleri* is a marine diatom and is a particularly valuable species in the aquaculture industry in Australia and Mexico (Brown *et al.*, 1997; López Elías *et al.*, 2003). It is widely used in feeding larvae of scallops, prawns and oysters (Brown *et al.*, 1997).

*Chaetoceros muelleri* has been found to contain more ascorbic acid and riboflavin than other common aquaculture microalgae (Brown *et al.*, 1997). Its common usage in aquaculture is linked to increases in larval development and survivability which is attributed to a high proportion of unsaturated fatty acids such as: palmitoleic acid, hexadecadienoic acid and EPA (D'Souza and Loneragan, 1999). It was also a species previously found to contain suitable amounts of the three important PUFAs:

ARA, EPA and DHA (Parrish *et al.*, 1998; D'Souza and Loneragan, 1999). Overall, this makes *C. muelleri* an important species in terms of nutritional value and promoting survivability in the aquaculture industry.

The increasing understanding of diatom biochemical and physiological capacity has steadily increased the potential of diatoms as a candidate for other industrial applications (Lebeau and Robert, 2003a, 2003b). In order to optimize diatom production for industrial applications, one must consider many environmental factors that affect growth, such as: temperature (Montagnes and Franklin, 2001), nutrient concentration (Fabregas *et al.*, 1986), and irradiance (Falkowski, Dubinsky and Wyman, 1985). The impact of these abiotic factors on biomass production and metabolite composition have been extensively characterized; however, the implementation of such research in aquaculture has been less common.

#### 3.1.4. Light emitting diodes and their potential role in aquaculture

As previously discussed in Chapter 2, many aquaculture facilities rely on fluorescent and metal halide lamps as light sources. Light emitting diodes (LEDs) offer several economic advantages over these traditional light sources, such as: lower heat generated when emitting light, has longer life-expectancy (up to 50,000 h) and have higher energy conversion efficiency (produce more light per Watt) (section 2.1.5). As seen in Chapter

2, increased biomass and growth rates were achieved in *C. muelleri* with higher light and carbon availability. Also, conventional light sources (such as fluorescent lamps) have a wide emission spectrum which include wavelengths that are not generally used by microalgae.

### 3.1.5. Selecting light quality to grow microalgae

When considering a light source for growing microalgae two properties are vital for high biomass productivity: light quality and intensity (Lee, 1999). While light intensity and its impact on growth has been relatively well characterised (Thompson, Harrison and Parslow, 1991; Carvalho *et al.*, 2011; Beardall and Raven, 2013), light quality and its impact on growth and the metabolic content is not well understood in diatoms.

Light quality or spectral quality refers to the spectral distribution of wavelengths and their intensity of the chosen light source used to grow photosynthetic microalgae. Light quality can be described as being either monochromatic or polychromatic.

Monochromatic light refers to a light source that has a single narrow-band emission spectrum (e.g. single wavelength LEDs) and polychromatic light being a light source that has a wideband emission spectrum (e.g. sunlight, white LEDs, fluorescence lamps).

It is also noteworthy that white LEDs will vary in light quality depending on the type, “warm-white” LEDs will have a pronounced red spectra, while a “cool-white” LED will



have a pronounced blue spectra. This should be noted when selecting and examining results of different studies using white LEDs (Glemser *et al.*, 2016).

In selecting light quality, one must consider the photosynthetic pigments of the desired microalgae. Microalgae typically capture light with 3 main groups of photosynthetic pigments: chlorophyll, phycobilins and carotenoids (Metting, 1996). The common chlorophylls (*a*, *b*, and *c*) have major absorption bands in blue ( $\approx 430\text{-}475\text{ nm}$ ) and red ( $\approx 630\text{-}675\text{ nm}$ ), and other groups of pigments are present to extend the range of light absorption, these include phycobilins (520-670 nm) and carotenoids (400-550 nm) (Falkowski and Raven, 2007; Nobel, 2009; Schulze *et al.*, 2014). The pigment composition of phototrophs can vary greatly between phyla, classes and species. For example, green algae generally possess Chl *a* and *b* as well as the primary carotenoid violaxanthin, while cyanobacteria and red algae possess Chl *a* and phycobilins and diatoms possess Chl *a* and *c* as well as the primary carotenoid fucoxanthin (Bertrand, 2010; Borowitzka, 2013; Richmond, 2004; Schulze *et al.*, 2014).

Carotenoids consist of two main classes: carotenes (e.g.  $\alpha$ -carotene,  $\beta$ -carotene) and xanthophylls which collectively fulfil a vital role in both light capture and photoprotection via a mechanism known as the xanthophyll cycle (Jin *et al.*, 2003; Falkowski and Raven, 2007). The xanthophyll cycle is triggered in phototrophs exposed to excessive light via the enzymatic interconversion between xanthophyll pigments to

dissipate excess energy (Lohr and Wilhelm, 1999; Müller, Li and Niyogi, 2001). For example, in higher plants and green algae the cycling of violaxanthin, antheraxanthin and zeaxanthin is present as the violaxanthin cycle (Lohr and Wilhelm, 1999; Falkowski and Raven, 2007; Bertrand, 2010) and in dinoflagellates the cycling of diadinoxanthin and diatoxanthin is present as the diadinoxanthin cycle (van de Poll and Buma, 2009).

While phototrophs using xanthophyll cycles generally use either the violaxanthin cycle or the diadinoxanthin cycle, some diatoms are unique in having the capacity to use both xanthophyll cycles, the violaxanthin cycle and the diadinoxanthin cycle (Lohr and Wilhelm, 1999). Additionally to the photoprotective role, xanthophylls such as fucoxanthin play a critical role in light capture by absorbing blue/green light which chlorophylls are unable to absorb (Papagiannakis *et al.*, 2005). Since blue/green is the dominant region of light in deep waters, fucoxanthin therefore gives diatoms a competitive advantage by being able to harness this light for photosynthesis (Shimura and Fujita, 1975). As well as their activity in light capture, fucoxanthin have been thought to provide beneficial bioactivity in aquaculture feed by improving survivability (Kawakami *et al.*, 1998).

### 3.1.6. Defining cost efficiencies in using LEDs for microalgae culturing

Operational costs of running microalgal production facilities in commercial hatcheries are known to be high, approximately 30 – 40% of total hatchery operational costs (Borowitzka, 1997; Knauer and Southgate, 1999; Camacho-Rodríguez *et al.*, 2016; Nielsen *et al.*, 2017).

Hence, in assessing LEDs for use in hatcheries for microalgal production, the cost efficiency should be taken into account. While LEDs are generally superior to conventional light sources (section 2.1.5), in order to select LEDs that will be most cost efficient the light quality must be suitable for the desired microalga. For instance, of all LEDs, white LEDs are used most commonly in microalgal research (Crawford, 2009; Carvalho *et al.*, 2011; Lucker *et al.*, 2014; Tamburic *et al.*, 2014; Glemser *et al.*, 2016).

However, some studies comparing multiple LED light qualities on the growth and energy efficiency in various microalgae species indicate that white LEDs may not be the most productive (Wang, Fu and Liu, 2007; Okumura *et al.*, 2015). Okumura *et al.*

(2015) assessed the economic efficiency (mg dry biomass per watt per day per mL per \$) of different LEDs (OptoSupply, Asada Electronic, Japan) on the green algae

*Botryococcus braunii* (NIES-836). Okumura *et al.* (2015) observed the highest growth rate and energy efficiency using blue LEDs (OSUB5161P) which was almost five times more efficient at producing the same amount of biomass than white LEDs (unspecified).

Additionally, red LEDs (OSHR5161P) were approximately twice as efficient compared to white and green LEDs (OSPG5161P), which were almost identical in performance (Okumura *et al.*, 2015). In a similar study, the growth rate and economic efficiency (g dry biomass per L per \$) of different LEDs (OSRAM, Germany) were assessed on the cyanobacterium *Arthrospira platensis* (Nordstedt) Gomont (ATCC-29408) (Wang, Fu and Liu, 2007). Compared to *B. braunii* in Okumura *et al.* (2015), Wang, Fu and Liu (2007) observed that blue, yellow and green LEDs (AL-R1001NB, AL-R1001NY, AL-R1001NG respectively) were very inefficient at growing *A. platensis*, while white LEDs (AL-R10001NW) were quite economically efficient. However, red LEDs were determined to have the highest growth rate and economic efficiency at producing the same amount of biomass (Wang, Fu and Liu, 2007). In the work by Okumura *et al.* (2015), all light qualities were set at the same light intensity of  $30 \mu\text{mol photons m}^{-2} \text{s}^{-1}$  on a 12:12 (light:dark) cycle and in the work by Wang, Fu and Liu (2007), all light qualities were set at the same light intensities in increments from 750 to 3000  $\mu\text{mol photons m}^{-2} \text{s}^{-1}$ , while the light:dark cycle was not specified. In investigating the effects of light quality, it was determined that cost efficiency of each light quality will be vital information for the aquaculture feed industry to assess the viability of LEDs of different light quality at producing microalgal feed.

### 3.1.7. Balancing light quality

Before using different wavelengths to culture microalgae, one must consider that different wavelengths of light are not utilized for photosynthesis equally. This is because photons of different wavelengths are absorbed proportionally to their antenna pigments; therefore, the pigment composition will determine the efficiency of absorbing photons of differing light quality (Schreiber, Klughammer and Kolbowski, 2011). Costa *et al.* (2013), Jungandreas *et al.* (2014) and Valle *et al.* (2014) had recognized this and had adjusted the irradiance of each wavelength by calculating either photosynthetically absorbed radiation ( $Q_{\text{phar}}$ ) according to Gilbert *et al.* (2000) or photosynthetically utilizable radiation (PUR) (Morel, 1978). The light quality will also be affected by the degree of attenuation in the water column, while this is less significant in smaller scale photobioreactor (with shorter path lengths), in larger scale photobioreactor (with longer light path lengths) this will significantly affect the light availability of cultures. For example, Costa *et al.* (2013) used  $120 \mu\text{mol photons m}^{-2} \text{s}^{-1}$  of white light,  $123 \mu\text{mol photons m}^{-2} \text{s}^{-1}$  of red light and  $72 \mu\text{mol photons m}^{-2} \text{s}^{-1}$  of blue light to achieve a balanced irradiance level by calculating  $Q_{\text{phar}}$  between each light quality (Costa *et al.*, 2013). Hence, experiments that set a constant irradiance for all wavelengths (e.g. Okumura *et al.* 2015; Wang, Fu and Liu (2007)) may be inadvertently observing light intensity effects when attempting to measure effects of light quality. Therefore, in order

to correctly observe the effect of wavelength dependent responses from diatoms, the photons absorbed by each wavelength must be normalized, by methods such as:  $Q_{\text{phar}}$  (Gilbert *et al.*, 2000), PUR (Morel, 1978) or absolute rate of photosystem II (PSII) turnover per quanta (PAR(II)) (Schreiber, Klughammer and Kolbowski, 2012). It is also difficult to compare experiments that investigate different wavelengths or different microalgal species as some publications do not disclose the spectra or peak wavelength of light quality investigated. Therefore, it is essential to characterise and quantify the metabolites of high nutritional value under defined light qualities. As previously discussed, LEDs produce higher intensities, have longer life expectancy (up to 50,000 h) and generate  $\approx 10\%$  less heat when converting energy into photons compared to conventional fluorescence lamps (Carvalho *et al.*, 2011).

However, in order to evaluate the different light qualities to grow microalgae, one must also assess the photosynthetic performances during the growth; which is often difficult to measure *in situ*. Hence, rapid light curves were explored as a technique to estimate photosynthetic performances of microalgae grown in different light qualities.

### 3.1.8. Measuring photosynthetic performance from cultures grown using different light qualities

The photosynthetic performance of microalgae as a function of increasing irradiances can be observed with a standard photosynthesis vs. irradiance (PI) curve. Steady-state light curves (SSLC) were used in Chapter 2 (section 2.4.3) to measure the long-term acclimation states and potential photosynthetic performance which are less influenced by previous light history. In this study, rapid light curves (RLC) were used to measure short-term acclimation and effective photosynthetic capacity. Unlike SSLC, RLC are strongly influenced by previous light history (e.g. light intensity, light quality), hence 'effective' photosynthetic capacity (Ralph and Gademann, 2005; Herlory, Richard and Blanchard, 2007; Perkins *et al.*, 2010; Houliez *et al.*, 2017). Another key distinction is that a steady state light curve (SSLC) measures photosynthesis rate at steady state (i.e. each irradiance interval is long enough ( $\geq 5$  min) to allow photosynthetic processes to stabilize) (2.1.5 for details). Rapid light curves are measured with short irradiance interval ( $< 10$  s), which does not allow for photosynthetic processes to stabilize (Ralph and Gademann, 2005; Perkins *et al.*, 2010; Houliez *et al.*, 2017). Both SSLC and RLC have three regions: the rise of the curve in the light limited region ( $\alpha$ ) which is virtually linear as irradiance increases, the light-saturated region, which begins at the minimum saturating irradiance ( $I_k$ ) which is determined by finding the intercept of  $\alpha$  with the

maximum relative electron transfer rate between PSII and photosystem I (PSI) ( $rETR_{max}$ ) and the light inhibited region ( $\beta$ ) where relative electron transfer rate ( $rETR$ ) begins to decrease as irradiance increases (Sakshaug *et al.*, 1997; MacIntyre *et al.*, 2002; Schreiber, 2005).

### 3.1.9. Light quality research in diatoms

Research in light quality using LEDs to investigate growth, high value products or cost efficiencies have been more common in green algae, red algae and cyanobacteria (Katsuda *et al.*, 2004; Wang, Fu and Liu, 2007; Fu *et al.*, 2013; Okumura *et al.*, 2015; Baer *et al.*, 2016; Schulze *et al.*, 2016). In diatoms, investigation has focused on physiology, such as chloroplast migration (a phenomena typically observed when chloroplast migrate to the nucleus to avoid strong light) (Furukawa, Watanabe and Shihira-Ishikawa, 1998), sinking rate (Fisher, Berges and Harrison, 1996) and zygote germination (Shikata *et al.*, 2011). More recent research investigating light quality in diatoms have focused on photophysiology and have aimed to understand the influence of light quality on photoacclimation and photoprotection in model diatoms such as *Phaeodactylum tricornutum* (Costa *et al.*, 2013; Jungandreas *et al.*, 2014; Valle *et al.*, 2014).



There are however other examples investigating light quality in different microalgae that demonstrate the potential for this approach to be utilized in aquaculture hatcheries. For instance, it has been demonstrated that blue/green light, as well as red light increased lipid content in *Chlorella* sp. (Pérez-Pazos and Fernández-Izquierdo, 2011; Shu *et al.*, 2012). In *Isochrysis* sp., cultures grown under blue fluorescent tubes exhibited higher protein content compared to standard white fluorescent tubes (Marchetti *et al.*, 2013). In both *Nannochloropsis oceanica* and *Tetraselmis suecica*, an increase in EPA content was observed under red LEDs, as well as blue LEDs in *N. oceanica* (Chen *et al.*, 2013; Abiusi *et al.*, 2014). While these examples indicate the potential for increasing the nutritional content in some microalgae, most exhibit relatively low growth rates (Pérez-Pazos and Fernández-Izquierdo, 2011; Shu *et al.*, 2012; Abiusi *et al.*, 2014). This may be indicative of the relatively low light intensities used in these studies (approximately 20 – 150  $\mu\text{mol photons m}^{-2} \text{ s}^{-1}$ ) (Pérez-Pazos and Fernández-Izquierdo, 2011; Shu *et al.*, 2012; Abiusi *et al.*, 2014). However, in the diatom *P. tricornutum*, Costa *et al.* (2013) and Jungandreas *et al.* (2014) concluded that under low irradiances (calculated  $Q_{\text{phar}}$ ) of blue, red and white light (24  $\mu\text{mol photons m}^{-2} \text{ s}^{-1}$ , 41  $\mu\text{mol photons m}^{-2} \text{ s}^{-1}$  and 40  $\mu\text{mol photons m}^{-2} \text{ s}^{-1}$  respectively) no significant differences in growth rate ( $\approx 0.43 \mu \text{ day}^{-1}$ ) were observed.

In order to further evaluate light quality as a strategy for use in hatcheries, light qualities must be tested at higher irradiances for it to be economically viable.

### **3.2. Aims and Objectives**

While the study of microalgae cultivated using different light qualities by LEDs have steadily increased in recent years, important gaps in the knowledge still exist as to how diatoms respond to light quality. The metabolic response of diatoms to light quality, and how that may improve growth, cultivation yields and cost efficiency of diatom cultivation in aquaculture remains poorly described. The present study will investigate the effect of light quality on the growth rate, primary metabolite content and photosynthetic response of *C. muelleri* by applying blue, green and red monochromatic light, as well as white light and assess their cost efficiency in producing biomass and metabolites.

The goal of this work is to investigate the effects of light quality on growth rate and primary metabolite production. This will provide information for industries such as aquaculture, cosmetics and pharmaceuticals to potentially tailor the light quality to increase production of desired primary metabolites using a non-invasive and simple techniques that may change the conventional culturing standard which uses traditional light sources for diatom culturing.

### 3.3. Material and Methods

#### 3.3.1. Culturing *Chaetoceros muelleri*

*Chaetoceros muelleri* (Lemmermann, 1898) (CS-176) obtained from the Australian National Algae Culture Collection (ANACC; CSIRO, Hobart, Australia) was grown in artificial seawater enriched with F/2 nutrients with silica following the methods of Guillard (1975). Artificial seawater was prepared by filter-sterilising artificial sea salt (Aquasonic) dissolved in Milli-Q water through a 0.2  $\mu\text{m}$  filter made to 35 practical salinity units (PSU). Stock cultures were maintained in 250 mL conical flasks in an incubator (Labec Pty. Ltd.) at 22°C under white LEDs with a 12 h:12 h light:dark cycle with an incident irradiance of approximately 40  $\mu\text{mol photons m}^{-2} \text{s}^{-1}$ .

#### 3.3.2. Photobioreactor system

*Chaetoceros muelleri* was cultured in photobioreactors (ePBR, Phenometrics, Lansing, MI, USA) with an inverted conical frustum geometry and a working volume of 450 mL (Figure 3.2; Tamburic *et al.*, 2014). Temperature was constantly maintained at  $22 \pm 0.5^\circ\text{C}$  using a peltier heater-cooler jacket and logged every 5 min with a temperature sensor (Phenometrics, Lansing, MI, USA). All ePBRs were aerated constantly with 0.2  $\mu\text{m}$  filtered (oil-free) ambient air ( $\text{CO}_2 \approx 0.04\%$ ) which was humidified by passing it through Milli-Q water and delivered from the bottom of the

vessel with a 0.4 mm hypodermic needle. pH was maintained via 5% CO<sub>2</sub> addition (Food Grade, BOC) using an inbuilt solenoid valve programmed to maintain the pH at approximately  $8.0 \pm 0.2$ . CO<sub>2</sub> was bubbled from the bottom of the ePBR with syringe needles (5/10 ADT (N) 6cm); SGE Analytical Science, Ringwood, VIC, Australia). The ePBR culture was magnetically stirred at a rate of 120 rpm.

### 3.3.3. Growth light

A custom LED (Side-LED) panel was built to fit between the two peltier heater-cooler units both front and back of the ePBR (Figure 3.2). Six LED chips (3 CREE® XLamp® XM-L Color and 3 Cree® XLamp® XP-E photo-red) were used for the custom LED panel. The chips were arranged equidistant apart and arranged in an alternating pattern between panels to avoid bright and dark spots in the water column, such that the light was as homogenous as possible (Figure 3.13 in Supplementary Materials). Four LED colours: blue, green, red, and white was used to culture *C. muelleri*. Emission spectra of the LED panel was measured with a Jaz spectrometer (Ocean Optics, USA) shown in Figure 3.1 alongside the absorption spectra of *C. muelleri* which was measured with a microplate reader (Infinite 200 PRO, Tecan, Switzerland). To ensure the irradiance is balanced between the colours, photosynthetically usable radiation (PUR) of 500  $\mu\text{mol}$

photons  $\text{m}^{-2} \text{s}^{-1}$  equivalent of white light was estimated based on the work by Morel (1978) (Eqn. 3.1).

$$\text{PUR} = \text{PAR}(a_{\phi}/a_{\phi_{\max}}) \quad \text{Eqn. 3.1}$$

where  $a_{\phi}$  is the mean absorption and  $a_{\phi_{\max}}$  is the maximum absorption ( $\approx 440 \text{ nm}$ ).

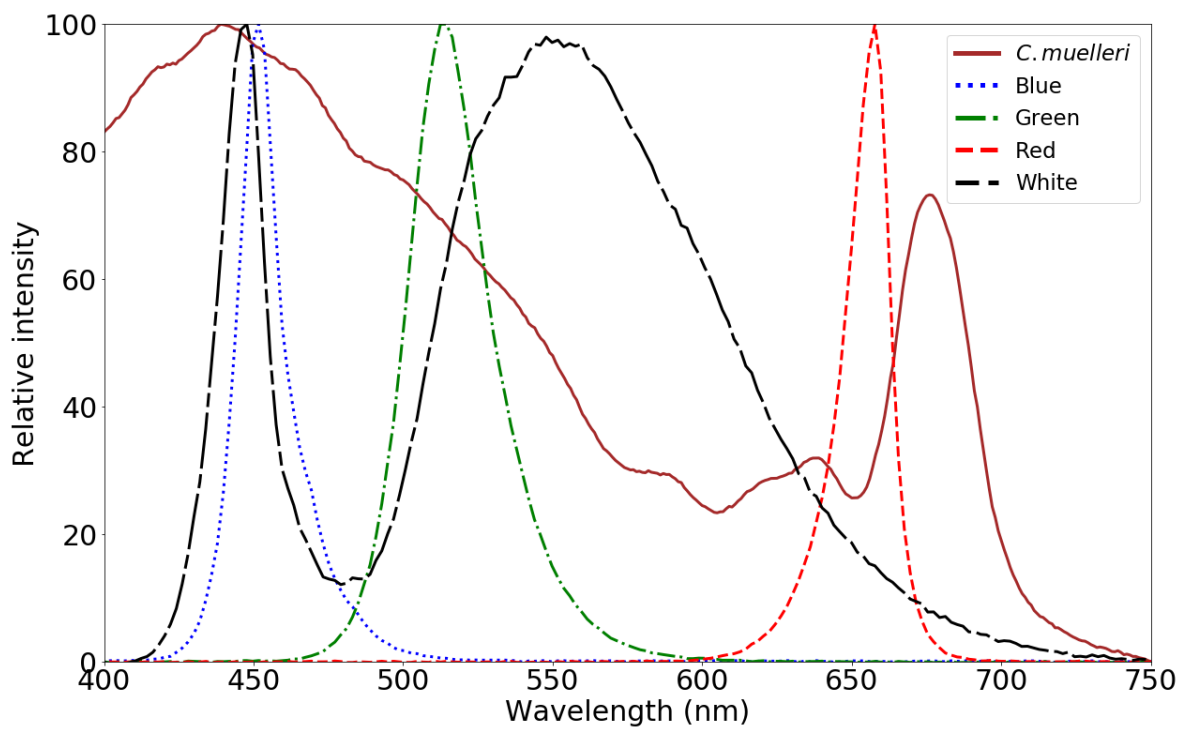


**Figure 3.1** Wavelength spectra of LEDs used in experiment and the relative absorption spectra of *C. muelleri*. Brown line represents the absorption spectra of *C. muelleri*, blue dotted line represents blue LED spectra, green ‘line & dot’ style line represents green LED spectra, red broken line represents red LED spectra, and black ‘long line & short line’ style line represents white LED spectra.

From Eqn. 3.1, PUR in  $\mu\text{mol photons m}^{-2} \text{ s}^{-1}$  was calculated to be approximately 371, 455 and 655 for blue light, green light and red light respectively which is estimated to be the equivalent of 500  $\mu\text{mol photons m}^{-2} \text{ s}^{-1}$  white light. The PUR calculated was found to be similar in ratio to other estimation methods, for example, the ratio of blue:red in Jungandreas *et al.* (2014) was  $\approx 1.71$  (for each blue photon there are 1.7 red photons) and the ratio of blue:red in this study was  $\approx 1.76$ .

In summary, *C. muelleri* cultured using: blue light (BL) were illuminated with 371  $\mu\text{mol photons m}^{-2} \text{ s}^{-1}$ , green light (GL) were illuminated with 455  $\mu\text{mol photons m}^{-2} \text{ s}^{-1}$ , red light (RL) were illuminated with 655  $\mu\text{mol photons m}^{-2} \text{ s}^{-1}$  and white light (WL) were illuminated with 500  $\mu\text{mol photons m}^{-2} \text{ s}^{-1}$ . All cultures were allowed to pre-acclimate to the respective light quality for seven days (Jungandreas *et al.* 2014). Cultures were operated as a semi-batch mode on a 12 h:12 h (light:dark) cycle.

#### 3.3.4. Calculating growth rate

Cell counts were recorded twice a day throughout the experiment, 2 h after the start of light cycle and 2 h before the end of light cycle (2.4.5 for details). Specific growth rate ( $\mu$ ) was calculated using Eqn. 3.2 outlined in Wood, Everroad and Wingard (2005) (Harrison, Thompson and Calderwood, 1990; Borowitzka and Moheimani, 2013; Huang

*et al.*, 2013; Gorai *et al.*, 2014; Han *et al.*, 2017). Doubling time ( $t_d$ ) was calculated using Eqn. 3.3.

$$\mu = \frac{\ln(N_1/N_0)}{t_1 - t_0} \quad \text{Eqn. 3.2}$$

where  $\mu$  = specific growth rate,  $N_1$  and  $N_0$  are cell densities in  $\text{mL}^{-1}$  at  $t_1$  = final time (day three) and  $t_0$  = initial time.

$$t_d = \frac{\ln(2)}{\mu} \quad \text{Eqn. 3.3}$$

where  $\mu$  = specific growth rate.

During the experiment, cultures were maintained under semi-batch mode, where cultures were grown to a target cell density of  $> 6 \times 10^6$  cells  $\text{mL}^{-1}$  for harvesting and diluted to the starting cell density of  $\approx 5 \times 10^5$  cells  $\text{mL}^{-1}$  after each experimental cycle. BL, GL and WL cultures were grown under a growth cycle of 3 days and RL cultures given 5 days, as its growth rate was significantly slower during preliminary experiments (data not shown). The spectra and light intensity of each light quality is detailed in section 3.3.3. The growth cycle time was determined based on the biomass requirements for chemical analysis of total protein, total lipids, fatty acid methyl esters (FAME), and total carbohydrates (3.3.10, 3.3.11 & 3.3.12). Biomass (dry weight) was measured at the end of each cycle, however due to low culture volume, dry weights were not taken periodically during each cycle.

### 3.3.5. Light measurements and calibration

A quantum  $4\pi$  sensor (4-pi LI-COR Inc., Lincoln, Nebraska, U.S.) and light meter (LI-250A, LI-COR Inc., Lincoln, Nebraska, U.S.) was used to calibrate the initial photon flux density (PFD) in media with no cells and measure the PFD at the longest path length of the ePBR vessel to determine the light attenuated by the culture (Figure 3.2).

The  $4\pi$  sensor (after sterilizing with 75% ethanol) was suspended approximately 2.5 cm inside the culture to measure PFD from the centre of the culture. The attenuation was measured twice a day prior to sampling for cell counts.

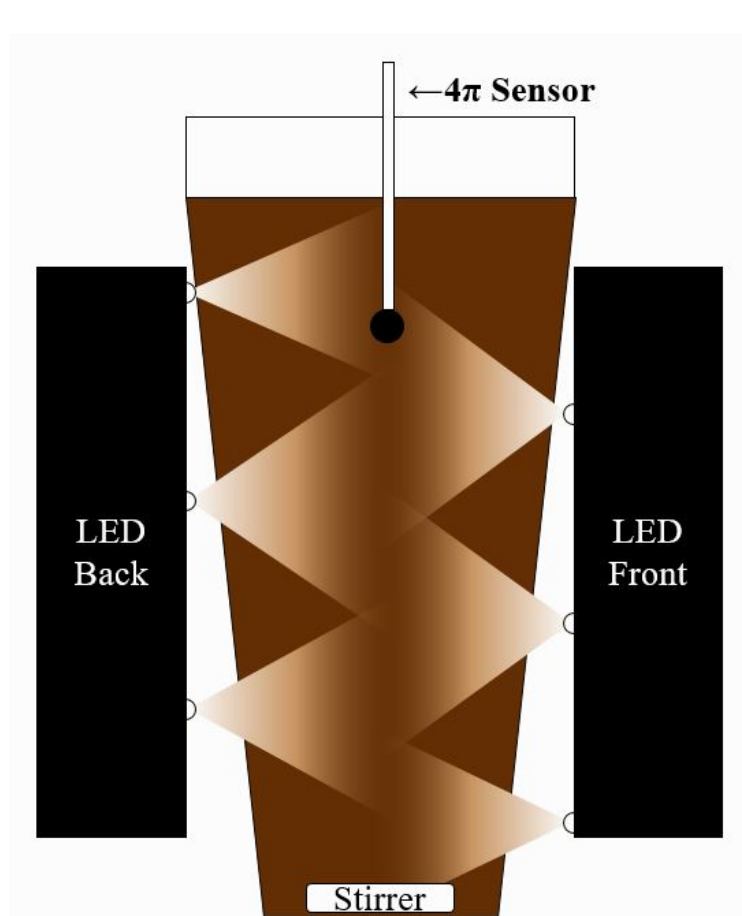


**Figure 3.2** Schematic of ePBR geometry (inverted conical frustum) and light

measurement. A quantum  $4\pi$  sensor were used to measure PFD *in situ*. There are three



LED chips in each LED panel mounted at the front and back of ePBR vessel. LED illumination is showed for demonstrative purposes and are not illustrative of the actual LED emission angles.

### 3.3.6. Dissolved oxygen measurements and measuring net photosynthesis using optical sensors

Dissolved oxygen (DO) was logged every 30 s (FireSting logger, PyroScience GmbH) with 3 mm oxygen optical minisensors with optical isolation (OXROB10-OI, PyroScience GmbH). A two-point calibration against air-saturated water and sodium dithionate solution (zero DO) was performed prior to all experiments. A solenoid valve (SMC Pneumatics Pty. Ltd.) controlled via an Arduino was used to intermittently stop the aeration in the ePBRs for 10 min every 2 h to monitor the linear change of DO concentration due to photosynthesis during the light cycle and respiration during the dark cycle, respectively. Net photosynthesis (photosynthesis – respiration) and respiration rates were calculated by applying a linear regression to each increase in DO, which is then normalized to cell density (Tamburic *et al.*, 2015, 2018).

### 3.3.7. Rapid light curve measurement

The multi-colour pulse amplitude modulation fluorometer (MC-PAM, Heinz Walz GmbH, Germany) was used to measure RLC (Eqn. 3.4; Schreiber, Klughammer and Kolbowski, 2012). Cultures of *C. muelleri* grown using different light qualities were sampled at midday of the first ( $t_0$ ) and last day ( $t_f$ ) of each growth cycle to evaluate the photosynthetic performance of each light quality. Sample volumes were 2 mL for  $t_0$  samples (dilute culture) and 0.5 mL for  $t_f$  samples (dense culture). Dense culture samples ( $t_f$ ) were diluted with F/2 media to normalise  $F_0$  to similar values ( $F_0 \approx 1.2$ ). A set of increasing light intensities (PAR list) used for the RLC measurement was determined by calibrating the MC-PAM LEDs with the  $4\pi$  sensor attached to the MC-PAM using the calibration mode of the PamWin-3 software (Walz GmbH, Germany). The PAR list determined was: 4, 21, 40, 78, 116, 173, 247, 339, 482, 638, 804, 997, 1183, 1408, 1672, 1935, 2229, 2620, 3018 and 3559  $\mu\text{mol photons m}^{-2} \text{s}^{-1}$  of white light.

Measuring light and saturation pulse intensity of the MC-PAM LEDs were determined to be approximately 0.4  $\mu\text{mol photons m}^{-2} \text{s}^{-1}$  (440 nm) and approximately 2900  $\mu\text{mol photons m}^{-2} \text{s}^{-1}$  (white light) respectively and saturation pulse length was 0.8 s. White light was used as actinic light and 440 nm was used as measuring light. Each irradiance interval was set to 10 s. Empirical data was fitted to the function detailed in Platt,

Gallegos and Harrison (1980) (Eqn. 3.4) using the curve fitting protocol of PamWin-3 (Schreiber, Klughammer and Kolbowski, 2012).

$$P = P_{max}(1 - e^{-\alpha I/P_{max}})e^{-\beta I/P_{max}} \quad \text{Eqn. 3.4}$$

where  $P$  is rate of photosynthesis (rETR) at a given irradiance,  $P_{max}$  is maximum rate of photosynthesis (rETR<sub>max</sub>) (Eqn. 3.7),  $\alpha$  is the initial slope of the curve before the onset of light saturation,  $I$  is irradiance and  $\beta$  is the slope of the curve after the onset of photoinhibition (Falkowski & Raven 2007).

Photoinhibition is defined as the inhibition of PSII from exposure to high irradiance (Powles, 1984). Maximum and effective quantum yield ( $\Phi$ PSII and  $F_v/F_m$  respectively) is also measured as an indicator of photosynthetic health when dark-adapted (Eqn. 3.5) and light-adapted (Eqn. 3.6). Non-photochemical quenching (NPQ) of Chl  $a$  was calculated according to the formula detailed in Bilger and Björkman (1990) as Eqn. 3.8.

$$\Phi\text{PSII} = \Delta F/F'_m = (F'_m - F)/F'_m \quad \text{Eqn. 3.5}$$

where  $F'_m$  and  $F$  are the maximum and minimum fluorescence of light-adapted samples.

$$F_v/F_m = (F_m - F_0)/F_m \quad \text{Eqn. 3.6}$$

where  $F_m$  and  $F_0$  are the maximum and minimum fluorescence yield of PSII in dark-adapted samples.

$$\text{rETR}_{\max} = P_s(a/[a + \beta])(\beta/[a + \beta])^{\beta/a} \quad \text{Eqn. 3.7}$$

where  $a$  is the slope of the light limited region and  $\beta$  is the slope of the light inhibited region and  $P_s$  is a scaling factor defined as the maximum potential rETR ( $\mu\text{mole electron m}^{-2} \text{ s}^{-1}$ ).

$$\text{NPQ} = F_m/F'_m - 1 \quad \text{Eqn. 3.8}$$

where  $F_m$  is the maximum fluorescence of dark-adapted sample, and  $F'_m$  is the maximal fluorescence in light-adapted sample.

### 3.3.8. Pigment analysis with high performance liquid chromatography

Pigment analysis was conducted by high-performance liquid chromatography (HPLC).

Culture samples (30 mL) were filtered through a GF/F (47 mm) filter paper in low light, followed by immediate flash freezing in liquid nitrogen and stored at  $-80^\circ\text{C}$  until further analysis. The filters were freeze-dried (2-4 Alpha LDplus, Christ, John Morris

Scientific, Australia) overnight and extracted in chilled 5 mL 90% HPLC-grade acetone

with three runs of sonication (FXP, 50 Hz, Unisonics Australia) for 30 s followed by

10 s of vortexing and stored at  $4^\circ\text{C}$  overnight. Freeze-drying and extraction were

conducted in the dark. Sample slurry (1 mL) was filtered through a  $0.2 \mu\text{m}$  13 mm

syringe filter (polytetrafluoroethylene) and loaded into amber colour HPLC glass vials.

Samples were analysed using an Agilent 1290 LC HPLC equipped with a binary pump

with an integrated vacuum degasser, thermostatic column compartment modules, photo-diode array detector and an Agilent 1290 Infinity autosampler. Pigments were separated using a Zorbax Eclipse XDB C8 HPLC 4.6 mm × 150 mm and guard column (Agilent) using a gradient of tetrabutyl alkylammonium acetate: methanol mix (3:7) (A) and methanol (B) as solvents. Column temperature was maintained at 55°C. The elution profile was: 0–22 min, 5–95% B; 22–29 min, 95% B; 29–31 min, 95–5%; 31–40 min, 5% B. The mobile phase flow rate was 1.1 mL min<sup>-1</sup>. Pigments were detected at 450 nm (Chl *a* at 665 nm) and quantified by comparing with the retention time of analytical standards.

### 3.3.9. Sample preparation for protein, lipid and carbohydrate analysis

Cultures were grown to a minimum cell density of > 6 × 10<sup>6</sup> cells mL<sup>-1</sup> for harvesting. Wet biomass (≈ 400 mL) was harvested at the end of the experiment via centrifugation (Rotanta 460R, Hettich GmbH & Co. KG, Tuttlingen, Germany) at 3000 g for 5 min in pre-weighed centrifugation tubes for dry weight measurements, washed twice with phosphate buffer and once in Milli-Q water, freeze-dried overnight and followed by storage in -80°C until further analysis. After all experiments had been completed, cultures were homogenised with mortar and pestle for protein, lipid, FAME, and carbohydrate analysis (sections 3.3.10, 3.3.11 and 3.3.12).

### 3.3.10. Total protein analysis from total nitrogen measurements

Total protein was estimated using a carbon and nitrogen analyser (Leco TruSpec, LECO Corporation, St. Joseph, Michigan, USA). Elemental nitrogen content was measured by combusting approximately 15 mg of biomass in triplicate. The elemental nitrogen content was then converted to the total protein content by a literature factor of 4.78 (Lourenço *et al.*, 2004).

### 3.3.11. Total lipid and fatty acid methyl ester extraction and analysis

Total lipid content was measured gravimetrically according to Folch *et al.* (1957), whereby biomass samples (10-15 mg) were resuspended in 6 mL of chloroform methanol (2:1 v/v) in 10 mL centrifuge tubes. Tubes of samples were then sonicated (FXP, 50 Hz, Unisonics Australia) at 4°C for 45 min and held at 4°C for 24 h, followed by sonication at 4°C for a further 45 min. 1.5 mL of NaCl (0.9% v/v) was added to each tube and centrifuged at 1500 g for 8 min to separate the phases. The lower lipid containing phase was recovered and the extraction steps were repeated with a further 2 mL of chloroform. The extracts were combined and dried under nitrogen gas and weighed. Transmethylation of lipid samples was performed as described in Carreau & Dubacq (1978). Nonadecanoic acid (C19:0) of known concentration (10 µL of 1 mg mL<sup>-1</sup>) was spiked into lipid samples as internal standard.

Fatty acid methyl ester samples were analysed by gas chromatography (GC) using an Agilent 7890 series GC coupled to an Agilent quadrupole MS (5975N) equipped with a HP-5MS fused capillary column (5%-phenyl-methylpolysiloxane, 30 m long, 0.25 mm internal diameter, film thickness 0.25  $\mu\text{m}$ , Agilent Technologies). Gas chromatography carrier gas was helium at a flow rate of 0.9  $\text{mL min}^{-1}$ . Gas chromatography inlet temperature was 280°C using the splitless mode of injection with a purge time of 1 min with an injection volume of 5  $\mu\text{L}$ . Fatty acid methyl ester peaks in the samples were identified by comparing their retention times with commercial standards (Sigma Aldrich, NSW, Australia). All conditions were analysed in triplicate.

### 3.3.12. Total carbohydrate analysis

Total carbohydrate was analysed as described in Dubois *et al.* (1951, 1956). Biomass of known weight ( $\approx 15$  mg) was boiled at 100°C in concentrated 2.5 M hydrochloric acid for 6 h. The samples were cooled to room temperature and neutralized with sodium carbonate ( $\text{Na}_2\text{CO}_3$ ) to approximately pH 7. Samples were then filtered (0.25  $\mu\text{m}$ ) and made up to 25 mL with Milli-Q water. The samples are analysed via phenol-sulphuric acid method giving an orange-yellow colour in response to carbohydrates (Dubois *et al.*, 1951). The absorption of the sample was measured at 485 nm with a microplate reader (Infinite M1000Pro, Tecan) (Masuko *et al.*, 2005).

### 3.3.13. Cost efficiency of different light qualities

In order to investigate the cost efficiency of the different LEDs used, a multimeter (Tenma digital multimeter 72-7770, Tenma Test Equipment) and DC power supply (Jaytech MP-3080) was setup to measure the current in milliamps (mA) and voltage (V) of the LED panel. The LED panel was attached to an ePBR in a mock calibration setup to measure the mA and V for a given PFD (Figure 3.2). Watt hours per day was calculated using equation Eqn. 3.9.

$$\text{Wh day}^{-1} = V \times A \times t \quad \text{Eqn. 3.9}$$

where V is voltage, A is current in amps, t is hours of light cycle in a day.

And finally cost efficiency of biomass or metabolite production was calculated with a modified equation (Eqn. 3.10) detailed in Wang, Fu and Liu (2007).

$$\text{cost efficiency} = \frac{x_f}{VAt} \quad \text{Eqn. 3.10}$$

where  $x_f$  is concentration of biomass or metabolite at the time of cultivation (3 days for BL, GL and WL, 5 days for RL; section 3.3.4).

As electricity costs vary depending on country or on time of year, the ‘cost’ efficiency was calculated based on the energy consumed in the commonly used kWh unit for each light quality for each experimental cycle (3 days for BL, GL and WL, 5 days for RL).



Statistical analysis was performed with Minitab (Minitab 17.1.0 Statistical Software, Minitab Inc.) and data visualization using Python 3.6, both on Windows 10.

### 3.4. Results

#### 3.4.1. Effects of light quality on *Chaetoceros muelleri* growth

The specific growth rates and maximum cell density of *C. muelleri* cultures were largely unaffected grown using blue, green and white light (Figure 3.3; Table 3.1). While, cultures grown using red light significantly decreased the growth rate as well as decreased maximum cell number (Figure 3.3; Table 3.1). Blue, green and white light grown cultures reached the target cell density ( $> 6 \times 10^6$  cells mL<sup>-1</sup>) on day three with over  $0.80 \times 10^7$  cells mL<sup>-1</sup>, while red light grown cultures, which exhibited the lowest growth rate, reached it on day five with approximately  $0.67 \times 10^7$  cells mL<sup>-1</sup> (Figure 3.3). While no significant difference in final dry weight (mg mL<sup>-1</sup>) were observed between light quality treatments at the time of cultivation (Table 3.1).

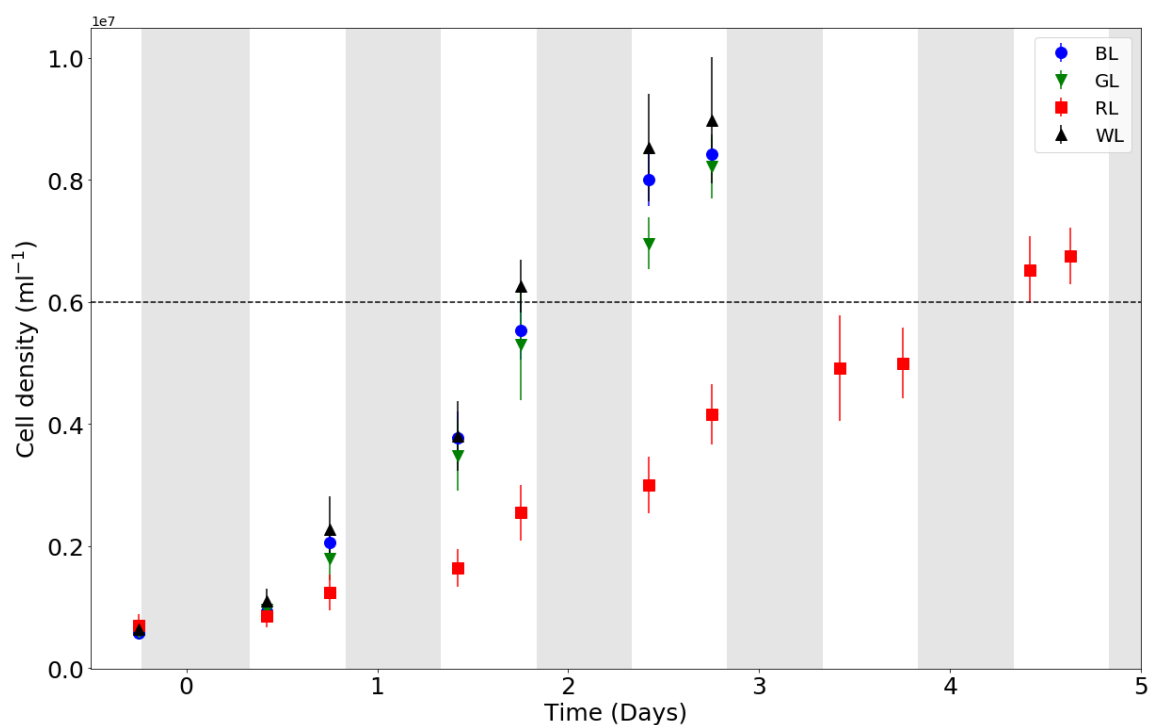


**Figure 3.3** Cell density are shown as a function of time for four light qualities of equal photosynthetically utilized radiation ( $500 \mu\text{mol photons m}^{-2} \text{s}^{-1}$ ). Blue circles indicate cultures grown using blue light (BL), green inverted triangles indicate cultures grown using green light (GL), red squares indicate cultures grown using red light (RL) and black triangles indicate cultures grown using white light (WL). The data points prior to day zero indicate the cell density of the starting inoculum of cultures before the first experimental cell count (day one). The black dotted line indicates the target cell density of  $> 6 \times 10^6 \text{ cells mL}^{-1}$  for metabolite analysis. Values represent the mean and standard deviation ( $n = 5$ ).

**Table 3.1** Specific growth rates ( $\mu$ ), approximate doubling time ( $t_d$ ), mean final dry weight (mean dw) in  $\text{mg mL}^{-1}$  and mean final cell density (mean  $t_f$  cells) in  $\text{cells mL}^{-1}$ . Treatments were BL for blue light grown cultures, GL for green light grown cultures, RL for red light grown cultures and WL for white light grown cultures. One-way ANOVA performed with Tukey method at 95% confidence: same or no letters indicate no significant difference and different letters indicate significant difference. Values represent mean and standard deviation (SD) ( $n = 5$ ).

Treatments	$\mu$	$t_d$	mean dw	mean $t_f$ cells
BL	$1.12 \pm 0.22^a$	$1.62 \pm 0.32^a$	$0.12 \pm 0.04$	$8.42 \times 10^6 \pm 0.26 \times 10^6^a$
GL	$1.12 \pm 0.29^a$	$1.63 \pm 0.42^a$	$0.09 \pm 0.02$	$8.22 \times 10^6 \pm 0.53 \times 10^6^a$
RL	$0.65 \pm 0.05^b$	$0.94 \pm 0.06^b$	$0.11 \pm 0.02$	$6.75 \times 10^6 \pm 0.46 \times 10^6^b$
WL	$1.08 \pm 0.10^a$	$1.56 \pm 0.15^a$	$0.12 \pm 0.05$	$8.98 \times 10^6 \pm 1.03 \times 10^6^a$

#### 3.4.2. Light attenuation in *Chaetoceros muelleri* cultures

To establish if light quality affected the rates of light attenuation in *C. muelleri* cultures, light intensity was measured twice a day (2 h before and after light phase). Data at day 0 ( $t_0$ ) show irradiance values with no cells at the calculated PUR irradiance level (section 3.3.3). Cultures grown with RL attenuated the most rapidly at  $t_1$  recording under  $350 \mu\text{mol photons m}^{-2} \text{s}^{-1}$ ; however, the rate of attenuation was slower compared to

other cultures with only an approximate  $100 \mu\text{mol photons m}^{-2} \text{s}^{-1}$  difference in irradiance during culture growth, complimenting the low rate of cell growth rate (Figure 3.4). The lowest irradiance at  $t_f$  was observed in BL cultures at under  $50 \mu\text{mol photons m}^{-2} \text{s}^{-1}$ . Similar trends in light attenuation were recorded in GL and WL, starting approximately with  $400 \mu\text{mol photons m}^{-2} \text{s}^{-1}$  and ended with approximately  $150 \mu\text{mol photons m}^{-2} \text{s}^{-1}$  (Figure 3.4).

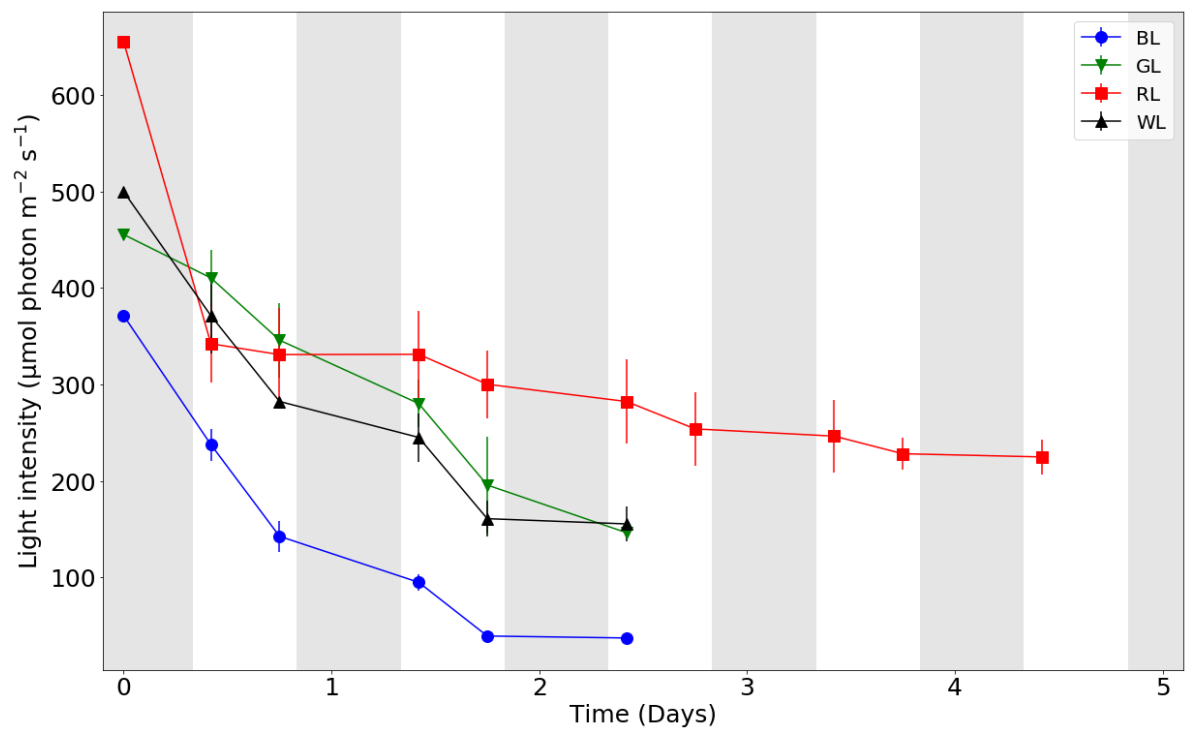


**Figure 3.4** Irradiance measured *in situ* from cultures grown using different light

qualities as a function of time. Blue circles represent BL, green inverted triangles

represent GL, red squares represent RL and black triangles represent WL. Note that RL

cultures were grown for five days and BL, GL and WL cultures were grown for three

days, as growth rates were significantly lower and was hence grown for longer to

harvest enough biomass for analysis. Irradiance at  $t_0$  represents the irradiance levels in media with no cells as detailed in section 3.3.5. Values represent the mean and standard deviation ( $n = 5$ ).

#### 3.4.3. Primary metabolic composition of *Chaetoceros muelleri* grown with different light qualities

In order to investigate whether different light qualities could affect the metabolite content in *C. muelleri*, total protein, lipid and carbohydrate content was analysed from samples harvested at the end of the growth cycle (Figure 3.5). A significantly higher total carbohydrate content was observed in BL cultures and higher total protein content was observed in RL cultures respectively, though a significantly lower total lipid content was also observed in RL (Figure 3.5).

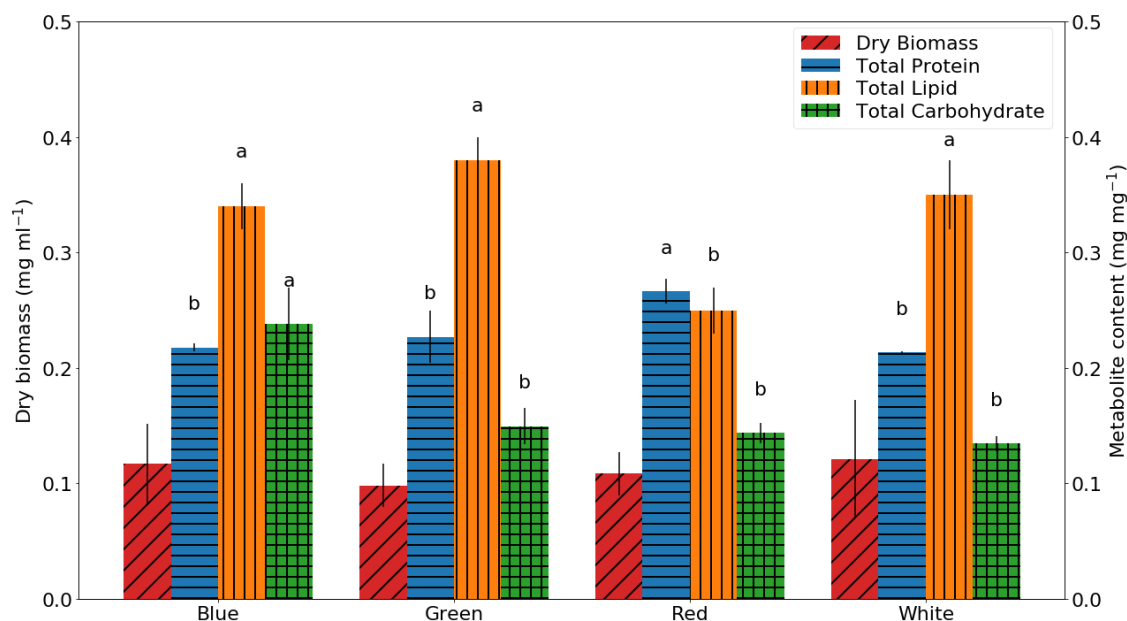


**Figure 3.5** Cellular content of total dry biomass ( $\text{mg ml}^{-1}$ ) on the left y-axis, total protein, lipid and carbohydrates ( $\text{mg mg}^{-1}$ ) on the right y-axis are shown for each light quality used to grow *C. muelleri*. Red bars with diagonal patterns represent dry weight, blue bars with horizontal patterns represent total protein, orange bars with vertical patterns represent total lipid and green bars with cross patterns represent total carbohydrates. Values represent mean and standard deviation of total metabolite samples ( $n = 3$ ) and dry biomass samples ( $n = 9$ ). One-way ANOVA performed with Tukey method at 95% confidence: the same letter indicates no significant difference, or if no letters are present, no significant differences between conditions were detected, and different letters indicate significant difference between light treatments.

#### 3.4.4. Effects of light quality on the FAME composition of *Chaetoceros muelleri*

Figure 3.6 shows the FAME composition of *C. muelleri* cultured using different light qualities. Cultures grown using GL and WL exhibited the highest FAME content, while BL cultures produced significantly less short chain fatty acids such as C16:1 (n-7) and C16:0 (Figure 3.6). Red light cultures overall had lower FAME content in the short chain fatty acids (C:14-C:16) and C20:5 (n-3) in comparison to GL and WL cultures and lower total lipid content ( $0.25 \text{ mg mg}^{-1}$ ) in comparison to all other treatments (Figure 3.5 & Figure 3.6).

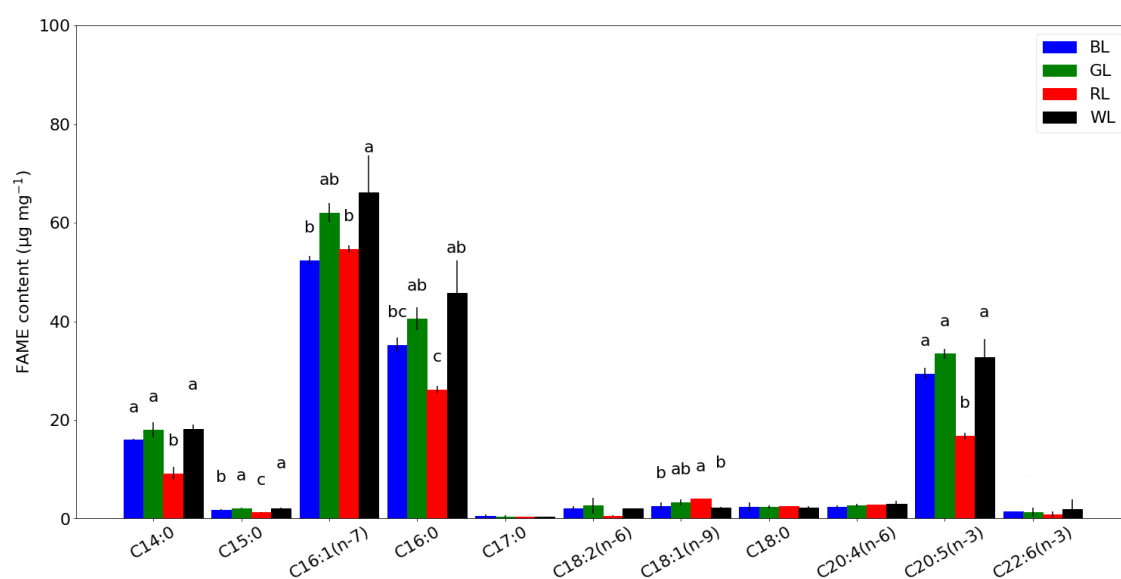


**Figure 3.6** Fatty acid methyl ester (FAME) content per mg dry weight ( $\mu\text{g mg}^{-1}$ ) of *C. muelleri* grown using different light qualities. Blue bars: BL cultures, green bars: GL cultures, red bars: RL cultures and black bars: WL cultures. One-way ANOVA performed with Tukey method at 95% confidence: same letter indicate no significant

difference, different letters indicate significant difference, and where no letters are present no significant differences were detected between conditions. Values represents mean and standard deviation ( $n = 3$ ).

#### 3.4.5. Effects of different light quality on the pigment composition of *C. muelleri*

In order to investigate whether different light qualities could affect the pigment composition of *C. muelleri*, pigment content was analysed from samples harvested at the end of the growth cycle and is presented in Figure 3.7. White light and GL grown cultures exhibited the highest pigment contents with the exception of Chl *a* content being highest in WL grown cultures (Figure 3.7). A notably lower diadinoxanthin content and reciprocally higher diatoxanthin content was observed in RL cultures compared to other conditions (Figure 3.7). While trace amounts of  $\beta$ -carotene were detected in BL, no  $\beta$ -carotene was detected in RL (Figure 3.7).



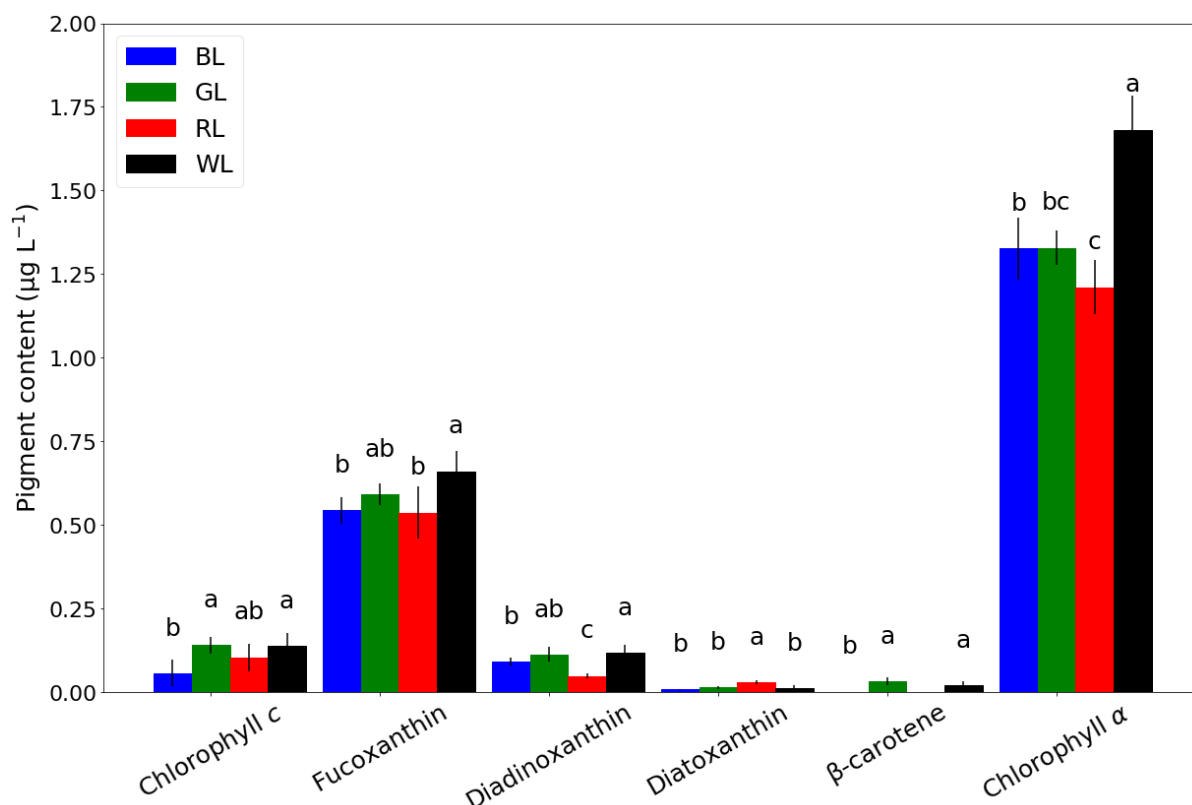


**Figure 3.7** Pigment content per culture volume (µg L<sup>-1</sup>) of *C. muelleri* harvested after grown using different light qualities. Values are mean and error bars indicating standard deviation (n = 5). Blue bars: BL grown cultures, green bars: GL grown cultures, red bars: RL grown cultures and black bars: WL grown cultures. One-way ANOVA performed with Tukey method at 95% confidence: the same letter indicates no significant difference and different letters indicate significant difference.

#### 3.4.6. Light quality and production efficiency

From Eqn. 3.9, it was calculated that blue LEDs required  $29.52 \times 10^{-3}$  kWh per growth cycle (3 days),  $61.20 \times 10^{-3}$  kWh (3 days) for green LEDs,  $109.20 \times 10^{-3}$  kWh (5 days) for red LEDs and  $60.69 \times 10^{-3}$  kWh (3 days) for white LEDs. The amount of energy

consumption (kWh) for dry biomass ( $\text{mg mL}^{-1}$ ) and metabolite ( $\text{mg/mg dry weight}$ )

production was calculated and is presented in Figure 3.8.

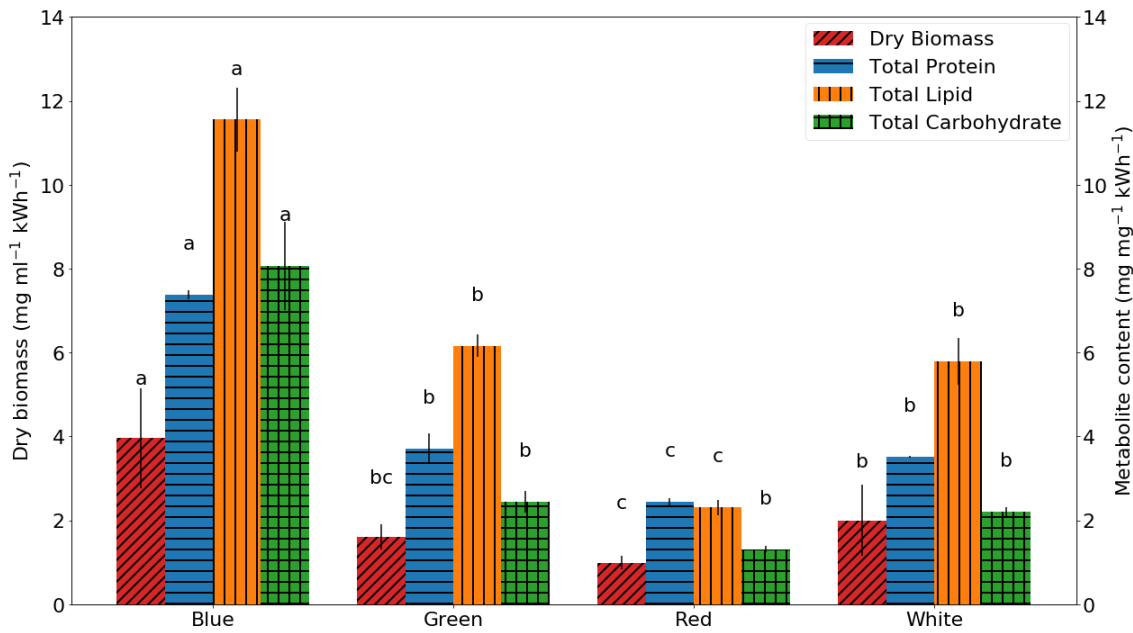


**Figure 3.8** Dry biomass ( $\text{mg mL}^{-1} \text{kWh}^{-1}$ ; left y-axis) and total metabolite ( $\text{mg mg}^{-1} \text{kWh}^{-1}$ ; right y-axis) yield based on power consumption for each light quality is shown. Red bars with diagonal patterns represent dry weight, blue bars with horizontal patterns represent total protein, orange bars with vertical patterns represent total lipid and green bars with cross patterns represent total carbohydrates. One-way ANOVA performed with Tukey method at 95% confidence: the same letter indicates no significant difference and different letters indicate significant difference. Values represent mean and standard deviation of total metabolite samples ( $n = 3$ ) and dry biomass samples ( $n = 9$ ).

A clear difference was seen in biomass and metabolite production per unit power consumed from lighting between the experimental light qualities (Figure 3.8). Blue LEDs were shown to be the most energy-efficient in producing both biomass and metabolites compared to green, red and white LEDs. Little differences were seen between green and white LEDs, while red LEDs were shown to be the least energy-efficient LEDs to grow *C. muelleri*.

A clear difference was seen in FAME production per unit power consumed from lighting between the experimental light qualities (Figure 3.9).

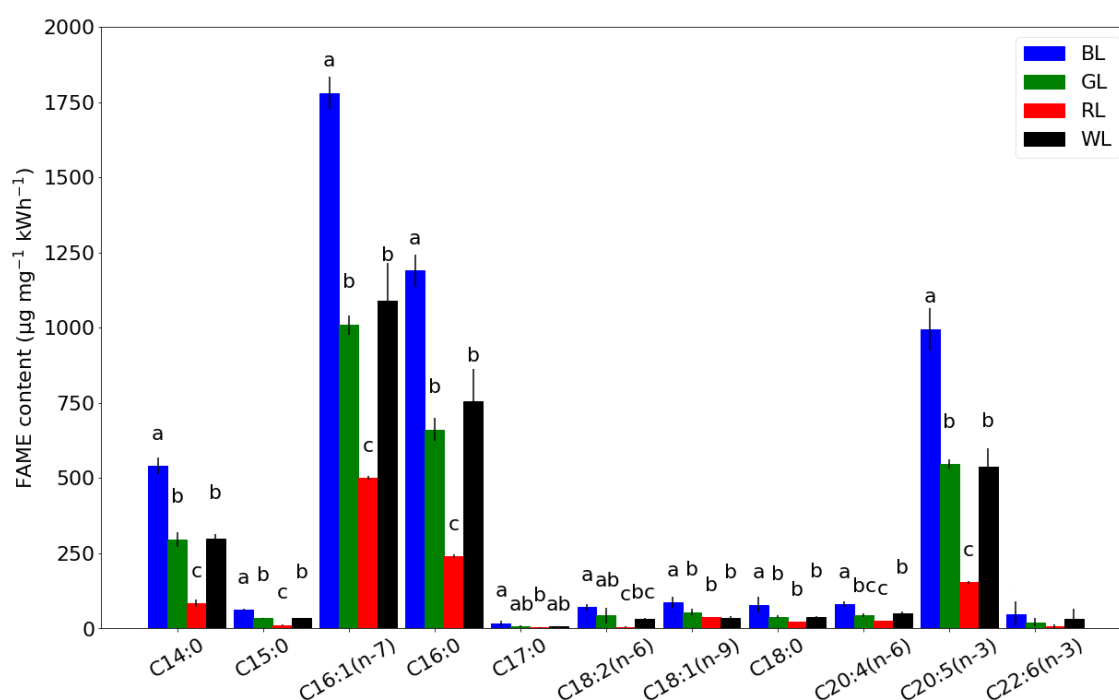


**Figure 3.9** FAME content based on power consumption ( $\mu\text{g mg}^{-1} \text{kWh}^{-1}$ ) for each light quality is shown. Blue bars: BL grown cultures, green bars: GL grown cultures, red bars: RL grown cultures and black bars: WL grown cultures. One-way ANOVA

performed with Tukey method at 95% confidence: same letter indicate no significant difference, different letters indicate significant difference, and where no letters are present no significant differences were detected between conditions. Values represents mean and standard deviation ( $n = 3$ ).

Blue LEDs were shown to be the most cost efficient in producing fucoxanthin, followed by green and white LEDs and red LEDs being the least efficient to produce fucoxanthin in *C. muelleri* (Figure 3.10).

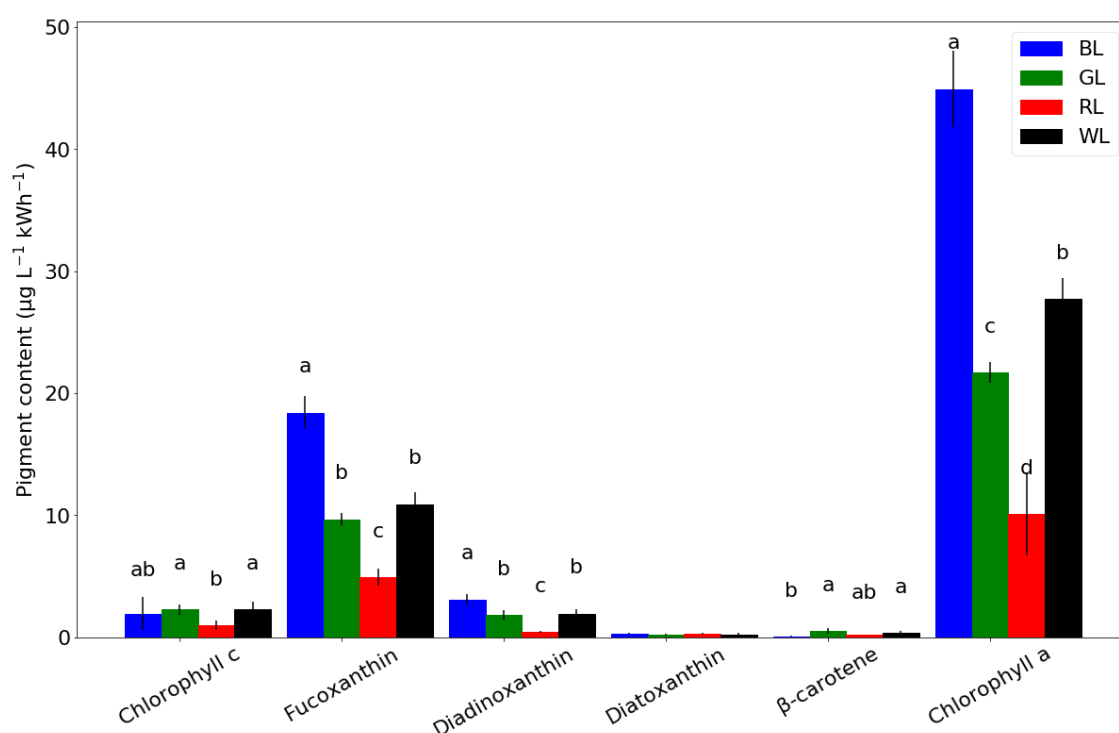


**Figure 3.10** Pigment content as a function of power consumption ( $\mu\text{g L}^{-1} \text{kWh}^{-1}$ ) for each light quality is shown. Blue bars: BL grown cultures, green bars: GL grown cultures, red bars: RL grown cultures and black bars: WL grown cultures. One-way ANOVA performed with Tukey method at 95% confidence: same letter indicate no

significant difference, different letters indicate significant difference, and where no letters are present no significant differences were detected between conditions. Values are mean and error bars indicating standard deviation ( $n = 5$ ).

#### 3.4.7. Effects of different light quality on net photosynthesis rates of *Chaetoceros muelleri*

To determine whether different light qualities influence the net photosynthesis rates of *C. muelleri* DO concentration was monitored over the course of the experiment and artificially ‘spiked’ to monitor the accumulation of DO when aeration is temporarily stopped (section 2.5.4.). A linear regression is fitted to each DO spike and normalized to cell density to calculate net photosynthesis for each wavelength throughout the experiment (Figure 3.11).

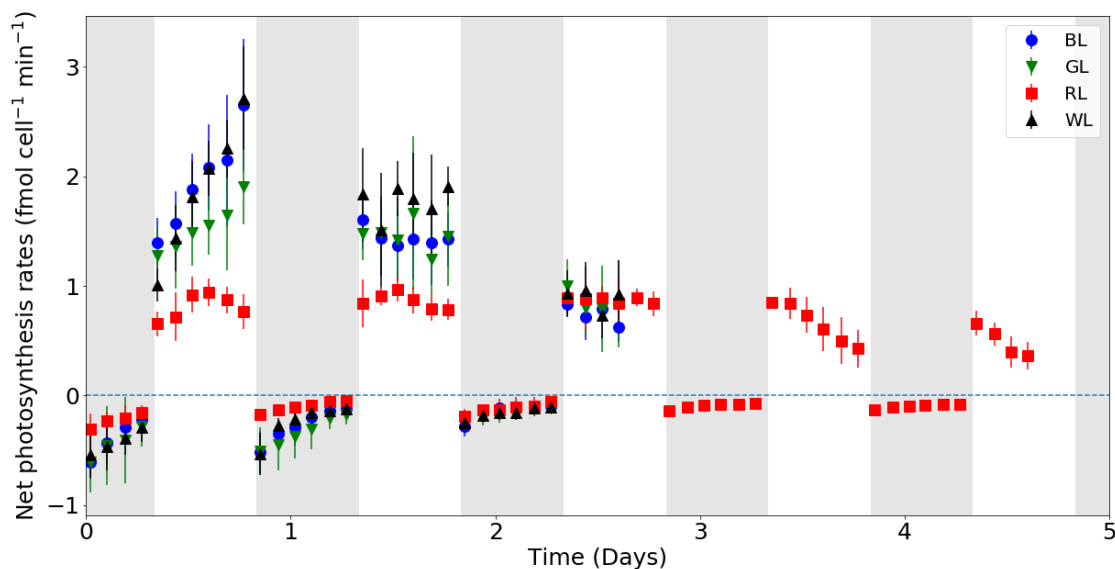


**Figure 3.11** Net photosynthesis of cultures grown using different light qualities as a function of time. Blue circle: BL grown cultures, green inverted triangle: GL grown cultures, red squares: RL grown cultures and black triangles: WL grown cultures. Dotted line indicates zero net photosynthesis. Values represent mean and standard deviation ( $n = 5$ ).

The steepest rise in net photosynthesis was detected in WL cultures compared to the BL and GL cultures in day one and RL cultures exhibited the lowest rate of net photosynthesis. On day two, net photosynthesis became largely stagnant as cultures entered light-limited linear growth phase. By day three, net photosynthesis had gradually decreased during the light phase as cultures entered stationary phase, with the exception of RL cultures, where it appeared to enter stationary phase on day four.

#### 3.4.8. Effects of light quality on rapid light curve

Many significant differences were observed in the RLCs between *C. muelleri* samples grown using different light qualities at both time points  $t_0$  and  $t_f$  (Table 3.2). Red light cultures consistently performed poorer in both  $\Phi_{PSII}$  and  $rETR_{max}$  while also exhibiting the lowest NPQ compared to all other treatments at both time points. Green and WL cultures were mostly similar with the exception of  $t_0$   $\Phi_{PSII}$  and NPQ. While BL and WL cultures also shared many similarities during  $t_0$ , however, by  $t_f$  parameters such as  $rETR_{max}$  and NPQ were significantly different.

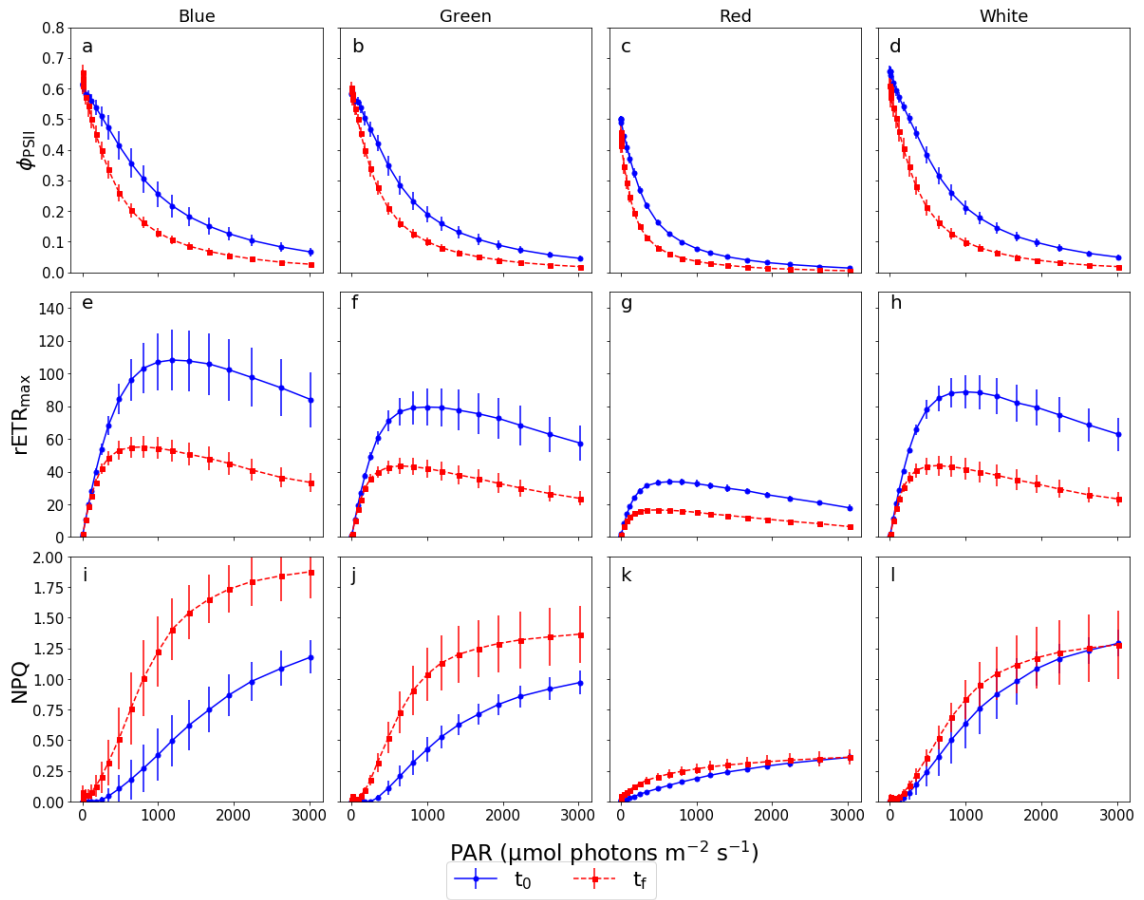


**Figure 3.12** Rapid light curve plot parameters where  $\Phi_{\text{PSII}}$  (maximum quantum yield of photosystem II) are shown in boxes a, b, c and d,  $\text{rETR}_{\text{max}}$  (relative maximum electron transfer rate) in boxes e, f, g and h and NPQ (non-photochemical quenching) in boxes i, j, k and l. Condition blue light are shown in boxes a, e, and i, green light in boxes b, f and j, red light in boxes c, g, and k, and white light in boxes d, h and l. Measurements were taken at day one ( $t_0$ ) represented as blue circles and at day three ( $t_f$ ) represented as red squares. All samples at  $t_f$  were diluted with F/2 media to achieve similar  $F_0$  values prior to the measurement. Values represent mean and standard deviation ( $n = 5$ ).



The RLC parameters generated as detailed in section 3.3.7 are shown below in Table

3.2. Red light cultures from both time points had the lowest  $\alpha$ ,  $rETR_{\max}$ ,  $I_k$  and  $\Phi_{PSII}$  compared to all other cultures. There were no significant differences in  $\alpha$  in all other cultures. At  $t_0$ , WL cultures had the highest  $\Phi_{PSII}$  while comparable values of  $rETR_{\max}$  and  $I_k$  with BL cultures, while slightly lower values were observed in GL cultures. However, at  $t_f$ , BL cultures had significantly higher values of  $rETR_{\max}$  and  $I_k$  compared to GL and WL cultures, while no significant differences in  $\Phi_{PSII}$  were observed.

**Table 3.2** Rapid light curve parameters are shown for cultures grown under blue (BL), green (GL), red (RL) and white (WL) light where  $F_0$  and  $F_m$  is minimum and maximum fluorescence yield of PSII in dark-adapted  $a$  is slope of light-limited region,  $rETR_{max}$  is maximum electron transfer rate,  $I_k$  is minimum saturating irradiance and  $\Phi_{PSII}$  is maximum quantum yield of photosystem II. Two RLC measurements were taken during each growth cycle at  $t_0$  and  $t_f$ . One-way ANOVA performed with Tukey method at 95% confidence: same or no letters indicates no significant difference and different letters indicate significant difference. Values indicate mean and standard deviation ( $n = 5$ ).

	Parameters	BL	GL	RL	WL
$t_0$	$F_0$	$0.82 \pm 0.11$	$0.92 \pm 0.17$	$0.84 \pm 0.10$	$0.93 \pm 0.17$
	$F_m$	$2.16 \pm 0.36^{ab}$	$2.23 \pm 0.45^{ab}$	$1.68 \pm 0.18^b$	$2.71 \pm 0.54^a$
	$a$	$0.27 \pm 0.01^a$	$0.28 \pm 0.01^a$	$0.22 \pm 0.01^b$	$0.29 \pm 0.01^a$
	$rETR_{max}$	$104.10 \pm 14.39^a$	$81.10 \pm 11.34^b$	$34.38 \pm 2.05^c$	$90.02 \pm 10.18^{ab}$
	$I_k$	$383.44 \pm 55.41^a$	$293.04 \pm 45.18^b$	$156.28 \pm 7.96^c$	$313.78 \pm 45.33^{ab}$
	$\Phi_{PSII}$	$0.62 \pm 0.02^b$	$0.59 \pm 0.02^c$	$0.50 \pm 0.01^d$	$0.66 \pm 0.02^a$
$t_f$	$F_0$	$1.13 \pm 0.03$	$1.19 \pm 0.04$	$1.24 \pm 0.06$	$1.16 \pm 0.07$
	$F_m$	$3.27 \pm 0.26^a$	$3.00 \pm 0.22^a$	$2.32 \pm 0.09^b$	$2.99 \pm 0.40^a$
	$a$	$0.28 \pm 0.02^a$	$0.26 \pm 0.01^a$	$0.19 \pm 0.01^b$	$0.27 \pm 0.01^a$
	$rETR_{max}$	$56.03 \pm 6.48^a$	$44.15 \pm 4.95^b$	$17.40 \pm 0.99^c$	$44.40 \pm 6.06^b$
	$I_k$	$203.78 \pm 17.90^a$	$168.65 \pm 15.86^b$	$89.90 \pm 3.78^c$	$167.30 \pm 15.94^b$
	$\Phi_{PSII}$	$0.65 \pm 0.02^a$	$0.60 \pm 0.02^a$	$0.47 \pm 0.01^b$	$0.61 \pm 0.03^a$

### 3.5. Discussion

This study investigated the response of *C. muelleri* to different light qualities (BL, GL, RL and WL) to assess its feasibility for use in feed production in commercial hatcheries. Applying irradiances that were equal in PUR and allowing cultures to pre-acclimate (7 days) to the different light qualities, this study aimed to investigate the effects of light quality without interfering factors such as light intensity influencing the results.

#### 3.5.1. Growth

From the cell count data shown in Figure 3.3 and other growth parameters shown in Table 3.1 there was no significant difference in the growth rate, dry weight, division rate or final cell densities between BL, GL and WL cultures. This is in spite of the limited capability of chlorophylls to absorb GL and is likely due to the high efficiency of the carotenoid fucoxanthin in transferring energy to Chl *a* during photosynthesis (Mann and Myers, 1968). Other microalgae, such as *Chlorella* sp. have been shown to grow poorly in GL (Shu *et al.*, 2012), this gives additional flexibility when selecting light quality for *C. muelleri* as it is able to utilise GL efficiently. It was previously mentioned (section 3.1.9.) that no significant differences in growth rate ( $\approx 0.43 \mu \text{ day}^{-1}$ ) was observed in the diatom *P. tricornutum* using BL, RL and WL ( $24 \mu \text{mol photons m}^{-2} \text{ s}^{-1}$ ,  $41 \mu \text{mol photons m}^{-2} \text{ s}^{-1}$  and  $40 \mu \text{mol photons m}^{-2} \text{ s}^{-1}$  respectively) (Costa *et al.*, 2013;

Jungandreas *et al.*, 2014). Costa *et al.* (2013) however observed a significant difference in growth rate when the irradiance of BL, RL and WL was increased to 72  $\mu\text{mol photons m}^{-2} \text{s}^{-1}$ , 123  $\mu\text{mol photons m}^{-2} \text{s}^{-1}$  and 120  $\mu\text{mol photons m}^{-2} \text{s}^{-1}$  respectively. Growth rates ( $\mu \text{ day}^{-1}$ ) increased to  $\approx 1.01^b$ ,  $\approx 0.78^c$  and  $\approx 1.08^b$  for BL, RL and WL respectively (same letters indicating no significant difference) suggesting that RL strongly correlates to a higher quantum requirement for biomass production (Costa *et al.*, 2013). This similarity in growth rates indicates a potentially common pattern in diatom growth rates in response to light quality, as similar growth rates were observed in this study at higher irradiances (Table 3.1). However, in the work by Mouget *et al.* (2004), the opposite trend was observed in the marine pennate diatom *Haslea ostrearia*. Mouget *et al.* (2004) reported that in BL (20  $\mu\text{mol photons m}^{-2} \text{s}^{-1}$ ) cultures a significantly higher growth rate ( $\mu \text{ day}^{-1}$ ) was observed compared to WL cultures, while no significant differences were observed in RL cultures compared to WL cultures. However, in higher irradiances (100  $\mu\text{mol photons m}^{-2} \text{s}^{-1}$ ) no significant difference between BL, RL nor WL were observed. The observations by Mouget *et al.* (2004) indicates that further investigation is required to fully understand the growth response of diatoms to different light quality.

### 3.5.2. Metabolite production

Jungandreas *et al.* (2014) has previously shown that in BL and RL (24  $\mu\text{mol photons m}^{-2} \text{ s}^{-1}$  and 41  $\mu\text{mol photons m}^{-2} \text{ s}^{-1}$  respectively) grown cultures of *P. tricornutum* no significant difference ( $p \leq 0.05$ ) in lipid content (% dry matter) was observed. However, in this study a significant difference in total lipids was observed between BL and RL cultures (Figure 3.5). Moreover, Jungandreas *et al.* (2014) also observed an increase in protein and a decrease in carbohydrate in BL cultures compared to RL cultures; a reciprocal result to this study (Figure 3.5). The contradicting observation may be due to the different source of irradiance used, as shown by Costa *et al.* (2013) different irradiance levels in the same species can lead to different results. While *P. tricornutum* is also a diatom, it is a pennate diatom as opposed to *C. muelleri*, a centric diatom, that have significantly different genetic makeups (Bowler *et al.*, 2008). This may contribute to different metabolic responses to light quality and requires further investigation to elucidate.

### 3.5.3. Pigments

Mouget *et al.* (2004) has previously shown in BL, GL and WL (100  $\mu\text{mol photons m}^{-2} \text{ s}^{-1}$ ) grown cultures of *H. ostrearia*, that BL cultures exhibited less  $\beta$ -carotene ( $\approx 0.10 \mu\text{g } 10^6 \text{ cells}^{-1}$ ) than those grown with GL ( $\approx 0.19 \mu\text{g } 10^6 \text{ cells}^{-1}$ ). Similar

observations have also been made in this work with BL and GL cultures, where BL cultures produced lower  $\beta$ -carotene in  $\mu\text{g L}^{-1}$  ( $0.12 \times 10^{-2} \pm 0.03 \times 10^{-2}$ ) than GL cultures ( $3.15 \times 10^{-2} \pm 1.23 \times 10^{-2}$ ) (Figure 3.7). Differences were, however, present between the works. While Mouget *et al.* (2004) observed no significant differences in fucoxanthin content ( $\mu\text{g } 10^6 \text{ cells}^{-1}$ ) between BL and WL cultures, significantly less fucoxanthin ( $\mu\text{g L}^{-1}$ ) was observed in BL cultures ( $5.43 \times 10^{-1} \pm 0.39 \times 10^{-1}$ ) compared to WL cultures ( $6.61 \times 10^{-1} \pm 0.62 \times 10^{-1}$ ) in this work (Figure 3.7). Additionally, Mouget *et al.* (2004) observed no significant differences in Chl *a* content in all light qualities tested, while in this work significant differences in Chl *a* content compared to WL cultures was observed (Figure 3.7). However, the correlation may be weak for a number of reasons. Firstly, Mouget *et al.* (2004) used a halogen lamp with broadband filters to produce the different light qualities, which results in a very broad emission peak for each light quality. Secondly, the author also statistically analysed samples compared to white light, but not between blue, green and red light grown samples directly, so the correlations discussed above between blue, green and red light, may not be significant. And finally, the author had not used equivalent PFD for each light quality (such as PUR) and had instead used a constant PFD ( $100 \mu\text{mol photons m}^{-2} \text{ s}^{-1}$ ) and therefore the results may be due to the intensity of the light which is known to have a dramatic influence over photosynthetic performance (Jeon, Cho and Yun, 2005).

The significant increase in diatoxanthin in RL cultures may be an indication that the xanthophyll cycle, an important photoprotection mechanism (by quenching the excited states of chlorophyll), had been triggered (Lohr and Wilhelm, 2001). It is known that diatoms accumulate diatoxanthin in prolonged high-light (Lohr and Wilhelm, 1999).

The increase of diatoxanthin using RL had also been observed in *P. tricornutum* by Valle *et al.* (2014), whereby upon exposure to high RL ( $730 \mu\text{mol photons m}^{-2} \text{s}^{-1}$ ), diatoxanthin content significantly increased within 30 mins. However, while Costa *et al.* (2013) and Jungandreas *et al.* (2014) have also reported significantly lower concentration of diadinoxanthin in RL grown cultures compared to BL grown cultures (and WL in Costa *et al.* (2013) for low and moderate irradiances neither works reported diatoxanthin content in neither BL nor RL grown cultures. Also, an accurate comparison cannot be made from the significant increase in diatoxanthin in RL from this work in comparison to the works by Mouget *et al.* (2004) who report on total xanthophyll cycle pigments (diadinoxanthin and diatoxanthin) and not individual diadinoxanthin and diatoxanthin pigment contents in different light qualities. However, Costa *et al.* (2013) observed a significantly lower diadinoxanthin cycle activity and diatoxanthin content in *P. tricornutum* cultured in high RL ( $1000 \mu\text{mol photons m}^{-2} \text{s}^{-1}$ ).

### 3.5.4. Photosynthesis

In this study, photosynthetic activity was monitored continuously in the form of photosynthetic oxygen evolution and periodically in the form of RLCs. As seen in Figure 3.11, the net photosynthesis rates in BL, GL and WL cultures were relatively comparable throughout the experiment. The light attenuation observed in BL, GL and WL cultures complements the net photosynthesis and the cell density data (Figure 3.3, Figure 3.4 and Figure 3.11). However, in RL cultures, the light attenuation was largely static with only a small decrease of approximately  $100 \mu\text{mol photons m}^{-2} \text{ s}^{-1}$  was observed after five days of culturing (Figure 3.4). This may be due to the progressive loss of photosynthetic activity which was observed in Figure 3.12 and Table 3.2, resulting in an incremental decrease in absorbed photons and net photosynthesis rates despite the increased cell density of the culture (Figure 3.3). Jungandreas *et al.* (2014) had previously reported that no significant difference was observed in oxygen evolution rate ( $\mu\text{mol O}_2 \text{ mg Chl } a^{-1} \text{ h}^{-1}$ ) with BL or RL ( $24 \mu\text{mol photons m}^{-2} \text{ s}^{-1}$  and  $41 \mu\text{mol photons m}^{-2} \text{ s}^{-1}$  respectively) grown *P. tricornutum* cultures. However, despite this they had observed a significant ( $p \leq 0.001$ ) decrease in  $\Phi_{\text{PSII}}$  in BL cultures ( $0.65 \pm 0.002$ ) compared to RL cultures ( $0.67 \pm 0.001$ ) and approximately half the NPQ in RL cultures ( $0.50 \pm 0.12$ ) compared to BL cultures ( $1.05 \pm 0.17$ ) (Jungandreas *et al.*, 2014). The work by Costa *et al.* (2013) complements this finding as they also observed no



significant difference in photosynthesis rates in blue, red or white light (24  $\mu\text{mol photons m}^{-2} \text{ s}^{-1}$ , 41  $\mu\text{mol photons m}^{-2} \text{ s}^{-1}$  and 40  $\mu\text{mol photons m}^{-2} \text{ s}^{-1}$  respectively) grown *P. tricornutum* cultures. However, in higher irradiance of blue, red and white light (72  $\mu\text{mol photons m}^{-2} \text{ s}^{-1}$ , 123  $\mu\text{mol photons m}^{-2} \text{ s}^{-1}$  and 120  $\mu\text{mol photons m}^{-2} \text{ s}^{-1}$  respectively), Costa *et al.* (2013) had observed a significantly lower photosynthesis rate ( $\mu\text{mol O}_2 \text{ mg Chl } a^{-1} \text{ h}^{-1}$ ) in increased red light ( $> 400 \mu\text{mol photons m}^{-2} \text{ s}^{-1}$ ) compared to BL and WL cultures, despite observing significantly lower NPQ in RL cultures, compared to BL and WL cultures. As Costa *et al.* (2013) has shown, in higher irradiances the difference in photosynthesis rates and photosynthetic parameters (such as NPQ) become more apparent than in lower irradiances. A significantly lower  $\Phi_{\text{PSII}}$  and net photosynthesis rate was consistently observed in  $t_0$  RL cultures compared to BL, GL and WL cultures (Table 3.2 & Figure 3.11) and while the  $\Phi_{\text{PSII}}$  of BL and GL cultures recovered by  $t_f$ ,  $\Phi_{\text{PSII}}$  in RL cultures had remained approximately the same (Table 3.2). The progressive loss of photosynthetic activity under high RL was also observed in *P. tricornutum* by Valle *et al.* (2014) through PAM fluorometry. Valle *et al.* (2014) observed the progressive decrease of  $\Phi_{\text{PSII}}$ ,  $a$  and  $r\text{ETR}_{\text{max}}$  over 96 h and concluded that diatoms have not evolved mechanisms to acclimate to high intensities of RL. This is not surprising given the scarcity of RL in deep aquatic environments (Levine and MacNichol, 1982; Austin and Petzold, 1986; Kirk, 1994). Also, in natural

aquatic environments, high RL will not be encountered without the presence of high BL, which diatoms highly depend upon to acclimate to high light (Costa *et al.*, 2013; Valle *et al.*, 2014).

### 3.5.5. Cost efficiency

In this study, the cost efficiency of each light quality was calculated. The most cost efficient light quality for biomass production was found to be BL at  $\approx 4 \text{ mg mL}^{-1} \text{ kWh}^{-1}$ , while other LEDs (GL, RL and WL) were less than half of that value (Figure 3.8).

While biomass and metabolite production per unit time showed small differences, in estimating production as a function of energy consumption, it was shown that BL significantly improved production of proteins, lipids and carbohydrates per unit energy consumed (Figure 3.8). The cost efficiency of fucoxanthin production was also significantly higher in BL than in all other light qualities (Figure 3.10). In aquaculture, fucoxanthin has been shown to improve antioxidant activities and is recognised as a beneficial reactive oxygen scavenger (Kawamura, Roberts and Nicholson, 1998; Xia *et al.*, 2013; Foo *et al.*, 2017). Significantly higher cost efficiency was also observed in ARA and EPA production, the PUFAs commonly correlated to higher survivability and development in aquaculture larvae (D'Souza and Loneragan, 1999; Brown, 2002).

Green light and WL had similar cost efficiencies in both biomass and metabolite

production, consuming approximately  $61 \times 10^{-3}$  kWh over three days, twice that of BL (approximately  $30 \times 10^{-3}$  kWh). Red light consumed approximately 44% more than GL and WL (approximately  $109 \times 10^{-3}$  kWh) and more than three times than BL.

Compounded with the progressive loss of photosynthetic activity (section 3.5.4., Figure 3.12 and Table 3.2), RL overall exhibited the poorest cost efficiency of production. For hatcheries, the use of blue LEDs are recommend, as superior biomass production can be achieved per unit energy consumed, compared with, for example WL, potentially reducing operational costs relating to microalgal production (Figure 3.3 & Figure 3.5).

Blue LEDs have been demonstrated in this work as a highly cost efficient irradiance source, though further experiments are required before applying them to commercial scale production. For example, as blue LEDs attenuated more rapidly than other LEDs (Figure 3.4), experiments that assess blue LEDs using multiple sources will give further insights into its usage in bags while minimising the early onset of light limitation.

### 3.6. Conclusions

This study has demonstrated the potential of blue LEDs applied in aquaculture facilities as a cost efficient light quality to cultivate biomass in the diatom *C. muelleri*. The study provides methods that can be transferable to investigate light quality in other photobioreactors and microalgal species. To the author's knowledge, this was the first

work to investigate LED light qualities in produce biomass and metabolites of *C. muelleri* and assess the cost efficiency for use in aquaculture hatcheries. At present, this study was conducted on laboratory-scale photobioreactors and further research is required on larger commercial-scale photobioreactors are required for industrial validation.

### 3.7. References

- Abiusi, F., Sampietro, G., Marturano, G., Biondi, N., Rodolfi, L., D'Ottavio, M. and Tredici, M. R. (2014) 'Growth, photosynthetic efficiency, and biochemical composition of *Tetraselmis suecica* F&M-M33 grown with LEDs of different colors', *Biotechnology and Bioengineering*, 111(5), pp. 956–964. doi: 10.1002/bit.25014.
- Baer, S., Heining, M., Schwerna, P., Buchholz, R. and Hübner, H. (2016) 'Optimization of spectral light quality for growth and product formation in different microalgae using a continuous photobioreactor', *Algal Research*, 14, pp. 109–115. doi: 10.1016/j.algal.2016.01.011.
- Beardall, J. and Raven, J. A. (2013) 'Limits to phototrophic growth in dense culture: CO<sub>2</sub> supply and light', in *Algae for Biofuels and Energy*. Dordrecht: Springer Netherlands, pp. 91–97. doi: 10.1007/978-94-007-5479-9\_5.
- Becker, W. (2004) 'Microalgae for aquaculture: The nutritional value of microalgae for

aquaculture’, in Richmond, A. (ed.) *Handbook of Microalgal Culture: Biotechnology and Applied Phycology*. Oxford, UK, pp. 380–391.

Bertrand, M. (2010) ‘Carotenoid biosynthesis in diatoms’, *Photosynthesis research*, 106(1–2), pp. 89–102. doi: 10.1007/s11120-010-9589-x.

Bilger, W. and Björkman, O. (1990) ‘Role of the xanthophyll cycle in photoprotection elucidated by measurements of light-induced absorbance changes, fluorescence and photosynthesis in leaves of *Hedera canariensis*’, *Photosynthesis Research*, 25(3), pp. 173–185. doi: 10.1007/BF00033159.

Blackburn, S. I. and Volkman, J. K. (2012) ‘Microalgae: A renewable source of bioproducts’, in Dunford, N. T. (ed.) *Food and Industrial Bioproducts and Bioprocessing*. 1st edn. Iowa: Iowa State University Press, pp. 221–241. doi: 10.1002/9781119946083.ch9.

Borowitzka, M. A. (1997) ‘Microalgae for aquaculture: Opportunities and constraints’, *Journal of Applied Phycology*, 9(5), pp. 393–401. doi: 10.1023/A:1007921728300.

Borowitzka, M. A. (2013) ‘High-value products from microalgae-their development and commercialisation’, *Journal of Applied Phycology*, 25(3), pp. 743–756. doi: 10.1007/s10811-013-9983-9.

Borowitzka, M. A. and Moheimani, N. R. (eds) (2013) *Algae for biofuels and energy*. Dordrecht: Springer Netherlands. doi: 10.1007/978-94-007-5479-9.

- Bowler, C., Allen, A. E., Badger, J. H., Grimwood, J., Jabbari, K., Kuo, A., Maheswari, U., Martens, C., Maumus, F., Otilar, R. P., Rayko, E., Salamov, A., Vandepoele, K., Beszteri, B., Gruber, A., Heijde, M., Katinka, M., Mock, T., Valentin, K., *et al.* (2008) 'The *Phaeodactylum* genome reveals the evolutionary history of diatom genomes', *Nature*, 456(7219), pp. 239–44. doi: 10.1038/nature07410.
- Bozarth, A., Maier, U. G. and Zauner, S. (2009) 'Diatoms in biotechnology: Modern tools and applications', *Applied Microbiology and Biotechnology*, 82(2), pp. 195–201. doi: 10.1007/s00253-008-1804-8.
- Brown, M. R. (2002) 'Nutritional value and use of microalgae in aquaculture', in Cruz-Suárez, L. E., Ricque-Marie, D., Tapia-Salazar, M., Gaxiola-Cortés, M. G., and Simoes, N. (eds) *Avances en nutrición acuícola VI. Memorias del VI Simposio Internacional de Nutrición Acuícola*. Quintana Roo, México, pp. 281–292. doi: 10.5772/1516.
- Brown, M. R., Jeffrey, S. W., Volkman, J. K. and Dunstan, G. A. (1997) 'Nutritional properties of microalgae for mariculture', *Aquaculture*, 151(1–4), pp. 315–331. doi: 10.1016/S0044-8486(96)01501-3.
- Brown, M. R., Mular, M., Miller, I., Farmer, C. and Trenerry, C. (1999) 'The vitamin content of microalgae used in aquaculture', *Journal of Applied Phycology*, 11(3), pp. 247–255. doi: 10.1023/A:1008075903578.
- Camacho-Rodríguez, J., Cerón-García, M. C., Macías-Sánchez, M. D., Fernández-

Sevilla, J. M., López-Rosales, L. and Molina-Grima, E. (2016) ‘Long-term preservation of concentrated *Nannochloropsis gaditana* cultures for use in aquaculture’, *Journal of Applied Phycology*, 28(1), pp. 299–312. doi: 10.1007/s10811-015-0572-y.

Carreau, J. P. and Dubacq, J. P. (1978) ‘Adaptation of a macro-scale method to the micro-scale for fatty acid methyl transesterification of biological lipid extracts’, *Journal of Chromatography A*, 151(3), pp. 384–390. doi: 10.1016/S0021-9673(00)88356-9.

Carvalho, A. P., Silva, S. O., Baptista, J. M. and Malcata, F. X. (2011) ‘Light requirements in microalgal photobioreactors: An overview of biophotonic aspects’, *Applied Microbiology and Biotechnology*, 89(5), pp. 1275–1288. doi: 10.1007/s00253-010-3047-8.

Chen, C.-Y., Chen, Y.-C., Huang, H.-C., Huang, C.-C., Lee, W.-L. and Chang, J.-S. (2013) ‘Engineering strategies for enhancing the production of eicosapentaenoic acid (EPA) from an isolated microalga *Nannochloropsis oceanica* CY2’, *Bioresource Technology*, 147, pp. 160–167. doi: 10.1016/j.biortech.2013.08.051.

Costa, B. S., Jungandreas, A., Jakob, T., Weisheit, W., Mittag, M. and Wilhelm, C. (2013) ‘Blue light is essential for high light acclimation and photoprotection in the diatom *Phaeodactylum tricornutum*’, *Journal of Experimental Botany*, 64(2), pp. 483–93. doi: 10.1093/jxb/ers340.

Crawford, M. H. (2009) ‘LEDs for solid-state lighting: Performance challenges and

recent advances', *IEEE Journal on Selected Topics in Quantum Electronics*, 15(4), pp. 1028–1040. doi: 10.1109/jstqe.2009.2013476.

D'Souza, F. M. L. and Loneragan, N. R. (1999) 'Effects of monospecific and mixed-algae diets on survival, development and fatty acid composition of penaeid prawn (*Penaeus* spp.) larvae', *Marine Biology*, 133(4), pp. 621–633.

Dubois, M., Gilles, K., Hamilton, J. K., Rebers, P. A. and Smith, F. (1951) 'A colorimetric method for the determination of sugars', *Nature*, 168(4265), pp. 167–167. doi: 10.1038/168167a0.

Fabregas, J., Herrero, C., Cabezas, B. and Abalde, J. (1986) 'Biomass production and biochemical composition in mass cultures of the marine microalga *Isochrysis galbana* Parke at varying nutrient concentrations', *Aquaculture*, 53(2), pp. 101–113. doi: 10.1016/0044-8486(86)90280-2.

Falkowski, P. G., Barber, R. T. and Smetacek, V. (1998) 'Biogeochemical controls and feedbacks on ocean primary production', *Science*, 281(5374), pp. 200–207.

Falkowski, P. G., Dubinsky, Z. and Wyman, K. (1985) 'Growth-irradiance relationships in phytoplankton', *Limnology and Oceanography*, 30(2), pp. 311–321. doi: 10.4319/lo.1985.30.2.0311.

Falkowski, P. G. and Raven, J. A. (2007) *Aquatic photosynthesis*. 2nd Ed. New Jersey, USA: Princeton University Press.



Field, C. B., Behrenfeld, M. J., Randerson, J. T. and Falkowski, P. (1998) 'Primary production of the biosphere: Integrating terrestrial and oceanic components', *Science*, 281(5374), pp. 237–240. doi: 10.1126/science.281.5374.237.

Fisher, A. E., Berges, J. A. and Harrison, P. J. (1996) 'Does light quality affect the sinking rates of marine diatoms?', *Journal of Phycology*, 32, pp. 353–360.

Folch, J., Lees, M. and Stanley, G. H. S. (1957) 'A simple method for the isolation and purification of total lipides from animal tissues', *Journal of Biological Chemistry*, 226(1), pp. 497–509.

Foo, S. C., Yusoff, F. M., Ismail, M., Basri, M., Yau, S. K., Khong, N. M. H., Chan, K. W. and Ebrahimi, M. (2017) 'Antioxidant capacities of fucoxanthin-producing algae as influenced by their carotenoid and phenolic contents', *Journal of Biotechnology*, 241, pp. 175–183. doi: 10.1016/j.jbiotec.2016.11.026.

Fu, W., Guðmundsson, Ó., Paglia, G., Herjólfsen, G., Andr sson,  . S., P lsson, B.  . and Brynj lfsen, S. (2013) 'Enhancement of carotenoid biosynthesis in the green microalga *Dunaliella salina* with light-emitting diodes and adaptive laboratory evolution', *Applied Microbiology and Biotechnology*, 97(6), pp. 2395–2403. doi: 10.1007/s00253-012-4502-5.

Furukawa, T., Watanabe, M. and Shihira-Ishikawa, I. (1998) 'Green-and blue-light-mediated chloroplast migration in the centric diatom *Pleurosira laevis*', *Protoplasma*,

203, pp. 214–220. doi: 10.1007/bf01279479.

Gilbert, M., Domin, A., Becker, A. and Wilhelm, C. (2000) 'Estimation of primary productivity by chlorophyll *a* in vivo fluorescence in freshwater phytoplankton', *Photosynthetica*, pp. 111–126. doi: 10.1023/a:1026708327185.

Glemser, M., Heining, M., Schmidt, J., Becker, A., Garbe, D., Buchholz, R. and Brück, T. (2016) 'Application of light-emitting diodes (LEDs) in cultivation of phototrophic microalgae: Current state and perspectives', *Applied Microbiology and Biotechnology*, 100(3), pp. 1077–1088. doi: 10.1007/s00253-015-7144-6.

Gorai, T., Katayama, T., Obata, M., Murata, A. and Taguchi, S. (2014) 'Low blue light enhances growth rate, light absorption, and photosynthetic characteristics of four marine phytoplankton species', *Journal of Experimental Marine Biology and Ecology*, 459, pp. 87–95. doi: 10.1016/j.jembe.2014.05.013.

Guedes, A. C. and Malcata, F. X. (2012) 'Nutritional value and uses of microalgae in aquaculture', *Aquaculture*, p. 390. doi: 10.5772/1516.

Guillard, R. R. L. (1975) 'Culture of phytoplankton for feeding marine invertebrates', in Smith, W. L. and Chanley, M. H. (eds) *Culture of marine invertebrate animals*. Boston, MA: Springer US, pp. 29–60. doi: 10.1007/978-1-4615-8714-9\_3.

Guiry, M. D. (2012) 'How many species of algae are there?', *Journal of Phycology*, 48(5), pp. 1057–1063. doi: 10.1111/j.1529-8817.2012.01222.x.

- Han, P., Shen, S., Wang, H.-Y., Yao, S., Tan, Z., Zhong, C. and Jia, S. (2017) 'Applying the strategy of light environment control to improve the biomass and polysaccharide production of *Nostoc flagelliforme*', *Journal of Applied Phycology*, 29(1), pp. 55–65. doi: 10.1007/s10811-016-0963-8.
- Harrison, P. J., Thompson, P. A. and Calderwood, G. S. (1990) 'Effects of nutrient and light limitation on the biochemical composition of phytoplankton', *Journal of Applied Phycology*, 2(1), pp. 45–56. doi: 10.1007/BF02179768.
- Herlory, O., Richard, A. P. and Blanchard, G. F. (2007) 'Methodology of light response curves: Application of chlorophyll fluorescence to microphytobenthic biofilms', *Marine Biology*, 153, pp. 91–101. doi: 10.1007/s00227-007-0787-9.
- Hildebrand, M., Davis, A. K., Smith, S. R., Traller, J. C. and Abbriano, R. (2012) 'The place of diatoms in the biofuels industry', *Biofuels*, 3(2), pp. 221–240. doi: 10.4155/bfs.11.157.
- Houliez, E., Lefebvre, S., Lizon, F. and Schmitt, G. F. (2017) 'Rapid light curves (RLC) or non-sequential steady-state light curves (N-SSLC): Which fluorescence-based light response curve methodology robustly characterizes phytoplankton photosynthetic activity and acclimation status?', *Marine Biology*, 164(174), pp. 1–17. doi: 10.1007/s00227-017-3208-8.
- Huang, H.-H., Feng, L., Liu, Y., Jiang, J., Jjiang, W.-D., Hu, K., Li, S.-H. and Zhou, X.-

- Q. (2011) 'Effects of dietary thiamin supplement on growth, body composition and intestinal enzyme activities of juvenile Jian carp (*Cyprinus carpio* var. Jian)', *Aquaculture Nutrition*, 17(2), pp. e233–e240. doi: 10.1111/j.1365-2095.2010.00756.x.
- Huang, X., Huang, Z., Wen, W. and Yan, J. (2013) 'Effects of nitrogen supplementation of the culture medium on the growth, total lipid content and fatty acid profiles of three microalgae (*Tetraselmis subcordiformis*, *Nannochloropsis oculata* and *Pavlova viridis*)', *Journal of Applied Phycology*, 25(1), pp. 129–137. doi: 10.1007/s10811-012-9846-9.
- Janech, M. G., Krell, A., Mock, T., Kang, J.-S. and Raymond, J. A. (2006) 'Ice-binding proteins from sea ice diatoms (Bacillariophyceae)', *Journal of Phycology*, 42(2), pp. 410–416. doi: 10.1111/j.1529-8817.2006.00208.x.
- Jeffrey, S. W., Leroi, J.-M. and Brown, M. R. (1992) 'Characteristics of microalgal species needed for Australian mariculture', in *Proceedings of the Aquaculture Nutrition Workshop*. Salamander Bay, NSW: Orange: NSW Fisheries, pp. 164–173.
- Jeon, Y.-C., Cho, C.-W. and Yun, Y.-S. (2005) 'Measurement of microalgal photosynthetic activity depending on light intensity and quality', *Biochemical Engineering Journal*, 27(2), pp. 127–131. doi: 10.1016/j.bej.2005.08.017.
- Jin, E., Polle, J. E. W., Lee, H. K., Hyun, S. M. and Chang, M. (2003) 'Xanthophylls in microalgae: From biosynthesis to biotechnological mass production and application', *Journal of Microbiology and Biotechnology*, 13(2), pp. 165–174. doi: <http://dx.doi.org/>.

Jungandreas, A., Costa, B. S., Jakob, T., Von Bergen, M., Baumann, S. and Wilhelm, C.

(2014) 'The acclimation of *Phaeodactylum tricornutum* to blue and red light does not influence the photosynthetic light reaction but strongly disturbs the carbon allocation pattern', *PLoS ONE*, 9(8), pp. 5–15. doi: 10.1371/journal.pone.0099727.

Katsuda, T., Lababpour, A., Shimahara, K. and Katoh, S. (2004) 'Astaxanthin

production by *Haematococcus pluvialis* under illumination with LEDs', *Enzyme and Microbial Technology*, 35(1), pp. 81–86. doi: 10.1016/j.enzmictec.2004.03.016.

Kawakami, T., Tsushima, M., Katabami, Y., Mine, M., Ishida, A. and Matsuno, T.

(1998) 'Effect of  $\beta$ , $\beta$ -carotene,  $\beta$ -echinenone, astaxanthin, fucoxanthin, vitamin A and vitamin E on the biological defense of the sea urchin *Pseudocentrotus depressus*',

*Journal of Experimental Marine Biology and Ecology*, 226(2), pp. 165–174. doi: 10.1016/S0022-0981(97)00236-0.

Kawamura, T., Roberts, R. D. and Nicholson, C. M. (1998) 'Factors affecting the food

value of diatom strains for post-larval abalone *Haliotis iris*', *Aquaculture*, 160(1), pp. 81–88. doi: 10.1016/S0044-8486(97)00223-8.

Knauer, J. and Southgate, P. C. (1999) 'A review of the nutritional requirements of

bivalves and the development of alternative and artificial diets for bivalve aquaculture', *Reviews in Fisheries Science*, 7(3–4), pp. 241–280. doi: 10.1080/10641269908951362.

Lebeau, T. and Robert, J. M. (2003a) 'Diatom cultivation and biotechnologically

relevant products. Part I: Cultivation at various scales', *Applied Microbiology and Biotechnology*, 60, pp. 612–623. doi: 10.1007/s00253-002-1176-4.

Lebeau, T. and Robert, J. M. (2003b) 'Diatom cultivation and biotechnologically relevant products. Part II: Current and putative products', *Applied Microbiology and Biotechnology*, 60, pp. 624–632. doi: 10.1007/s00253-002-1177-3.

Lee, C.-G. (1999) 'Calculation of light penetration depth in photobioreactors', *Biotechnology and Bioprocess Engineering*, 4(1), pp. 78–81. doi: 10.1007/BF02931920.

Lemmermann, E. (1898) 'Der grosse Waterneverstorfer Binnensee. Eine biologische Studie', *Forschungsberichte aus der Biologischen Station zu Plön*, 6, pp. 166–205.

Lohr, M. and Wilhelm, C. (1999) 'Algae displaying the diadinoxanthin cycle also possess the violaxanthin cycle', *Proceedings of the National Academy of Sciences of the United States of America*, 96(15), pp. 8784–8789. doi: 10.1073/pnas.96.15.8784.

Lohr, M. and Wilhelm, C. (2001) 'Xanthophyll synthesis in diatoms: Quantification of putative intermediates and comparison of pigment conversion kinetics with rate constants derived from a model', *Planta*, 212(3), pp. 382–391. doi: 10.1007/s004250000403.

López Elías, J. A., Voltolina, D., Chavira Ortega, C. O., Rodríguez Rodríguez, B. B., Sáenz Gaxiola, L. M., Cordero Esquivel, B. and Nieves, M. (2003) 'Mass production of microalgae in six commercial shrimp hatcheries of the Mexican northwest',

*Aquacultural Engineering*, 29(3–4), pp. 155–164. doi: 10.1016/S0144-8609(03)00081-5.

Lourenço, S. O., Barbarino, E., Lavín, P. L., Lanfer Marquez, U. M. and Aida, E. (2004) 'Distribution of intracellular nitrogen in marine microalgae: Calculation of new nitrogen-to-protein conversion factors', *European Journal of Phycology*, 39(1), pp. 17–32. doi: 10.1080/0967026032000157156.

Lucker, B. F., Hall, C. C., Zegarac, R. and Kramer, D. M. (2014) 'The environmental photobioreactor (ePBR): An algal culturing platform for simulating dynamic natural environments', *Algal Research*, 6(PB), pp. 242–249. doi: 10.1016/j.algal.2013.12.007.

MacIntyre, H. L., Kana, T. M., Anning, T. and Geider, R. J. (2002) 'Photoacclimation of photosynthesis irradiance response curves and photosynthetic pigments in microalgae and cyanobacteria', *Journal of Phycology*, 38(1), pp. 17–38. doi: 10.1046/j.1529-8817.2002.00094.x.

Mann, D. G. and Vanormelingen, P. (2013) 'An inordinate fondness? The number, distributions, and origins of diatom species', *Journal of Eukaryotic Microbiology*, 60(4), pp. 414–420. doi: 10.1111/jeu.12047.

Mann, J. E. and Myers, J. (1968) 'On pigments, growth, and photosynthesis of *Phaeodactylum tricornutum*', *Journal of Phycology*, 4(4), pp. 349–355. doi: 10.1111/j.1529-8817.1968.tb04707.x.

- Marchetti, J., Bougaran, G., Jauffrais, T., Lefebvre, S., Rouxel, C., Saint-Jean, B., Lukomska, E., Robert, R. and Cadoret, J. P. (2013) 'Effects of blue light on the biochemical composition and photosynthetic activity of *Isochrysis* sp. (T-iso)', *Journal of Applied Phycology*, 25(1), pp. 109–119. doi: 10.1007/s10811-012-9844-y.
- Martin-Jezequel, V., Hildebrand, M. and Brzezinski, M. A. (2000) 'Silicon metabolism in diatoms: Implications for growth', *Journal of Phycology*, 36(5), pp. 821–840. doi: 10.1046/j.1529-8817.2000.00019.x.
- Masuko, T., Minami, A., Iwasaki, N., Majima, T., Nishimura, S.-I. and Lee, Y. C. (2005) 'Carbohydrate analysis by a phenol–sulfuric acid method in microplate format', *Analytical Biochemistry*, 339(1), pp. 69–72. doi: 10.1016/J.AB.2004.12.001.
- Metting, F. B. (1996) 'Biodiversity and application of microalgae', *Journal of Industrial Microbiology & Biotechnology*, 17(5–6), pp. 477–489. doi: 10.1007/bf01574779.
- Montagnes, D. J. S. and Franklin, M. (2001) 'Effect of temperature on diatom volume, growth rate, and carbon and nitrogen content: Reconsidering some paradigms', *Limnology and Oceanography*, 46(8), pp. 2008–2018. doi: 10.4319/lo.2001.46.8.2008.
- Morel, A. (1978) 'Available, usable, and stored radiant energy in relation to marine photosynthesis', *Deep Sea Research*, 25(8), pp. 673–688. doi: 10.1016/0146-6291(78)90623-9.
- Mouget, J.-L., Rosa, P. and Tremblin, G. (2004) 'Acclimation of *Haslea ostrearia* to



light of different spectral qualities – confirmation of ‘chromatic adaptation’ in diatoms’,

*Journal of Photochemistry and Photobiology B: Biology*, 75(1–2), pp. 1–11. doi:

10.1016/j.jphotobiol.2004.04.002.

Müller, P., Li, X.-P. and Niyogi, K. K. (2001) ‘Non-Photochemical Quenching. A

Response to Excess Light Energy’, *Plant Physiology*, 125, pp. 1558–1566. doi:

10.1104/pp.124.1.273.

Nelson, D. M., Tréguer, P., Brzezinski, M. A., Leynaert, A. and Quéguiner, B. (1995)

‘Production and dissolution of biogenic silica in the ocean: Revised global estimates,

comparison with regional data and relationship to biogenic sedimentation’, *Global*

*Biogeochemical Cycles*, 9(3), pp. 359–372. doi: 10.1029/95gb01070.

Nichols, D. S. (2003) ‘Prokaryotes and the input of polyunsaturated fatty acids to the

marine food web’, *FEMS Microbiology Letters*, 219(1), pp. 1–7. doi: 10.1016/S0378-

1097(02)01200-4.

Nielsen, R., Nielsen, M., Abate, T. G., Hansen, B. W., Jepsen, P. M., Nielsen, S. L.,

Støttrup, J. G. and Buchmann, K. (2017) ‘The importance of live-feed traps - farming

marine fish species’, *Aquaculture Research*, 48(6), pp. 2623–2641. doi:

10.1111/are.13281.

Nobel, P. S. (2009) *Physicochemical and environmental plant physiology*. 4th edn.

Amsterdam: Academic Press.

- Okumura, C., Saffreena, N., Rahman, M. A., Hasegawa, H., Miki, O. and Takimoto, A. (2015) 'Economic efficiency of different light wavelengths and intensities using LEDs for the cultivation of green microalga *Botryococcus braunii* (NIES-836) for biofuel production', *Environmental Progress & Sustainable Energy*, 34(1), pp. 269–275. doi: 10.1002/ep.11951.
- Papagiannakis, E., Van Stokkum, I. H. M., Fey, H., Büchel, C. and Van Grondelle, R. (2005) 'Spectroscopic characterization of the excitation energy transfer in the fucoxanthin-chlorophyll protein of diatoms', *Photosynthesis Research*, 86(1–2), pp. 241–250. doi: 10.1007/s11120-005-1003-8.
- Parrish, C. C., Wells, J. S., Yang, Z. and Dabinett, P. (1998) 'Growth and lipid composition of scallop juveniles, *Placopecten magellanicus*, fed the flagellate *Isochrysis galbana* with varying lipid composition and the diatom *Chaetoceros muelleri*', *Marine Biology*, 133(3), pp. 461–471. doi: 10.1007/s002270050486.
- Pérez-Pazos, J.-V. and Fernández-Izquierdo, P. (2011) 'Synthesis of neutral lipids in *Chlorella* sp. under different light and carbonate conditions', *Tecnología y Futuro*, 4.
- Perkins, R. G., Kromkamp, J. C., Serôdio, J., Lavaud, J., Jesus, B., Mouget, J. L., Lefebvre, S. and Forster, R. M. (2010) 'The application of variable chlorophyll fluorescence to microphytobenthic biofilms', in Suggett, D. J., Borowitzka, M. A., and Prášil, O. (eds) *Chlorophyll a Fluorescence in Aquatic Sciences: Methods and*

*Applications*. Dordrecht: Springer Netherlands, pp. 237–275. doi: 10.1007/978-90-481-9268-7\_12.

Platt, T., Gallegos, C. and Harrison, W. (1980) ‘Photoinhibition of photosynthesis in natural assemblages of marine phytoplankton’, *Journal of Marine Research*, 38(4), pp. 687–701.

van de Poll, W. H. and Buma, A. G. J. (2009) ‘Does ultraviolet radiation affect the xanthophyll cycle in marine phytoplankton?’, *Photochemical & Photobiological Sciences*, 8(9), pp. 1295–1301. doi: 10.1039/b904501e.

Powles, S. B. (1984) ‘Photoinhibition of photosynthesis induced by visible light’, *Annual Review of Plant Physiology*, 35(1), pp. 15–44. doi: 10.1146/annurev.pp.35.060184.000311.

Ralph, P. J. and Gademann, R. (2005) ‘Rapid light curves: A powerful tool to assess photosynthetic activity’, *Aquatic Botany*, 82(3), pp. 222–237. doi: 10.1016/j.aquabot.2005.02.006.

Richmond, A. (ed.) (2004) *Handbook of microalgal culture: Biotechnology and applied phycology*. Oxford, UK: Blackwell Science. doi: 10.1002/9780470995280.

Sakshaug, E., Bricaud, A., Dandonneau, Y., Falkowski, P. G., Kiefer, D. A., Legendre, L., Morel, A., Parslow, J. and Takahashi, M. (1997) ‘Parameters of photosynthesis: Definitions, theory and interpretation of results’, *Journal of Plankton Research*, 19(11),

pp. 1637–1670. doi: 10.1093/plankt/19.11.1637.

Scala, S. and Bowler, C. (2001) ‘Molecular insights into the novel aspects of diatom biology’, *Cellular and Molecular Life Sciences CMLS*, 58(11), pp. 1666–1673. doi: 10.1007/pl00000804.

Schreiber, U. (2005) ‘Pulse-amplitude-modulation (PAM) fluorometry and saturation pulse method: An overview’, in Papageorgiou, G. C. and Govindjee (eds) *Advances in Photosynthesis and Respiration*. Dordrecht: Springer Netherlands, pp. 279–319. doi: 10.1007/978-1-4020-3218-9\_11.

Schreiber, U., Klughammer, C. and Kolbowski, J. (2011) ‘High-end chlorophyll fluorescence analysis with the MULTI-COLOR-PAM I. Various light qualities and their applications’, *PAM Application Notes*, 1, pp. 1–21.

Schreiber, U., Klughammer, C. and Kolbowski, J. (2012) ‘Assessment of wavelength-dependent parameters of photosynthetic electron transport with a new type of multi-color PAM chlorophyll fluorometer’, *Photosynthesis Research*, 113(1–3), pp. 127–144. doi: 10.1007/s11120-012-9758-1.

Schulze, P. S. C., Barreira, L. A., Pereira, H. G. C., Perales, J. A. and Varela, J. C. S. (2014) ‘Light emitting diodes (LEDs) applied to microalgal production’, *Trends in Biotechnology*, 32(8), pp. 422–430. doi: 10.1016/j.tibtech.2014.06.001.

Schulze, P. S. C., Pereira, H. G. C., Santos, T. F. C., Schueler, L., Guerra, R., Barreira,

L. A., Perales, J. A. and Varela, J. C. S. (2016) 'Effect of light quality supplied by light emitting diodes (LEDs) on growth and biochemical profiles of *Nannochloropsis oculata* and *Tetraselmis chuii*', *Algal Research*, 16, pp. 387–398. doi:

10.1016/j.algal.2016.03.034.

Shikata, T., Iseki, M., Matsunaga, S., Higashi, S., Kamei, Y. and Watanabe, M. (2011)

'Blue and red light-induced germination of resting spores in the red-tide diatom

*Leptocylindrus danicus*', *Photochemistry and Photobiology*, 87(3), pp. 590–597. doi:

10.1111/j.1751-1097.2011.00914.x.

Shimura, S. and Fujita, Y. (1975) 'Changes in the activity of fucoxanthin-excited

photosynthesis in the marine diatom *Phaeodactylum tricornutum* grown under different

culture conditions', *Marine Biology*, 33(3), pp. 185–194. doi: 10.1007/bf00390922.

Shu, C.-H., Tsai, C.-C., Liao, W.-H., Chen, K.-Y. and Huang, H.-C. (2012) 'Effects of

light quality on the accumulation of oil in a mixed culture of *Chlorella* sp. and

*Saccharomyces cerevisiae*', *Journal of Chemical Technology & Biotechnology*, 87(5),

pp. 601–607. doi: 10.1002/jctb.2750.

Sims, P. A., Mann, D. G. and Medlin, L. K. (2006) 'Evolution of the diatoms: Insights

from fossil, biological and molecular data', *Phycologia*, 45(4), pp. 361–402. doi:

10.2216/05-22.1.

Spolaore, P., Joannis-Cassan, C., Duran, E. and Isambert, A. (2006) 'Commercial

applications of microalgae', *Journal of Bioscience and Bioengineering*, 101(2), pp. 87–

96. doi: <http://dx.doi.org/10.1263/jbb.101.87>.

Tamburic, B., Evenhuis, C. R., Crosswell, J. R. and Ralph, P. J. (2018) 'An empirical process model to predict microalgal carbon fixation rates in photobioreactors', *Algal*

*Research*, 31, pp. 334–346. doi: 10.1016/j.algal.2018.02.014.

Tamburic, B., Evenhuis, C. R., Suggett, D. J., Larkum, A. W. D., Raven, J. A. and

Ralph, P. J. (2015) 'Gas transfer controls carbon limitation during biomass production by marine microalgae', *Chem Sus Chem*, 8(16), pp. 2727–2736. doi:

10.1002/cssc.201500332.

Tamburic, B., Guruprasad, S., Radford, D. T., Szabó, M., Lilley, R. M., Larkum, A. W.

D., Franklin, J. B., Kramer, D. M., Blackburn, S. I., Raven, J. A., Schliep, M. and Ralph,

P. J. (2014) 'The effect of diel temperature and light cycles on the growth of

*Nannochloropsis oculata* in a photobioreactor matrix', *PLoS ONE*, 9(1), pp. 1–13. doi:

10.1371/journal.pone.0086047.

Thompson, P. A., Harrison, P. J. and Parslow, J. S. (1991) 'Influence of irradiance on cell volume and carbon quota for ten species of marine phytoplankton', *Journal of*

*Phycology*, 27(3), pp. 351–360. doi: 10.1111/j.0022-3646.1991.00351.x.

Tréguer, P., Nelson, D. and Bennekom, A. Van (1995) 'The silica balance in the world ocean: a reestimate', *Science*, 268(5209), pp. 375–379.

- Valle, K. C., Nymark, M., Aamot, I., Hancke, K., Winge, P., Andresen, K., Johnsen, G., Brembu, T. and Bones, A. M. (2014) 'System responses to equal doses of photosynthetically usable radiation of blue, green, and red light in the marine diatom *Phaeodactylum tricornutum*', *PLoS ONE*, 9(12), pp. 1–37. doi: 10.1371/journal.pone.0114211.
- Wang, C.-Y., Fu, C.-C. and Liu, Y.-C. (2007) 'Effects of using light-emitting diodes on the cultivation of *Spirulina platensis*', *Biochemical Engineering Journal*, 37(1), pp. 21–25. doi: 10.1016/j.bej.2007.03.004.
- Webb, K. L. and Chu, F. E. (1983) 'Phytoplankton as a food source for bivalve larvae', in Pruder, G. D., Langdon, C., and Conklin, D. (eds) *Proceedings of the Second International conference on Aquaculture Nutrition: Biochemical and physiological approaches to shellfish nutrition, Lewes/Rehoboth Beach, Delaware, October 27-29 1981*. LA: Louisiana State University, pp. 272–291.
- Williams, P. and Laurens, L. (2010) 'Microalgae as biodiesel biomass & feedstocks: Review & analysis of the biochemistry, energetics & economics', *Energy & Environmental Science*, 3(5), p. 554. doi: 10.1039/b924978h.
- Wood, M. A., Everroad, R. C. and Wingard, L. M. (2005) 'Measuring growth rates in microalgal cultures', in Andersen, R. A. (ed.) *Algal Culturing Techniques*. Massachusetts: Elsevier Academic Press, pp. 269–285.

Xia, S., Wang, K., Wan, L., Li, A., Hu, Q. and Zhang, C. (2013) ‘Production, characterization, and antioxidant activity of fucoxanthin from the marine diatom *Odontella aurita*’, *Mar. Drugs*, 11, pp. 2667–2681. doi: 10.3390/md11072667.

Zhu, W., Mai, K. and Wu, G. (2002) ‘Thiamin requirement of juvenile abalone, *Haliotis discus hannai* Ino’, *Aquaculture*, 207(3–4), pp. 331–343. doi: 10.1016/S0044-8486(01)00749-9.

### 3.8. Supplementary Materials

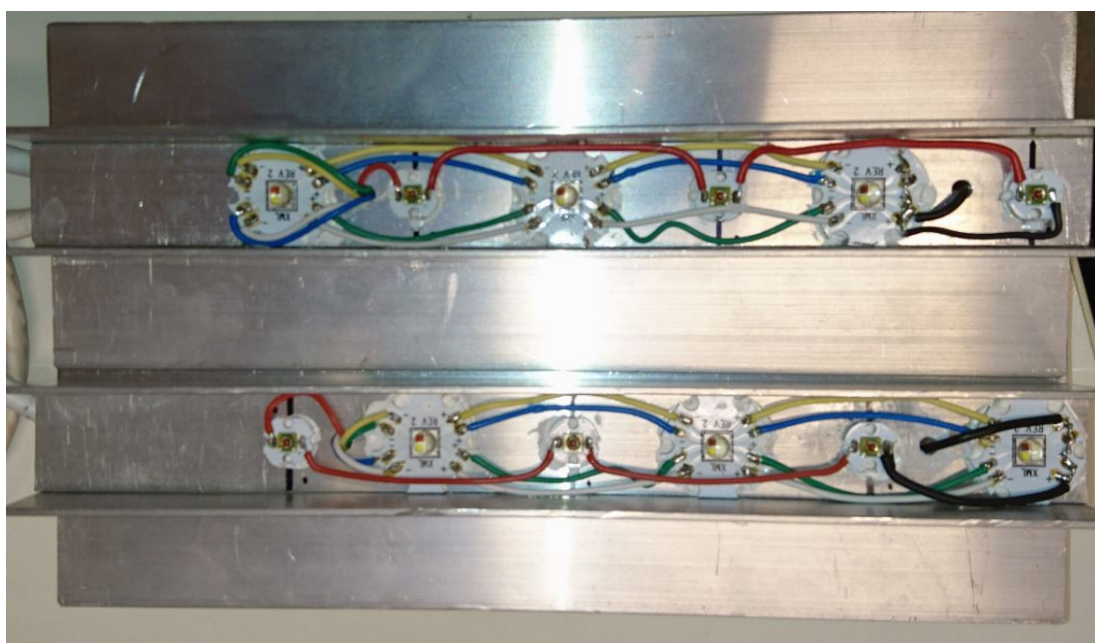


**Figure 3.13** View of the LED chips and their arrangements in the custom LED panel used in the study. The larger chips are the CREE® XLamp® XM-L Color and the smaller chips are the Cree® XLamp® XP-E photo-red.



## Chapter 4 Change in photon diet – Light quality shifting to tailor metabolite content and their digestibility in *Chaetoceros muelleri*

Kenji Iwasaki, Janice McCauley, Milán Szabó, Bojan Tamburic,

Unnikrishnan Kuzhiumparambil & Peter Ralph

Climate Change Cluster (C3), Faculty of Science, University of Technology Sydney,

Australia

### 4.1. Introduction

#### 4.1.1. Diatoms in aquaculture

The global annual microalgae production is estimated to be 5000 t yr<sup>-1</sup> with a turnover of approximately US\$ 1.25 billion yr<sup>-1</sup> (Pulz and Gross, 2004; Hemaiswarya *et al.*, 2011). Microalgae production for feed in aquaculture is one of the fastest growing industries with an estimated value of US\$ 700 million (Pulz and Gross, 2004). Less than twenty species are used as feed in commercial aquaculture today, of which notable diatom (Bacillariophyceae) species include: *Chaetoceros* sp., *Thalassiosira* sp., *Skeletonema* sp. and *Nitzschia* sp. (Brown, 2002). Diatoms have been cultured in large-scale production systems for aquaculture feed for decades and are particularly important in feeding bivalve, mollusc and shrimp larvae (Brown *et al.*, 1997; Lebeau and Robert, 2003a, 2003b). While protein and vitamin contents are determining factor when

determining the nutritional value of feed, polyunsaturated fatty acids (PUFAs) are an essential dietary requirement for marine animals (Nichols, 2003; Hemaiswarya *et al.*, 2011). Diatoms have been shown to contain balanced levels of important PUFAs: eicosapentaenoic acid (EPA C20:5 omega-3), docosahexaenoic acid (DHA C22:6 omega-3) and arachidonic acid (ARA C20:5 omega-6) which have been linked to benefit larval growth (Blackburn and Volkman, 2012). Various strategies have been employed to improve PUFA content in microalgae, such as light intensity, nutrient stresses, and temperature (Hemaiswarya *et al.*, 2011). One such strategy involves the manipulation of light quality used to culture microalgae.

#### 4.1.2. Selecting light quality to grow diatoms in aquaculture

Two properties are vital for high biomass productivity of diatoms in aquaculture: light quality and intensity (Lee, 1999). While intensive research has been conducted on light intensity and its impact on growth (Thompson, Harrison and Parslow, 1991; Carvalho *et al.*, 2011; Beardall and Raven, 2013), the effect of light quality and its impact on growth and metabolic content is not yet understood in diatoms.

Light quality (or spectral quality) refers to the distribution of wavelengths of a light source. In selecting light quality, one must consider the pigment makeup of the desired microalga. As diatoms are equipped with chlorophylls (Chl) *a* and *c*, as well as the

carotenoid fucoxanthin, they are able to utilize blue, green, and red wavelength bands for photosynthesis (Bertrand, 2010; Borowitzka, 2013; Richmond, 2004; Schulze *et al.*, 2014). After determining the optimum light quality, the cost efficiency in producing biomass and metabolite content should be considered. As shown in Chapter 3, different monochromatic light emitting diodes (LED) were used to grow the centric diatom *Chaetoceros muelleri* and a significant difference in cost efficiency was observed between LEDs in producing biomass and metabolite content.

#### 4.1.3. Light shifting in microalgae

Another aspect of researching light quality in microalgae has been to investigate the capability of using light quality shifts as a technique to manipulate the metabolism of microalgae to produce desired metabolites (section 3.1.).

Light shifting (also known as spectral shift and wavelength shift) refers to a shift in the spectrum of light during culture growth (e.g. blue light to red light). It is hypothesized that shifting the wavelength of light can stimulate a growth or metabolic response. For example, in the model chlorophytes *Chlamydomonas reinhardtii* and *Chlorella vulgaris* blue light was observed to significantly increase cell size, while red light promoted cell division (Oldenhof, Zachleder and Van Den Ende, 2006; Kim *et al.*, 2014). Therefore, in contrast to the traditional white light, a strategy was proposed to shift the light quality

from blue to red light (Kim *et al.*, 2014). During the first stage, *C. vulgaris* was grown using blue light to increase the cell size during the lag phase (Kim *et al.*, 2014). In the second stage, growth light was shifted from blue light to red light, where by the large cells would be triggered to divide at a more rapid rate during the exponential phase (Kim *et al.*, 2014; Figure 4.1).

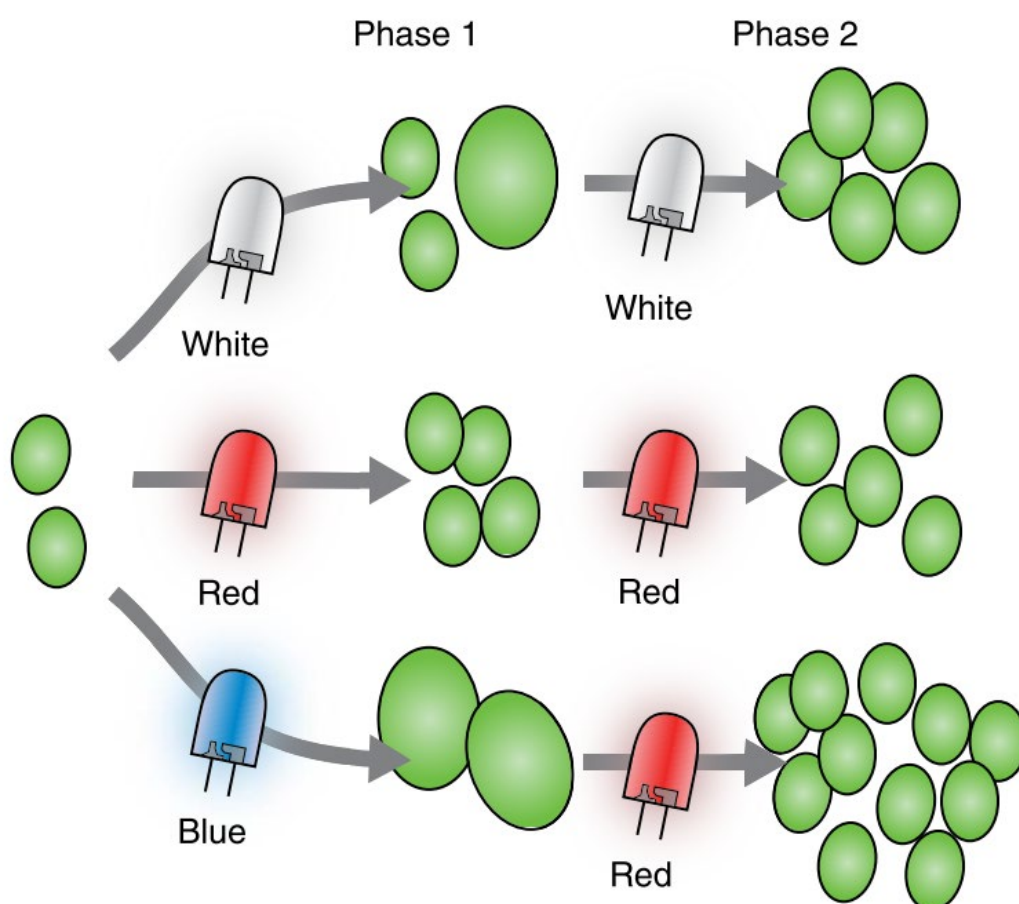


**Figure 4.1** Conceptual diagram of a) traditional illumination of microalgae with white light b) illumination with constant red light c) a light shift from blue light to red light which induces an increase in division in *Chlamydomonas vulgaris* by increasing cell

volume in blue light and subsequently shifting to red light to induce division (image adapted by Ooms *et al.* 2016; original image from Kim *et al.* 2014).

It should also be noted that Kim *et al.* (2014) investigated different scenarios of light shifts, whereby the shift in light quality occurred at different times. Kim *et al.* (2014) demonstrated that higher biomass yields were observed in *C. vulgaris* cultures where a light shift from blue to red occurred during the third and fourth day (out of a five day experiment duration). Other scenarios shifting to red light too early (the second day) or late (fifth day) did not improve the biomass yield (Kim *et al.*, 2014). Kim *et al.* (2014) therefore hypothesized that in order to increase biomass yields with a red light shift it must correspond to the late exponential phase.

Another example of research utilizing light shift was Ra *et al.* (2016) to manipulate the lipid content of *Nannochloropsis oculata*, *N. oceanica* and *N. salina*. They observed that all *Nannochloropsis* species grown under green light (520 nm) achieved a higher percentage of lipids when compared to the 5 other light qualities: white fluorescent light, purple (405 nm), blue (465 nm), yellow (640 nm) and red light (660 nm) (Ra *et al.*, 2016). However, the specific growth rate was less than half when compared to other light qualities tested at  $0.01 \text{ h}^{-1}$  (Ra *et al.*, 2016). Ra *et al.* (2016) hypothesized

that a shift between the growth light with the highest specific growth rate (blue light at  $\approx 0.03 \text{ h}^{-1}$ ) and the growth light with the highest lipid content (green light  $\approx 35\%$  dry weight) will improve the growth rate of the culture whilst increasing lipid content. This hypothesis was tested and all *Nannochloropsis* species were grown using blue light for 18 days then followed by a light shift to green light for 3 days (Ra *et al.*, 2016). All cultures exhibited an improved specific growth rate with lipid content over 50% (of dry weight), in contrast to constant blue light which exhibited lipid content of 30% (of dry weight) (Ra *et al.*, 2016).

#### 4.1.4. Light shifts in diatoms

Currently, there is a lack of research into light shifts in diatoms. One of the few studies to the author's knowledge is by Jungandreas *et al.* (2014), who investigated light shifts in *Phaeodactylum tricornutum*. Jungandreas *et al.* (2014) observed that shifting the light quality from blue to red light, significantly increased the carbohydrate content and significantly decreased protein content. Conversely, minimal changes were observed in protein and carbohydrate content when cultures were shifted from red light to blue light (Jungandreas *et al.*, 2014). No significant changes in growth rate ( $\text{d}^{-1}$ ) was observed in blue to red light shifted *P. tricornutum* cultures ( $\approx 0.4 \text{ d}^{-1}$ ); however a temporary arrest in growth rate was observed within 24 hr of red to blue light shift in *P. tricornutum*

cultures which stabilized to approximately  $0.4 \text{ d}^{-1}$  by day three (Jungandreas *et al.*, 2014).

As a result of limited studies, the knowledge of light shifting and its corresponding physiological, biochemical and behavioural responses of diatoms remain largely unknown (Depauw *et. al.* 2012, Fu, Wichuk & Brynjólfsson 2015). Regardless, evidence suggests that metabolite profiles may be influenced through light shifting and manipulating the diatoms metabolite content for enhanced production of specific metabolites remains a challenge for both the food and feed industries.

Within the aquaculture industry, reducing the high costs associated in producing microalgal feed remains a major challenge (Borowitzka, 1997; Knauer and Southgate, 1999; Camacho-Rodríguez *et al.*, 2016; Nielsen *et al.*, 2017). While there is a need to produce more microalgal feed at reduced cost, this must not reduce the quality of the feed.

#### 4.1.5. Digestibility analysis

Understanding the digestibility of major nutrients is a crucial step to evaluate the value and quality of feed ingredients for a desired aquaculture species. The digestibility of a feed is the measure of how much of the feed is made available for uptake, post-digestion (Cavonius, Albers and Undeland, 2016). Digestibility can be investigated through

enzymatic digestion assays which utilize a variety of digestive enzymes such as: pepsin, trypsin, papain, pronase, pancreatin (a mixture of amylase, lipase and protease) and renin (Buchanan, 1969; Saunders *et al.*, 1973; Taverner and Farrell, 1981; Bhatti, 1982; Parsons, 1991). Such enzymes can be commercially purchased or freshly isolated from the organism of interest. However, the simplest form of this assay involves a protein substrate (e.g. feed, foodstuff) incubated under specific conditions (e.g. pH, incubation time, temperature) with a number of digestive enzymes (mentioned above) and upon completion of the reaction both digested and non-digested samples are quantified (Moyano *et al.*, 2015).

The utilization of enzymatic digestion assays on microalgae have been steadily increasing, coupled with the increasing interest of microalgae supplements for animal feed and human consumption (Morris *et al.*, 2008; Goh *et al.*, 2009; Graziani *et al.*, 2013; Rodríguez De Marco *et al.*, 2014; Cavonius, Albers and Undeland, 2016; Tibbetts *et al.*, 2016). Within aquaculture industries long-term feeding trials are the conventional method to assess the value of feed (Grabner, 1985). While dependable, traditional feeding trials are resource intensive, low throughput, expensive, laborious and involve ethical consideration (Grabner, 1985; Moyano *et al.*, 2015). *In vitro* digestion assays in comparison are inexpensive, are significantly less resource intensive and are a high throughput assessment of relative feed quality (Grabner, 1985; McCauley *et al.*, 2019).



According to Moyano *et al.* (2015), 64 studies have been published utilizing digestibility assays in aquatic animals, including 45 with fish, 15 with crustaceans and 4 with molluscs. Most notably, of the four studies assessing digestibility in molluscs, two studies assessed the digestibility of phytoplankton species in the freshwater pearl mussel, *Hyriopsis bialatus*. Areekijseeree *et al.* (2006) assessed the digestibility of carbohydrate, protein and lipids in 4 phytoplankton species, while Supannapong *et al.* (2008) assessed the digestibility of carbohydrates and protein in 4 phytoplankton species, both using enzyme extracts from *H. bialatus*. The two other studies used commercially available enzyme mixes from bovine, porcine and fungal sources to simulate digestion in two molluscs; *Crassostrea gigas* and *Haliotis midae*, to measure C<sub>14</sub> and protein digestibility respectively (Langdon, 1989; Shipton and Britz, 2002). While using enzymes extracted from the desired organism can provide a more accurate physiological representation of the specific digestion kinetics of the organism, it is common to use enzymes that are commercially available instead as sourcing enzyme extracts from animals which is more difficult, requires ethical consideration and present difficulties in replicating accurately across independent trials. At present, works focusing on the digestibility of diatoms in bivalves are limited and there is a general lack of knowledge of how different experimental growth conditions can affect the digestibility of diatom biomass.

Enzymatic digestion will therefore be utilised herein to investigate whether or not any observed changes in the primary metabolite production correlated with an increase or decrease in the apparent digestibility of these components. Improved *in vitro* digestibility assay techniques could reduce the need for expensive feeding trials to screen diatoms and other microalgae as feedstock for aquaculture.

## **4.2. Aims and Objectives**

While the studies of microalgae utilizing light shifting is still in its infancy, it could revolutionize industrial applications of microalgae if such a relatively simple and non-invasive method could be fully characterized. At present, the physiological and metabolic response of diatoms to light shifts and how it may affect the digestibility remains unknown. As discussed in Chapter 3, an increase in protein production was observed in red light (section 3.4.3). However, it yielded lower biomass productivity and was deemed not commercially feasible, while blue and white light exhibited superior growth (Table 3.1). This study will hence, investigate the effect of light shifts of monochromatic blue to red light and white to red light (including blue and white light control) on the growth rate, metabolite content and photosynthetic response of *C. muelleri*, as well as assessing its digestibility. To the knowledge of the author, no

works have been published investigating light shifts followed by analysis of its digestibility.

The goal of this work was to investigate the effects of light shift on growth rate, metabolite production and digestibility. This will provide vital information for the aquaculture industry regarding diatom culturing conditions potentially to tailor light quality to increase production of desired metabolites and their digestibility to assess relative feed quality.

### **4.3. Material and Methods**

#### **4.3.1. Culturing *Chaetoceros muelleri***

*Chaetoceros muelleri* (Lemmermann 1898) (CS-176) obtained from the Australian National Algae Culture Collection (ANACC; CSIRO, Hobart, Australia) was grown in artificial seawater enriched with F/2 nutrients with silica following the methods of Guillard (1975). Artificial seawater was prepared by filter sterilising artificial sea salt (Aquasonic) dissolved in milli-Q water through a 0.2  $\mu\text{m}$  filter made to 35 practical salinity units (PSU). Medium was made fresh and stored in the dark at 4°C until needed. Stock cultures were maintained in 250 mL conical flasks in an incubator (Labec Pty. Ltd.) at 22°C under a 12 h:12 h light:dark cycle at incident irradiance of approximately 40  $\mu\text{mol photons m}^{-2} \text{ s}^{-1}$ .

During the experiment, cultures were operated under semi-batch mode, where cultures were harvested at a minimum density of  $\approx 6 \times 10^6$  cells mL<sup>-1</sup> and diluted to the starting cell density of  $\approx 5 \times 10^5$  cells mL<sup>-1</sup> after each experimental cycle. Blue light control (BLctrl), blue light red shifted (BLRL), white light control (WLctrl) and white light red shifted (WLRL) grown cultures were under a growth cycle of 3 days. The growth cycle time was determined based on the biomass requirements for chemical analysis.

#### 4.3.2. Photobioreactor system

*Chaetoceros muelleri* was cultured in photobioreactors (ePBR, Phenometrics, Lansing, MI, USA) with an inverted conical frustum geometry and a working volume of 450 mL (Tamburic *et al.*, 2014). Temperature was constantly maintained at  $22 \pm 0.5^\circ\text{C}$  using a peltier heater-cooler jacket and constantly logged every 5 min (Phenometrics sensors). All PBRs were aerated constantly with 0.2  $\mu\text{m}$  filtered (oil-free) ambient air ( $\text{CO}_2 \approx 0.04\%$ ) which was humidified by passing it through Milli-Q water and delivered from the bottom of the vessel with a 0.4 mm hypodermic needle. The pH was maintained via 5%  $\text{CO}_2$  addition (food grade, BOC) using an inbuilt solenoid valve programmed to maintain the pH at approximately  $8.0 \pm 0.2$ . Carbon dioxide was bubbled from the bottom of the PBR with syringe needles (5/10 ADT (N) 6cm); SGE

Analytical Science, Ringwood, VIC, Australia). The PBR culture was magnetically stirred at a rate of 120 rpm.

#### 4.3.3. Growth light

All PBRs were illuminated with different colour LEDs from the side (Figure 4.2) at equivalent photon flux density (PFD) of  $500 \mu\text{mol photons m}^{-2} \text{s}^{-1}$  under a 12 h:12 h (light:dark) cycle. Emission spectra of the LED panel was measured with a Jaz spectrometer (Ocean Optics, USA) shown in alongside the absorption spectra of *C. muelleri* which was measured with a microplate reader (Infinite 200 PRO, Tecan, Switzerland). Photosynthetically utilizable/usable radiation (PUR) was calculated based on the equation outlined in Morel (1978) shown below (Eqn. 4.1). Each *C. muelleri* samples were allowed to pre-acclimate to the respective light quality for 7 days as per the work by Jungandreas *et al.* (2014). Two cultures were grown under blue light and white light without light shifting, while two other cultures were grown under blue and white light then red shifted for the final 10 h of the experiment.

$$\text{PUR} = \text{PAR}(a_{\phi}/a_{\phi\max}) \quad \text{Eqn. 4.1}$$

where  $a_{\phi}$  is the mean absorption and  $a_{\phi\max}$  is the maximum absorption ( $\approx 440 \text{ nm}$ ).

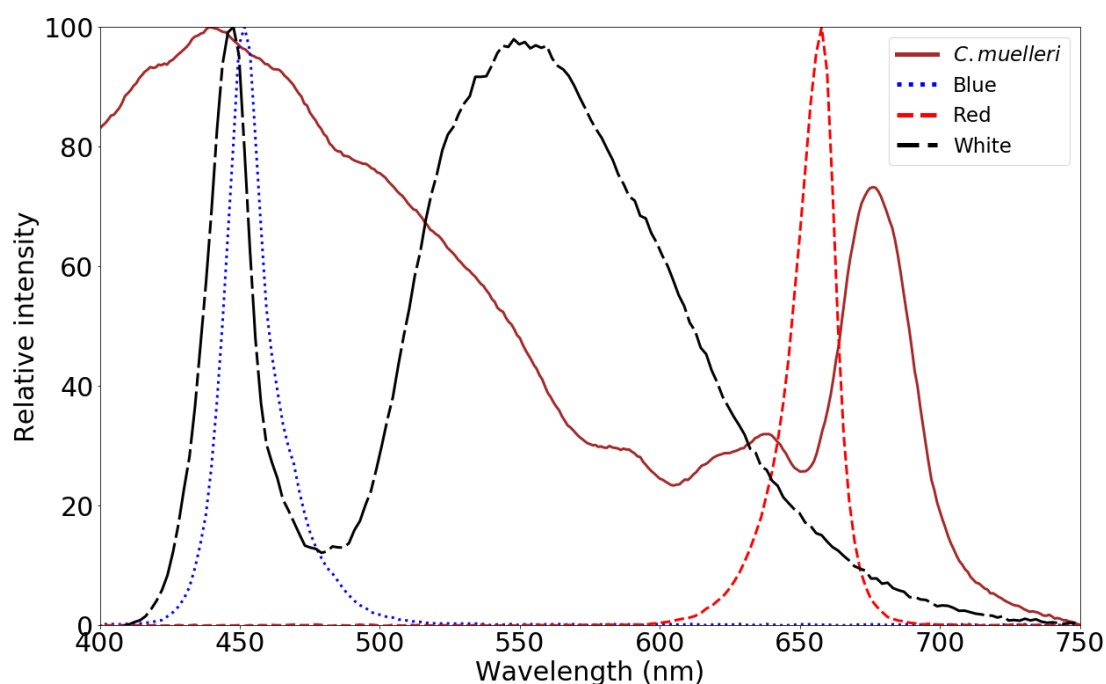


**Figure 4.2** Wavelength spectra of LEDs used in experiment and the relative absorption spectra of *C. muelleri*. Brown line represents the absorption spectra of *C. muelleri*, blue dotted line represents blue LED spectra, red broken line represents red LED spectra, and black ‘long line & short line’ style line represents white LED spectra.

#### 4.3.4. Growth rate

Cell counts were taken twice a day throughout the experiment, 2 h after the start of light cycle and 2 h before the end of light cycle (2.4.5 for details). Specific growth rate ( $\mu$ ) was calculated using Eqn. 4.2 outlined in Wood, Everroad and Wingard (2005) which has been used frequently to calculate specific growth rates in microalgae (Harrison,

Thompson and Calderwood, 1990; Borowitzka and Moheimani, 2013; Huang *et al.*, 2013; Gorai *et al.*, 2014; Han *et al.*, 2017).

$$\mu = \frac{\ln(N_1/N_0)}{t_1 - t_0} \quad \text{Eqn. 4.2}$$

where  $\mu$  = specific growth rate,  $N_1$  and  $N_0$  are cell densities in  $\text{mL}^{-1}$  at  $t_1$  = final time (day three) and  $t_0$  = initial time

Division rate was calculated using Eqn. 4.3.

$$t_d = \frac{\ln(2)}{\mu} \quad \text{Eqn. 4.3}$$

where  $\mu$  = specific growth rate

During the experiment, cultures were maintained under semi-batch mode, where cultures were harvested after three days and diluted to the starting cell density of  $\approx 5 \times 10^5$  cells  $\text{mL}^{-1}$  after each experimental cycle. Blue control (BLctrl) was used to inoculate the next BLctrl and BLRL condition, and WLctrl was used to inoculate the next WLctrl and WLRL condition. The harvested biomass was then used for dry weight measurements and for chemical analysis of total protein, total lipids and fatty acid methyl esters (FAME) (4.3.10, 3.3.11 & 3.3.12). Biomass (dry weight), was measured at the end of each cycle, however due to low culture volume, dry weights were not taken periodically during each cycle.

#### 4.3.5. Light attenuation measurements

A quantum sensor (4-pi LI-COR Inc., Lincoln, Nebraska, U.S.) and light meter (LI-250A, LI-COR Inc., Lincoln, Nebraska, U.S.) was used to measure the attenuated PFD at the longest path length of the PBR vessel to determine the attenuated light of the two light configurations. After sterilizing with 75% ethanol, the  $4\pi$  sensor was suspended inside the culture to measure PFD from the centre of the culture. The attenuation was measured twice a day prior to sampling for cell counts. The LEDs were calibrated as detailed in Chapter 3 (section 3.3.5).

#### 4.3.6. Rapid light curve measurements

The rapid light curve (RLC) measures relative electron transfer rate (rETR) as a function of irradiance (Ralph and Gademann, 2005). A RLC is measured with short irradiance interval ( $<10$  s), which does not allow for photosynthetic processes to stabilize (Ralph and Gademann, 2005; Perkins *et al.*, 2010; Houliez *et al.*, 2017). Both SSLC and RLC have three regions: the rise of the curve in the light limited region ( $\alpha$ ) which is virtually linear as irradiance increases, light-saturated region, which begins at the minimum saturating irradiance ( $I_k$ ) which is determined by finding the intercept of  $\alpha$  with the maximum relative electron transfer rate between PSII and photosystem I (PSI) ( $rETR_{max}$ ) (Eqn. 4.4) and light inhibited region ( $\beta$ ) where relative electron transfer rate



(rETR) begins to decrease as irradiance increases (MacIntyre *et al.* 2002; Sakshaug *et al.* 1997; Schreiber 2004).

$$\text{rETR}_{\text{max}} = P_s(a/[a + \beta])(\beta/[a + \beta])^{\beta/a} \quad \text{Eqn. 4.4}$$

where  $a$  is the slope of the light limited region and  $\beta$  is the slope of the light inhibited region and  $P_s$  is a scaling factor defined as the maximum potential rETR.

The multi-colour-PAM (Pulse Amplitude Modulation) fluorometer (MC-PAM, Heinz Walz GmbH, Germany) was used to measure a RLC with seven biological replicates.

Cultures of *C. muelleri* grown under different light conditions were sampled on day one ( $t_0$ ) and on day three ( $t_f$ ) at three time points: 0 h, 5 h and 8 h after light shift  $t_{f0}$ ,  $t_{f5}$  and  $t_{f8}$  respectively). Day three ( $t_f$ ) samples were diluted with F/2 media normalise  $F_0$  to similar values ( $F_0 \approx 1.1$ ). The PAR list used was 6, 28, 52, 100, 149, 222, 318, 436, 620, 819, 1033, 1281, 1520, 1816, 2151, 2487, 2866, 3371, 3889 and 4578  $\mu\text{mol photons m}^{-2} \text{s}^{-1}$ . Measuring light and saturation pulse intensity were approximately 0.4  $\mu\text{mol photons m}^{-2} \text{s}^{-1}$  at 440 nm and approximately 2900  $\mu\text{mol photons m}^{-2} \text{s}^{-1}$  white light respectively and saturation pulse length was 0.8 s. White light was used as actinic light and 440 nm was used as measuring light. Each irradiance interval was set to 10 s. Each irradiance interval was set to 10 s. Empirical data was fitted to the function detailed in Platt, Gallegos and Harrison (1980) (Eqn. 4.5) using the curve fitting protocol of PamWin-3 (Schreiber, Klughammer and Kolbowski, 2012). The rise of the

curve in the light limited region ( $\alpha$ ) is virtually linear to irradiance as irradiance increases light-saturated region begins at the minimum saturating irradiance ( $I_k$ ) which is determined by finding the intercept of  $\alpha$  with the relative maximum electron transfer rate between photosystem II (PSII) and photosystem I (PSI) (rETR<sub>max</sub>) (MacIntyre *et al.* 2002; Sakshaug *et al.* 1997; Schreiber 2004).

$$P = P_{\max} \left( 1 - e^{-\alpha I / P_{\max}} \right) e^{-\beta I / P_{\max}} \quad \text{Eqn. 4.5}$$

where  $P$  is rate of photosynthesis at a given irradiance,  $P_{\max}$  is maximum rate of photosynthesis,  $\alpha$  is the initial slope of the curve before the onset of light saturation,  $I$  is irradiance and  $\beta$  is the slope of the curve after the onset a condition known as photoinhibition (Falkowski & Raven 2007).

Photoinhibition is defined as the inhibition of photosystem II (PSII) from exposure to high irradiance (Powles, 1984). Unlike conventional light curves, a rapid light curve (RLC) measures effective quantum yield ( $\Phi_{\text{PSII}}$ ) as a function of irradiance (Ralph and Gademann, 2005). And while a steady state light curve (SSLC) measures photosynthesis rate at steady state (i.e. each irradiance interval is long enough ( $\geq 5$  min) to allow photosynthetic processes to stabilize) a RLC is measured with short irradiance interval ( $< 60$  s), which does not allow for photosynthetic processes to stabilize (Ralph and Gademann, 2005; Perkins *et al.*, 2010; Houliez *et al.*, 2017). This means SSLC are used to measure long-term acclimation states and potential photosynthetic performance and

are less influenced by light history, while RLC are used to measure short-term acclimation and effective photosynthetic capacity and are strongly influenced by long-term light history (such as high/low light or light quality acclimated) (Ralph and Gademann, 2005; Herlory, Richard and Blanchard, 2007; Perkins *et al.*, 2010; Houliez *et al.*, 2017). Maximum and effective quantum yield ( $\Phi_{PSII}$  and  $F_v/F_m$  respectively) is also measured as an indicator of photosynthetic health when dark-adapted (Eqn. 4.6) and light-adapted (Eqn. 4.7). Non-photochemical quenching (NPQ) of Chl *a* was calculated according to Eqn. 4.8 detailed in Bilger and Björkman (1990).

$$\Phi_{PSII} = \Delta F / F'_m = (F'_m - F) / F'_m \quad \text{Eqn. 4.6}$$

where  $F'_m$  and  $F$  are the maximum and minimum fluorescence of light-adapted samples.

$$F_v/F_m = (F_m - F_0) / F_m \quad \text{Eqn. 4.7}$$

where  $F_m$  and  $F_0$  are the maximum and minimum fluorescence of dark-adapted samples.

$$NPQ = F_m / F'_m - 1 \quad \text{Eqn. 4.8}$$

where  $F_m$  is the maximum fluorescence of dark-adapted sample, and  $F'_m$  is the maximal fluorescence in light-adapted sample.

#### 4.3.7. Pigment analysis with HPLC

Pigment analysis was conducted by high-performance liquid chromatography (HPLC).

Diatom samples (30 mL) were filtered through a GF/F (47 mm) filter paper in low light,

followed by immediate flash freezing in liquid nitrogen and stored at  $-80^{\circ}\text{C}$  until further analysis. The filters were freeze-dried (2-4 Alpha LDplus, Christ, John Morris Scientific, Australia) overnight and extracted in 5 mL 90% HPLC-grade acetone with three runs of sonication (FXP, 50 Hz, Unisonics Australia) for 30 s followed by 10 s of vortexing and stored at  $4^{\circ}\text{C}$  overnight. Freeze-drying and extraction was conducted in the dark. Sample slurry (1 mL) was filtered through a  $0.2\ \mu\text{m}$  13mm syringe filter (polytetrafluoroethylene) and loaded into amber colour HPLC glass vials. Samples were analysed using an Agilent 1290 LC HPLC equipped with a binary pump with an integrated vacuum degasser, thermostatic column compartment modules, photo-diode array detector and an Agilent 1290 Infinity autosampler. Pigments were separated using a Zorbax Eclipse XDB C8 HPLC  $4.6\ \text{mm} \times 150\ \text{mm}$  and guard column (Agilent) using a gradient of tetrabutyl alkylammonium acetate methanol mix (3:7) and methanol as solvents. Column temperature was maintained at  $55^{\circ}\text{C}$ . Pigments were detected at 450 nm (Chl *a* at 665 nm) and quantification was done by comparing results with the retention time of analytical standards.

#### 4.3.8. *In vitro* digestion assay

Conditions for the digestion assay are outlined in Table 4.1 and which were based on modifications of Moyano & Savoie (2001). Approximately 450 mL fresh culture was

harvested via centrifugation (3500 rpm, 3 min), followed by two washing steps with phosphate buffer. Samples were collected into two 50 mL Falcon tubes yielding approximately 55 mg of dry weight. In the first stage of the digestion model which simulates stomach digestion, sample biomass was suspended in 9.6 mL of 0.25 mg mL<sup>-1</sup> pepsin (MP Biomedicals, NSW, Australia) in 0.02 M HCl (pH 2) and incubated at 37°C for 30 min. Incubation was followed by inactivation of pepsin via addition of 800 µL of 0.1 sodium borate buffer adjusted to pH 9 using 0.5 M NaOH. The second stage of the digestion assay which simulates intestinal digestion utilized 800 µL of 2.5 mg mL<sup>-1</sup> pancreatin (MP Biomedicals, NSW, Australia) in 0.1 M sodium borate buffer and further incubated at 37°C for 60 min. Incubation was followed by inactivation of pancreatin via briefly submerging reaction tubes in boiling water for approximately 1 min before centrifugation to remove the supernatant. The digested samples were then stored in -80°C until further chemical analysis. Any metabolites detected after the assay will be assumed to not be available for absorption and will be referred to as 'released' metabolites. Blanks were also prepared as negative controls.

**Table 4.1** Conditions for the *in vitro* static digestion model using typical monogastric proteolytic enzymes pepsin and pancreatin. Based on modifications of Moyano & Savoie (2001).

Enzyme	Steps	Simulation	Enzyme quantity (mg)	Algal sample mass (mg dw)	Time (min)	pH	Temp (°C)
Pepsin	1	Stomach Digestion	2.4	55.0	30	2.0	37
Pancreatin	2	Final hydrolysis in intestine	2.0		60	9.0	37

#### 4.3.9. Sample preparation for protein and lipid analysis

All cultures were grown to a minimum cell density of  $\approx 6 \times 10^6$  cells mL<sup>-1</sup> for harvesting. Wet biomass ( $\approx 400$  mL) was harvested at the end of the experiment via centrifugation (Rotanta 460R, Hettich GmbH & Co.KG, Tuttlingen, Germany) at 3000 g for 5 min in pre-weighed centrifugation tubes (for dry weight measurements), subsequently washed twice with phosphate buffer and once in Milli-Q water, freeze-dried overnight and followed by storage in -80°C until further analysis. After all experiments had been completed, cultures were homogenised with mortar and pestle for protein, lipid and carbohydrate analysis.

#### 4.3.10. Total protein analysis from total nitrogen measurements

Total protein of freeze-dried biomass samples (undigested samples) were analysed by the Leco TruSpec carbon and nitrogen analyser (LECO Corporation, St. Joseph, Michigan, USA) as detailed in section 3.3.10. Digested samples (detailed in 4.3.8) were analysed for elemental nitrogen content measured by combusting 1 mL of liquid digested extracts in triplicate. The elemental nitrogen content was then converted to the total protein content by a literature factor of 4.78 (Lourenço *et al.*, 2004). Protein digestibility, a percentage measure of the proteins broken down by the simulated digestive enzyme mixture was calculated with the equation below (Eqn. 4.9).

$$x_d = 1 - (x_{di}/x_{wb}) \quad \text{Eqn. 4.9}$$

where  $x_{di}$  is total metabolite in digested samples in mg,  $x_{wb}$  is total metabolite in undigested biomass samples per unit weight (mg).

#### 4.3.11. Total lipid and fatty acid methyl ester extraction and analysis

Total lipid content and FAME for undigested samples were analysed as detailed in section 3.3.11. For total lipid content and FAME of digested samples, liquid to liquid partitioning of 5 mL of aqueous digest extract was performed three times with 3 mL of chloroform methanol (2:1 v/v). The organic extract was dried under nitrogen and measured gravimetrically for total lipids. Dried lipids were saponified with 1 mL 1%

NaOH for 15 min at 55°C and allowed to cool. Nonadecanoic acid (C19:0) of known concentration (10 µL of 1 mg mL<sup>-1</sup>) was spiked into lipid samples as internal standard and transesterified in the presence of 2 mL 5% methanolic HCl for 15 min at 55°C.

Fatty acid methyl ester was extracted with 1 mL hexane twice and dried under nitrogen gas. Hexane (100 µL) was added and transferred to amber gas chromatography (GC) vials. Samples were analysed by GC using an Agilent 7890 series GC coupled to an Agilent quadrupole MS (5975N) equipped with a HP-5MS fused capillary column (5%-phenyl-methylpolysiloxane, 30 m long, 0.25 mm internal diameter, film thickness 0.25 µm, Agilent Technologies). Gas chromatography carrier gas was helium at a flow rate of 0.9 mL min<sup>-1</sup>. Gas chromatography inlet temperature was 280°C using the splitless mode of injection with a purge time of 1 min with an injection volume of 5 µL.

Results were analysed using Agilent GC Chemstation software to identify peaks by comparing their retention times with commercial standards (Sigma Aldrich, NSW, Australia). All conditions were analysed in triplicate. Total FAME and individual FAME species digestibility was calculated with the equation noted above (Eqn. 4.9).

Statistical analysis was done with Minitab (Minitab 17.1.0 Statistical Software, Minitab Inc.) and data visualization were done with Python 3.6 on Windows 10.



## 4.4. Results

### 4.4.1. Effects of light shift on *Chaetoceros muelleri* growth

Investigating the effect of light shift on the growth of *C. muelleri* indicated that cell growth rates were largely unaffected in BL and WL control cultures as shown in Figure

4.3.

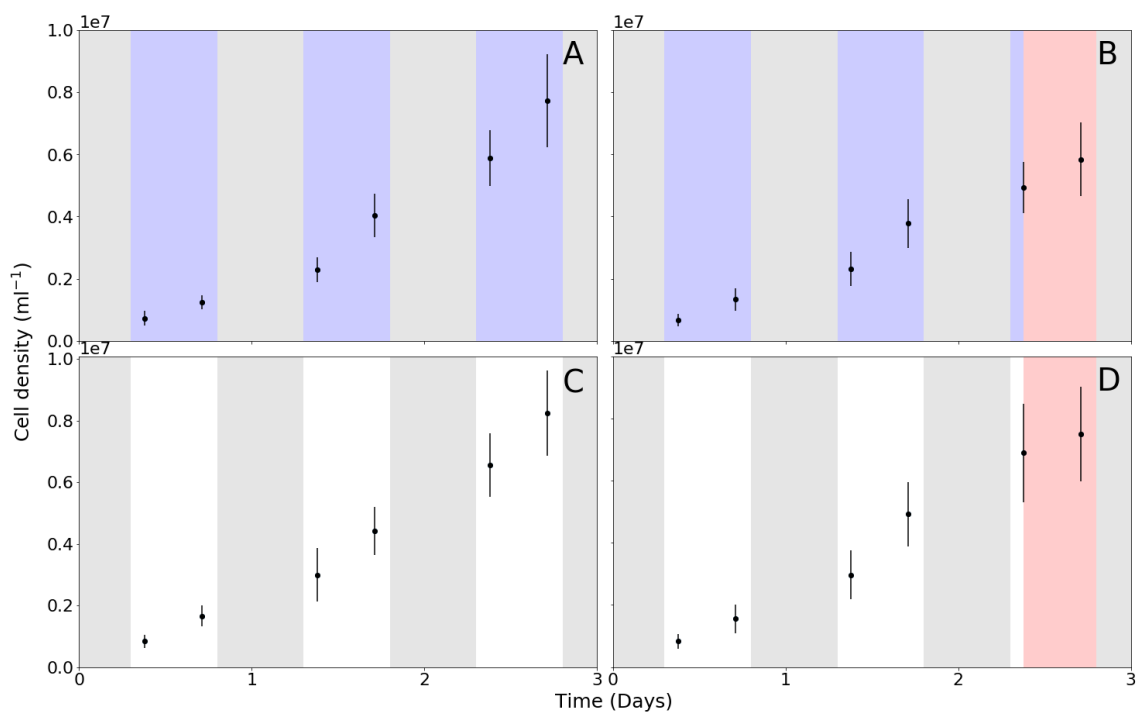


**Figure 4.3** Cell concentration as a function of time and treatment. Black dots: cell count data, coloured shades indicating the light quality of growth light: blue for blue light, red for red light, white for white light and grey for dark phase. A) Constant blue light (BLctrl), B) BL shifted to red light for 10 h during day three (BLRL), C) constant white light (WLctrl) and D) WL shifted to red light for 10 h during day three (WLRL). Values represents the mean and standard deviation (n = 7).

Figure 4.3 and Table 4.2 shows the details of growth as well as biomass production with respect to time (days) for BLctrl, BLRL, WLctrl and WLRL grown cultures. Final cell density at the end of day three was between  $\approx 7.80 \times 10^6$  and  $\approx 8.00 \times 10^6$  cells  $\text{mL}^{-1}$  for BLctrl, WLctrl and WLRL grown cultures (Table 4.2). While BLRL grown cultures, exhibited the lowest growth rate and final cell density with approximately  $6.03 \times 10^6$  cells  $\text{mL}^{-1}$  (Table 4.2). No significant difference in dry weight ( $\text{mg mL}^{-1}$ ) were observed between BLctrl and BLRL nor between WLctrl and WLRL cultures (Table 4.2).

**Table 4.2** Specific growth rates ( $\mu$ ), division rate (td), average dry weight (mean dw) in  $\text{mg mL}^{-1}$ , average final cell density (mean  $t_f$  cells) in cells  $\text{mL}^{-1}$ . One-way ANOVA performed with Tukey method at 95% confidence: same or no letters indicate no significant difference and different letters indicate significant difference. Data represents the mean and standard deviation ( $n = 7$ ).

Treatments	Specific growth rate ( $\mu$ )	td (days)	mean dw	mean $t_f$ cells
BLctrl	$1.02 \pm 0.09$	$1.47 \pm 0.12$	$0.10 \pm 0.01^{ab}$	$7.86 \times 10^6 \pm 1.07 \times 10^6^a$
BLRL	$0.93 \pm 0.12$	$1.34 \pm 0.17$	$0.09 \pm 0.01^b$	$6.03 \times 10^6 \pm 0.95 \times 10^6^b$
WLctrl	$0.97 \pm 0.09$	$1.40 \pm 0.13$	$0.12 \pm 0.02^a$	$8.20 \times 10^6 \pm 1.00 \times 10^6^a$
WLRL	$0.95 \pm 0.12$	$1.37 \pm 0.17$	$0.11 \pm 0.02^{ab}$	$7.80 \times 10^6 \pm 1.37 \times 10^6^a$

#### 4.4.2. Light attenuations of *Chaetoceros muelleri* culture

To observe how light shift affected the PFD in *C. muelleri* cultures, irradiance was intermittently measured. We observed that BLctrl cultures attenuated the most rapidly at  $t_0$  recording under  $275 \mu\text{mol photons m}^{-2} \text{s}^{-1}$  as well as the lowest light intensity at  $t_{\text{rat}}$  approximately  $50 \mu\text{mol photons m}^{-2} \text{s}^{-1}$  (Figure 4.4). WLctrl cultures recorded similar trends in light attenuation, starting approximately at  $350 \mu\text{mol photons m}^{-2} \text{s}^{-1}$  and ended with approximately  $150 \mu\text{mol photons m}^{-2} \text{s}^{-1}$  (Figure 4.4). Both results correlate to the results seen in Chapter 3. When blue and white light was shifted to red light in BLRL and WLRL cultures, the measured irradiance increased in both cultures (Figure 4.4).

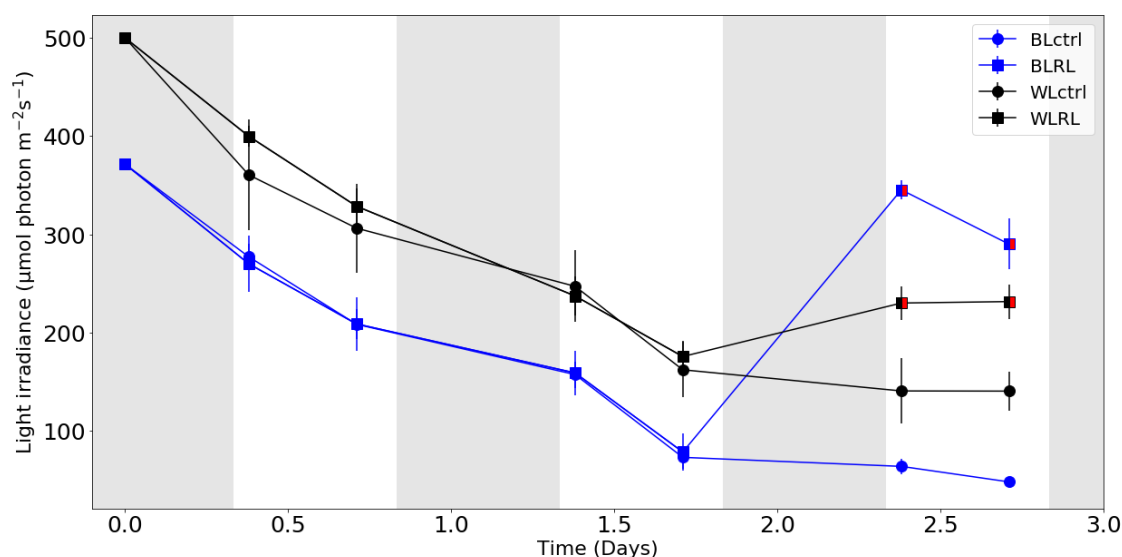


**Figure 4.4** Rate of light attenuation of different light qualities as a function of time.

Blue circles: blue light grown (BL), blue squares: blue light grown subsequently red shifted on day three shown as blue/red square (BLRL), black circles: white light grown

(WL) and black squares: white light grown subsequently red shifted on day three shown as black/red square (WLRL). Irradiance at  $t_0$  represents the initial irradiances as detailed in section 4.3.3. Grey area indicates dark phase and white area indicates light phase.

Values represents the mean and standard deviation ( $n = 7$ ).

A significant increase was observed in both BLRL and WLRL cultures after undergoing a RL shift. An increase of approximately  $50 \mu\text{mol photons m}^{-2} \text{s}^{-1}$  in WLRL cultures and an increase of approximately  $300 \mu\text{mol photons m}^{-2} \text{s}^{-1}$  was observed in BLRL cultures.

#### 4.4.3. Effects of light shift on rapid light curve parameters of *Chaetoceros muelleri*

Rapid light curves were conducted to measure photosynthetic performance parameters during the first and last day of the study, as well as at three time points following the light shift as shown in Figure 4.5. Relative  $\text{ETR}_{\text{max}}$ ,  $\Phi_{\text{PSII}}$  and NPQ were consistent between blue (BLctrl & BLRL) and white (WLctrl & WLRL) acclimated cultures at  $t_0$  and  $t_f 0$ . However upon reaching  $t_f 5$  and  $t_f 8$  a major change in  $\text{rETR}_{\text{max}}$  was seen in BLRL compared to BLctrl (Figure 4.5). At  $t_f 0$ , all cultures exhibited a  $\Phi_{\text{PSII}}$  approximately 0.65 indicating physiologically ‘healthy’ cells, typical of diatoms (Ihnken, Roberts and Beardall, 2011; Jungandreas *et al.*, 2014). However upon shifting to red light, the  $\Phi_{\text{PSII}}$  in both BLRL & WLRL fell below 0.50 at  $t_f 5$ , then to 0.34 in BLRL and 0.42 in WLRL at  $t_f 8$ . NPQ capacity also changed dramatically as the red light

shift progressed (Figure 4.5). In BLRL, NPQ continued to decrease until reaching approximately 0.22 at  $t_{f8}$ , while in BLctrl, NPQ remained at approximately 1.60 at  $t_{f8}$ . A similar observation was made in WLRL, where NPQ at  $t_{f8}$  decreased to approximately 0.35 compared to 0.80 in WLctrl at  $t_{f8}$ .

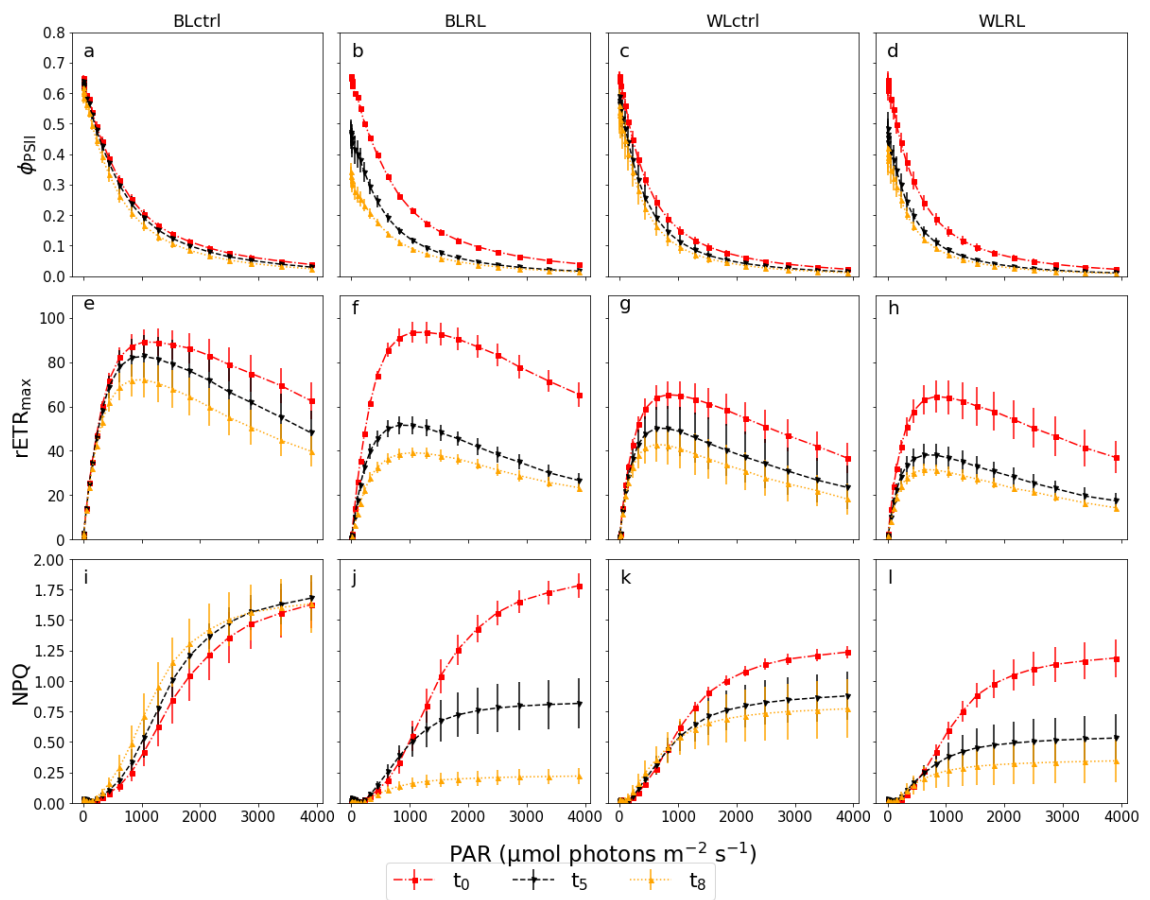


**Figure 4.5** Rapid light curve plots where  $\Phi_{PSII}$  (a, b, c, d) is maximum electron transfer rate,  $rETR_{max}$  (e, f, g, h) is maximum quantum yield of photosystem II and NPQ (i, j, k, l) is non-photochemical quenching. Condition are grouped as: BLctrl (a, e, i), BLRL (b, f, j), WLctrl (c, g, k) and WLRL (d, h, l). Rapid light curve measurements were taken at day one ( $t_0$ ) represented as blue circle and at 3 time points at day three ( $t_f$ ): 0 h ( $t_{f0}$ ), 5 h ( $t_{f5}$ ) and 8 h after light shift ( $t_{f8}$ ); represented as red square, black inverted

triangle and orange triangle respectively. All samples at  $T_f$  were diluted with F/2 media by  $\frac{1}{4}$  as to not oversaturate the measurement. Values represents the mean and standard deviation ( $n = 7$ ).

#### 4.4.4. Effect light shift on the pigment composition of *Chaetoceros muelleri*

Pigment content was analysed from samples harvested at the end of the growth cycle in order to investigate changes in pigment content in *C. muelleri* cultures grown under light shifts. A significantly higher diadinoxanthin (ddx) and lower diatoxanthin (dtx) was observed in BLctrl cultures compared to all other conditions (Figure 4.6). Both red light shifted cultures (BLRL & WLRL) had an increased pool of dtx than their non-shifted counterparts (BLctrl & WLctrl). No significant differences were observed in the other pigments.

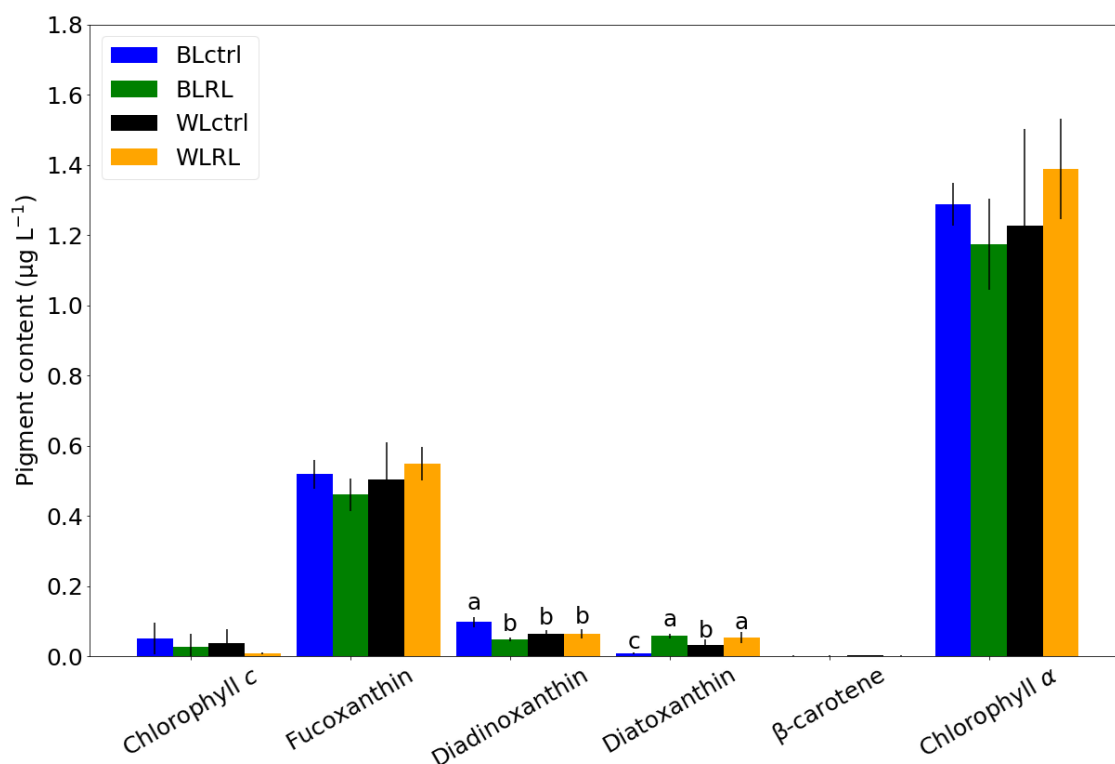


**Figure 4.6** Pigment content of *C. muelleri* harvested after grown in different light

qualities in  $\mu\text{g L}^{-1}$ . Blue bars: BLctrl, green bars: BLRL, black bars: WLctrl and orange:

WLRL. One-way ANOVA performed with Tukey method at 95% confidence: same

letter indicate no significant difference, different letters indicate significant difference,

and where no letters are present no significant differences were detected between

conditions. Values represents the mean and standard deviation ( $n = 7$ ).

#### 4.4.5. Primary metabolic composition of *Chaetoceros muelleri* with light shift

To determine whether light shifts could affect the biochemical composition of

*C. muelleri*, total protein and FAME content were analysed from samples harvested at

the end of each growth cycle. No significant difference in total FAME was observed in

all culture conditions and no significant differences were observed in total protein between the pairs BLctrl and BLRL nor WLctrl and WLRL; however a significant difference was observed between the control cultures with BLctrl with significantly higher total protein content (Figure 4.7; Total Protein and Total FAME).

#### 4.4.6. Digestibility of desired metabolites

To establish if light shifts could affect the digestibility of total proteins and total FAME, the digested samples were analysed to determine protein and FAME content released post-enzymatic digestion. The total protein and FAME released from the digested samples are shown in Figure 4.7 (Released Protein and Released FAME). The values indicate the total protein and FAME that was not broken down during the simulated enzymatic digestion. No significant differences were observed between the conditions, indicating that light shifting does not affect the protein and FAME digestion of *C. muelleri* significantly.



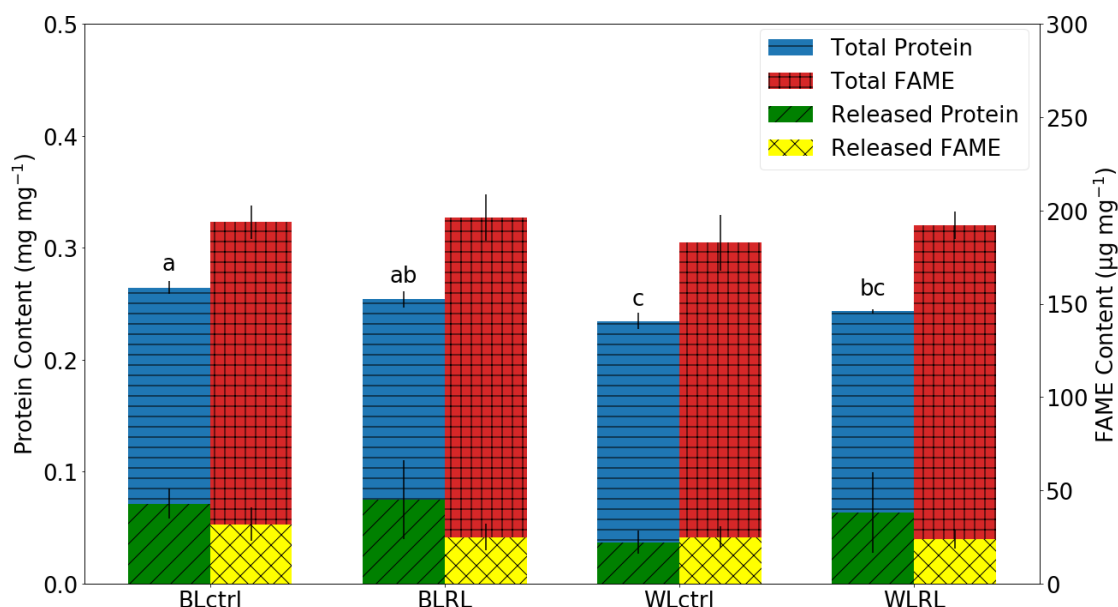


**Figure 4.7** Total and released protein and FAME from undigested and digested

*C. muelleri* cultures grown under different light qualities. Blue bars with horizontal line pattern represent total protein in mg mg<sup>-1</sup> dry weight (left y-axis), red bars with cross line pattern represent total FAME in μg mg<sup>-1</sup> dry weight (right y-axis), green bars with diagonal line pattern represent released protein in mg mg<sup>-1</sup> dry weight, and yellow bars with diagonal crossing line pattern represent released FAME in μg mg<sup>-1</sup> dry weight.

One-way ANOVA performed with Tukey method at 95% confidence: same letter

indicate no significant difference, different letters indicate significant difference, and

where no letters are present no significant differences were detected between conditions.

Values represents the mean and standard deviation (n = 3).

The results presented in Figure 4.7 can be expressed as percentage digestion using Eqn.

4.9. While no significant differences were observed in the total FAME digestibility, a

significant difference in protein digestibility was observed between WLctrl and BLRL; however no significant differences were observed as a result of light shifting (between BLctrl and BLRL & WLctrl and WLRL) (Figure 4.10).

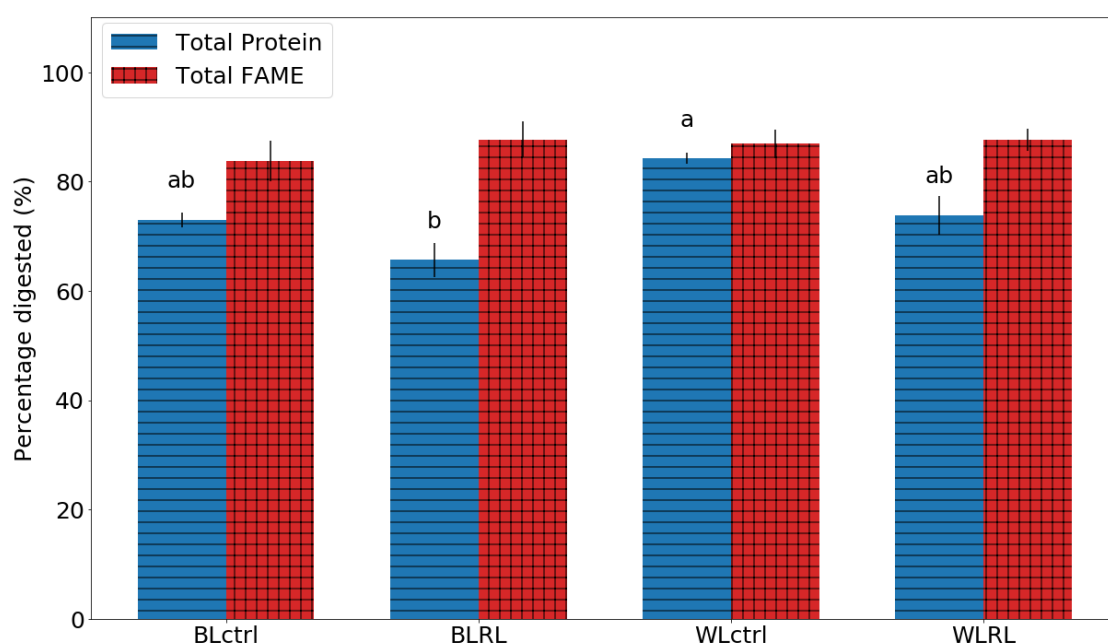


**Figure 4.8** Percentage digested protein and total FAME shown where blue bars with horizontal line pattern represent total protein and red bars with crossing line pattern represent total FAME. One-way ANOVA performed with Tukey method at 95% confidence: same letter indicate no significant difference, different letters indicate significant difference, and where no letters are present no significant differences were detected between conditions. Values represents the mean and standard deviation ( $n = 3$ ).

#### 4.4.7. Effects of light shift on the fatty acid methyl ester composition of *Chaetoceros muelleri*

Fatty acid methyl ester content was analysed from samples harvested at the end of the growth cycle in order to investigate changes in FAME content in *C. muelleri* cultures grown under light shifts. Of the desired PUFAs, significant differences in EPA (C20:5(n-3)) were observed in BLctrl cultures compared to all other conditions (Figure 4.8). Significantly higher ARA (C20:4(n-6)) were observed in WLRL cultures in comparison to BLRL cultures, where both control (BLctrl and WLctrl) cultures showed no significant differences (Figure 4.9; with no pattern). Among the prominent shorter chain fatty acids, C16:0 was shown to significantly increase after shifting from blue light to red light (Figure 4.9; with no pattern).

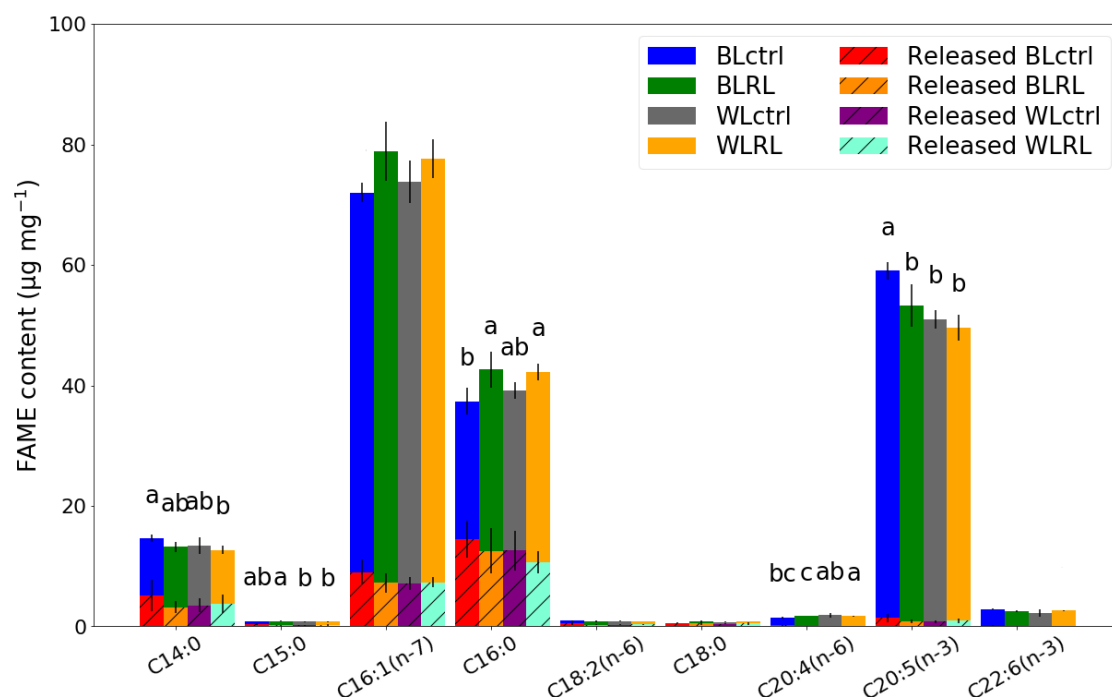


**Figure 4.9** Total and released individual fatty acid species from undigested and digested *C. muelleri* cultures grown under different light qualities in  $\mu\text{g mg}^{-1}$  dry weight. Total FAME is represented by coloured bars with no line pattern, and released FAME is shown with diagonal line pattern. One-way ANOVA performed with Tukey method at 95% confidence: same letter indicate no significant difference, different letters indicate significant difference, and where no letters are present no significant differences were detected between conditions. Data represents the mean  $\pm$  standard deviation ( $n = 3$ ).

#### 4.4.8. Digestibility of fatty acid methyl ester

Total and released individual FAME species from undigested and digested *C. muelleri* cultures grown under different light qualities are shown in Figure 4.9 (with diagonal line pattern). Total FAME is represented by coloured bars with no line pattern, and released

FAME is shown with diagonal line pattern. No significant differences in released FAMEs were observed between the conditions, indicating that light shifting does not affect the digestibility of individual FAME species in *C. muelleri* (Figure 4.9).

From the results in Figure 4.9, percentage digestion can be calculated (Figure 4.10).

While no significant differences were observed between each condition, it was observed that the long chain PUFAs, specifically ARA, EPA and DHA (C20:4 (n-6), C20:5 (n-3) and C22:6 (n-3) respectively) were highly digested compared to shorter chain fatty acids (< C18). This indicates that while no differences were observed between conditions, long chain PUFAs produced by *C. muelleri* are readily digestible and is a suitable species for aquaculture feed. While no significant differences were observed in the total FAME digested (Figure 4.9), significant difference in individual FAME digestibility was observed between both control cultures (BLctrl and WLctrl) and both shifted cultures (BLRL and WLRL); while no significant differences were observed as a result of shifting (BLctrl and BLRL, WLctrl and WLRL).

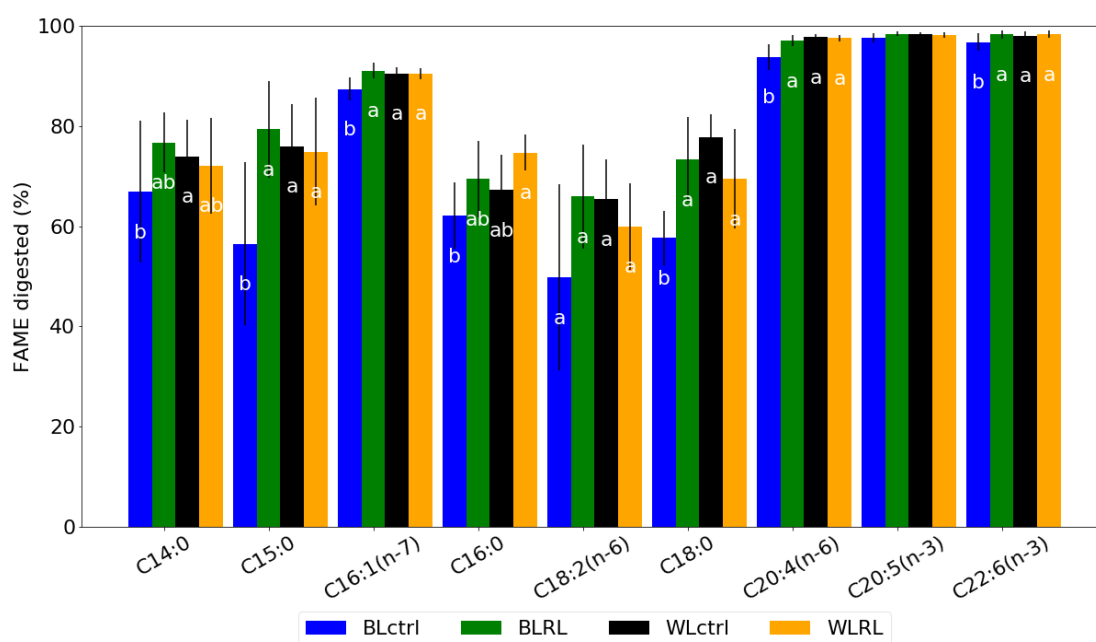


**Figure 4.10** Percentage FAME digestibility of *C. muelleri* grown under different light qualities are shown. One-way ANOVA performed with Tukey method at 95%

confidence: same letter indicate no significant difference, different letters indicate significant difference, and where no letters are present no significant differences were detected between conditions. Data represents the mean  $\pm$  standard deviation ( $n = 3$ ).

## 4.5. Discussion

This study investigated the response of *C. muelleri* to light shifts (blue to red and white to red light). By applying irradiances that were equal in PUR, as well as allowing cultures to pre-acclimate (7 days) to the different light qualities, this study aimed to investigate the effects of light shifts without interfering factors such as light intensity and acclimation state to influencing the results.

#### 4.5.1. Growth rate

From the cell count data shown in Figure 4.3 and other growth dynamics data shown in Table 4.2 there did not appear to be a distinct difference in the growth rates of each treatment. However, a significant difference in  $t_f$  cell densities were observed in BLRL cultures (Table 4.2). There were no significant differences between the BL cultures (BLctrl & BLRL) nor the WL cultures (WLctrl & WLRL) prior to light shift, indicating the difference in  $t_f$  cell density can be attributed to the red light shift. In a previous study, Jungandreas *et al.* (2014) had investigated light shifts in a pennate diatom, *P. tricornutum*, using ‘low’ irradiance of blue light and red light (of equal  $Q_{phar}$ : 24 and 40  $\mu\text{mol photons m}^{-2} \text{s}^{-1}$  respectively). Light shift experiments were conducted to observe the growth, metabolite content and photosynthetic parameters in both the long-term (days) and short-term (hours) following light shift (Jungandreas *et al.*, 2014). Jungandreas *et al.* (2014) demonstrated that during the first day after light shift from blue light to red light, the growth rates had decreased ( $\approx 0.30 \text{ d}^{-1}$ ) and then recovered after 3 days from the shift ( $\approx 0.42 \text{ d}^{-1}$ ); as the cells presumably re-acclimated to RL. As discussed in section 3.5.1, Jungandreas *et al.* (2014) had not observed any significant differences in growth rates in the blue light nor the red light acclimated cultures, indicating that light shifts disrupt cell division in diatoms. It is also noteworthy that during the 6 day observation period after the light shift, growth rates never increased

beyond the growth rates observed before the light shift ( $\approx 0.42 \text{ d}^{-1}$ ). While not conclusive, observations made by Jungandreas *et al.* (2014) and this study may suggest that light shifts negatively impact growth; rather than positively (e.g. in the green algae *C. vulgaris* (Kim *et al.*, 2014)) or neutrally (e.g. in *Nannochloropsis* species (Ra *et al.*, 2016)). However, it is also important to note that the studies mentioned above, with the exception of Jungandreas *et al.* (2014) and this study, had used fixed PAR for their investigation instead of equalizing the intensity proportionally to the organism (such as with PUR or  $Q_{\text{phar}}$ ; section 3.1.7). This makes the studies difficult to draw comparisons, and indicates that further investigation is required with a standardized methodology.

#### 4.5.2. Metabolite production

In this study cultures of *C. muelleri* were grown under blue light, blue light shifted to red light, white light and white light shifted to red light. We determined total protein, total FAME content as well as individual FAMES and pigment contents measured after 10 h from the light shift. In the previous work by Jungandreas *et al.* (2014), a major increase in carbohydrate content and a decrease in protein content was observed during a blue to red light shift in cultures of *P. tricornutum* measured incrementally for 13 h after light shift. At the 10 h mark, Jungandreas *et al.* (2014) observed an approximate 12% decrease in protein content after the blue to red light shift and while a



decrease in total protein was detected in the blue to red light shift cultures in this study ( $\approx 4\%$ ), it was not statistically significant. While no significant differences in total lipid (appendix) nor total FAME were detected in this study despite a decrease in total lipids observed in red light previously (section 3.4.3). Other studies suggest that a light shift to green light increases cellular content of lipids in *Nannochloropsis* sp. (Ra *et al.*, 2016; Sung *et al.*, 2018) and may prove to be an avenue of further research in diatoms.

However the cellular mechanism causing this relationship between green light and increased lipid biosynthesis is currently unknown (Sung *et al.*, 2018). In a previous study investigating light qualities in *Nannochloropsis* sp., no growth was observed under green light (Vadiveloo *et al.*, 2015). One may therefore speculate the increase in lipids after a green light shift may be a stress response, as *Nannochloropsis* sp. grows poorly under green light, and other microalgae are known to increase lipid content in response to stresses such as nitrogen limitation (Su *et al.*, 2011; Gao, Yang and Wang, 2013). While the results discussed in this study offers new insight into how the biochemical composition of *C. muelleri* changes in response to a short-term light shift, many new questions have also been raised: mainly, the differences discussed in comparison to Jungandreas *et al.* (2014). As studies of light shifts in diatoms are still limited, more studies focusing on comparing multiple diatom species under the same light conditions would improve the understanding of this emerging technique with

potential for application in aquaculture, as well as being relevant in photophysiology research.

#### 4.5.3. Digestibility

There are a myriad of studies investigating different species or strategies to improve biomass or biochemical productivity of lipids, proteins and FAMEs in microalgae as a sustainable feed for aquaculture (Hemaiswarya *et al.*, 2011). While studies reporting improved biomass and/or biochemical content can be broadly defined as potentially bioaccessible nutrients; in practice, it is often unknown what fraction of that is digested and made available for absorption. This disconnect exists as not all studies can readily conduct feeding trials to measure digestibility. However, simulated digestibility assays can be an inexpensive method to provide a qualitative estimation of feed quality in a short time period (Moyano *et al.*, 2015).

To test the feed quality of *C. muelleri* grown under different light conditions, digestibility assays were performed on blue and white light control cultures, as well as red light shifted cultures. The scope of this assay was to estimate the digestibility of the two most important metabolites for bivalve spat growth, protein and FAME. Note that, while total lipids were measured in undigested and digested biomass samples (Figure 4.11 in Supplementary Materials), the digestibility of total lipid was not

analysed. As total lipids were measured gravimetrically, the total lipid values in the digested samples were too low to be measured accurately. Therefore, total FAME values were used for the analysis as GC is a more sensitive instrument for measuring smaller concentrations of metabolites. There were no significant differences between the different light conditions for total FAME digestibility, however it appears that protein digestibility is decreased in blue light acclimated cultures, while red light shifting in both blue and white light acclimated cultures resulted in a minor decrease in protein digestibility (Figure 4.7).

#### 4.5.4. Pigments

Pigment content was quantified with HPLC and compared between cultures grown under blue and white light and blue and white light shifted to red light. The main differences in the pigment content between the control cultures and shifted cultures of *C. muelleri* occurred in xanthophyll pigments (diadinoxanthin and diatoxanthin) (Figure 4.6). In both the red light shifted cultures (BLRL & WLRL) dtx content were significantly higher than the respective control cultures (BLctrl & WLctrl). Jungandreas *et al.* (2014) observed a similar trend in blue to red light shifted cultures, where a decrease of ddx of approximately 15 mmol mol Chl  $a^{-1}$  was observed within the first 24 h of the light shift, while dtx content was not shown or detected; possibly due to the

low irradiance of red light used ( $40 \mu\text{mol photons m}^{-2} \text{s}^{-1}$ ). Since xanthophyll pigments are integral to photoprotection by quenching the excited states of chlorophyll (Lohr and Wilhelm, 2001), this may indicate red light shifted cultures experienced a state similar to high light stress, as dtx in diatoms are known to increase upon exposure to high light (Nymark *et al.*, 2009). A study by Valle *et al.* (2014) confirmed this in *P. tricornutum* where it was observed that under high red light ( $730 \mu\text{mol photons m}^{-2} \text{s}^{-1}$ ) illumination (0.5 h) dtx content had significantly increased while it was not detected at lower red light ( $230 \mu\text{mol photons m}^{-2} \text{s}^{-1}$ ).

#### 4.5.5. Photosynthesis

Maintaining photosynthetic health of all microalgae cultures is a crucial factor in ensuring high biomass productivity. Rapid light curves were conducted during the first day ( $t_0$ ) (Table 4.3 in Supplementary Materials) and at three time points after the light shift during the last day ( $t_f$ ) (Figure 4.5) to monitor the effect of light shifts on photosynthetic parameters (Table 4.4 in Supplementary Materials). As discussed in section 4.5.4, indications that red light constrains the photosynthetic performance in *C. muelleri* were also observed in the series of RLC measurements upon shifting blue and white light acclimated cultures to red light (Figure 4.5). The most drastic changes were observed in  $\Phi_{\text{PSII}}$  measurements with values falling as low as 0.34 and 0.42 in

BLRL and WLRL, respectively. A similar observation was made by Valle *et al.* (2014) in *P. tricornutum* cultures shifted from white light ( $100 \mu\text{mol photons m}^{-2} \text{s}^{-1}$ ) to red light ( $730 \mu\text{mol photons m}^{-2} \text{s}^{-1}$ , with 48 h of dark treatment prior to light shift to synchronize the growth stage), where  $\Phi_{\text{PSII}}$  decreased from  $\approx 0.60$  to  $\approx 0.30$  in 6 h. This observation is in contrast to the observations made in Jungandreas *et al.* (2014), where a minor increase in  $\Phi_{\text{PSII}}$  (from  $\approx 0.66$  to  $\approx 0.69$ ) was observed incrementally over a 10 h period in *P. tricornutum* cultures shifted from low blue light ( $24 \mu\text{mol photons m}^{-2} \text{s}^{-1}$ ) to low red light ( $40 \mu\text{mol photons m}^{-2} \text{s}^{-1}$ ). The different observations made in *P. tricornutum* are most likely due to the difference in total irradiance used, while it appears that light shifting in lower irradiance levels does not hinder photosynthetic performances (Jungandreas *et al.*, 2014), at higher irradiances photosynthetic performance is significantly hindered (Valle *et al.*, 2014). Photosynthetic capacity ( $\text{rETR}_{\text{max}}$ ) also followed a similar trend as  $\Phi_{\text{PSII}}$  in the two red light shifted cultures also fell significantly compared to pre-shifted conditions ( $t_{f0}$ ). In BLctrl the  $\text{rETR}_{\text{max}}$  fell by approximately 20% by  $t_{f8}$ , while in BLRL  $\text{rETR}_{\text{max}}$  fell by approximately 60%, also by  $t_{f8}$ . The change was less significant in WL cultures as a decrease in  $\text{rETR}_{\text{max}}$  of 35% was observed in WLctrl and approximately 50% in WLRL by  $t_{f8}$ . A substantial shift in NPQ capacity was observed following red light shifts in BLRL cultures ( $t_{f0}$ :  $1.78 \pm 0.10$  to  $t_{f8}$ :  $0.22 \pm 0.07$ ) and in WLRL cultures ( $t_{f0}$ :  $1.19 \pm 0.15$  to  $t_{f8}$ :  $0.35 \pm 0.18$ ) compared to the

non-shifted counterparts (BLctrl & WLctrl) (Figure 4.5). Costa *et al.* (2013) had previously demonstrated that NPQ in *P. tricornutum* was largely dependent on the light quality rather than light intensity, observing higher NPQ in blue light than white light, while lower NPQ in red light compared to white light. A similar observation was made by Jungandreas *et al.* (2014) in *P. tricornutum* cultures shifted from low blue light to low red light, where maximum NPQ values fell from approximately 1.12 to 0.59 in three days following light shift. The observation made in this study further solidifies the idea that NPQ capacity in diatoms are largely determined by light quality; however, under higher light intensities, there change occur in hours as opposed to days.

#### **4.6. Conclusions**

This study sought to assess the feasibility of light shifts for use in aquaculture facilities to increase metabolite productivity and increase nutritional value, as well as the resulting feed quality of the cultures which was also assessed via digestibility assays.

This was the first work to investigate light shifts and assess the feed quality by utilizing digestibility assay, a technique rarely utilized in diatom research. As anticipated, no increase in biomass production was detected and while an increase in protein production was hypothesized; no significant increase in protein was observed as a result of light

shifts. Significant differences were observed however in the digestibility of proteins and individual FAME species.

This study was conducted using laboratory-scale photobioreactors under limited irradiances and monitored for a short period of three days. Further insights could be observed by investigating the effects of light shifts under a wider range of irradiance levels, monitoring for a longer period of time after light shift and conducting light shifts with several other diatoms.

#### 4.7. References

- Areekijserree, M., Engkagul, A., Kovitvadhi, S., Kovitvadhi, U., Thongspan, A. and Rungruangsak-Torrissen, K. (2006) ‘Development of digestive enzymes and *in vitro* digestibility of different species of phytoplankton for culture of early juveniles of the freshwater pearl mussel, *Hyriopsis (Hyriopsis) bialatus* Simpson, 1900’, *Invertebrate Reproduction & Development*, 49(4), pp. 255–262. doi: 10.1080/07924259.2006.9652215.
- Beardall, J. and Raven, J. A. (2013) ‘Limits to phototrophic growth in dense culture: CO<sub>2</sub> supply and light’, in *Algae for Biofuels and Energy*. Dordrecht: Springer Netherlands, pp. 91–97. doi: 10.1007/978-94-007-5479-9\_5.
- Bertrand, M. (2010) ‘Carotenoid biosynthesis in diatoms’, *Photosynthesis research*,

106(1–2), pp. 89–102. doi: 10.1007/s11120-010-9589-x.

Bhatty, R. S. (1982) ‘*In vitro* hydrolysis of skim milk and pea proteins by pepsin and rennin’, *Canadian Institute of Food Science and Technology Journal*, 15(2), pp. 101–108. doi: 10.1016/S0315-5463(82)72373-9.

Bilger, W. and Björkman, O. (1990) ‘Role of the xanthophyll cycle in photoprotection elucidated by measurements of light-induced absorbance changes, fluorescence and photosynthesis in leaves of *Hedera canariensis*’, *Photosynthesis Research*, 25(3), pp. 173–185. doi: 10.1007/bf00033159.

Blackburn, S. I. and Volkman, J. K. (2012) ‘Microalgae: A renewable source of bioproducts’, in Dunford, N. T. (ed.) *Food and Industrial Bioproducts and Bioprocessing*. 1st edn. Iowa: Iowa State University Press, pp. 221–241. doi: 10.1002/9781119946083.ch9.

Borowitzka, M. A. (1997) ‘Microalgae for aquaculture: Opportunities and constraints’, *Journal of Applied Phycology*, 9(5), pp. 393–401. doi: 10.1023/A:1007921728300.

Borowitzka, M. A. (2013) ‘High-value products from microalgae-their development and commercialisation’, *Journal of Applied Phycology*, 25(3), pp. 743–756. doi: 10.1007/s10811-013-9983-9.

Borowitzka, M. A. and Moheimani, N. R. (eds) (2013) *Algae for biofuels and energy*.



Dordrecht: Springer Netherlands. doi: 10.1007/978-94-007-5479-9.

Brown, M. R. (2002) 'Nutritional value and use of microalgae in aquaculture', in Cruz-Suárez, L. E., Ricque-Marie, D., Tapia-Salazar, M., Gaxiola-Cortés, M. G., and Simoes, N. (eds) *Avances en nutrición acuícola VI. Memorias del VI Simposio Internacional de Nutrición Acuícola*. Quintana Roo, México, pp. 281–292. doi: 10.5772/1516.

Brown, M. R., Jeffrey, S. W., Volkman, J. K. and Dunstan, G. A. (1997) 'Nutritional properties of microalgae for mariculture', *Aquaculture*, 151(1–4), pp. 315–331. doi: 10.1016/S0044-8486(96)01501-3.

Buchanan, R. A. (1969) 'In vivo and in vitro methods of measuring nutritive value of leaf-protein preparations', *British Journal of Nutrition*, 23(03), p. 533. doi: 10.1079/BJN19690062.

Camacho-Rodríguez, J., Cerón-García, M. C., Macías-Sánchez, M. D., Fernández-Sevilla, J. M., López-Rosales, L. and Molina-Grima, E. (2016) 'Long-term preservation of concentrated *Nannochloropsis gaditana* cultures for use in aquaculture', *Journal of Applied Phycology*, 28(1), pp. 299–312. doi: 10.1007/s10811-015-0572-y.

Carvalho, A. P., Silva, S. O., Baptista, J. M. and Malcata, F. X. (2011) 'Light requirements in microalgal photobioreactors: An overview of biophotonic aspects', *Applied Microbiology and Biotechnology*, 89(5), pp. 1275–1288. doi: 10.1007/s00253-

010-3047-8.

Cavonius, L. R., Albers, E. and Undeland, I. (2016) ‘*In vitro* bioaccessibility of proteins and lipids of pH-shift processed *Nannochloropsis oculata* microalga’, *Food & Function*, 7(4), pp. 2016–2024. doi: 10.1039/c5fo01144b.

Costa, B. S., Jungandreas, A., Jakob, T., Weisheit, W., Mittag, M. and Wilhelm, C. (2013) ‘Blue light is essential for high light acclimation and photoprotection in the diatom *Phaeodactylum tricornutum*’, *Journal of experimental botany*, 64(2), pp. 483–93. doi: 10.1093/jxb/ers340.

Falkowski, P. G. and Raven, J. A. (2007) *Aquatic photosynthesis*. 2nd Ed. New Jersey, USA: Princeton University Press.

Gao, Y., Yang, M. and Wang, C. (2013) ‘Nutrient deprivation enhances lipid content in marine microalgae’, *Bioresource Technology*, 147, pp. 484–491. doi: 10.1016/j.biortech.2013.08.066.

Goh, L. P., Loh, S. P., Fatimah, M. Y. and Perumal, K. (2009) ‘Bioaccessibility of carotenoids and tocopherols in marine microalgae, *Nannochloropsis* sp. and *Chaetoceros* sp.’, *Malasian Journal of Nutrition*, 15(1), pp. 77–86.

Gorai, T., Katayama, T., Obata, M., Murata, A. and Taguchi, S. (2014) ‘Low blue light enhances growth rate, light absorption, and photosynthetic characteristics of four marine

phytoplankton species', *Journal of Experimental Marine Biology and Ecology*, 459, pp. 87–95. doi: 10.1016/j.jembe.2014.05.013.

Grabner, M. (1985) 'An *in vitro* method for measuring protein digestibility of fish feed components', *Aquaculture*, 48(2), pp. 97–110. doi: 10.1016/0044-8486(85)90097-3.

Graziani, G., Schiavo, S., Nicolai, M. A., Buono, S., Fogliano, V., Pinto, G. and Pollio, A. (2013) 'Microalgae as human food: Chemical and nutritional characteristics of the thermo-acidophilic microalga *Galdieria sulphuraria*', *Food & Function*, 4(1), pp. 144–152. doi: 10.1039/c2fo30198a.

Guillard, R. R. L. (1975) 'Culture of phytoplankton for feeding marine invertebrates', in Smith, W. L. and Chanley, M. H. (eds) *Culture of marine invertebrate animals*. Boston, MA: Springer US, pp. 29–60. doi: 10.1007/978-1-4615-8714-9\_3.

Han, P., Shen, S., Wang, H.-Y., Yao, S., Tan, Z., Zhong, C. and Jia, S. (2017) 'Applying the strategy of light environment control to improve the biomass and polysaccharide production of *Nostoc flagelliforme*', *Journal of Applied Phycology*, 29(1), pp. 55–65. doi: 10.1007/s10811-016-0963-8.

Harrison, P. J., Thompson, P. A. and Calderwood, G. S. (1990) 'Effects of nutrient and light limitation on the biochemical composition of phytoplankton', *Journal of Applied Phycology*, 2(1), pp. 45–56. doi: 10.1007/BF02179768.

Hemaiswarya, S., Raja, R., Kumar, R. R., Ganesan, V. and Anbazhagan, C. (2011)

‘Microalgae: A sustainable feed source for aquaculture’, *World Journal of Microbiology and Biotechnology*, 27(8), pp. 1737–1746. doi: 10.1007/s11274-010-0632-z.

Herlory, O., Richard, A. P. and Blanchard, G. F. (2007) ‘Methodology of light response curves: Application of chlorophyll fluorescence to microphytobenthic biofilms’, *Marine Biology*, 153, pp. 91–101. doi: 10.1007/s00227-007-0787-9.

Houliez, E., Lefebvre, S., Lizon, F. and Schmitt, G. F. (2017) ‘Rapid light curves (RLC) or non-sequential steady-state light curves (N-SSLC): Which fluorescence-based light response curve methodology robustly characterizes phytoplankton photosynthetic activity and acclimation status?’, *Marine Biology*, 164(174), pp. 1–17. doi: 10.1007/s00227-017-3208-8.

Huang, X., Huang, Z., Wen, W. and Yan, J. (2013) ‘Effects of nitrogen supplementation of the culture medium on the growth, total lipid content and fatty acid profiles of three microalgae (*Tetraselmis subcordiformis*, *Nannochloropsis oculata* and *Pavlova viridis*)’, *Journal of Applied Phycology*, 25(1), pp. 129–137. doi: 10.1007/s10811-012-9846-9.

Ihnken, S., Roberts, S. and Beardall, J. (2011) ‘Differential responses of growth and photosynthesis in the marine diatom *Chaetoceros muelleri* to CO<sub>2</sub> and light availability’, *Phycologia*, 50(2), pp. 182–193. doi: 10.2216/10-11.1.

- Jungandreas, A., Costa, B. S., Jakob, T., Von Bergen, M., Baumann, S. and Wilhelm, C. (2014) 'The acclimation of *Phaeodactylum tricornutum* to blue and red light does not influence the photosynthetic light reaction but strongly disturbs the carbon allocation pattern', *PLoS ONE*, 9(8), pp. 5–15. doi: 10.1371/journal.pone.0099727.
- Kim, D. G., Lee, C., Park, S.-M. and Choi, Y.-E. (2014) 'Manipulation of light wavelength at appropriate growth stage to enhance biomass productivity and fatty acid methyl ester yield using *Chlorella vulgaris*', *Bioresource Technology*, 159, pp. 240–248. doi: 10.1016/j.biortech.2014.02.078.
- Knauer, J. and Southgate, P. C. (1999) 'A review of the nutritional requirements of bivalves and the development of alternative and artificial diets for bivalve aquaculture', *Reviews in Fisheries Science*, 7(3–4), pp. 241–280. doi: 10.1080/10641269908951362.
- Langdon, C. J. (1989) 'Preparation and evaluation of protein microcapsules for a marine suspension-feeder, the Pacific oyster *Crassostrea gigas*', *Marine Biology*, 102(2), pp. 217–224. doi: 10.1007/BF00428283.
- Lebeau, T. and Robert, J. M. (2003a) 'Diatom cultivation and biotechnologically relevant products. Part I: Cultivation at various scales', *Applied Microbiology and Biotechnology*, 60, pp. 612–623. doi: 10.1007/s00253-002-1176-4.
- Lebeau, T. and Robert, J. M. (2003b) 'Diatom cultivation and biotechnologically

relevant products. Part II: Current and putative products', *Applied Microbiology and Biotechnology*, 60, pp. 624–632. doi: 10.1007/s00253-002-1177-3.

Lee, C.-G. (1999) 'Calculation of light penetration depth in photobioreactors', *Biotechnology and Bioprocess Engineering*, 4(1), pp. 78–81. doi: 10.1007/BF02931920.

Lourenço, S. O., Barbarino, E., Lavín, P. L., Lanfer Marquez, U. M. and Aida, E. (2004) 'Distribution of intracellular nitrogen in marine microalgae: Calculation of new nitrogen-to-protein conversion factors', *European Journal of Phycology*, 39(1), pp. 17–32. doi: 10.1080/0967026032000157156.

MacIntyre, H. L., Kana, T. M., Anning, T. and Geider, R. J. (2002) 'Photoacclimation of photosynthesis irradiance response curves and photosynthetic pigments in microalgae and cyanobacteria', *Journal of Phycology*, 38(1), pp. 17–38. doi: 10.1046/j.1529-8817.2002.00094.x.

McCauley, J. I., Umarova, J., Pernice, M. and Ralph, P. J. (2019) 'Using a simulated monogastric digestion model to explore the digestibility of different species of microalgae', *Unpublished work*.

Morris, H. J., Almarales, A., Carrillo, O. and Bermúdez, R. C. (2008) 'Utilisation of *Chlorella vulgaris* cell biomass for the production of enzymatic protein hydrolysates', *Bioresource Technology*, 99(16), pp. 7723–7729. doi: 10.1016/j.biortech.2008.01.080.

Moyano, F. J., Saénz de Rodrigáñez, M. A., Díaz, M. and Tacon, A. G. J. (2015)

‘Application of *in vitro* digestibility methods in aquaculture: Constraints and perspectives’, *Reviews in Aquaculture*, 7(4), pp. 223–242. doi: 10.1111/raq.12065.

Moyano, F. J. and Savoie, L. (2001) ‘Comparison of *in vitro* systems of protein

digestion using either mammal or fish proteolytic enzymes’, *Comparative Biochemistry and Physiology Part A: Molecular & Integrative Physiology*, 128(2), pp. 359–368. doi: 10.1016/S1095-6433(00)00315-9.

Nichols, D. S. (2003) ‘Prokaryotes and the input of polyunsaturated fatty acids to the marine food web’, *FEMS Microbiology Letters*, 219(1), pp. 1–7. doi: 10.1016/S0378-1097(02)01200-4.

Nielsen, R., Nielsen, M., Abate, T. G., Hansen, B. W., Jepsen, P. M., Nielsen, S. L.,

Støttrup, J. G. and Buchmann, K. (2017) ‘The importance of live-feed traps - farming marine fish species’, *Aquaculture Research*, 48(6), pp. 2623–2641. doi: 10.1111/are.13281.

Nymark, M., Valle, K. C., Brembu, T., Hancke, K., Winge, P., Andresen, K., Johnsen, G. and Bones, A. M. (2009) ‘An integrated analysis of molecular acclimation to high light in the marine diatom *Phaeodactylum tricornutum*’, *PLoS ONE*, 4(11). doi: 10.1371/journal.pone.0007743.

Oldenhof, H., Zachleder, V. and Van Den Ende, H. (2006) 'Blue- and red-light regulation of the cell cycle in *Chlamydomonas reinhardtii* (Chlorophyta)', *European Journal of Phycology*, 41(3), pp. 313–320. doi: 10.1080/09670260600699920.

Ooms, M. D., Dinh, C. T., Sargent, E. H. and Sinton, D. (2016) 'Photon management for augmented photosynthesis', *Nature Communications*, 7, p. 12699. doi: 10.1038/ncomms12699.

Parsons, C. M. (1991) 'Use of pepsin digestibility, multienzyme pH change and protein solubility assays to predict *in vivo* protein quality of feedstuffs', in Fuller, M. F. (ed.) *In vitro Digestion for Pigs and Poultry*. Wallingford, U.K.: CAB International Publishing, pp. 105–115.

Perkins, R. G., Kromkamp, J. C., Serôdio, J., Lavaud, J., Jesus, B., Mouget, J. L., Lefebvre, S. and Forster, R. M. (2010) 'The application of variable chlorophyll fluorescence to microphytobenthic biofilms', in Suggett, D. J., Borowitzka, M. A., and Prášil, O. (eds) *Chlorophyll a Fluorescence in Aquatic Sciences: Methods and Applications*. Dordrecht: Springer Netherlands, pp. 237–275. doi: 10.1007/978-90-481-9268-7\_12.

Powles, S. B. (1984) 'Photoinhibition of photosynthesis induced by visible light', *Annual Review of Plant Physiology*, 35(1), pp. 15–44. doi:



10.1146/annurev.pp.35.060184.000311.

Pulz, O. and Gross, W. (2004) 'Valuable products from biotechnology of microalgae', *Applied Microbiology and Biotechnology*, 65(6), pp. 635–648. doi: 10.1007/s00253-004-1647-x.

Ra, C.-H., Kang, C.-H., Jung, J.-H., Jeong, G.-T. and Kim, S.-K. (2016) 'Effects of light-emitting diodes (LEDs) on the accumulation of lipid content using a two-phase culture process with three microalgae', *Bioresource Technology*, 212, pp. 254–261. doi: 10.1016/j.biortech.2016.04.059.

Ralph, P. J. and Gademann, R. (2005) 'Rapid light curves: A powerful tool to assess photosynthetic activity', *Aquatic Botany*, 82(3), pp. 222–237. doi: 10.1016/j.aquabot.2005.02.006.

Richmond, A. (ed.) (2004) *Handbook of microalgal culture: Biotechnology and applied phycology*. Oxford, UK: Blackwell Science. doi: 10.1002/9780470995280.

Rodríguez De Marco, E., Steffolani, M. E., Martínez, C. S. and León, A. E. (2014) 'Effects of *spirulina* biomass on the technological and nutritional quality of bread wheat pasta', *LWT - Food Science and Technology*, 58(1), pp. 102–108. doi: 10.1016/j.lwt.2014.02.054.

Sakshaug, E., Bricaud, A., Dandonneau, Y., Falkowski, P. G., Kiefer, D. A., Legendre,

- L., Morel, A., Parslow, J. and Takahashi, M. (1997) 'Parameters of photosynthesis: Definitions, theory and interpretation of results', *Journal of Plankton Research*, 19(11), pp. 1637–1670. doi: 10.1093/plankt/19.11.1637.
- Saunders, R. M., Connor, M. A., Booth, A. N., Bickoff, E. M. and Kohler, G. O. (1973) 'Measurement of digestibility of *Alfalfa* protein concentrates by *in vivo* and *in vitro* methods', *The Journal of Nutrition*, 103(4), pp. 530–535. doi: 10.1093/jn/103.4.530.
- Schreiber, U. (2005) 'Pulse-amplitude-modulation (PAM) fluorometry and saturation pulse method: An overview', in Papageorgiou, G. C. and Govindjee (eds) *Advances in Photosynthesis and Respiration*. Dordrecht: Springer Netherlands, pp. 279–319. doi: 10.1007/978-1-4020-3218-9\_11.
- Schulze, P. S. C., Barreira, L. A., Pereira, H. G. C., Perales, J. A. and Varela, J. C. S. (2014) 'Light emitting diodes (LEDs) applied to microalgal production', *Trends in Biotechnology*, 32(8), pp. 422–430. doi: 10.1016/j.tibtech.2014.06.001.
- Shipton, T. A. and Britz, P. J. (2002) 'Evaluation of an *in vitro* digestibility technique for the prediction of protein digestibility in the South African abalone, *Haliotis midae* L.', *Aquaculture Nutrition*, 8(1), pp. 15–21. doi: 10.1046/j.1365-2095.2002.00187.x.
- Su, C. H., Chien, L. J., Gomes, J., Lin, Y. S., Yu, Y. K., Liou, J. S. and Syu, R. J. (2011) 'Factors affecting lipid accumulation by *Nannochloropsis oculata* in a two-stage

cultivation process', *Journal of Applied Phycology*, 23(5), pp. 903–908. doi: 10.1007/s10811-010-9609-4.

Sung, M.-G., Han, J.-I., Lee, B. and Chang, Y. K. (2018) 'Wavelength shift strategy to enhance lipid productivity of *Nannochloropsis gaditana*', *Biotechnology for Biofuels*, 11(70), pp. 1–12. doi: 10.1186/s13068-018-1067-2.

Supannapong, P., Pimsalee, T., A-komol, T., Engkagul, A., Kovitvadhi, U., Kovitvadhi, S. and Rungruangsak-Torrissen, K. (2008) 'Digestive enzymes and in-vitro digestibility of different species of phytoplankton for culture of the freshwater pearl mussel, *Hyriopsis (Hyriopsis) bialatus*', *Aquaculture International*, 16(5), pp. 437–453. doi: 10.1007/s10499-007-9156-4.

Tamburic, B., Guruprasad, S., Radford, D. T., Szabó, M., Lilley, R. M., Larkum, A. W. D., Franklin, J. B., Kramer, D. M., Blackburn, S. I., Raven, J. A., Schliep, M. and Ralph, P. J. (2014) 'The effect of diel temperature and light cycles on the growth of *Nannochloropsis oculata* in a photobioreactor matrix', *PLoS ONE*, 9(1), pp. 1–13. doi: 10.1371/journal.pone.0086047.

Taverner, M. R. and Farrell, D. J. (1981) 'Availability to pigs of amino acids in cereal grains: 3. A comparison of ileal availability values with faecal, chemical and enzymic estimates', *British Journal of Nutrition*, 46(1), pp. 173–180. doi: 10.1079/bjn19810019.

Thompson, P. A., Harrison, P. J. and Parslow, J. S. (1991) 'Influence of irradiance on cell volume and carbon quota for ten species of marine phytoplankton', *Journal of Phycology*, 27(3), pp. 351–360. doi: 10.1111/j.0022-3646.1991.00351.x.

Tibbetts, S. M., MacPherson, T., McGinn, P. J. and Fredeen, A. H. (2016) 'In vitro digestion of microalgal biomass from freshwater species isolated in Alberta, Canada for monogastric and ruminant animal feed applications', *Algal Research*, 19, pp. 324–332. doi: 10.1016/j.algal.2016.01.016.

Vadiveloo, A., Moheimani, N. R., Cosgrove, J. J., Bahri, P. A. and Parlevliet, D. (2015) 'Effect of different light spectra on the growth and productivity of acclimated *Nannochloropsis* sp. (Eustigmatophyceae)', *Algal Research*, 8, pp. 121–127. doi: 10.1016/j.algal.2015.02.001.

Valle, K. C., Nymark, M., Aamot, I., Hancke, K., Winge, P., Andresen, K., Johnsen, G., Brembu, T. and Bones, A. M. (2014) 'System responses to equal doses of photosynthetically usable radiation of blue, green, and red light in the marine diatom *Phaeodactylum tricornutum*', *PLoS ONE*, 9(12), pp. 1–37. doi: 10.1371/journal.pone.0114211.

Wood, M. A., Everroad, R. C. and Wingard, L. M. (2005) 'Measuring growth rates in microalgal cultures', in Andersen, R. A. (ed.) *Algal Culturing Techniques*.

Massachusetts: Elsevier Academic Press, pp. 269–285.

## 4.8. Supplementary Materials

**Table 4.3** Rapid light curve data at  $t_0$  where,  $a$  is photosynthetic rate in light-limited region of RLC,  $rETR_{\max}$  is maximum electron transfer rate,  $I_k$  is minimum saturating irradiance,  $F_0$  is minimum fluorescence of dark-adapted microalgal culture,  $F_m$  is maximum fluorescence yield of dark-adapted microalgal culture and  $\Phi_{PSII}$  is maximum quantum yield of photosystem II. One-way ANOVA performed with Tukey method at 95% confidence: same letter indicate no significant difference and different letters indicate significant difference. Values shown are mean  $\pm$  standard deviation ( $n = 7$ ).

<b>T<sub>0</sub></b>	<b>a</b>	<b>rETR<sub>max</sub></b>	<b>I<sub>k</sub></b>	<b>F<sub>0</sub></b>	<b>F<sub>m</sub></b>	<b>Φ<sub>PSII</sub></b>
<b>BLctrl</b>	0.27 $\pm$ 0.01 <sup>b</sup>	140.67 $\pm$ 5.64 <sup>a</sup>	529.13 $\pm$ 24.95 <sup>a</sup>	0.70 $\pm$ 0.09	1.67 $\pm$ 0.25 <sup>ab</sup>	0.58 $\pm$ 0.02 <sup>b</sup>
<b>BLRL</b>	0.26 $\pm$ 0.00 <sup>b</sup>	137.63 $\pm$ 5.04 <sup>a</sup>	521.23 $\pm$ 25.00 <sup>a</sup>	0.66 $\pm$ 0.09	1.57 $\pm$ 0.25 <sup>b</sup>	0.58 $\pm$ 0.01 <sup>b</sup>
<b>WLctrl</b>	0.29 $\pm$ 0.01 <sup>a</sup>	131.02 $\pm$ 6.78 <sup>ab</sup>	456.48 $\pm$ 27.02 <sup>b</sup>	0.79 $\pm$ 0.16	2.17 $\pm$ 0.50 <sup>a</sup>	0.63 $\pm$ 0.01 <sup>a</sup>
<b>WLRL</b>	0.29 $\pm$ 0.01 <sup>a</sup>	122.15 $\pm$ 11.78 <sup>b</sup>	419.88 $\pm$ 49.80 <sup>b</sup>	0.80 $\pm$ 0.11	2.19 $\pm$ 0.34 <sup>a</sup>	0.63 $\pm$ 0.01 <sup>a</sup>

**Table 4.4** Rapid light curve data at  $t_f$  where,  $a$  is photosynthetic rate in light-limited region of RLC,  $rETR_{max}$  is maximum electron transfer rate,  $I_k$  is minimum saturating irradiance,  $F_0$  is minimum fluorescence of dark-adapted microalgal culture,  $F_m$  is maximum fluorescence yield of dark-adapted microalgal culture and  $\Phi_{PSII}$  is maximum quantum yield of photosystem II. Measurements were taken at 3 time points during day three ( $T_f$ ): 0 h ( $T_f 0$ ), 5 h ( $T_f 5$ ) and 8 h after light shift ( $T_f 8$ ). One-way ANOVA performed with Tukey method at 95% confidence: same letter indicate no significant difference and different letters indicate significant difference. One-way ANOVA was used to analyse the same cultures at different time points. Values shown are mean  $\pm$  standard deviation ( $n = 7$ ).

	Time	$a$	$rETR_{max}$	$I_k$	$F_0$	$F_m$	$\Phi_{PSII}$
<b>BLctrl</b>	$T_f 0$	$0.29 \pm 0.01^a$	$91.96 \pm 4.43^a$	$314.50 \pm 14.89^a$	$1.06 \pm 0.10^a$	$3.04 \pm 0.31^a$	$0.65 \pm 0.01^a$
	$T_f 5$	$0.27 \pm 0.01^b$	$83.34 \pm 8.68^a$	$310.74 \pm 27.40^a$	$1.15 \pm 0.04^a$	$3.16 \pm 0.21^a$	$0.64 \pm 0.01^{ab}$
	$T_f 8$	$0.26 \pm 0.01^c$	$72.94 \pm 7.68^b$	$286.46 \pm 35.02^a$	$1.15 \pm 0.08^a$	$3.04 \pm 0.33^a$	$0.62 \pm 0.02^b$
<b>BLRL</b>	$T_f 0$	$0.29 \pm 0.01^a$	$94.80 \pm 4.77^a$	$330.61 \pm 25.40^a$	$1.01 \pm 0.06^a$	$2.93 \pm 0.24^a$	$0.66 \pm 0.01^a$
	$T_f 5$	$0.20 \pm 0.02^b$	$52.51 \pm 3.91^b$	$271.04 \pm 24.36^b$	$1.00 \pm 0.12^a$	$1.90 \pm 0.34^b$	$0.47 \pm 0.04^b$
	$T_f 8$	$0.13 \pm 0.02^c$	$39.59 \pm 2.54^c$	$306.81 \pm 24.07^a$	$0.78 \pm 0.07^b$	$1.20 \pm 0.15^c$	$0.34 \pm 0.03^c$
<b>WLctrl</b>	$T_f 0$	$0.29 \pm 0.01^a$	$66.26 \pm 6.40^a$	$229.46 \pm 15.00^a$	$1.17 \pm 0.07^a$	$3.42 \pm 0.23^a$	$0.66 \pm 0.01^a$
	$T_f 5$	$0.25 \pm 0.03^b$	$51.04 \pm 10.32^b$	$203.63 \pm 15.62^b$	$1.14 \pm 0.12^a$	$2.83 \pm 0.67^a$	$0.59 \pm 0.05^b$
	$T_f 8$	$0.24 \pm 0.03^b$	$43.64 \pm 8.36^b$	$184.61 \pm 13.29^b$	$1.15 \pm 0.14^a$	$2.69 \pm 0.75^a$	$0.56 \pm 0.06^b$
<b>WLRL</b>	$T_f 0$	$0.28 \pm 0.02^a$	$65.27 \pm 7.53^a$	$232.31 \pm 13.66^a$	$1.12 \pm 0.08^a$	$3.15 \pm 0.42^a$	$0.64 \pm 0.03^a$
	$T_f 5h$	$0.20 \pm 0.03^b$	$38.79 \pm 5.04^b$	$194.66 \pm 15.29^b$	$1.06 \pm 0.16^a$	$2.11 \pm 0.53^b$	$0.48 \pm 0.05^b$
	$T_f 8h$	$0.17 \pm 0.03^b$	$32.03 \pm 2.77^b$	$186.14 \pm 18.74^b$	$0.97 \pm 0.16^a$	$1.71 \pm 0.41^b$	$0.42 \pm 0.05^c$

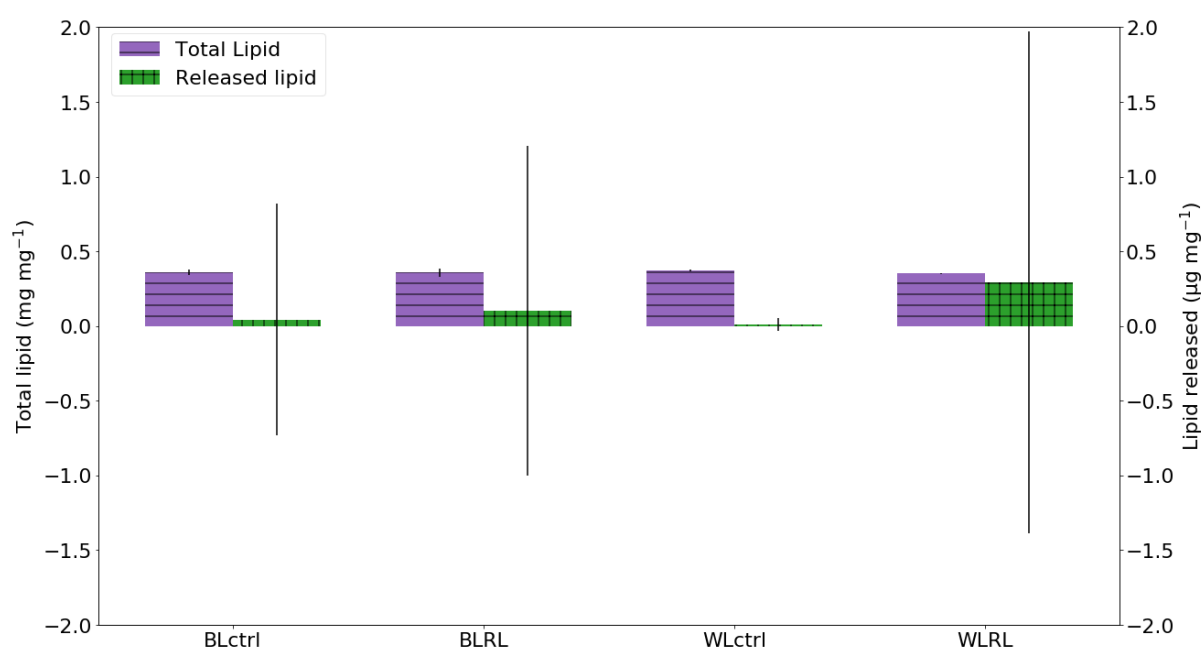


**Figure 4.11** Total lipids from undigested and digested *C. muelleri* cultures grown under different light qualities. Purple bars with horizontal patterns represent total lipids in  $\mu\text{g mg}^{-1}$  dry weight from undigested samples and green bars with crossing patterns represent total lipids in  $\mu\text{g mg}^{-1}$  dry weight from digested samples. One-way ANOVA performed with Tukey method at 95% confidence: no letters indicate no significant difference and different letters indicate significant difference. Data represents the mean  $\pm$  standard deviation ( $n = 3$ ).



## Chapter 5 General Discussion

Food security is projected to be one of the major challenges facing humanity in the immediate future (Godfray *et al.*, 2010). Today, aquaculture is regarded globally as one of the fastest growing food-producing industries (Ahmed and Lorica, 2002; FAO, 2016). With the world population predicted to surpass 8.5 billion people by the year 2030 (United Nation, 2015), in order to meet the increasing food demand, aquaculture production must increase. In order to improve aquaculture productions, microalgae which feed many aquaculture species must also increase. Major challenges must be addressed to make production economically feasible and environmentally sustainable, whilst maintaining high feed quality.

This study has investigated the two main factors limiting biomass production experienced in commercial microalgal production in hatcheries. *Chaetoceros muelleri* (CS-176) was used as a candidate species to assess strategies to overcome these limitations, while assessing the feasibility of different light conditions to improve growth, nutrient content and the cost efficiency. These strategies were simulated with photobioreactors (ePBRs) that allows for the continuous monitoring of abiotic factors, which are difficult to conduct in operational hatcheries.

## 5.1. Key Findings

### 5.1.1. Chapter 2

In this chapter, strategies to minimise the two main limitations restricting microalgal growth, light and CO<sub>2</sub> availability, were assessed. Four scenarios of light and CO<sub>2</sub> availabilities were tested, low light and low CO<sub>2</sub>, low light and high CO<sub>2</sub>, high light and low CO<sub>2</sub> and high light and high CO<sub>2</sub>. Light availability scenarios were tested by changing the areal availability of light, as opposed to simply increasing light intensity. By using two different LED setups that changed the path length of light (long and short), the distribution of light (low and high) was changed. CO<sub>2</sub> availability scenarios were tested by bubbling air and CO<sub>2</sub> gas (high availability) and bubbling with just air (low availability). From the observations made in this chapter, it was concluded that the availability of both light and CO<sub>2</sub> were essential to maximise biomass productivity, and the presence of one limitation (light and/or CO<sub>2</sub>) resulted in low productivity. These results indicate that, in order to improve biomass production of diatoms in commercial hatcheries, one must increase the availability of light, as well as CO<sub>2</sub>.

### 5.1.2. Chapter 3

From the observations made in Chapter 2, the scenario with the highest biomass productivity (high light and high CO<sub>2</sub>) was selected to assess the feasibility of using LEDs with different light qualities to test the growth rate, metabolic content and the cost efficiency of production.

The feasibility of blue, green, red and white LEDs as growth lights in commercial hatcheries. Blue, green and white LEDs had similar performances in biomass productivity, while red LEDs had significantly lower performance. Total metabolites (mg mg<sup>-1</sup> dry weight) was also quantified for proteins, lipids and carbohydrates. While most values were comparable to between the treatments, carbohydrates in blue light and proteins in red light were found to be significantly higher. Blue light was found to be the most cost efficient in biomass and metabolite production, requiring less than half the energy input (kilowatt hours) of other light qualities. The findings in this chapter indicate that with a suitable light configuration (as shown in Chapter 2), a light quality of high cost efficiency (blue LEDs) may be a viable option to reduce the hatchery operational costs, while maintaining high biomass productivity and metabolic content.

### 5.1.3. Chapter 4

In this chapter, the wavelength of the growth light was shifted to assess its effectiveness as a possible non-invasive method to manipulate diatom metabolic content for use in aquaculture feed production, as well as investigating its effects on growth, photosynthesis and feed quality. As hypothesised, no increase in biomass production was detected and while an increase in protein production was hypothesized, based on the findings in Chapter 3; no significant increase in protein was observed as a result of red light shifting. Significant changes were, however observed in rapid light curve measurements as a result of red light shifting. A significant reduction of  $\Phi_{PSII}$  and  $rETR_{max}$  was observed as a result of shifting from blue light to red light. To the author's knowledge this was the first work to investigate feed quality through the use of digestibility assays with experimental *C. muelleri* cultures.

## 5.2. Future Research

This thesis has provided new insights into the potential use of LEDs as a light source in microalgal production facilities used in aquaculture. The importance of light and CO<sub>2</sub> availability has been demonstrated to significantly improve biomass production, as well as the usage of blue LEDs to significantly improve the cost efficiency of biomass production. Also the potential useability of digestibility assays as a high throughput

method to test feed quality. However, this thesis has also raised further questions to be addressed in future research:

#### 5.2.1. Chapter 2

- In Chapter 2, the physiological and photosynthetic response of the marine diatom, *C. muelleri*, was analysed under different scenarios of light and CO<sub>2</sub> availability.

Further research should focus on strategies to increase the light and CO<sub>2</sub> availability in larger commercial bioreactor systems (e.g. bags). As larger systems have longer path lengths for the light to travel, the challenge will be to provide the available light as efficiently as possible. It is recommended that several LED panels are used to surround a bag to increase the areal light availability, instead of providing light from a single side of a bag.

#### 5.2.2. Chapter 3

- We observed that different light qualities of equal PUR have significant impact on the growth and metabolite content in *C. muelleri*. Further research should aim to investigate the metabolome in detail to fully characterise the changes in the metabolite content (e.g. proteins grown under red light).

- In addition to the future research prospects from Chapter 2 (above), different light quality of lights was observed to attenuate differently. In order to assess the findings made in Chapter 3, further experiments are required to assess the effects and cost efficiency of light qualities in larger production systems.
- Also, a future study investigating combined light qualities (i.e. combining 2 or more monochromatic lights) may yield further valuable insights in cost efficient light usage in hatcheries. For example, a previous study observed that combined blue/green treatment increased cost efficiency of growing *Botryococcus* sp. (Okumura *et al.*, 2015).

#### 5.2.3. Chapter 4

- In Chapter 4, the feasibility of light shifts in manipulating the metabolic content of *C. muelleri* for use in microalgal production facilities in hatcheries was investigated. While significant differences were observed in photosynthetic activities in response to the light shifts, no significant effects were observed in the physiology. This is in contrast to several studies investigating light shifts in several microalgae, and highlights the need for further research into light shifts in diatoms. For example, many studies have investigated light shifts in relatively low irradiances ( $< 100 \mu\text{mol photons m}^{-2} \text{ s}^{-1}$ ), while in this study an equivalent

irradiance of  $500 \mu\text{mol photons m}^{-2} \text{ s}^{-1}$  was used. An investigation of light shifts at multiple irradiance levels may give further insights to the feasibility of light shifts.

- In both Chapters 3 and 4, irradiances were estimated to be equal (PUR), the estimate is based on absorption but not photosynthetic output. To further improve light quality research, a photosynthetic action spectrum of *C. muelleri* will need to be conducted. An action spectrum measures photosynthesis in response to different monochromatic light (Haxo and Blinks, 1950). A photosynthetic action spectra based on oxygen evolution or carbon fixation of *C. muelleri* will improve the knowledge required to choose irradiance levels at different monochromatic lights.

### 5.3. Conclusion

The results outlined in this thesis has investigated growth limiting factors and light conditions with a matrix of photobioreactors (ePBR), physiological measurements as well as photosynthetic measurements to provide new understandings and strategies to grow *C. muelleri* in microalgal production facilities for the aquaculture industry. The new insights will improve our understanding of culturing techniques in hatcheries, as well as providing possible strategies to improve the cost efficiency of *C. muelleri* feed production.

With the looming global food security crisis, it is imperative that food producing industries, such as aquaculture, to meet the increasing production demand. With recent projections estimating that in order to meet the rising food demand the aquaculture industry will need to produce between 93.6 - 109.4 million tonnes by 2030 from the current (2016) 80.0 million tonnes (World Bank, 2013; FAO, 2018). With wild catchments are not projected to significantly increase production in 2030 from current figures: 90.9 million tonnes in 2016 and 91.0 million tonnes projected for 2030 (FAO, 2018), the aquaculture industry will need to increase production by 17% – 37% by 2030.

The cost efficient production of microalgal biomass and strategies to improve metabolic content of feed is a small step towards meeting the increasing demand.

## 5.4. References

Ahmed, M. and Lorica, M. H. (2002) 'Improving developing country food security through aquaculture development-lessons from Asia', *Food Policy*, 27, pp. 125–141.

FAO (2016) *The state of world fisheries and aquaculture 2016: Contributing to food security and nutrition for all*. Rome. doi: 10.5860/choice.50-5350.

FAO (2018) *The state of world fisheries and aquaculture 2018: Meeting the sustainable development goals*. Rome.



Godfray, H. C. J., Beddington, J. R., Crute, I. R., Haddad, L., Lawrence, D., Muir, J. F.,

Pretty, J., Robinson, S., Thomas, S. M. and Toulmin, C. (2010) 'Food security: The challenge of feeding 9 billion people', *Science*, 327, pp. 812–818.

Haxo, F. T. and Blinks, L. R. (1950) 'Photosynthetic action spectra of marine algae', *The Journal of General Physiology*, 33(4), pp. 389–422. doi: 10.1085/JGP.33.4.389.

Okumura, C., Saffreena, N., Rahman, M. A., Hasegawa, H., Miki, O. and Takimoto, A. (2015) 'Economic efficiency of different light wavelengths and intensities using LEDs for the cultivation of green microalga *Botryococcus braunii* (NIES-836) for biofuel production', *Environmental Progress & Sustainable Energy*, 34(1), pp. 269–275. doi: 10.1002/ep.11951.

United Nation (2015) *World Population Prospects: The 2015 Revision, Key Findings and Advance Tables*.

World Bank (2013) *FISH TO 2030: Prospects for Fisheries and Aquaculture*.

Washington DC. Available at: [www.worldbank.org](http://www.worldbank.org).